

**Sulfated phenolic acids as readily activatable
storage forms of antifouling agents
in marine plants**

Dissertation

zur Erlangung des akademischen Grades
doctor rerum naturalium (Dr. rer. nat.)

Vorgelegt dem Rat der chemisch-geowissenschaftlichen Fakultät
der Friedrich-Schiller-Universität Jena

von

M. Sc. (Chemie) Caroline Kurth

geboren am 13.07.1981 in Freiburg i. Br.

Gutachter:

1. Prof. Dr. Georg Pohnert (Friedrich-Schiller-Universität Jena)
2. Prof. Dr. Rainer Beckert (Friedrich-Schiller-Universität Jena)

Tag der öffentlichen Verteidigung: 13.05.2015

To my family

Acknowledgments

This thesis is based on more than three years research, whose accomplishment and finalization would not have been possible without the support of numerous people. First, I would like to thank Prof. Georg Pohnert for accepting me to his research group, for providing this exciting interdisciplinary topic, and for his trust in me and my scientific work. He always left me the freedom to plan and pursue the project by myself but at the same time guaranteed support by many constructive discussions. I would also like to thank the Volkswagen Stiftung and the Friedrich-Schiller-Universität Jena for funding this research project.

Special thanks go to my parents, Eike, my sister and Pablo, who always supported me in many respects during my entire studies.

Thanks, belong to the whole former and present research group not only for the many lively scientific discussions but also for the great time I had with them. Special thanks go to Andrea, Katha, Charles, Matt and Astrid for their introduction to the group, the algae- and the analytical world. Katha, Michi, Conny, Thomas and Anett prevented me during many biological discussions from a lot of mistakes a chemist probably would do when entering the world of microorganisms. I would also like to thank Stefanie, Phillip and Björn for the discussions concerning chemical issues. My thanks also belong to Stefanie and Jenny for algae extraction during their stays in Georgia and Florida and to Stefanie and Michi for proofreading this thesis. Last but not least I would like to thank the "UPLC-MS rescue team" Stefanie, Raphael and Michael who made the numerous hours and days in front of it bearable and occasionally even entertaining. Finally I would like to thank Jan Grüneberg and Dr. Carsten Paul for providing marine bacteria for the filter disc assay, and Dr. Levent Cavas for the successful cooperation and for performing the field assay in Turkey.

Contents

List of Figures	VI
List of Tables	IX
Zusammenfassung	X
Abstract	XII
Abbreviations	XIV
1 Introduction	1
1.1 Wound reaction of siphonous green algae	1
1.1.1 Wound plug formation in <i>Caulerpa</i> spp.	3
1.1.2 Wound plug formation in <i>Dasycladus</i> spp.	4
1.1.3 Wound reaction in <i>Codium</i> spp.	6
1.2 Sulfated secondary metabolites of aquatic origin	7
1.3 Bacterial biofilm development	10
1.4 Biofouling in the marine environment	15
1.5 Aim of the thesis	19
2 Sulfated phenolic acids of <i>Dasycladus</i> spp.	21
2.1 Synthesis of sulfated phenolic acids, phenols and coumarines	22
2.1.1 Formation of the sulfate ester raw product	24
2.1.2 Purification - analytical scale (a.s.)	25
2.1.3 Purification - large scale (l.s.)	26
2.1.4 Summary of the synthesized products	28
2.2 Stability of sulfated phenolic acids	33
2.2.1 pH dependent stability of 3,4CAS	33
2.2.2 Stability of sulfated phenolic acids in sterile medium	35
2.2.3 Hydrolysis of sulfated phenolic acids by an arylsulfatase	36
2.2.4 Summary of sulfated phenolic acid stability	38

2.3	Identification of sulfated phenolic acids in <i>Dasycladus</i> spp.	39
2.3.1	Sulfated phenolic acids in <i>Dasycladus vermicularis</i>	39
2.3.2	Sulfated phenolic acids in <i>Cymopolia barbata</i>	42
2.3.3	Sulfated phenolic acids in <i>Neomeris annulata</i>	43
2.3.3.1	Hydrolysis of sulfated metabolites in <i>N. annulata</i>	46
2.3.4	Summary of sulfated metabolites from <i>Dasycladus</i> spp.	48
3	Filter disc assay	50
3.1	Impact of AS, BS, A and B on bacterial growth	51
3.2	Summary of the filter disc assay	53
4	Biofilm assay at the air-liquid-interface	55
4.1	Experimental design	56
4.2	Impact of AS, BS, ZS and their non-sulfated forms on biofilm formation of <i>Escherichia coli</i>	58
4.3	Impact of AS, BS, ZS and their non-sulfated forms on biofilm formation of <i>Vibrio natriegens</i>	67
4.4	Summary of biofilm assays at the air-liquid-interface	72
5	Biofilm assay on PTFE plates	74
5.1	Biofilm surface test for <i>E. coli</i> and <i>V. natriegens</i>	74
5.2	Experimental design and image evaluation	76
5.3	Impact of AS, A, BS, B, ZS and Z on <i>E. coli</i> biofilm formation	79
5.4	Impact of ZS and Z on biofilm formation of <i>V. natriegens</i>	84
5.5	Impact of AS, A, BS and B on biofilm formation of <i>V. natriegens</i>	94
5.6	Summary of biofilm formation on PTFE plates	96
6	Biofouling field assay with AS, BS and ZS at the coast of İzmir	98
6.1	Experimental design and evaluation	98
6.2	Impact of AS, BS and ZS on marine fouling	99

7	UPLC-MS screening for secondary metabolites in <i>Codium fragile</i>	104
7.1	Wound response of <i>Codium fragile</i>	105
7.2	UPLC-MS screening for sulfated metabolites	109
7.3	Summary	109
8	Conclusions	110
9	Materials and Methods	114
9.1	Instruments and materials	114
9.1.1	NMR	114
9.1.2	UPLC-ESI-MS (UPLC-MS)	114
9.1.3	HPLC-ESI-Triple-Quad-MS	115
9.1.4	GC-MS	116
9.1.5	Mithras plate reader	116
9.1.6	Microscopes	116
9.1.7	Solvents and chemicals	117
9.1.8	Buffer solutions	117
9.1.8.1	Phosphate buffered saline	117
9.1.8.2	TRIS-HCl buffer	117
9.2	Synthesis of sulfated phenolic acids	118
9.2.1	General method	118
9.2.1.1	Purification - analytical scale	119
9.2.1.2	Purification - large scale	119
9.2.2	4-(Sulfooxy)benzoic acid (BS)	120
9.2.3	3-(Sulfooxy)benzoic acid (mBS)	122
9.2.4	4-(Sulfooxy)phenylacetic acid (AS)	123
9.2.5	Zosteric acid (ZS)	124
9.2.6	3-(Sulfooxy)-4-hydroxycinnamic acid, 4-(sulfooxy)-3-hydroxycinnamic acid (3,4CAS)	125
9.2.7	2-(Sulfooxy)-3-hydroxycinnamic acid, 3-(sulfooxy)-2-hydroxycinnamic acid (2,3CAS)	126

9.2.8	2-(Sulfooxy)-4-hydroxycinnamic acid, 4-(sulfooxy)-2-hydroxycinnamic acid (2,4CAS)	128
9.2.8.1	Sulfatation with Pyr*SO ₃	128
9.2.8.2	Sulfatation with chlorosulfonic acid	129
9.2.9	5-(Sulfooxy)-2-hydroxycinnamic acid (2,5CAS)	129
9.2.10	1-(Sulfooxy)-2-methoxybenzene (2MOPS)	131
9.2.11	1-(Sulfooxy)-3-methoxybenzene (3MOPS)	131
9.2.12	1-(Sulfooxy)-4-methoxybenzene (4MOPS)	132
9.2.13	2-(Sulfooxy)benzoic acid (oBS)	132
9.3	Stability of sulfated phenolic acids	133
9.3.1	pH dependent stability of 3,4CAS	133
9.3.2	HCl hydrolysis of sulfated metabolites in <i>N. annulata</i>	134
9.3.3	Enzymatic hydrolysis by an arylsulfatase	135
9.3.4	Stability of sulfated phenolic acids in sterile medium	135
9.4	Cultivation and extraction of algae	136
9.4.1	<i>Codium fragile</i>	136
9.4.1.1	UPLC-MS measurements of <i>Codium</i> sp. extracts	137
9.4.2	<i>Dasycladus vermicularis</i>	137
9.4.2.1	UPLC-MS measurements of <i>D. vermicularis</i> extracts	137
9.4.3	<i>Neomeris annulata</i> and <i>Cymopolia barbata</i>	138
9.4.3.1	UPLC-MS measurements of <i>N. annulata</i> and <i>C. bar-</i> <i>bata</i> extracts	138
9.4.4	Extraction of zosteric acid from <i>Zostera marina</i>	138
9.4.4.1	UPLC-MS measurements of <i>Z. marina</i> extracts	138
9.5	Identification of sulfated metabolites by UPLC-MS	139
9.6	Cultivation and storage of bacteria	139
9.7	Bioassays	140
9.7.1	Filter disc assay	140
9.7.2	Biofilm formation at the air-liquid-interface	142

9.7.3	Biofilm formation below the air-liquid-interface	145
9.7.3.1	Surface test for biofilms of <i>E. coli</i> and <i>V. natriegens</i>	145
9.7.3.2	Biofilm growth test of <i>V. natriegens</i> on PTFE plates	146
9.7.3.3	Biofilm formation of <i>E.coli</i> and <i>V. natriegens</i> on PTFE plates with additives	146
9.7.3.4	Calibration of ZS and Z in ZS samples after presence of <i>V. natriegens</i> by UPLC-MS	150
9.7.4	Biofouling field assay at the coast of İzmir, Turkey	152
	Bibliography	154
	Appendix	175
	Selbständigkeitserklärung	186

List of Figures

1.1	Schematic draft showing different thallus morphologies of siphonous green algae.	2
1.2	Wound plug formation in <i>Caulerpa prolifera</i> and <i>Dasycladus vermicularis</i>	4
1.3	Sulfate esters of aquatic origin.	8
1.4	Schematic draft showing different steps of biofilm development	11
1.5	Scanning electron images of biofilm from the nontypeable <i>Haemophilus influenzae</i>	13
1.6	Development of a biofouling community	16
2.1	General sulfatation procedure of substituted phenols	23
2.2	UPLC-MS screening during the large scale purification process of 4-hydroxybenzoic acid sulfatation	27
2.3	UPLC-MS stability screening of AS, BS and ZS and their non-sulfated forms in sterile medium	36
2.4	UPLC-MS monitoring of the enzymatic cleavage of mBS by an aryl-sulfatase	37
2.5	UPLC-MS co-injection experiment of <i>D. vermicularis</i> extract with AS and BS	40
2.6	UPLC-MS co-injection of <i>C. barbata</i> extract with synthetic BS	43
2.7	UPLC-MS co-injection of <i>N. annulata</i> extract with 3,4CAS and 2,3CAS	45
2.8	Triple-Quad MS/MS of <i>N. annulata</i> extract	46
3.1	Filter disc assay with A, B, AS, BS and several antibiotics as growth inhibitors of marine bacteria	52
4.1	<i>E. coli</i> biofilm at the air-liquid-interface	59
4.2	<i>E. coli</i> growth during lag and exponential phase until the start of biofilm formation	60
4.3	UPLC-MS screening of additives in medium during biofilm formation of <i>E. coli</i>	61

4.4	Biofilms of <i>V. natriegens</i> at the air-liquid-interface	68
4.5	<i>V. natriegens</i> growth during lag and exponential phase until the start of biofilm formation	69
4.6	UPLC-MS screening of medium containing additives during biofilm formation of <i>V. natriegens</i>	70
5.1	Biofilm formation of <i>E. coli</i> and <i>V. natriegens</i> on different surfaces	75
5.2	Experimental setup for biofilm development on PTFE tubes	77
5.3	Image evaluation of <i>V. natriegens</i> biofilm	78
5.4	<i>E. coli</i> biofilm on PTFE plates without additives	80
5.5	<i>E. coli</i> biofilm on PTFE plates with additives	81
5.6	UPLC-MS screening of additives in <i>E. coli</i> biofilm assay on PTFE plates	83
5.7	Biofilm coverage of <i>V. natriegens</i> on PTFE plates in the presence of Z and ZS	86
5.8	UPLC-MS chromatograms of ZS in presence of <i>V. natriegens</i>	88
5.9	Quantification of ZS and "Z in ZS" at RT and at 30 °C	90
5.10	Cell number estimation during biofilm development of <i>V. natriegens</i> in presence of Z and ZS at RT	93
5.11	Biofilm development of <i>V. natriegens</i> on PTFE plates in presence of AS, BS, A and B	95
5.12	Color change in <i>V. natriegens</i> samples during exposure to B and BS	96
5.13	UPLC-MS stability screening of AS, BS, A and B in presence of <i>V.</i> <i>natriegens</i>	97
6.1	Panels with addition of biocides BS, AS and ZS, with primer coating and biocide free paint, before and after immersion in seawater for 70 days	100
7.1	Microscopic images of the fragmentation of a <i>Codium fragile</i> thallus by rupture	105

7.2	Base peak ion chromatogram (BPI) obtained by UPLC-MS screening of unwounded and wounded methanolic <i>C. fragile</i> extracts	107
9.1	^1H and ^{13}C NMR of synthetic AS	175
9.2	^1H and ^{13}C NMR of synthetic BS	176
9.3	^1H and ^{13}C NMR of synthetic ZS	177
9.4	^1H of the isomeric mixture 3,4CAS	178
9.5	UPLC chromatograms and MS spectra of synthetic AS and BS	179
9.6	UPLC chromatogram and MS spectrum of synthetic ZS	180
9.7	UPLC-MS monitoring of the enzymatic cleavage of 3,4CAS by an arylsulfatase	181
9.8	UPLC-MS monitoring of the enzymatic cleavage of BS by an arylsulfatase	182
9.9	Field assay plates after two weeks with 2 and 10% biocide	183
9.10	Mass spectra of methanolic <i>Codium fragile</i> extracts 60 minutes after wounding.	184
9.11	Mass spectra of methanolic <i>Codium fragile</i> extracts 60 minutes after wounding.	185

List of Tables

2.1	Summary of synthesized sulfate esters 1	29
2.2	Summary of synthesized sulfate esters 2	30
2.3	Hydrolysis of 3,4CAS by HCl, H ₂ SO ₄ , HCOOH and KOH	34
9.1	UPLC method standard	115
9.2	UPLC method biofilm	115
9.3	UPLC method sulfmet	115
9.4	UPLC method co-injection	115
9.5	UPLC method co-injection 2	115
9.6	HPLC method sulfmetTQ	115
9.7	Bacteria and culture media used for filter disc assay	141
9.8	Additives and solvents used in filter disc assay	141
9.9	Filling scheme of a 96-well plate for biofilm at the air-liquid-interface	143
9.10	External calibration standards for Z	151
9.11	External calibration standards for ZS	151
9.12	Paint compositions for the biofouling field assay in İzmir, Turkey . . .	153

Zusammenfassung

Das Seegrass *Zostera marina* enthält eine sulfatierte phenolische Säure (Zosterische Säure, ZS), die seit vielen Jahren als biofilmhemmender Naturstoff diskutiert wird. Im Vorfeld dieser Arbeit wurden in einigen Dasycladaceae ebenfalls sulfatierte Metabolite detektiert, wobei angenommen wurde, dass diese strukturelle Ähnlichkeit zu ZS aufweisen.

Um die bislang unbekanntenen Strukturen dieser sulfatierten Metabolite zu ermitteln, wurden reine Standards synthetisiert und die vermuteten Substanzen 4-(Sulfooxy)benzoesäure (BS) und 4-(Sulfooxy)phenyllessigsäure (AS) mittels UPLC-MS (Ultra high performance liquid chromatography-mass spectrometry) Co-Injektionsexperimenten bestätigt. Aufgrund der strukturellen Ähnlichkeit zu ZS ergab sich die Frage, ob BS und AS eine mit ZS vergleichbare Wirkung zeigen würden und welche der strukturellen Einheiten für die Biofilmhemmung verantwortlich sind.

Die letztlich etablierte Kombination aus verschiedenen Bioassays, der Verwendung unterschiedlicher Testorganismen (*Escherichia coli*, *Vibrio natrie gens*), UPLC-MS Stabilitätskontrolle der Testsubstanzen und der Beobachtung eines möglichen Einflusses auf das bakterielle Wachstum, gewährte einen umfassenden Einblick in die Aktivität sulfatierter phenolischer Säuren im Vergleich zu ihren nicht-sulfatierten Formen. Es zeigte sich, dass der Einfluss beider Substanzklassen sowohl von der bakteriellen Art, als auch den experimentellen Bedingungen abhing. Dennoch konnten einige wichtige, allgemeingültige Schlüsse gezogen werden. So konnte weder in einem der angewandten Assays die bewuchshemmende Eigenschaft von ZS bestätigt, noch ein solcher Effekt bei den sulfatierten Metaboliten einiger Dasycladaceae (AS, BS) beobachtet werden. Stattdessen erwies sich die nicht-sulfatierte Form von ZS, 4-Hydroxyzimtsäure (Z), als hoch effektiv zur Eindämmung der Biofilmbildung aller Testorganismen.

UPLC-MS Messungen zeigten zudem, dass *V. natrie gens*, mittels enzymatischer Aktivität einer Sulfatase, ZS hydrolysierte und somit die aktive, nicht-sulfatierte Form Z in das bakterielle Medium freigesetzt wurde. Diese Verbindung konnte daraufhin die Biofilm-Neubildung hemmen, nicht jedoch einen bereits bestehenden Biofilm

reduzieren.

Der Einfluss von Z auf das bakterielle Wachstum war sowohl von deren Konzentration als auch vom Testorganismus abhängig. So wurde lediglich das Wachstum von *V. natriegens* in hohen Konzentrationen von Z negativ beeinflusst, das von *E. coli* nicht. Geringe Z-Konzentrationen hatten allerdings auch auf das Wachstum von *V. natriegens* keinen Einfluss, waren jedoch zur Biofilmhemmung ausreichend. Die Bildung eines Biofilms ist unter anderem von der Zellzahl abhängig. Da Z jedoch die Biofilmbildung auch ohne einen negativen Einfluss auf die Zellzahl inhibieren konnte, scheint ein toxischer, zellzahl-reduzierender Effekt nicht die alleinige Ursache für die Biofilmhemmung zu sein.

Die nicht sulfatierten Formen A und B der in einigen Dasycaldaceen identifizierten Metabolite (AS, BS) zeigten entweder nur eine kurzzeitig biofilmhemmende Wirkung (B) oder gar keine (A).

Ein kleineres Projekt im Rahmen dieser Arbeit beschäftigte sich mit der siphonalen Grünalge *Codium fragile*. Mittels UPLC-MS Messungen sollte das Vorhandensein sulfatierter Metabolite überprüft, sowie Erkenntnisse zur Verwundungsreaktion von *C. fragile* erlangt werden. UPLC-MS Messungen unverwundeter und verwundeter *C. fragile* Zellextrakte deuteten fundamental unterschiedliche Prozesse im Vergleich zu den bereits aufgeklärten Verwundungsreaktionen einiger Arten der Caulerpaceae und Dasycladaceae an. Auch konnten sulfatierte Metabolite mit dieser Methode nicht detektiert werden.

Anhand der Ergebnisse dieser Arbeit konnte die bisher angenommene Aktivität sulfatierter Phenolsäuren, insbesondere die von ZS, revidiert werden. Die Möglichkeit der enzymatischen Hydrolyse von ZS durch Sulfatasen, was die Freisetzung der aktiven, nicht-sulfatierten Substanz Z zur Folge hat, wurde in bisherigen Untersuchungen zur Aktivität von ZS nicht in Betracht gezogen. Der Sulfatester scheint daher eine inaktive Speicherform der wirksamen Substanz Z zu sein.

Abstract

The sea grass *Zostera marina* contains a sulfated phenolic acid (zosteric acid, ZS) that has been discussed during the recent years as a potent, natural biofilm inhibiting agent. Previously to this work have further sulfated metabolites been detected in members of the Dasycladaceae and it was assumed that these are structurally related to ZS.

In order to identify these hence unknown metabolites, pure standards were synthesized and the assumed compounds 4-(sulfooxy)benzoic acid (BS) and 4-(sulfooxy)-phenylacetic acid (AS) confirmed by UPLC-MS (Ultra high performance liquid chromatography-mass spectrometry) co-injection experiments. Based on the structural relation of AS and BS to ZS the question arose, if the novel sulfated compounds would exhibit similar properties as ZS and which structural elements define their activity.

The final combination of different bioassays and test organisms (*Escherichia coli*, *Vibrio natriegens*), UPLC-MS stability screening of the test compounds and monitoring of a possible impact on bacterial growth, provided a comprehensive overview of the activity of sulfated phenolic acids in comparison to their non-sulfated forms. Although impacts of these two molecular classes were found to be dependent on the bacterial species and experimental setups, some common conclusions could be drawn. In neither of the employed assays could the previously suggested antifouling activity of ZS be confirmed, nor any effect observed from the structurally related sulfated phenolic acids of some Dasycladaceae. Instead, the non-sulfated form of ZS, 4-hydroxy-cinnamic acid (Z), proved highly efficient to inhibit bacterial settlement. UPLC-MS measurements revealed sulfatase activity in *V. natriegens*, leading to a release of the active, non-sulfated form Z into the bacterial medium. This compound could then inhibit biofilm formation, but not reduce an already developing biofilm. The influence of Z on bacterial growth was both dependent on the Z concentrations as well as the test organisms. Thus, only growth of *V. natriegens* was negatively affected by high Z concentrations, growth of *E. coli*, in contrast, not. Low concentrations of Z, however, had no influence on cell numbers of *V. natriegens*, although

they were sufficient to reduce biofilm formation effectively. Biofilm formation is among others dependent on the cell number. Since Z, however, could still reduce biofilm formation without negatively influencing bacterial growth, seems a toxic, cell number reducing effect not to be the sole reason for biofilm inhibition.

The non-sulfated forms (A, B) of metabolites isolated from members of the Dasycladaceae (AS, BS) showed either only a short term effect on biofilm inhibition (B), or none (A).

A smaller project of this work was concerned with the siphonous green alga *Codium fragile*. UPLC-MS measurements were applied to screen cell extracts for the presence of sulfated metabolites and to provide insights concerning the wound response of *C. fragile* on a molecular level. UPLC-MS measurements of unwounded and wounded *C. fragile* cell extracts indicated fundamentally different processes to those recently unveiled in some members of the Caulerpaceae and Dasycladaceae. Also were sulfated metabolites with this method not detected.

Based on the results obtained during this study, could the common consent concerning the activity of sulfated phenolic acids, especially that of ZS, be revised. The possibility of enzymatic hydrolysis of ZS by a sulfatase and the subsequent release of the non-sulfated form Z into the bacterial medium was not included in earlier studies. The sulfate ester seems thus to constitute a storage form of the active compound Z.

Abbreviations

A	4-hydroxyphenylacetic acid
AF	antifouling
AS	4-(sulfooxy)phenylacetic acid
AHL	N-acyl-homoserine lactones
B	4-hydroxybenzoic acid
mBS	3-(sulfooxy)benzoic acid
oBS	2-(sulfooxy)benzoic acid
BPI	base peak intensity
BS	4-(sulfooxy)benzoic acid
CA	<i>trans</i> -cinnamic acid
2,3CA	2,3-dihydroxycinnamic acid
2,4CA	2,4-dihydroxycinnamic acid
2,5CA	2,5-dihydroxycinnamic acid
3,4CA	3,4-dihydroxycinnamic acid
2,3CAS	2-(sulfooxy)-3-hydroxycinnamic acid, 3-(sulfooxy)-2-hydroxycinnamic acid
2,4CAS	2-(sulfooxy)-4-hydroxycinnamic acid, 4-(sulfooxy)-2-hydroxycinnamic acid
2,5CAS	5-(sulfooxy)-2-hydroxycinnamic acid
3,4CAS	3-(sulfooxy)-4-hydroxycinnamic acid, 4-(sulfooxy)-3-hydroxycinnamic acid
C.L.	<i>Cellulophaga lytica</i>
CV	crystal violet (tris(4-(dimethylamino)phenyl)methyl)chloride)
DHyCS	6,7-dihydroxycoumarin-3-sulfate
DINO	<i>Dinoroseobacter shibae</i>
DMF	N,N-dimethylformamide
DMSO	dimethylsulfoxide
DTT	dithiothreitol
EA	elementary analysis

EPS	extracellular polymeric substance
ESI	electro spray ionization
EWG	external wound plug
GC	gaschromatography
HILIC	hydrophilic interaction liquid chromatography
HPLC	high pressure liquid chromatography
M+	inoculated medium
M-	sterile medium
MB	marine broth
2MOPS	1-(sulfooxy)-2-methoxybenzene
3MOPS	1-(sulfooxy)-3-methoxybenzene
4MOPS	1-(sulfooxy)-4-methoxybenzene
MS	mass spectrometry
MSTFA	N-methyl-N-(trimethylsilyl) trifluoroacetamide
MTBE	2-methoxy-2-methylpropan
NMR	nuclear magnetic resonance
OD	optical density
PBS	phosphate buffered saline
PDA	photo diode array
PTFE	polytetrafluoroethylene
QTof	quadrupole time-of-flight
rel. int.	relative intensity
R.T.	retention time
RT	room temperature
SDS	sodium dodecyl sulfate
SDS-PAGE	SDS polyacrylamide gel electrophoresis
T	tailingfactor at 10% peak height
T3SS	type III secretion system
TBT	tributyltin
THyC	3,6,7-trihydroxycoumarine

TIC	total ion current
TRIS	tris(hydroxymethyl)aminomethan
QqQ	triple quadrupole
UPLC	ultra high performance liquid chromatography
UV-Vis	ultraviolett visible
ZOI	zone of inhibition
Z	4-hydroxycinnamic acid
ZS	zosteric acid (4-(sulfooxy)cinnamic acid)

1 Introduction

1.1 Wound reaction of siphonous green algae

Among green macroalgae (Chlorophyta), siphonous species represent a unique group. They are composed of one giant single cell, often with several nuclei (coenocytic) distributed across the thallus (plant body), whose form often resembles a siphon lacking cross cell walls. This allows cell contents to move around freely.[1] Menzel [1] defined three distinct types of siphons that can be distinguished as schematically shown in Figure 1.1. The first consists of one cylindrical siphon, which is lined inside with cytoplasm and contains a central vacuole, occupying most of the cell's volume. The diameters of these siphons are in the mm range, the length of these siphons can reach several meters (Figure 1.1 A). Typical members of this type are found in the genus *Bryopsis*. A second type is represented by the Caulerpaceae, where principle setup and size resemble type one, but the siphon is modified by the formation of interior cellwall extensions (trabeculae) which function as an internal skeleton (Figure 1.1 B). Members of the Codiaceae constitute a third type (Figure 1.1 C). Here, the diameter of single siphons lays below the mm range. Single colorless siphons are called medullary filaments ending in pigmented utricles. Single siphons are highly branched or tightly interwoven and can be constricted or even plugged.[1] Most siphonous species posses rhizoids (root like structures) for adhesion, and thalli are often composed of stolons (slender horizontal branches) with photosynthetically active filaments attached (assimilators).[2]

Cell wounding of siphonous green algae, caused by herbivore grazing, fragmentation during storms or by ships' propellers, sand abrasions, parasites or epiphytes requires cell repair mechanisms to prevent loosing cell contents and perish.[3] In

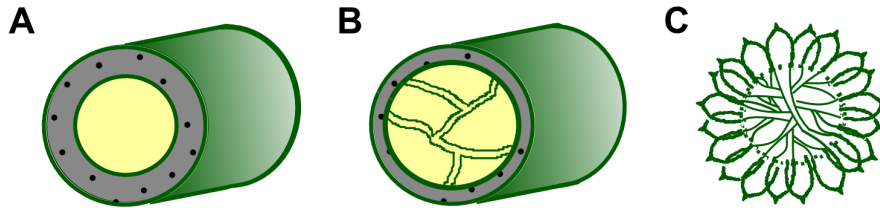


Figure 1.1: Schematic draft showing different thallus morphologies of siphonous green algae, adapted from [1]. **A:** Simplest type consisting of a cylindrical siphon, lined inside with cytoplasm and a central vacuole. A typical representative of this type is the genera *Bryopsis*. **B:** Similar structure as in **A**, but slightly modified by the formation of interior cellwall extensions (trabeculae), as found in the Caulerpaceae. **C:** Members of the Codiaceae constitute a third type. Single colorless siphons (medullary filaments) end in pigmented utricles. Single siphons are branched, interwoven and can be constricted or plugged.

plants wound-healing generally involves necrosis of damaged cells, upon which regenerative tissue can be formed adjacent to the wound.[4] These mechanisms are unavailable for a single celled organism. Thus, siphonous green algae have developed mechanisms to endure wounding, as for example cytoplasmic retraction away from the wound site concurrent with a turgor pressure loss and subsequent sealing of the wound.[5, 6] Wounds in some siphonous green algae can also be sealed by rapid formation a gelatinous external wound-plug.[7, 8] The external wound plug prevents loss of cell contents and lethal contact between the remaining cytoplasm and the surrounding seawater. Beneath the external polymer an insoluble plug is formed functioning as an internal wound barrier. Today's state of knowledge is that in many siphonous green algae wounding is responded by lectin-carbohydrate-interactions and subsequent protein crosslinking. Lectins are a broad category of proteins that can bind selected carbohydrates in a specific, reversible manner.[6] Chemical processes leading to wound plug formation by protein crosslinking were recently investigated in species belonging to the families of Caulerpaceae and Dasycladaceae. In both species an inactivated main secondary metabolite is rapidly transformed upon wounding into a highly reactive molecule, able to crosslink proteins. The activated crosslinking agents have at least two functional sites, so that crosslinking processes can be repeated many times. Thereby, a large and complex matrix can be created.[9–12]

1.1.1 Wound plug formation in *Caulerpa* spp.

Caulerpa taxifolia is a highly abundant and widely distributed species in tropical oceans.[10] It has been accidentally introduced into the Mediterranean Sea in 1984 and spread rapidly, causing a major threat for the ecosystems.[13–16] As early as 1978 a main secondary metabolite, the acetylenic sesquiterpene caulerpenyne 1 (Figure 1.2 B) was isolated and identified.[17] It occurs both in invasive and non-invasive *Caulerpa* species.[10] This secondary metabolite was found to play a crucial role in the alga's chemical defense against herbivores and could inhibit first cleavage of seaurchin eggs without affecting fertilization.[18–27]

Other siphonous green algae belonging to the *Bryopsidales* have similar secondary metabolites. The genus *Halimeda* contains halimedatetraacetate [28], which upon injury is rapidly transformed to the highly reactive halimedatrial, containing three aldehyde groups. Halimedatrial also proved to be a potent feeding deterrent.[29] Caulerpenyne exhibits a close structural relationship to the metabolite halimedatetraacetate, with respect to the masked aldehyde groups. Besides its function as a chemical defense metabolite, caulerpenyne has also been identified to play a crucial role during wound-plug formation of several *Caulerpa* species both invasive and non-invasive.[9, 10] In extracts of unwounded *C. taxifolia* cells caulerpenyne could be readily detected via normal phase HPLC-UV analysis. In extract of wounded algae the content of caulerpenyne was reduced by 80% after 30 seconds and after 10 minutes none was detectable.[9] The labile transformation product of caulerpenyne was identified as the reactive 1,4-dialdehyde, oxytoxin 2.[9, 30] Reactivity of oxytoxin 2 was assigned to the dialdehyde function adjacent to a Michael acceptor system, as is schematically shown in Figure 1.2 B.[9, 30] Since dialdehydes are potential protein cross-linkers, the transformation of caulerpenyne was suggested to be related to wound plug formation. The rapid cleavage of the three acetate groups was found to be catalyzed enzymatically by an esterase (Figure 1.2 B).[10] Figure 1.2 A shows a wound plug formed only minutes after cutting of a *C. prolifera* thallus. Sodium dodecyl sulfate polyacrylamide gel electrophoresis (SDS-PAGE) investigations showed that upon wounding, the *in situ* transformed oxytoxin 2 is involved in

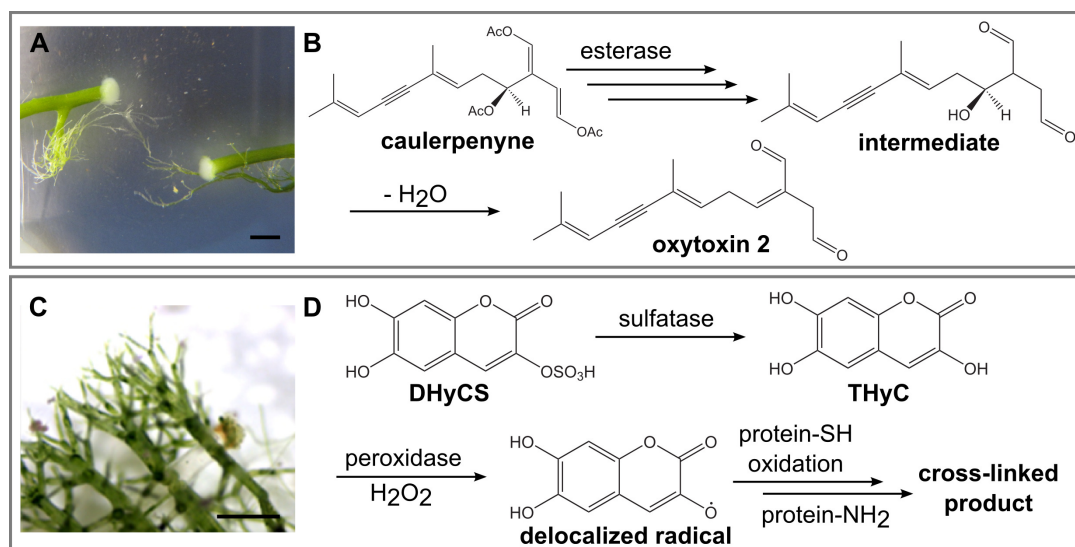


Figure 1.2: Wound plug formation in *Caulerpa prolifera* and *Dasycladus vermicularis*. **A:** Microscopic image of the wound plug in *C. prolifera*. **B:** Upon wounding, acetyl groups of caulerpenyne are subsequently cleaved by esterase activity. Loss of water from the intermediate provides the highly reactive protein cross-linker oxytoxin 2.[10] **C:** Microscopic image of the wound plug in *D. vermicularis*, adapted from [6]. **D:** Upon wounding the sulfate ester of 6,7-dihydroxycoumarin-3-sulfate (DHyCS) is hydrolyzed by a sulfatase. 3,6,7-trihydroxycoumarin (THyC) is then oxidized by H_2O_2 and peroxidase activity, upon which a delocalized radical forms that readily reacts with adjacent proteins, forming a highly cross-linked biopolymer.[12]

the wound plug formation by cross-linking nucleophilic groups of proteins, present in the wounded tissue material.[10, 11] Excessive boiling of material extracted from wounded cells with SDS and dithiothreitol (DTT) did not dissolve the proteinous material, which indicated a covalently linked polymer. Dialdehyde and algal proteins were found to be the essential factors required for wound plug formation.[11] The bifunctionality and high reactivity of oxytoxin 2 allows intra- as well as inter-protein linkages, thus enabling the rapid formation of the wound plug biopolymer.

1.1.2 Wound plug formation in *Dasycladus* spp.

As in diverse *Caulerpa* species wound plug formation can also be observed in members of the Dasycladaceae. *Dasycladus vermicularis* is a cosmopolitan, siphonous green algae, distributed in shallow waters from tropical to temperate shores and has been found off the coasts of Spain, Japan and Florida. Ross *et al.* proposed

the wound plug formation in *D. vermicularis* to proceed through two steps. Step one represents the rapid under water gelling within the first few minutes, which is assumed to require a lectin-carbohydrate system. Within an hour, browning of the plug (Figure 1.2 C) and increased hardening could be observed (step two). Ross *et al.* reported an oxidative burst and the release of nitric oxide species and H_2O_2 within the boundaries of the wound plug with a short delay after the injury.[31]

A major secondary metabolite present in *D. vermicularis* was reported to be the 3,6,7-trihydroxycoumarin (THyC). THyC was first isolated after acid hydrolysis from *D. vermicularis* extracts.[32] Coumarins can readily be oxidized to form reactive quinones [33], thus THyC was assumed to represent a potential precursor for a protein cross-linker. In chemical profiling experiments in intact and wounded algae, using ultra performance liquid chromatography, coupled to mass spectrometry (UPLC-MS), surprisingly no THyC, but a dominant metabolite with a similar UV spectrum and a m/z mass difference of plus 80 was detected. The authors assumed that the metabolite might be masked as a sulfate ester, which was identified as 6,7-dihydroxycoumarin-3-sulfate (DHyCS). By using UPLC-MS techniques it could be observed that the amount of DHyCS in methanolic extracts, collected at different time intervals after wounding, decreases until two minutes post wounding. The non-sulfated form, THyC, could only be detected in trace amounts. The rapid transformation of DHyCS was assumed to be enzymatic and could be assigned to the presence of a sulfatase by both *in vitro* and *in vivo* assays.[12] Additionally, peroxidases were isolated from *D. vermicularis*, which might catalyze the oxidation of THyC in presence of H_2O_2 , provided during the oxidative burst (Figure 1.2 D).[34] This would explain why after enzymatic hydrolyzation of DHyCS only traces of THyC were found. In model reactions with synthetic THyC, horse radish peroxidase and H_2O_2 , the coumarin was completely transformed in presence of all components, indicating the oxidation to a quinone via a delocalized radical (Figure 1.2 D). The catechol functionality of THyC (position 6, 7) can be oxidized to the *ortho*-quinone, which can tautomerize to the more reactive *para*-quinone methide. Quinones are known to react with S- and N-nucleophiles via a Michael reaction

and in case of N-nucleophiles additionally by reaction of the R-NH₂ terminus with the carbonyl moiety of the quinone, forming an imine (Schiff base).[12] Oxidized THyC was indeed found to react with thiols and amines both in *in vitro* and *in vivo* experiments. Since multiple thiol adducts were detected, THyC can obviously be oxidized to a quinone several times, thus providing multiple reaction sites. These could contribute to the rapid formation of a stable biopolymer with proteins present close to the wound site.[12]

Thus, the two algal species *C. taxifolia* and *D. vermicularis* despite belonging to different classes, show in principle very similar mechanisms during wound-plug formation. In both species a secondary metabolite is present in an inactivated form, rapidly transformed by enzyme activity, providing highly potent protein-cross-linking agents. Adjacent proteins at the wound site are readily cross-linked leading to a stable wound plug ensuring the alga's survival.

1.1.3 Wound reaction in *Codium* spp.

Siphonous species of the Codiaceae also have raised interest in the last decades, since *Codium fragile* ssp. *tomentosoides* is one of the major invasive species around the world. Subspecies of *Codium fragile*, originally from Japan, are found in temperate waters around the globe, covering now shores of North and South America, Australia, and Europe.[35–48] Much research has been performed on their dispersal potential and their abilities to adapt to new environments. Upon wounding new fragments can be produced from regeneration of isolated utricles and medullary filaments.[49–53] For *C. fragile* two different types of thalli have been described, called spongy and filamentous, which are nowadays considered as two independent life stages. Spongy thalli have pigmented utricles and the medullary filaments are interwoven. Filamentous thalli consist of branched medullary filaments.[50, 54] It has been found that spongy thalli grow preferably in fast flowing water with high irradiance, whereas filamentous thalli form in calm waters, where their growth can be inhibited when irradiation is too high.[53] Fusiform chloroplasts of isolated utri-

cles can be transferred to basal parts and medullary filaments immediately after isolation, leading to the formation of a filamentous thallus. Utricles then lose the ability to form filamentous thalli, but begin to attach to a substratum by rapidly elongating thalli.[52] It has also been observed that after cell disruption an aggregation of protoplasts takes place. During the first few minutes clumps are formed which are later drawn together by gelatinous threads, then formation of a lipid based membrane takes place. In case of *C. fragile* however no formation of cell walls could be observed, so the protoplast cannot be transformed into new, viable cells, as it has been observed for *Bryopsis* species.[55]

Although it is known that *Codium* species can reproduce by fragmentation and even form new cells from isolated utricles and medullary filaments, the underlying chemical processes involved in wound sealing assumed to be taking place right after wounding are not yet investigated in detail.[49–55]

1.2 Sulfated secondary metabolites of aquatic origin

During his investigation of the wound responses in *Dasycladus* species, Dr. Matthew Welling also found indications for the presence of further presumably sulfated metabolites besides DHyCS. These were not involved in metabolic changes during wounding.[56] Sulfate esters can be found in several aquatic organisms, covering a broad range of molecular features as well as functions attributed to them. A selection is shown in Figure 1.3.

The sulfate ester of the recently discovered DHyCS plays a crucial role in controlling reactivity of the trihydroxycoumarine, as just discussed in section 1.1.2.

In the marine sponge *Aplysinella rhaax* (Figure 1.3 D) the presumably enzymatic conversion of the secondary metabolite psammaphin A sulfate to psammaphin A could be observed within seconds after wounding by fish bites. During a choice feeding assay with a generalist herbivore, the sulfated form was deterred less. Thus, the release of the non-sulfated form was considered as an activated defense mechanism of the sponge. Sulfatation of the active compound hence was interpreted as a measure

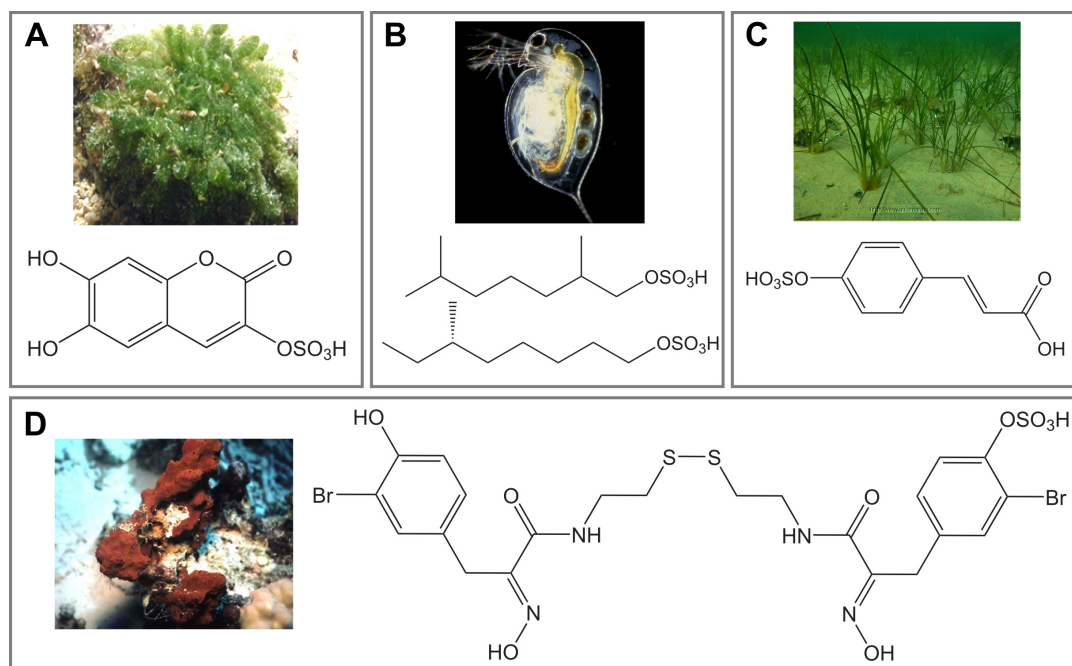


Figure 1.3: Sulfate esters of aquatic origin. **A:** DHyCS, found in the siphonous green alga *D. vermicularis*. Image source: www.algaebase.com. **B:** Sulfated aliphatics from the water flea *Daphnia*. Image source [58]. **C:** Zosteric acid, isolated from the seagrass *Zostera marina*. Image source: www.guiamarina.com by Dirk Schories. **D:** Psammaplin A sulfate from the sponge *Aplysinella rhax*. Image source: www.palaeontologie.geo.uni-muenchen.de.

of detoxification.[57]

The freshwater fleas belonging to the genus *Daphnia* excrete aliphatic sulfate esters (Figure 1.3 B), which cause the unicellular green algae *Scenedesmus subspicatus* to form colonies. The aliphatic sulfate esters can thus be considered as messenger molecules, so called kairomones, inducing a defense reaction. For unicellular algae, formation of colonies constitutes an important protection against grazers.[59]

Siphonous green algae belonging to *Codium* spp. are not only known for their huge dispersal potential (section 1.1.3), but also for their high content of sulfated polysaccharides.[60–64] These compounds can also be found in several other marine algae and are structurally complex.[65] They have an attributed immunostimulating effect [64] and exhibit strong antiviral activity during virus binding, host cell penetration and in early stage of viral reproduction [66–69]. They also show a strong anticoagulant activity, which increases with increasing amount of sulfatation.[70, 71] Sulfated polysaccharides are charged in seawater and, therefore

play a role as ionic and osmotic regulators. Hydration follows gel formation which might constitute a resistance against mechanical stress.[63]

Another compound that has been subject to recent research is the sulfate ester of 4-hydroxycinnamic acid (Z), also known as zosteric acid (ZS, Figure 1.3 C). ZS has been isolated from the seagrass *Zostera marina* (eelgrass) and its structure has been identified by Todd *et al.* in 1993.[72] Both *Z. marina* extracts and a synthetic analogue of ZS could inhibit attachment of an *Acinetobacter* species, isolated from eelgrass leaves.[72] In the years to follow, an impact on adhesion of other species was detected. Thus, ZS was found to inhibit fungal spore adhesion of a crop pathogen [73], biofilm formation by marine and fresh water bacteria [74–77], an *E. coli* K-12 strain [78] and the fungi *Candida albicans* [79]. *In vitro*, ZS could also slightly inhibit early steps of virus-cell interactions of the Dengue virus, although other, more complex compounds carrying amino groups were tested as well and proved more effective.[80] Despite its seemingly strong biofilm inhibiting potential, ZS was found to have a rather low toxicity.[81]

To each of these sulfate esters of aquatic origin a unique biological function could be attributed, but only in the case of DHyCS from *D. vermicularis* and psammaplin A sulfate from the sponge *A. rhax* the specific role of the sulfate ester was determined. [12, 57] In both cases sulfatation seems to have a "masking" purpose and only upon enzymatic cleavage, presumably by a sulfatase, the "activated" form developed its specific function. Although the anticoagulant activity of sulfated polysaccharides from *Codium* species seems to be dependent on the level of sulfatation [70, 71], specific pharmacological reasons for this observation are yet not known.

The same is true for the biofilm inhibiting properties of ZS. It is assumed that these are related to the sulfate ester, as based on one study by Todd *et al.* where the non-sulfated form was found to be inactive.[72] So far no systematic study has been performed concerning the query in how far other molecular moieties, such as the carboxylic acid or the double bond, affect the biofilm inhibiting properties and if minor changes of these would influence this function. For the presumably sulfated metabolites found by Dr. Matthew Welling in some *Dasycladus* species,

data obtained by UV-Vis absorption and mass spectrometry hinted a phenolic acid backbone.[56] Thus, these compounds in comparison to ZS seemed a reasonable basis for the present study to unveil the functional relationship between sulfate ester and phenolic acid backbone.

1.3 Bacterial biofilm development

Numerous studies are available on biofilm forming organisms. This section summarizes relevant insights for this work that have been accepted to be general phenomena in bacterial biofilm formation and is based on recent reviews.[82–85]

Biofilms are highly structured, matrix enclosed communities of microorganisms, irreversibly attached to a biotic or abiotic surface, producing extracellular polymeric substances (EPS).[82–85] Regarding their phenotype, cells within the biofilm community are profoundly different from their planktonic counterparts.[82] In the biofilm they can function in a co-ordinated manner, mimicking the behavior of multicellular organisms.[83] Bacteria are the most intensively studied organisms regarding biofilm formation, but also fungi, yeast, algae, protozoa and viruses are known to form biofilms.[83] As soon as sufficient nutrients are available, biofilms can be found in any aquatic environment. Almost all surfaces independent of their physical or chemical properties can be colonized, however, preferences often vary between different biofilm forming organisms.[85]

The presence of biofilms in various environments has been recognized for more than 100 years, but only during the last three decades the immense differences between planktonic and biofilm communities were revealed. Advanced microscopic techniques, such as confocal laser scanning microscopy, and genetic tools contributed to that.[85] In nature, biofilms are mostly formed by a complex community of several different species. An exception constitute some pathogenic bacterial biofilms developing on tissues, which are often just composed of one single species.[83, 84] Laboratory research so far mainly focused on single species biofilms. The follow-

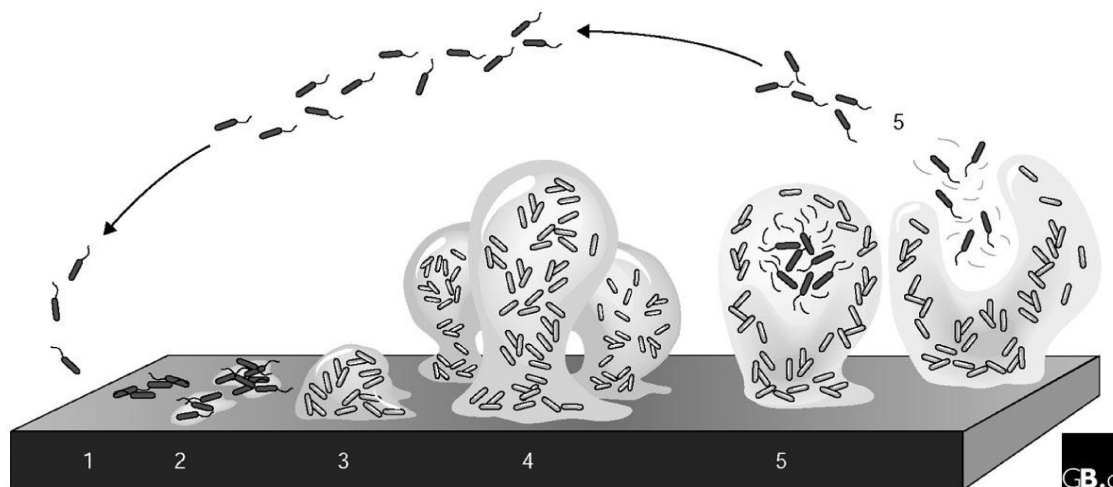


Figure 1.4: Schematic draft showing different steps of biofilm development. **1:** Surface conditioning by nutrients. **2:** Reversible attachment of planktonic bacteria. **3:** Irreversible attachment, start of EPS production. Cells are phenotypically different from their planktonic counterparts. **4:** Biofilm maturation. Channels and pores form. **5:** Microcolonies are detached from the biofilm for further colonization. Detached cells return to the planktonic state. Source: [84]

ing section summarizes aspects on bacterial biofilm development obtained during the last decade that are assumed to be universal phenomena. As in any biological system, there are exceptions for certain species. Biofilms are formed by both gram negative and gram positive bacteria, and both motile and non-motile species.[82–86] The development of a biofilm can be divided into several steps as is schematically shown in Figure 1.4. The first step in biofilm formation is described as surface conditioning (Figure 1.4 1). Surfaces absorb organic and inorganic nutrients, whose content influences initial attachment. The mode of a first contact between bacteria on surfaces is species dependent, regulated either by sedimentation, Brownian motion, convection currents, electrostatic and physical interactions between bacteria and the substratum, and for motile bacteria of course by active flagella governed movement.[83] Besides nutrient availability, biofilm initiation can also be triggered by temperature, osmolarity, pH, iron and oxygen supply. What conditions prove favorable for an organism can be highly species dependent. Some bacteria need certain nutrients or even prefer an oligotrophic (nutrient limited) environment, others grow under almost any condition.[85] Once a surface is approached, an equilibrium arises between suspended and adherent cells (Figure 1.4 2).[83] This phase is called

"reversible attachment". Here cells can still individually move, glide or creep and adhered cells are not phenotypically distinct from planktonic ones.[84]

A crucial factor for coordinating different phases of biofilm formation is the chemical communication between cells of a community by using signal molecules, a phenomenon called quorum sensing. This communication involves production, release, detection and the response to small, hormone like molecules called autoinducers.[87] Quorum sensing allows a bacterial community to monitor their environment and respond to changes in conditions, population size and species, thus acting like a multicellular organism.[87] Autoinducers also playing a crucial role in bacterial biofilm formation are acyl-homoserine lactones (AHL's), whose specificity is defined by different acyl-side chains.[85, 87] The concentration of autoinducers increases with expanding cell number and when a certain threshold is exceeded alterations in gene expression take place.[87]

The transition from reversible to "irreversible attachment" as well as biofilm maturation have been found to be quorum sensing dependent.[85] As soon as cells are attached, production of EPS starts to tighten the cell-surface-contact and build bridges between cells (Figure 1.4 3). It is assumed that membrane-bound sensory proteins stimulate EPS production. EPS is composed of polysaccharides, proteins and nucleic acids.[84] Once cells are irreversibly attached, maturation of the biofilm starts (Figure 1.4 4 and 5). The most obvious feature of biofilm maturation is the formation of a complex EPS matrix. Here bacteria are clustered in microcolonies which often appear mushroom shaped, connected by a complex system of channels (Figure 1.5). These allow the exchange of water, nutrients, oxygen and waste products.[82, 85] The EPS matrix, however, does not only serve as a nutrient distribution system, but also can function as a diffusion barrier for harmful substances and last but not least provides a stable niche, able to withstand even strong currents and shear forces. The EPS production rate is assumed to be nutrient dependent and can thus influence biofilm architecture.[84] During maturation

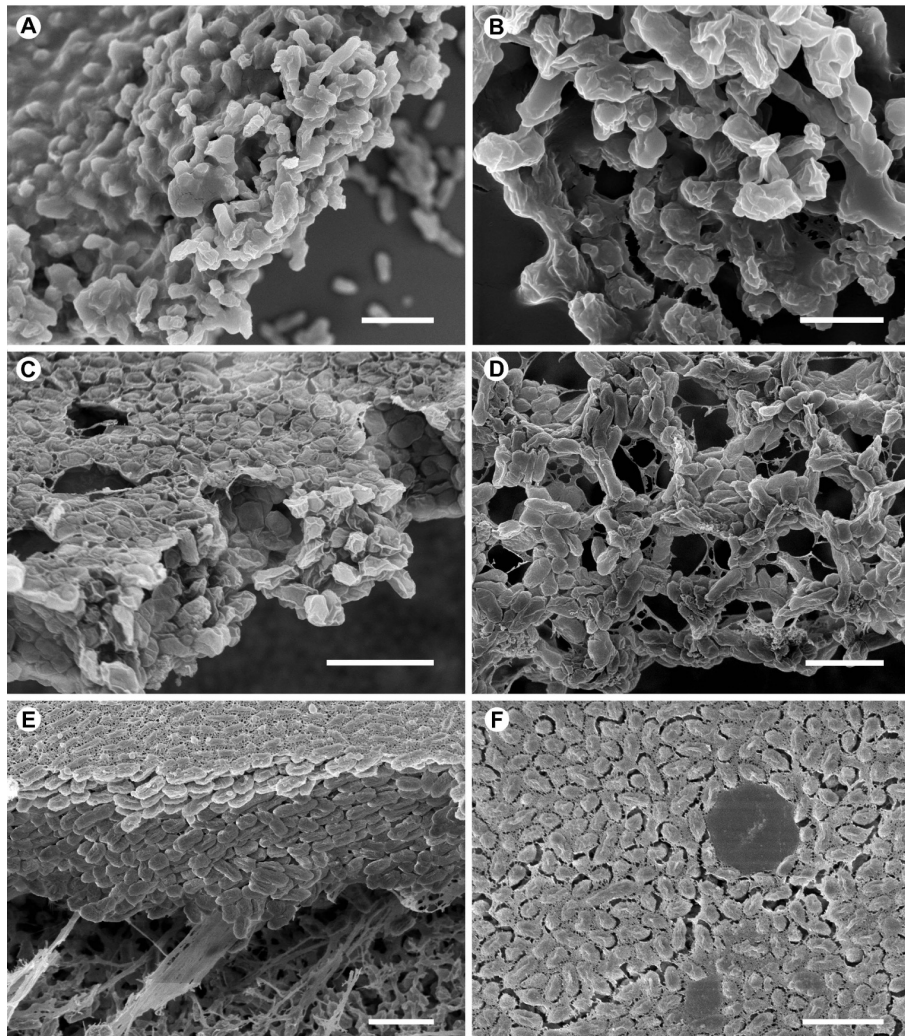


Figure 1.5: Scanning electron images of biofilm from the nontypeable *Haemophilus influenzae*, showing fine structures. **A:** Flat mats of bacteria in an amorphous EPS matrix (scale bar = 2 μm). **B:** Magnification shows that EPS layer covers bacterial surface (scale bar = 1 μm). **C and D:** Biofilm formation initiated on filter, then placed in medium for maturation. Different perspectives show the porous channel system. **E and F:** Biofilm formation initiated on filter, then placed in medium at the air-liquid-interface. Flat top surface exposed to air is covered by EPS, also covering bacteria free spaces (**F**) (scale bar (**C - F**) = 2 μm). Source: [88]

however, not only the visible environment of bacterial cells differs, most importantly a dramatic change also occurs within biofilm cells. Most cells are profoundly phenotypically different from their planktonic counterparts.[82] Different genes are expressed, mostly involving metabolism, phospholipid synthesis, membrane transport, secretion and protective mechanisms. Knock out of these genes often leads to less biofilm coverage and cells lacking differentiation.[84] A further important factor

during biofilm maturation is the so called twitching motility, a movement type developed presumably to redistribute colonies away from the substratum to extend the biofilm.[84] It has been observed that for some motile bacteria, motility is not flagella governed anymore, but replaced by a twitching motility approached by extension and retraction of type IV pili (e.g. in *Pseudomonas putida*).[84]. The development of antibiotic resistance mechanisms also takes place during biofilm maturation and many antibiotics have been found to be about 500 times less effective on bacteria organized in biofilm communities. Bacteria have been found to slow down growth and to start the expression of multi drug-resistance pumps, antibiotic modifying or degrading enzymes, or even altered antibiotic targets to resist these treatments.[85] However, the biofilm structure also seems to play a crucial role, since it has been observed that bacteria in a less complex biofilm matrix are more susceptible to antimicrobial agents.[84]

After biofilm maturation cells begin to detach from the biofilm, which is nowadays considered as a highly regulated process (Figure 1.4 5). Biofilm bacteria can thus disseminate into new areas for further colonization. During detachment different processes were observed. Cells can be released and return to the planktonic state (e.g. *P. aeruginosa*) [85], or they can form "swarmer cells" as observed for *Proteus mirabilis* [83]. Gliding bacteria can move along a slime trail, e.g. *Myxococcus xanthus*. [85] Cell surface alteration can also facilitate detachment as observed for some *Escherichia coli* strains. For all steps quorum sensing, the cell to cell signaling, is considered a crucial factor. During detachment EPS production is decreased. Starvation is considered one reason for detachment. The release of cells that return to the planktonic state allows the search for nutrient richer habitats. Thus, in a way the cycle is closed.[84] Hence, a biofilm exhibits a protected niche for bacteria, but as soon as growth conditions become less favorable, cells can be released again to ensure further survival.

The reasons why microorganisms are assumed to organize in biofilm communities are several fold. Within an oligotrophic environment it is assumed that nutrients accumulate on a surface and, thus, the overall content there is higher than in the

bulk fluid. Therefore, the surface constitutes a favorable growth niche. Due to the proximities of cells, quorum sensing is facilitated. Presumably, most importantly the biofilm constitutes a protection against detrimental external influences, such as UV-light, metal toxicity, acid exposure, dehydration, phagocytosis and antimicrobial agents. Biofilms provide an excellent protective niche for pathogens, when not associated with the host organism.[82] As beneficial the biofilm concept proves for participating organisms, as detrimental and hazardous can biofilms be for human health when harboring clinical pathogens. Biofilms, e.g. in industrial sewage or filter systems also cause enormous economical damage.[83, 89, 90]

Research within the last decades was concerned to unveil the fascinating and complex processes during biofilm formation and the factors that influence it. The understanding of biofilm seems thus a crucial starting point to be able to limit or prevent biofilm formation when undesired. Research concerning that quest included the search for substances that might inhibit biofilm initiation or that can even remove an existing biofilm. Among the substances tested with regards to biofilm inhibition was the already mentioned sulfated phenolic acid zosteric acid (ZS), which was found to reduce biofilm formation of an bacterial *E. coli* K12 strain and the fungus *Candida albicans*. [78, 79] The biofilm inhibiting potential of structurally related sulfated phenolic acids to ZS and the role of the sulfate ester remain to be investigated and parts of this thesis are concerned with this quest.

1.4 Biofouling in the marine environment

Since biofilms are known to develop on all types of surfaces immersed in water, marine environments provide numerous niches for their development. Surfaces exposed to seawater rarely harbor populations of single species but mixed communities. Further, in the marine environment, biofilms are not only composed of bacteria, but also provide a favorable environment for other organism of groups such as diatoms, fungi, unicellular algae and protozoa. They promote the settlement of macroalgae and invertebrates such as barnacles and mussels. This process is known as

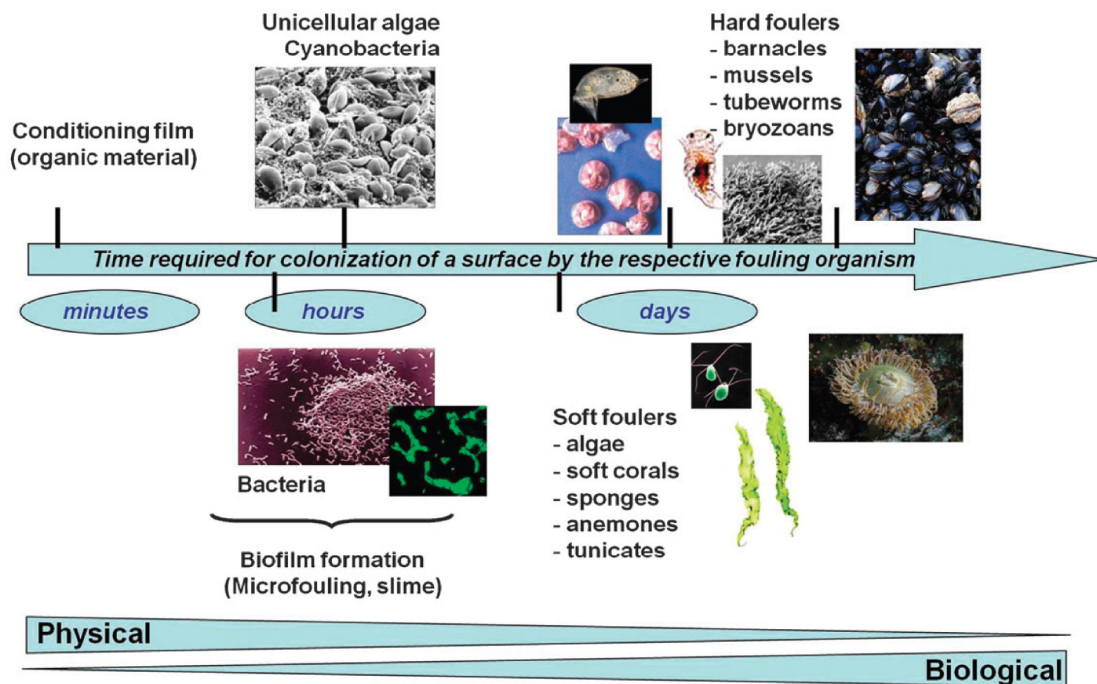


Figure 1.6: Development of a biofouling community. Adapted from Rosenhahn *et al.* 2010. [93] Within minutes after immersion in seawater, the surface is conditioned by organic and inorganic nutrients. During the following hours a biofilm forms, consisting e.g. of bacteria and unicellular algae. In the days to follow, macrofoulers such as algae and barnacles accumulate. The more organisms colonize the surface, the less surface properties are defined by physical parameters.

biofouling.[91, 92]

During biofouling, several distinct steps can be observed on a surface, e.g. immersed in seawater (Figure 1.6). Within the first few minutes, nutrients accumulate on the surface, upon which bacteria begin to adhere, usually within 24 hours (primary colonizers). A bacterial biofilm develops. During the following days, microorganisms as diatoms and other unicellular algae, planktonic propagules of algae and invertebrates (spores and larvae) join the community (secondary colonizers). Seaweeds and invertebrates begin to adhere around two to three weeks after immersion, forming the final "layer" of the community.[94] The role of marine biofilms as mediators for settlement of higher organisms has been reviewed by Qian *et al.* in 2007.[89] The formation of a biofilm constitutes the crucial feature for further settlement. Besides environmental conditions, already discussed in section 1.3, primary colonizers essentially determine the biochemical and physical properties of the biofilm, thus displaying either promoting or discouraging properties to secondary coloniz-

ers searching for a growth niche. Planktonic propagules can distinguish between different communities and either choose or reject a new habitat. They can sense composition, density, metabolic activity, age and origin. Whichever factor proves to be beneficial or discouraging for secondary colonizers, however, remains highly species dependent. That, and the fact that fouling communities are also highly adaptable to changes in environmental conditions, renders predictions what types of communities will form under certain conditions a rather difficult task.[89]

Biofouling ensures a protected growth niche within the marine environment. It thus plays an essential role in the rehabilitation of marine habitats and can also be beneficial for aquacultures. Biofouling research however is strongly focused on fouling inhibition strategies (antifouling, AF), due to the immense costs it causes for marine industries. Fouling negatively effects the hydrodynamic efficiency of ships and propellers, causes pipeline blockage or sensor malfunction, and enhances corrosion of stainless steel.[91, 92] For more than a hundred years, prevention of biofouling has been a huge field of research.[94–98] Surfaces constantly immersed in water, such as ship hulls are treated with so called antifouling paints, whose development during the last century was reviewed by Almeida *et al.* in 2007.[94] Ship hulls are first treated by an anticorrosive primer upon which the antifouling paint is applied. In general, three distinct types can be distinguished. In the 1950's so called soluble paints were used. These are composed of seawater soluble binders such as rosin (derivatives of the diterpene abietic acid, isolated e.g. from pine trees). Antimicrobial pigments containing copper, iron, arsenic and mercury were added. Upon immersion, the matrix gets dissolved continuously releasing AF compounds. Unfortunately, this matrix has a poor mechanical strength, can only incorporate low amounts of pigments and has to be renewed usually within a year. In order to evade this disadvantage, insoluble matrix paints were designed. Sea water insoluble high molecular mass binders such as acrylic polymers, exhibited an improved mechanical strength. Soluble AF components such as copper and so called booster biocides (further AF agents) are constantly released, whereby a porous material forms. Sea water passing through the pores will release AF agents from deeper layers. However,

after a while, pollutants can accumulate within the pores and block further release of AF compounds, thus, the long term activity of these paintings is also limited. The most efficient approach for many years proved to be self-polishing paints. Here, the highly effective AF tributyl-tin (TBT) derivatives were bound to an insoluble polymer which then became soluble and additionally pigments containing copper were added. Both copper ions and the TBT polymer were continuously released, preventing the formation of pores and the release rate could be adjusted based on the molecular properties of the polymer.[94]

As efficient TBT based self-polishing paints proved against various organisms under varying environmental conditions, as detrimental were their effects to numerous marine organisms and after accumulating in the food web, finally to humans.[99] Thus, the International Maritime Organization (IMO) demanded a total ban of TBT based compounds, finally valid from 2008.[100] Copper ions can also have toxic effects, but the contribution of copper ions from AF paints is considered to be much less than its natural occurrence in sea water. Usually "free" Cu^{2+} ions are readily complexed by organic ligands. Thus, their presence in common AF paint compositions are tolerated. However, many higher organisms proved to be highly tolerant towards copper ions, hence there is an urgent need for additional effective, non-toxic AF agents that can replace TBT compounds. [94, 101]

Various strategies to solve this acute problem can be distinguished. One approach is to modify the physical properties of a surface to inhibit biofouling.[93, 102–106] Since bacterial biofilms seem to represent the crucial step for biofouling, interference with biofilm formation seems a further promising attempt. Here, especially compounds that proved to interfere with quorum sensing processes such as acetylated homoserine lactones (AHL) or halogenated furanones from the red alga *Delisea pulchra* are of interest. Research with respect to screening of novel microbial compounds related to quorum sensing is however just at its beginning.[94] Another approach focuses on non-toxic biomimetic or bioinspired substances used for example by algae to protect themselves from fouling organisms.[103, 107–111] An overview of recently developed booster biocides and some of natural origin is provided by Omae in 2003. Among

these natural AF agents also the phenolic sulfate ester zosteric acid (ZS) can be found.[101]

1.5 Aim of the thesis

The emergence of both biofilm formation and biofouling can constitute more than just disturbing phenomena. Bacterial biofilms of clinical pathogens often bear a life threatening potential [83] and aquatic biofouling causes either enormous economical costs for aquatic industries or, if treated effectively, an ecologically not justifiable release of toxins into the environment [91, 92, 99, 100]. Thus, the development of, or screening for effective antifouling and biofilm inhibiting compounds with tolerable toxicities is a challenging field of research, comprising several disciplines.

Assuming that the sulfated metabolites detected by Dr. Matthew Welling in members of the Dasycladaceae [56] are structurally related to the as antifouling agent described zosteric acid (ZS), a comprehensive comparison was aimed to draw conclusions on a structure-function relation for sulfated phenolic acids. Questions concerned the specific roles the sulfate esters play and in how far other functional groups influence their biological activity. Another important aspect included the application of highly sensitive analytical tools, especially ultra-high-performance-liquid-chromatography coupled to electro-spray ionization mass spectrometry (UPLC-MS), to be able to monitor the fate of the sulfated compounds under various experimental conditions including reaction monitoring during synthesis as well as in presence of pure enzymes and metabolically active bacteria. This was intended to ensure that any observed effects would be attributed to the correct compound.

Chapter 2 focuses on structure identification of the novel sulfated metabolites found in members of the Dasycladaceae by using UPLC-MS. Both for identification and subsequent bioassays, standards of high purity were required. Thus, efficient synthesis and purification routines for these compounds were to be developed. Knowledge about the sensitivity of sulfated metabolites towards chemical and enzymatic hydrolyzation was considered a fundamental basis for intended bioassays.

Chapter 3 to 6 contain results from different bioassays with three sulfated phenolic acids and their non-sulfated forms. A filter disc assay was assumed to provide informations about the antimicrobial activity against marine bacteria of the novel compounds identified in members of the Dasycladaceae (chapter 3). The biofilm inhibiting and antifouling activities of the novel compounds in comparison to ZS and their non-sulfated forms were to be tested comparatively on different bacteria and under varying experimental conditions both in the laboratory and the field (chapter 4-6). The field assay was performed in co-operation with Dr. Levent Cavas from the University in İzmir, Turkey.

Results presented in chapter 7 of this thesis are based on a different motivation concerning the wound reaction of species belonging to the siphonous green algae *Codium*. These investigations were supposed to be pursued, if these organisms would possess a similar wound response as has been previously observed for species belonging to the Caulerpaceae and Dasycladaceae.

2 Sulfated phenolic acids of *Dasycladus* spp.

The hence unknown secondary metabolites found by Dr. Matthew Welling in members of the siphonous green algae family Dasycladaceae showed additionally to the molecular ion $[M-H]^-$ a characteristic fragment of $[M-H-80]^-$, indicating the loss of "SO₃".[56] A sulfated metabolite involved in the wound reaction of *Dasycladus vermicularis* and *Cymopolia barbata* could be identified as 6,7-dihydroxycoumarine-3-sulfate (DHyCS, Figure 1.2 D).[12, 56] For the remaining sulfated metabolites in the species *D. vermicularis*, *C. barbata* and *Neomeris annulata* that were not involved in the wound reaction, a phenolic acid backbone was assumed based on retention times, mass and UV-Vis spectra. The first eluting peak in the methanolic extract of *D. vermicularis* showing a MS fragment of $[M-H-80]^-$ was assumed to be the sulfate ester of a hydroxybenzoic acid, with a m/z of 217 $[M-H]^-$. The second peak showing a loss of - 80 was assigned to DHyCS. The third peak with a m/z of 231 $[M-H]^-$ was assumed to be the sulfate ester of a hydroxyphenylacetic acid, due to its mass increase of 14 compared to the first metabolite, indicating the presence of an additional CH₂ group. A metabolite with a m/z of 217 $[M-H]^-$, a congruent mass spectrum and retention time was also found in *C. barbata*. In *N. annulata* two closely eluting peaks with similar mass spectra were found, indicating isomers. Both had m/z values of 259 $[M-H]^-$ and showed a -80 fragment.[56]

Mass and UV-Vis spectra showed a close relationship to a known phenolic acid sulfate ester found in the sea grass *Zostera marina* named zosteric acid (ZS), which was first isolated by Todd *et al.* in 1993.[72] The two metabolites from *N. annulata* showed a mass increase of 16 compared to ZS, indicating an additional oxygen,

which potentially derived from a second phenolic hydroxy group. Sulfatation of either of the two hydroxy groups would result in two constitutional isomers, with similar mass spectra and only slightly different retention times.[56]

Based on these data, the structure of the novel sulfated compounds were to be identified. Not enough biomaterial was available for structure analysis by NMR. A reasonable way for structure elucidation therefore seemed co-injection experiments by UPLC-MS with synthetic analogues. Mass- and UV-Vis spectra obtained by Dr. Matthew Welling already provided valuable structural informations.[56] For identification and subsequent bioassays it was essential to obtain the sulfated phenolic acids in adequate amounts and high purity. Due to their two acidic protons, sulfated phenolic acids seemed also valuable LC-MS standards.

This chapter focuses on the development of a simple synthesis routine for a variety of sulfated phenolic acids, phenols and mono-hydroxycoumarines, their chemical properties towards acidic and enzymatic hydrolysis as a basis for later bioassays, and on the structure elucidation of the unknown sulfated phenolic acids from the three members of the Dasycladaceae.

2.1 Synthesis of sulfated phenolic acids, phenols and coumarines

For creating sulfate esters of many different types of compounds, including alcohols, aryls or carbohydrates, the highly reactive electrophile sulfur trioxide (SO_3) is the essential unit. Since reactivity of pure SO_3 is difficult to control, selectivity during synthesis is hardly achievable. Thus, reactive SO_3 has been stabilized in various forms to better navigate its reactivity. One of the first stabilized sulfatation agents used was chlorosulphonic acid (ClSO_3H).[112] Nowadays, various SO_3 complexes with different amines are known and commercially available, such as pyridine-, trimethylamine-, triethylamine- or *N,N*-dimethylaniline- SO_3 complexes. These are less sensitive to hydrolyzation e.g. by humidity than ClSO_3H , but still possess a high reactivity towards a variety of compounds to be sulfated.[113–115] An overview on

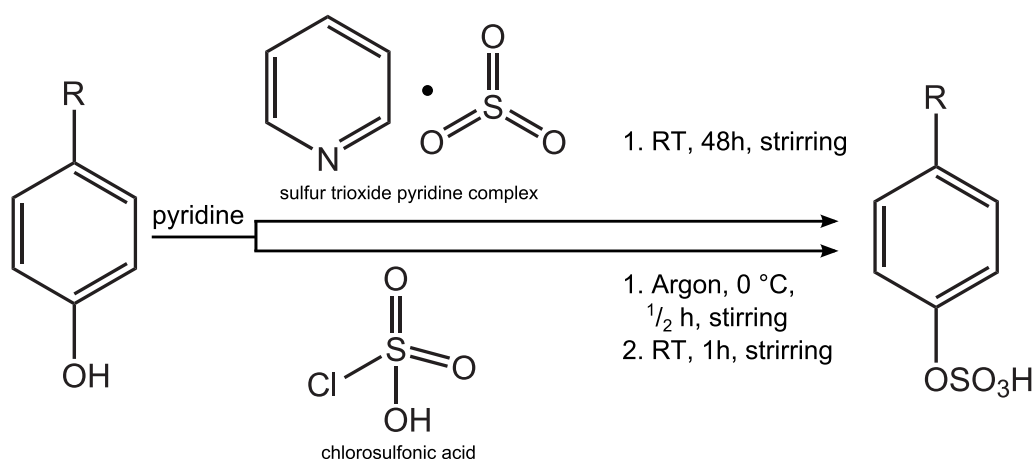


Figure 2.1: General sulfatation procedure of substituted phenols either by a sulfur trioxide pyridine complex (Pyr*SO₃) or chlorosulfonic acid (ClSO₃H) [72] in pyridine. R = organic rest; RT = room temperature

commercially available amine*SO₃ complexes is provided by Kusch.[116] The chemical property of the chosen base also influences the reactivity of the formed SO₃ complex and, thus, selectivity can be further adjusted. For the sulfatation of carbohydrates, flavonoids and aryl bearing peptides a variety of protected sulfatation agents have been designed, which proved highly applicable for sulfatation within a cascade of reaction steps.[117–124] These will not be further discussed here.

This study was solely focused on the synthesis and purification of phenolic acids, phenols and mono-hydroxycoumarines, therefore, only sulfatation procedures concerning this molecular family were considered. Published routines for creating sulfate ester from phenols or phenolic acids vary slightly in solvents, sulfatation agents and reaction conditions applied [72–79, 81, 113, 114, 125–127], but all procedures have in common that the purification of the products is not trivial, due to their increased water solubility and association with sulfate salts. Since ZS seemed most closely related to the molecules to be identified in members of *Dasycladus* spp., procedures described here are based on publications concerning ZS synthesis.[72, 77, 78] None of these publications however provided work-up strategies to obtain the product both in high quantity as well as in the desired purity.

As sulfatation agents for this study, pyridine sulfur trioxide complex (Pyr*SO₃) [127] and in rare cases ClSO₃H [72] were used in pyridine (Figure 2.1). Pyridine was

chosen, because it dissolves both product and educt, can be removed by rotor evaporation and is considered less toxic than, for example, N,N-dimethylformamid (DMF), which has been used by Villa *et al.* [78, 79, 126] The following description of the established synthesis routine and purification strategies refer to the use of Pyr*SO₃ as sulfatation agent. For the rare cases this did not lead to the desired result, ClSO₃H was used according to a method from Todd *et al.* 1993 (section 9.2.13). [72] After neutralization of the reaction mixture containing ClSO₃H, the work-up procedure followed that described for the reaction with Pyr*SO₃ in the following paragraph. UPLC-MS proved to be a valuable tool to improve reaction and purification procedures due to the straightforward identification of sulfated products by their specific loss of m/z -80. This method additionally allowed a fast screening for side products and educt residuals.

2.1.1 Formation of the sulfate ester raw product

An equimolar mixture of educt and Pyr*SO₃ in pyridine was stirred at room temperature for 48 hours, leading to an almost complete transformation of the educt. For sulfatation of phenolic acids containing two hydroxy groups the amount of Pyr*SO₃ was adjusted to double molar. With this agent di-sulfatation was not observed. After complete transformation of the educt, pyridine was removed to yield an oily product, which was then dissolved in water and the pH increased from 3 to 7 with potassium hydroxide (KOH). [127] KOH was chosen instead of sodium hydroxide (NaOH) [78, 79, 126, 128] due to the lower solubility of K₂SO₄ (110 g L⁻¹) in water at room temperature compared to the corresponding sodium salt (210 g L⁻¹). [129] The aqueous phase was repeatedly extracted with ethylacetate, until the formation of precipitate stopped. The latter did not contain product and was discarded. After removal of water from the raw product, two side products could be identified by UPLC-MS during sulfatation of phenolic acids: presumably the anhydride of educt and sulfated product (X/XS), and educt and educt (X/X) (Figure 2.2 A-E). The formation of Z/Z and Z/ZS side products during ZS synthesis have presumably been noticed by others, although they are described in current literature as diesters

with no further structural information.[73, 76] Protection of the carbon acid moiety as a tertiary butyl ester proved not to be a convenient solution, since during synthesis and cleavage of the tertiary butyl ester even more undesired side products accumulated in the reaction mixture. The amount of anhydride could be reduced, but never prevented completely, by using equimolar (or double molar) amounts of educt and sulfatation agent and by not increasing the reaction temperature above room temperature. Using the sulfatation agent in excess decreased the pH during synthesis below 3, which might be supportive for anhydride formation. The thus obtained raw product contained potassium sulfate, the two anhydrides, occasionally educt and an oily substance, which were all water soluble (Figure 2.2 E, F). Many published synthesis routines for ZS and related molecules either do not state any further purification steps [73, 74, 76] or used methanol to precipitate salts and used the crude product obtained for further experiments [77–79, 126, 128]. Todd *et al.* 1993 used HPLC to purify the raw product of ZS [72] and Edwards *et al.* 2012 recrystallized a sulfated chlorophenol from ethanol [127]. Nevertheless, preparative, reversed-phase HPLC is very time consuming and inconvenient for larger amounts in the gram range and recrystallization did not work with the molecules sulfated during this study. Thus, a non time consuming way had to be established to separate the product from side products and salts. Two ways were developed to obtain highly pure products, which will be introduced in the following section.

2.1.2 Purification - analytical scale (a.s.)

For co-injection experiments analytical amounts (mg) of product were sufficient and the raw product could successfully be purified by using a ZIC[®]-HILIC (hydrophilic interaction liquid chromatography) solid phase extraction (SPE) cartridge. The HILIC material of the cartridges is build based on silica gel carrying an alkyl chain with a quarternary amine and a sulphonic acid moiety, thus, being twitter ionic, which shows a high affinity for polar substances, but salts and organic side products can be removed. The phenolic acid sulfate ester is absorbed by the HILIC material, whereas salts remain dissolved in the mixture of water and organic solvent (here

acetonitrile) used to load the sample on the cartridge. The loaded cartridge was washed with acetonitrile to remove organic side products, including the two anhydrides and finally the product was eluted with water containing 0.1 % formic acid. The analytical scale purification routine was applicable for 2-, 3-, and 4-(sulfooxy)-benzoic acid (oBS, mBS, BS) and 4-(sulfooxy)phenylacetic acid (AS), which provided yields between 5 and 20 % of the amount of loaded material (table 2.1). The enormous "loss" is presumably due to the oily nature of the raw product and the high amount of salts. After passing the cartridge, neither in the loading solvent mixture, nor in the organic washing phase could the sulfated product be detected by UPLC-MS.

Neither for the purification of ZS nor any of the dihydroxycinnamic acid sulfate esters was this approach suitable. Here only a minor part of the product absorbed to the material and a high amount of analyte passed through during loading.

2.1.3 Purification - large scale (l.s.)

Since the restricted applicability of the analytical scale method and the fact that for bioassays much more material was needed, a large scale purification method was developed. The anhydrides of X/XS and X/X could readily be cleaved by increasing the pH of the aqueous phase to 10 with KOH after washing with ethylacetate. Therefore the solution was stirred in a water bath of 60 °C for an hour. After cooling to room temperature (RT) the pH was adjusted back to 6-7 with H₂SO₄. Then, water was removed and the raw product, now containing product, educt and potassium sulfate was dissolved in as little water as possible in a 40 °C water bath (Figure 2.2 G). To precipitate salts, two times the volume of the aqueous phase of methanol was added [72, 77–79, 126], upon which a white precipitate formed containing presumably potassium sulfate and only negligible amounts of product, as revealed by UPLC-MS. The precipitate was filtered off and one volume of methanol was added to the filtrate. Here, formation of precipitate did not occur anymore. The solution was left at RT overnight, upon which transparent crystals, presumably K₂SO₄, formed which did not contain product, as tested by UPLC-MS measurements. The

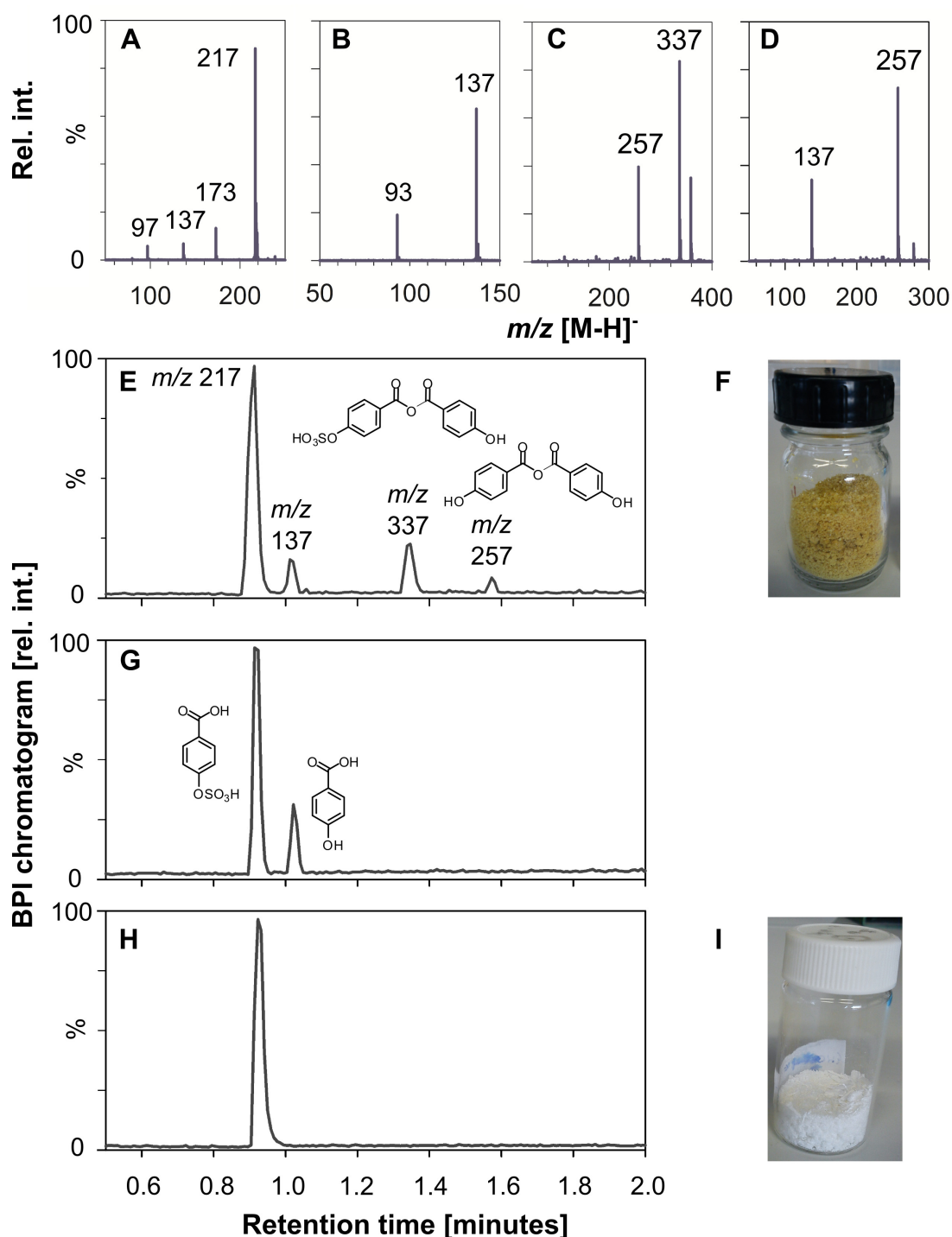


Figure 2.2: UPLC-MS screening during the large scale purification process of 4-hydroxybenzoic acid sulfation (BS). **A-D:** Mass spectra of the 4 detectable products BS (**A**; R.T. 0.92 min; m/z 217 [M-H]⁻), 4-hydroxybenzoic acid (**B**) (**B**; R.T. 1.01 min; m/z 137 [M-H]⁻), B/BS anhydride (**C**; R.T. 1.35 min; m/z 337 [M-H]⁻), B/B anhydride (**D**; R.T. 1.01 min; m/z 257 [M-H]⁻). **E-H:** UPLC-MS BPI chromatograms and pictures of raw product (**E**, **F**), product after anhydride cleavage with KOH (**G**) and pure product (**H**, **I**). R.T. = retention time.

crystals were filtered off and the solution was evaporated to dryness, usually yielding a white product in some yellow brownish oily side product (Figure 2.2 F). The oily product could be removed by adding one tenth of the volume of methanol used to precipitate salts. The batch was placed in an ultrasonic bath until a white suspension of product in methanol and dissolved side product was obtained. Methanol was removed by funnel filtration and a white powder consisting of product and educt was obtained. Removal of the educt was achieved by washing the solid in the filter with acetone until no trace of educt could be detected by UPLC-MS measurements anymore (Figure 2.2 H, I). After large scale purification yields ranging from 55 to almost 80 % were achieved.

2.1.4 Summary of the synthesized products

The selected sulfatation agents in pyridine and the developed purification routines proved applicable to a variety of substances. Several monohydroxylated phenolic acids including 4-hydroxybenzoic acid (B), 3-hydroxybenzoic acid (mB), 2-hydroxybenzoic acid (oB), 4-phenylacetic acid (A) and 4-hydroxycinnamic acid (Z) could be sulfated providing the high purity products BS, mBS, oBS, AS and ZS in good yields. Additionally sulfate esters of 3,4- and 2,3-dihydroxycinnamic acid (3,4CAS, 2,3CAS), mono-hydroxylated coumarines (6-, and 7-(sulfoxy)coumarine) and 2-, 3-, 4-methoxyphenols (2-, 3-, 4MOPS) could be obtained. Only sulfatation of 2,4-dihydroxycinnamic acid (2,4CAS) led to different products, depending on the sulfatation agent. All substances obtained are listed in tables 2.1 and 2.2, showing the synthesis routine, yields, properties and the analytics applied on each product. A detailed description of synthesis and analytical data for each substance can be found in section 9.2; NMR spectra and chromatograms in the appendix.

BS, mBS, AS and ZS, obtained with Pyr^*SO_3 , were isolated as highly pure, white powders, which can be stored for years at $-26\text{ }^\circ\text{C}$. NMR measurements of these four substances showed no traces of educt or any other side products. A downfield shift

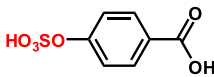
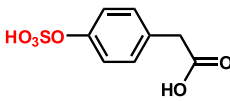
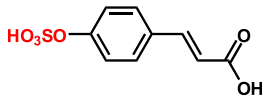
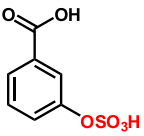
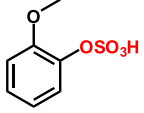
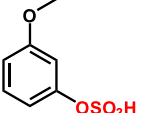
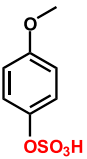
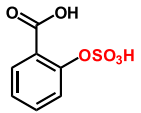
Product	Synthesis	Yield	Properties	Analytic
BS 	Pyr*SO ₃	a.s. 6.7 % l.s. 57.0 %	white powder pure product	UPLC-MS NMR EA
AS 	Pyr*SO ₃	a.s. 19.0 % l.s. 76.0 %	white powder pure product	UPLC-MS NMR EA
ZS 	Pyr*SO ₃	l.s. 58.0 %	white powder pure product	UPLC-MS NMR EA
mBS 	Pyr*SO ₃	a.s. 11.2 % l.s. 49.5 %	white powder pure product	UPLC-MS NMR
2MOPS 	Pyr*SO ₃	l.s. not est.	beige solid	UPLC-MS
3MOPS 	Pyr*SO ₃	l.s. not est.	beige solid	UPLC-MS
4MOPS 	Pyr*SO ₃	l.s. not est	beige solid	UPLC-MS
oBS 	ClSO ₃ H [72]	a.s. 13.8 %	white powder pure product unstable	UPLC-MS

Table 2.1: Summary of synthesized sulfate esters 1. Abbreviations: a.s. = analytical scale, l.s. = large scale, not est. = not estimated, NMR = nuclear magnetic resonance, EA = elementary analysis.

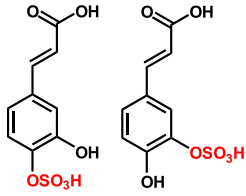
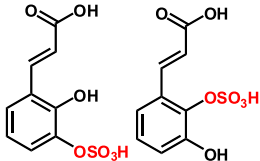
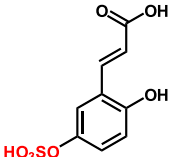
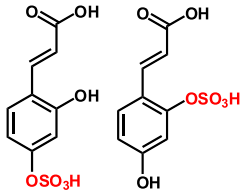
Product	Synthesis	Yield	Properties	Analytic
3,4CAS 	Pyr*SO ₃	l.s. 50.1%	ecru powder pure product isomeric mixture	UPLC-MS NMR
2,3CAS 	(1) 2,3 CA [130] (2) Pyr*SO ₃	not est. not est.	yellow oil yellow solid raw product isomeric mixture	UPLC-MS UPLC-MS
2,5CAS 	(1) Pyr*SO ₃ 6-(sulfoxy)- coumarine (2) coumarine hydrolysis [131]	not est. not est.	beige solid raw product beige solid raw product pure isomer	UPLC-MS UPLC-MS
2,4CAS 	(1) Pyr*SO ₃ (2) ClSO ₃ H	not est. not est.	brown solid raw product unidentified brown solid raw product one isomer	UPLC-MS UPLC-MS

Table 2.2: Summary of synthesized sulfate esters 2. Abbreviations: a.s. = analytical scale, l.s. = large scale, not est. = not estimated, NMR = nuclear magnetic resonance.

from protons or carbon atoms close to the sulfate ester was observed compared to the non-sulfated form. UPLC-MS investigations revealed no contaminations in pure products of mBS, BS, and AS, solely in measurements of ZS could minor amounts of educt (< 1%) be found, despite several washing steps with acetone. Elementary analysis of the large scale synthesis of AS, BS and ZS never showed an increased sulfur content, indicating that most of the potassium sulfate was indeed removed during purification.

Sulfatation of 2-hydroxybenzoic acid (oBS) was only achieved by using ClSO₃H as sulfatation agent. UPLC-MS measurements of the raw product showed several non-sulfated polymers of salicylic acid, which could be removed by the analytical scale HILIC workup. The obtained white powder, however, was not stable in an even slightly acidic solution, as present during UPLC-MS measurements, for a longer time. After a while first a dramatic reduction in retention time of a substance with m/z 217 [M-H]⁻, later the presence of the non-sulfated form (m/z 137 [M-H]⁻) could be observed. Even at -26 °C in dried form was the substance not stable for more than a few months. A possible explanation provided Benkovic *et al.* in 1966, who performed a kinetic study on arylsulfate ester hydrolysis. It was postulated that in salicyl sulfate an intra-molecular attack of the carboxylgroup on the sulfate ester, leading to rearrangement of the sulfate group, increases the hydrolysis rate at a pH between 3 and 4 by a factor of 200.[128]

Minor amounts of BS, mBS, oBS and AS were used for co-injection experiments with *D. vermicularis* and *C. barbata* (section 2.3). Several gram of highly pure AS and BS were used for a filter disc assay (chapter 3) and together with ZS for different biofilm assays (chapters 4, 5 and 6).

2-, 3- and 4-methoxyphenol were also applied to sulfatation with Pyr*SO₃, leading to 2MOPS, 3MOPS and 4MOPS. UPLC-MS measurements showed no side products or traces of educt in the raw product, which after desalting was a slightly oily beige solid. Treatment with methanol in an ultrasonic bath dissolved the oily compound and provided slightly beige powders. All three were used for co-injection experiments with *C. barbata* (section 2.3).

3,4-dihydroxycinnamic acid was also successfully sulfated with Pyr*SO₃, leading to 3,4CAS and purified using the large scale approach with comparable yields and purity to AS, BS and ZS. These substance were used for studies on chemical and enzymatic stability of sulfated phenolic acids (section 2.2) and for co-injection experiments with *N. annulata* (section 2.3).

Sulfatation of the remaining three dihydroxycinnamic acids, providing 2,3CAS, 2,5CAS and 2,4CAS was only performed on an analytical scale for co-injection tests

with *N. annulata* (section 2.3) and the products were not further purified after desalting. For the generation of 2,3CAS, 2,3-dihydroxycinnamic acid (2,3CA) was synthesized from 2,3-dihydroxybenzaldehyde according to a method described by Dupin *et al.* 1985.[130] The obtained raw product was identified by UPLC-MS and without further purification treated with Pyr*SO₃. UPLC-MS measurements showed two peaks with identical masses of m/z 259 [M-H]⁻, both showing a loss of -80, indicating the presence of two sulfated constitutional isomers. 5-(sulfoxy)cinnamic acid (2,5CAS) was obtained as the pure isomer from sulfatation of 6-hydroxycoumarin with Pyr*SO₃ and subsequent hydrolysis of the raw product after a method described by Adams *et al.* in 1948.[131] The raw product was identified by UPLC-MS. Sulfatation of commercially available 2,4-dihydroxycinnamic acid (2,4CAS) did not lead to obvious results. After Pyr*SO₃ addition, two products with m/z values of 259 [M-H]⁻ could be found in UPLC-MS measurements, but neither showed the [M-H-80]⁻ fragment usually observed. Instead, fragments of m/z 215, indicating the loss of CO₂ and of m/z 241, usually the m/z [M-H]⁻ of a mono-(sulfoxy)coumarin, were found. Sulfatation with ClSO₃H only provided one product with m/z 259 [M-H]⁻ and the typical [M-H-80]⁻ fragment. The other product found with m/z of 241 [M-H]⁻ was presumably a mono-(sulfoxy)coumarin. Here, obviously an intra-molecular reaction took place at the rather low pH of 2 during synthesis with this sulfatation agent. Although a 7-(sulfoxy)coumarin could be synthesized, subsequent coumarin hydrolysis as described for 6-(sulfoxy)coumarin, which would lead to 4-(sulfoxy)-2-hydroxycinnamic acid, was also not successful.

Thus, in cases where a hydroxy group in *ortho*-position to the carboxylic acid moiety was present, sulfatation was either only achievable with ClSO₃H (oBS) or lead to different products by using either of both sulfatation agents, as in the case of 2,4-dihydroxycinnamic acid. Intra-molecular reactions in oBS were only observed after synthesis, explaining the instability. For 2,4CAS these occurred already during synthesis. During the synthesis of 2,5CAS formation of an isomeric mixture and an intra-molecular reaction were prevented by first creating the 6-(sulfoxy)coumarin, which was then cleaved to provide the pure 5-(sulfoxy)-2-hydroxycinnamic acid

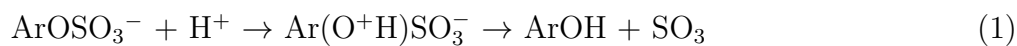
isomer. The latter was stable in solution during the measurement. Unfortunately, this routine was not applicable for 7-(sulfooxy)coumarine. During the sulfatation of 2,3CA no intra-molecular reactions were observed. Here, the close proximity of the two hydroxy groups presumably led to an electron distribution within the aromatic system unfavorable for a ring closure to the corresponding coumarine.

For all substances intended to be used for different bioassays or substance identification the developed purification routines on either analytical or large scale could successfully remove side products, such as the anhydrides of X/XS and X/X, traces of the educt and the unidentified oily side product. Although the presence of the anhydrides (termed diesters) have presumably been noticed by others during synthesis of ZS [73, 76], no further steps of purification were reported: Other published synthesis routines for ZS and related molecules, either do not state any further purification steps [73, 74, 76] or stopped after using methanol to precipitate salts [77–79, 126, 128]. The importance of the purification of the raw product of sulfated phenolic acids will be discussed in chapters 4 and 5.

2.2 Stability of sulfated phenolic acids

2.2.1 pH dependent stability of 3,4CAS

Arylsulfate esters are acid labile and decompose by the following mechanism, leading to phenol and sulfuric acid [132]:



Several kinetic studies during hydrolysis of different arylsulfate esters have been performed. These studies were concerned with the ability of different acids or alkalis (mineral and non mineral) to hydrolyze various sulfate esters [133, 134], but also investigated the influence of other ring substituents, both concerning their chemical nature (electron withdrawing or donating) and their position within the

Condition		HCl		H ₂ SO ₄		HCOOH		KOH	
t [h]	pH	3,4CAS	3,4CA	3,4CAS	3,4CA	3,4CAS	3,4CA	3,4CAS	3,4CA
0.5	1	✓	x	-	-	-	-	-	-
0.5	3	✓	x	-	-	-	-	-	-
0.5	5	✓	x	-	-	-	-	-	-
1	1	✓	✓	-	-	-	-	-	-
1	3	✓	x	-	-	-	-	-	-
1	5	✓	x	-	-	-	-	-	-
2	1	✓	✓	✓	x	-	-	-	-
2	3	✓	x	✓	x	-	-	-	-
2	5	✓	x	✓	x	-	-	-	-
4	1	x	✓	✓	✓	✓	x	-	-
4	3	✓	x	✓	x	✓	x	-	-
4	5	✓	x	✓	x	✓	x	-	-
4	7	-	-	-	-	-	-	✓	x
4	9	-	-	-	-	-	-	✓	x
4	11	-	-	-	-	-	-	✓	x
4	13	-	-	-	-	-	-	✓	x

Table 2.3: Hydrolysis of 3,4CAS by HCl, H₂SO₄, HCOOH (pH 1-5) and KOH (pH 7-13) at 80 °C during 0.5, 1, 2 and 4 hours. ✓ = 3,4CAS still present, x = 3,4CAS not present anymore, x = 3,4CA not present, indicating no hydrolysis, ✓ = 3,4CA present, indicating hydrolysis, - = no sample. Abbreviation: t = time in hours.

aromat [128, 132–134]. Hydrolysis in general seems to be promoted by electron withdrawing groups present at the ring. The individual chemical stability of each arylsulfate ester against acid (and alkaline) hydrolysis is thus dependent on the chemical nature of substituents and their position within the aromatic ring. Since no studies concerning hydrolysis of the phenolic acid sulfate esters used during this study have been published so far, this experiment was performed to estimate, if the synthetic compounds are stable under the conditions of UPLC-MS measurements and the various bioassays.

The isomeric mixture of 3,4CAS was used as a model substance, due to the two different positions of sulfate esters on the aromatic system (*meta*, *para*). Formic

acid was present in the solvents during UPLC-MS measurements and also during the analytical scale HILIC purification. HCl, H₂SO₄ and KOH were present during the sulfation reaction with Pyr*SO₃ and ClSO₃H and subsequent purification. Additionally, some microorganisms can decrease the pH value of their medium due to metabolic processes, so it was important to know, if there is a general critical pH range for hydrolyzation of 3,4CAS. Thus, the stability against these agents was tested at different pH values ranging from 1 to 13 at RT and 80 °C for a maximum period of 4 hours. All samples were then screened by UPLC-MS measurements for the presence of 3,4CAS (m/z 259 [M-H]⁻) and the appearance of the non-sulfated form 3,4CA (m/z 179 [M-H]⁻). At RT, no conversion of 3,4CAS could be observed during 4 hours, independent of pH and agent. Table 2.3 summarizes the result for the different agents at 80 °C. In the presence of HCl at pH 1, part of the substrate was already hydrolyzed to 3,4CA after one hour and after 4 hours no 3,4CAS could be detected anymore, indicating complete hydrolyzation. By using H₂SO₄, the presence of the non-sulfated form could be observed at pH 1 after 4 hours, but here no complete conversion took place within this time frame. In samples containing formic acid from pH 1 to 5 and KOH from pH 7 to 13 no traces of the non-sulfated form could be observed after 4 hours.

2.2.2 Stability of sulfated phenolic acids in sterile medium

The stability of the sulfated phenolic acids ZS, AS and BS as well as their non-sulfated forms was tested in sterile bacterial medium, at the conditions applied during the biofilm assays (section 9). Therefore A, B, Z, AS, BS and ZS were dissolved in Marine Broth at concentrations of 2.05 mmol/l and sterile filtered into autoclaved glass vials. Samples were taken immediately afterwards and after 11 days, at 30 °C and under permanent agitation on a shaker. By UPLC-MS measurements changes in concentrations of each substance were estimated using *trans*-cinnamic acid as internal standard for peak area normalization. Samples of the sulfated phenolic acids ZS, AS and BS were additionally screened for the presence of the corresponding non-sulfated forms, recognizable by a mass difference of m/z -80. Figure 2.3 shows

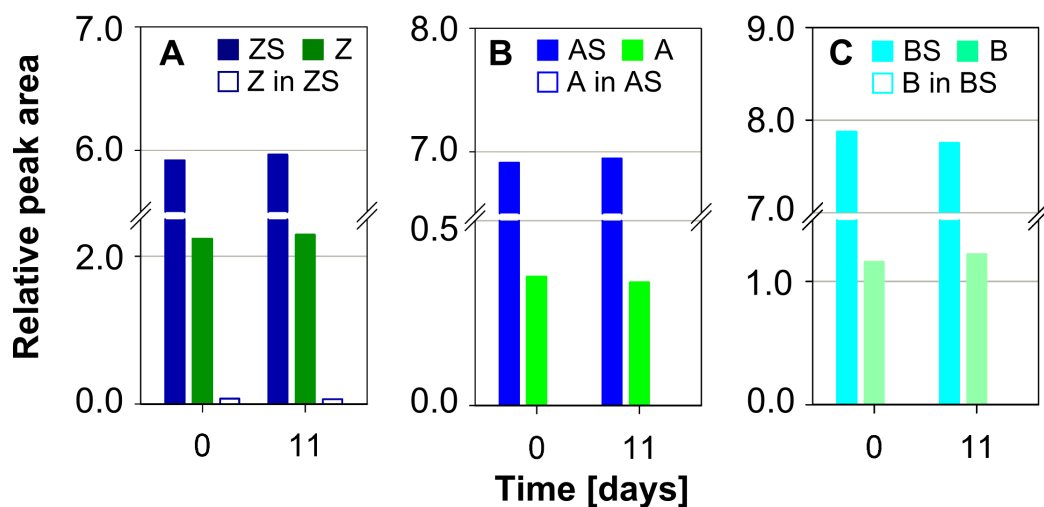


Figure 2.3: UPLC-MS screening of the sulfated metabolites ZS (A), AS (B) and BS (C) and their non-sulfated forms after 0 and 11 days in sterile Marine Broth (MB) at 30 °C. Internal standard used to normalize peak areas was *trans*-cinnamic acid.

that under the sterile conditions applied during the bioassays neither concentrations of sulfated or non-sulfated forms changed in ZS, AS and BS and that only in the ZS sample minor amounts of the non-sulfated Z from the synthesis were present. This content was estimated to be less than 1%. The compounds are thus stable even under the prolonged incubation under sterile conditions.

2.2.3 Hydrolysis of sulfated phenolic acids by an arylsulfatase

This experiment was supposed to provide insights, if the sulfated phenolic acids used during this study are in general accepted substrates for enzymatic hydrolysis by an arylsulfatase. So far no study has been performed on sulfated aryls bearing a carboxylic acid moiety either directly attached to the ring, as it is the case for the sulfated benzoic acids used (BS, oBS, mBS), or via an alkyl chain as in 3,4CAS. Substrates in arylsulfatase studies hence published had either stronger electron withdrawing (NO_2) or nucleophilic groups (NH_2) or were more complex. An overview is provided by Dodgson *et al.* from 1956 and Hanson *et al.* from 2004.[135, 136]

During this experiment no measures to quantify turnover rates were taken. In case of an apparent susceptibility of the substrates towards the sulfatase, the proto-

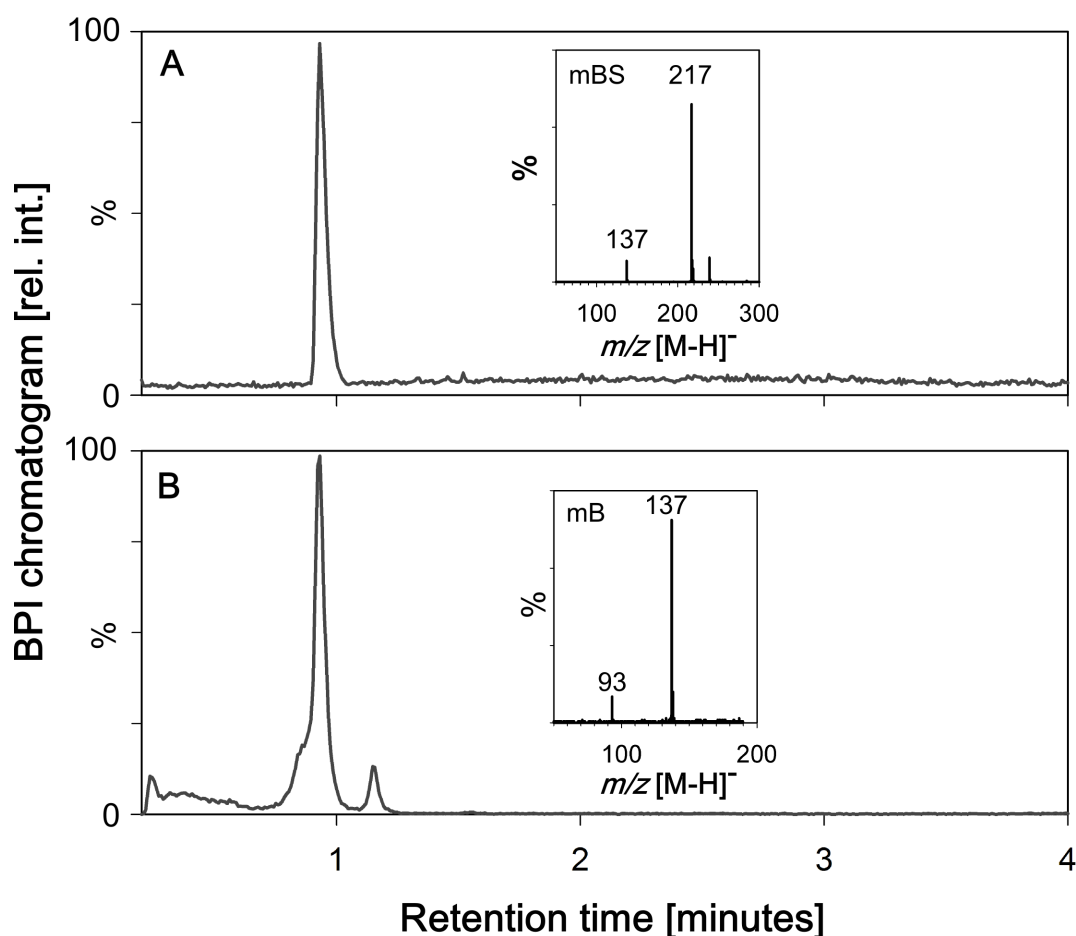


Figure 2.4: UPLC-MS monitoring of the enzymatic cleavage of mBS by an arylsulfatase. **A:** BPI chromatogram showing pure mBS at 0.92 minutes and the corresponding mass spectrum before sulfatase treatment. **B:** BPI chromatogram showing pure mBS at 0.92 minutes, and its cleavage product mB at 1.15 minutes with the corresponding mass spectrum, after sulfatase treatment.

col was supposed to be used to hydrolyze presumably sulfated metabolites from *N. annulata* for further structure analysis (see section 2.3). Additionally, it was assumed that these substrates might then also be hydrolyzed during bioassays as soon as bacteria possess sulfatase activity and, thus, their impact on these organisms might be changing during the assay. It is known that arylsulfatases are highly conserved enzymes. Therefore, the susceptibility for the substrates should be independent from the organism the sulfatase originates from.[136]

Enzymatic hydrolysis experiments of the synthetic phenolic sulfates 3,4CAS, BS, o- and mBS were performed with an arylsulfatase type VI from *Aerobacter aerogenes*,

according to a published protocol.[137] All samples were measured by UPLC-MS in methanol before sulfatase addition to confirm the absence of non-sulfated forms. Samples were then incubated with the sulfatase in TRIS buffer at 37°C. After 1.5 hours, solvents were evaporated, the samples dissolved again in the original amount of methanol, separated from precipitating salts and again measured by UPLC-MS. Chromatograms were then screened for the presence of non-sulfated forms, recognizable by the loss of m/z -80, compared to the m/z values of the sulfated substrates. In 3,4CAS (Figure 9.7, appendix), BS (Figure 9.8, appendix) and mBS (Figure 2.4) samples their non-sulfated forms were all present after sulfatase treatment, but in none of these samples hydrolyzation was completed within this time frame. The oBS sample showed no trace of the non-sulfated form salicylic acid after 1.5 hours. As discussed in section 2.1.4 oBS was highly unstable. After incubation with buffer and sulfatase, polymers of salicylic acid and the intra-molecular rearrangement product, visible by the shift of a peak with m/z 217 $[M-H]^-$ to a much earlier retention time, were immediately present. Since oBS did not play a further role in any of the performed bioassays, the experiment was not repeated. It thus cannot be distinguished if either the time frame was not sufficient for sulfatase hydrolysis, if the substrate released enzyme inhibiting components during transformation, or if the substrate simply is not susceptible to arylsulfatase activity. So far, the site of substitution in the aromatic ring close to the sulfate ester did not matter, as discussed in a study by Dodgson *et al.* from 1956, rather the nature of the substituents.[135] In case of the sulfated benzoic acids however, this was always the carboxylic acid moiety.

2.2.4 Summary of sulfated phenolic acid stability

The performed experiments concerning the stability of sulfated phenolic acids in environments of UPLC-MS measurements and under conditions that were assumed to might occur during bioassays showed that these molecules are relatively stable against hydrolysis by mineral acids. In contrast, they were hydrolyzed enzymatically within a short time by an arylsulfatase, with one exception (oBS). 3,4CAS was hydrolyzed completely by HCl and partly H₂SO₄ within 4 hours, but only at a

pH of 1 and a temperature of 80 °C. The conditions were neither reached during synthesis nor UPLC-MS measurements or bioassays. In sterile medium AS, BS and ZS proved also to be stable for 11 days at 30 °C. Only in the presence of an arylsulfatase were mBS, BS and 3,4CAS already partly hydrolyzed after 1.5 hours. This indicates that during bioassays including bacteria, which might possess an arylsulfatase, the stability of the sulfated phenolic acids whose impact is to be tested, should be monitored continuously by UPLC-MS. Only this way can be assured to which substance a possible observed impact can be assigned to.

2.3 Identification of sulfated phenolic acids in *Dasycladus* spp.

2.3.1 Sulfated phenolic acids in *Dasycladus vermicularis*

The established synthesis of highly pure standards of sulfated phenolic acids allowed the identification of the novel sulfated metabolites detected by Dr. Matthew Welling in members of the Dasycladaceae.[56] For identification of the two unknown phenolic sulfates in *D. vermicularis* (m/z 217 [M-H]⁻ and 231 [M-H]⁻) by UPLC-MS co-injection experiments, solvent from a methanolic algae extract was removed and the residue taken up in UPLC solvent composition A (98 % water, 2 % acetonitrile, 0.1 % formic acid, section 9). Dissolution in A and further dilution when necessary, considerably improved background noise and peak shape of these metabolites during measurement and near symmetrical peaks could be obtained. Peak symmetry was important for recognizing distortions, that might hint for closely but not co-eluting peaks. For the identification of the first sulfated metabolite in *D. vermicularis* extract, the three constitutional isomers oBS, mBS and BS were tested. The isomers oBS and mBS could be excluded due to their different retention times and co-injection resulted both times in two separated peaks. BS showed a similar retention time and mass spectrum as the first sulfated metabolite in *D. vermicularis* extract. Therefore, an external multipoint calibration by UPLC-MS of synthetic BS

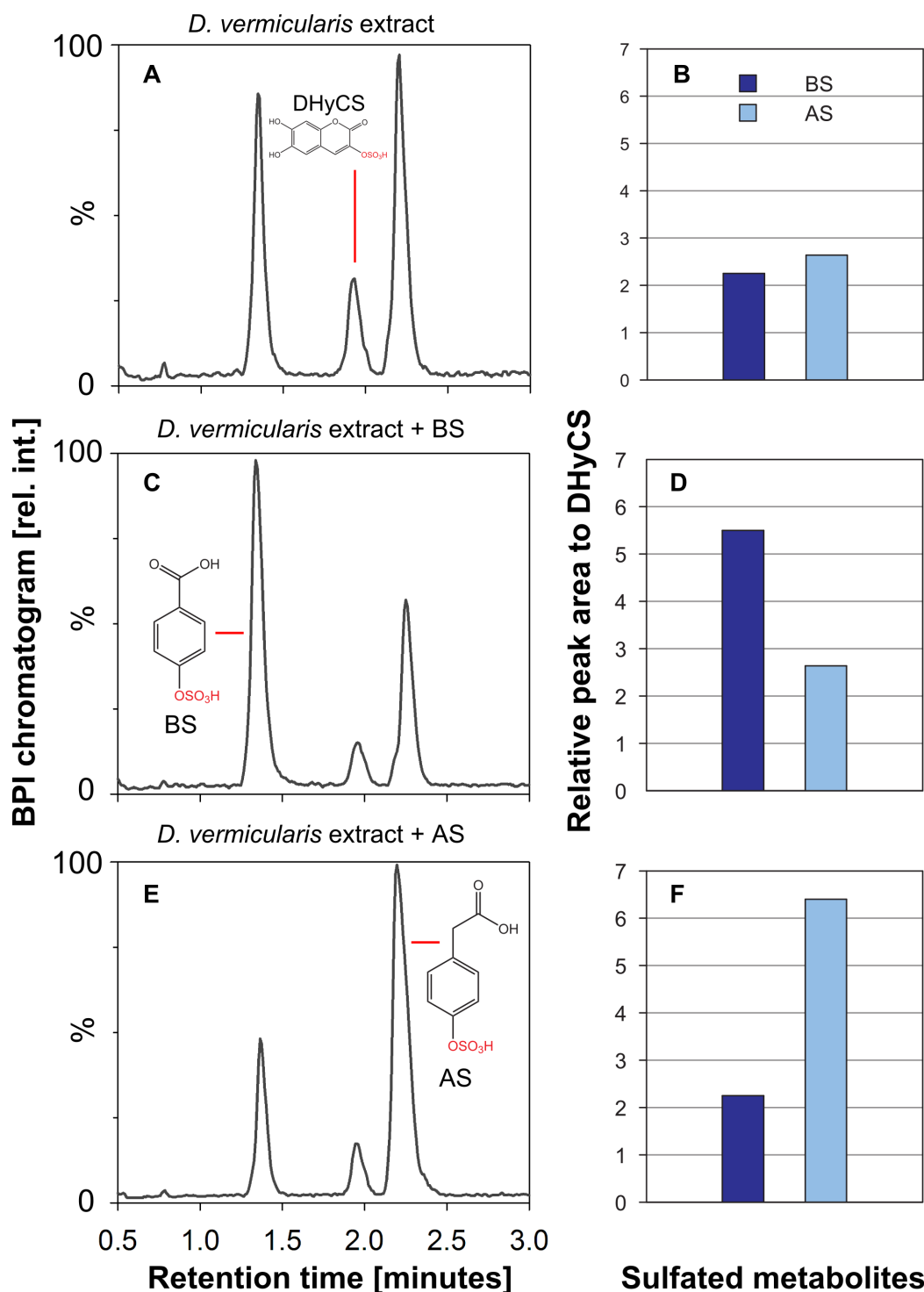


Figure 2.5: UPLC-MS co-injection experiment of *D. vermicularis* extract in solvent A with AS and BS. DHyCS was used as internal standard for peak area normalization. **A, B:** *D. vermicularis* extract, with the peak areas of BS (1st peak) and AS (3rd peak) normalized to DHyCS (2nd peak). **C, D:** Co-injection of synthetic BS and *D. vermicularis* extract with an increase of BS peak area (2 fold). **E, F:** Co-injection of synthetic AS and *D. vermicularis* extract with an increase of AS peak area (2.4 fold). In none of the samples was peak symmetry affected upon co-injection.

was performed, ranging from 10 to 80 $\mu\text{g ml}^{-1}$, in steps of 10. Comparison of peak areas showed that the 20 $\mu\text{g ml}^{-1}$ sample most closely represented the concentration in the extract. Hence, equal volumes of these two samples were thoroughly mixed, the solvent evaporated and the sample taken up in half the original volume of solvent A. The original extract and the extract with the additive were measured by UPLC-MS. Peak areas in the original extract (Figure 2.5 A) and the extract with the additive (Figure 2.5 C) were compared using DHyCS, present in the extract of *D. vermicularis*, as an internal standard. Comparison of relative peak areas showed an approximately doubled peak area (factor 2) in the extract with BS, compared to the pure extract (Figure 2.5 B and D). The same procedure was applied for co-injection of AS. Here the concentration during calibration ranged from 50 to 400 μg , in steps of 50. The most closely related sample was that of 150 $\mu\text{g ml}^{-1}$. The peak area in the sample with additional AS was increased by a factor of 2.4 (Figures 2.5 E and F). Neither upon addition of BS nor AS could a significant change in peak symmetry or the presence of a shoulder be observed (Figures 2.5 A, B and C). A shoulder would hint close but not co-eluting peaks. In the pure extract, peaks showed a minimal tailing at 10 % peak height, with tailing factors T of 1.12 for BS (a=0.17 and b=0.19 cm) and 1.18 for AS (a=0.17 and b=0.2 cm). *D. vermicularis* extract with additional BS still had a symmetric peak with a T value of 1.18 (a=0.17 and b=0.20 cm), extract with additional AS a T value of 1.33 (a= 0.15 and b=0.2 cm). The increased tailing factor upon addition of AS to the extract might be due to the fact that the peak area was more than doubled. It could be observed that the peak symmetry of sulfated phenolic acids is highly concentration dependent and the emergence of tailing sensitive to small increases in concentration. Thus, in *D. vermicularis* two further, hence unknown sulfated metabolites, 4-(sulfooxy)benzoic acid (BS) and 4-(sulfooxy)phenylacetic acid (AS) could be identified by using highly pure synthetic standards in UPLC-MS co-injection experiments.

2.3.2 Sulfated phenolic acids in *Cymopolia barbata*

In methanolic extracts of *C. barbata* Dr. Matt Welling found three substances with a m/z of $[M-H-80]^-$, indicating the presence of three sulfated metabolites. The first peak had a mass of m/z of 289 $[M-H]^-$, the second peak of 217 $[M-H]^-$ and the third of 273 $[M-H]^-$. The third peak was already identified as DHyCS, also present in *D. vermicularis*.^[56]

Unfortunately, there was none of the original extract left, but the alga was available from an aquarium shop in Florida (USA). The alga was ordered two times and extracted immediately after arrival by Dr. Jennifer Sneed in Florida (USA) and Stefanie Wolfram in Georgia (USA). In both cases, the water the algae arrived in was rather brownish and smelled strongly. Dr. Matt Welling used freshly harvested algae and liquid nitrogen to shock freeze the plants before grinding and thus quenched sulfatase activity initiated by wounding during extraction. During the extractions of the commercial algae in Florida only cold methanol (-24°C) was available, in Georgia, liquid nitrogen was used to extract *C. barbata*. In UPLC-MS measurements, metabolic profiles of both experiments showed no traces of the m/z 289 $[M-H]^-$ metabolite and in both extracts traces of m/z 193 $[M-H]^-$ with a later retention time than m/z 273 $[M-H]^-$ were present, indicating the presence of non-sulfated 3,6,7-trihydroxycoumarine (THyC). This might be an indicator of enzymatic activity before or during extraction due to a wound response and a general high stress level caused by the not optimal conditions the alga faced during delivery. This might be an explanation why m/z 289 $[M-H]^-$ could not be detected anymore, and THyC was detectable additionally to DHyCS, in higher amounts as observed before.^[56] Instead, traces of another metabolite with a loss of m/z -80 were detectable with a m/z of 203 $[M-H]^-$. It showed an UV-Vis absorption band in the aromatic region and was thus assumed to be a degradation product of the metabolite m/z 289. Here, the three isomers 2-, 3- and 4MOPS were co-injected, but none of these standards showed a co-eluting peak. However, the metabolite with m/z 217 $[M-H]^-$ seemed not to be affected and could be identified as BS by the procedure described for *D. vermicularis*. Peak shape of BS in pure extract and extract with BS added both

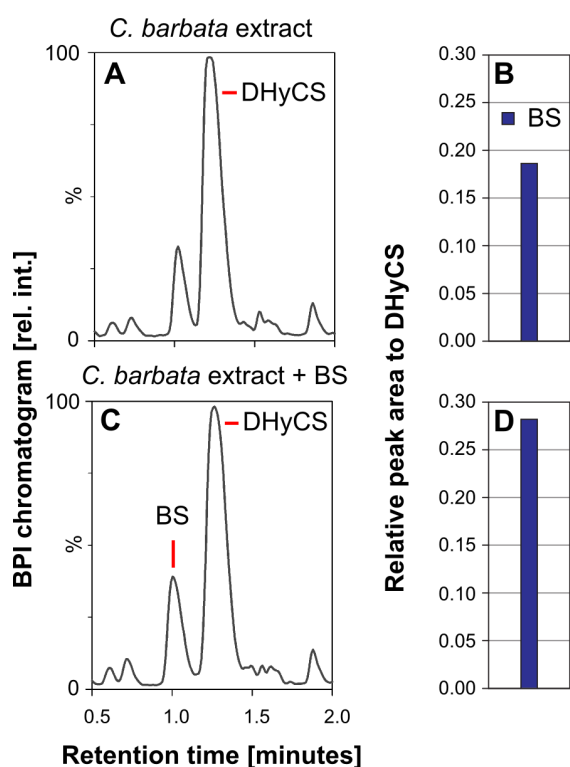


Figure 2.6: UPLC-MS co-injection of *C. barbata* extract in solvent A with synthetic BS. DHyCS was used as internal standard for peak area normalization. **A, B:** *C. barbata* extract and relative peak area of BS. **C, D:** *C. barbata* extract plus BS. Relative peak area of BS is increased without a significant change in peak symmetry.

showed a tailing factor T of 1.71 ($a=0.2$ and $b=0.36$ cm) (Figure 2.6 A) and of 1.73 ($a=0.22$ and $b=0.38$ cm) (Figure 2.6 C). There was no shoulder or significant change in peak symmetry suggesting the substance identity. Upon addition of BS, the peak area in the combined sample of pure extract and BS in A doubled (Figures 2.6 B and D). This confirms that *D. vermicularis* and *C. barbata* share this secondary metabolite additionally to DHyCS.

2.3.3 Sulfated phenolic acids in *Neomeris annulata*

In *N. annulata* methanolic extracts of both wounded and unwounded algae, two closely eluting metabolites, with identical m/z values of 259 and each with a fragment of $[M-H-80]^-$ were found.[56] Since all so far identified sulfated phenolic acids in the Dasycladaceae (BS, AS) carried the sulfate group in *para*- position, the sulfated isomers of 3,4CAS seemed promising candidates. Additionally, the non-sulfated form 3,4-dihydroxycinnamic acid (caffeic acid), is a well known secondary plant metabolite, present for example in coffee and the approximately 600 members of the Oleaceae (e.g. olives).[138] It was also identified in seagrass, namely in *Zostera ma-*

rina in addition to ZS, which also carries a sulfate ester group in *para*- position.[72] Unfortunately, neither MS/MS spectra nor retention times (R.T.) of the synthetic 3,4CAS isomeric mixture (Figures 2.7 D-F) were identical to the metabolites in the *N. annulata* extract (Figures 2.7 A-C). The MS/MS spectra of the synthetic 3,4CAS only had one dominant fragment of m/z 179 [M-H-80]⁻ (Figures 2.7 E, F), whereas the metabolites from the alga extract had an additional fragment of m/z 187 [M-H-72]⁻ (Figures 2.7 B,C). Co-injection of 3,4CAS and *N. annulata* extract showed clearly separated peaks (Figure 2.7 D). MS/MS spectra of the isomeric mixture of synthetic 2,3CAS also were not identical to the algal metabolites, showing additional fragments of m/z 215 [M-H-44]⁻, presumably the loss of CO₂, and m/z 179 [M-H-80]⁻ (Figures 2.7 H, I). Also the retention times of 2,3CAS were clearly different (Figure 2.7 G). The remaining two sulfated dihydroxycinnamic acids 2,4CAS (by chlorosulfonic acid) and the pure isomer 2-hydroxy-5-(sulfoxy)cinnamic acid (2,5CAS) also showed the fragment of m/z 179 [M-H-80]⁻ and additionally the fragment m/z 215 [M-H-44]⁻ (data not shown). This seems a common fragmentation pattern of dihydroxycinnamic acids with a substituent in *ortho*- position. Thus, these two isomers of dihydroxycinnamic acids could also be excluded. The MS/MS fragmentation patterns in the synthetic standards 3,4CAS, 2,3CAS, 2,4CAS and 2,5CAS could all be well interpreted with respect to their chemical nature. 3,4CAS seemed the most stable molecule, only showing the loss of SO₃ (-80). All derivatives carrying a hydroxy group in *ortho*-position, additionally showed a loss of CO₂ (-44). The metabolites of the *N. annulata* extract, however, additionally to the fragment [M-H-80]⁻ showed another one with [M-H-72]⁻, which could indicate the loss of C₂H₄CO₂. This would contradict the assumption of a double bond moiety in the side chain. Unfortunately, this fragment was not always reproducible by the ESI-QToF-MS system used. With the available amount of *N. annulata* extract, MS/MS spectra recorded with the QToF system were marked by a low signal to noise ratio. This additionally caused difficulties distinguishing background signals from metabolite fragments, that might have hinted further structural informations. Thus the algae extract was investigated also on a triple quadrupole mass spectrometer

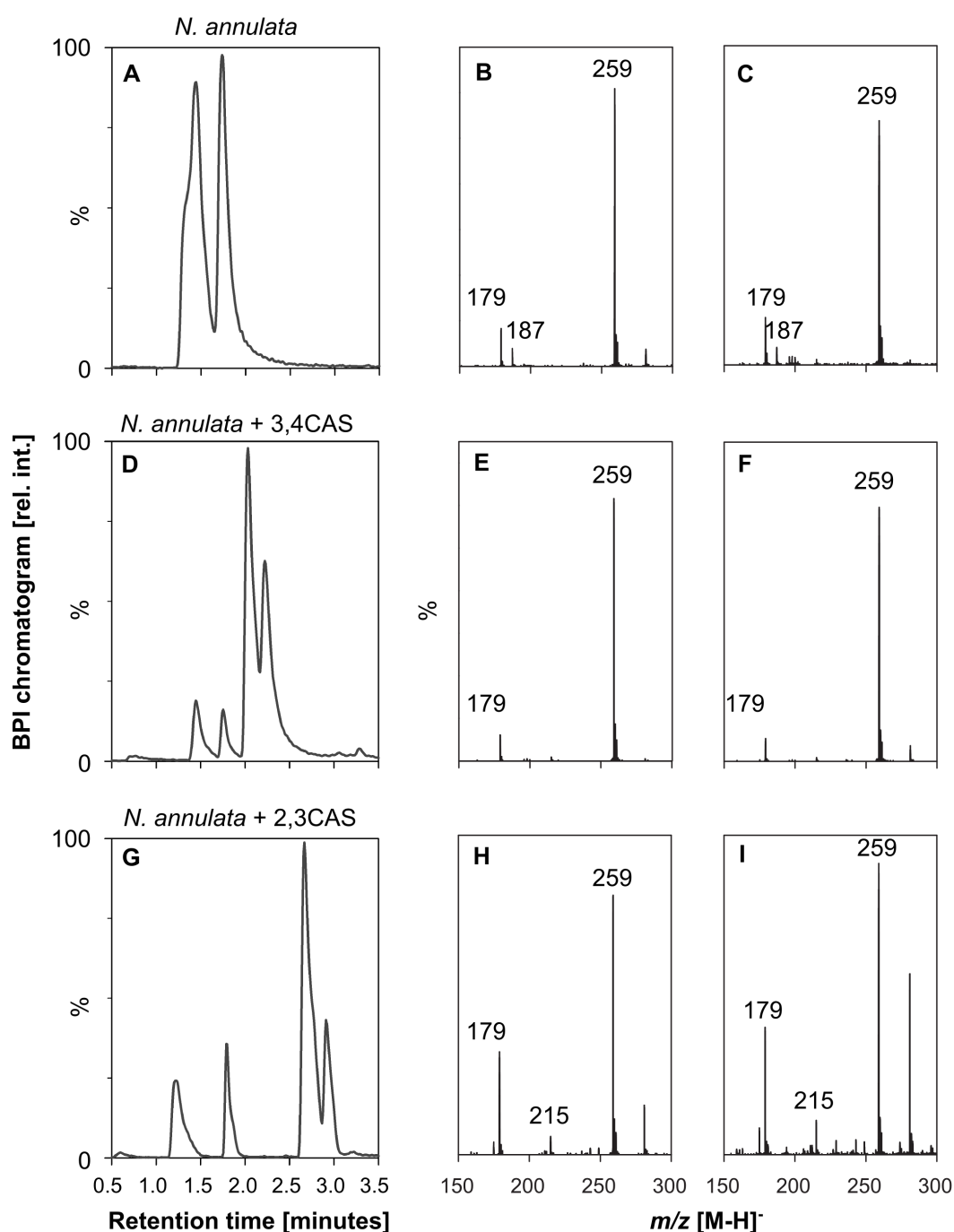


Figure 2.7: UPLC-MS co-injection of *N. annulata* extract in methanol with synthetic 3,4CAS and 2,3CAS. **A:** Chromatogram of *N. annulata* extract. **B:** MS/MS of peak one (**A**) at 1.45 minutes. **C:** MS/MS of peak two (**A**) at 1.74 minutes. **D:** Chromatogram of *N. annulata* extract plus synthetic 3,4 CAS. **E:** MS/MS of peak three (**D**) at 2.02 minutes. **F:** MS/MS of peak four (**D**) at 2.21 minutes. **G:** Chromatogram of *N. annulata* extract plus 2,3CAS. **H:** MS/MS of peak three (**G**) at 2.67 minutes. **I:** MS/MS of peak four (**G**) at 2.95 minutes. Retention time deviations in *N.annulata* extracts are due to different concentrations and the timespan of a few months between measurements of 3,4CAS and 2,3CAS.

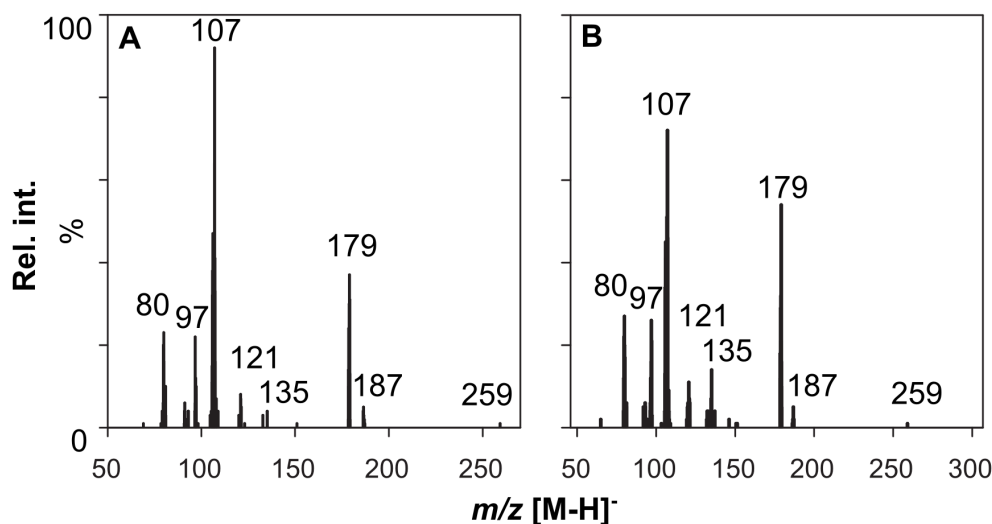


Figure 2.8: Triple-Quad MS/MS of *N. annulata* extract in methanol showing the two isomers (A, B) with m/z 259 $[M-H]^-$.

(QqQ-MS). The product ion scan mode allowed first a screening for the pseudo molecular ions of the two isomers m/z 259 $[M-H]^-$ and subsequent further fragmentation. With this technique, the fragments of m/z 187 $[M-H-72]^-$ and m/z 179 $[M-H-80]^-$ could be confirmed. Additionally fragments of m/z 135 $[M-H-80-44]^-$, 121 $[M-H-80-58]^-$, 107 $[M-H-80-72]^-$ and 97 $[M-H-80-82]^-$ could be found (Figures 2.8 A,B). Fragment m/z 135 indicated the presence of a carboxylic acid moiety and fragment m/z 121 might indicate the loss of CO_2 together with a CH_2 group. Fragment m/z 107 showed again the loss of a unit with m/z 72 together with the loss of m/z 80. These fragments contradict the assumption that the two compounds of *N. annulata* are based on a dihydroxycinnamic acid backbone. As mentioned before, the low availability of algae extract did not allow the use of NMR techniques for further structural analysis.

2.3.3.1 Hydrolysis of sulfated metabolites in *N. annulata*

One last attempt to identify the unknown metabolites in *N. annulata* was to cleave the ester that was hence assumed to be a sulfate ester either enzymatically or via acid hydrolysis. For both methods a protocol has been established with model sulfated

phenolic acids, such as 3,4CAS (see section 2.2). In case of successful hydrolysis, the metabolite should be analyzed by GC-MS measurements, which might provide further structural information due to increased fragmentation by electron impact ionization (EI) and the databases available for such measurements.

Acid hydrolysis of methanolic *N. annulata* extract by HCl was performed as described in section 9.3.2. Briefly, a control sample was measured before the acid treatment by UPLC-MS. The acid treated sample was divided into three parts. 100 μl were diluted once with solvent A (sample 2) and another 100 μl with methanol (sample 1). The remaining 300 μl were extracted with methyl-tert-butylether (MTBE), which proved a suitable extraction solvent for phenolic acids from aqueous solution (sample 3). The organic phase of sample 3 was evaporated to dryness and taken up in 150 μl of methanol. Samples 1-3 were screened by UPLC-MS for compounds with m/z 179 $[\text{M-H}]^-$, which would indicate a sulfate ester hydrolysis product. However, in neither of these samples could a substance of m/z 179 $[\text{M-H}]^-$ be found. Instead, traces of m/z 259 $[\text{M-H}]^-$ in samples 1 and 2 were still present additionally to a new compound of m/z 121 $[\text{M-H}]^-$ in samples 1-3. This compound was especially dominant in sample 3. Since a fragment of m/z 121 was also found by QqQ-MS measurements in the algal extract, it seemed reasonable that this was a product from acid degradation of the two compounds of interest with the m/z of 259 $[\text{M-H}]^-$. Sample 3 was thus derivatized according to a protocol from [139] for GC-MS analysis. Unfortunately, this measurement did not provide further insights. Besides the internal standards nothing was detected that might be related to the m/z 121 fragment, although it was the dominant compound in the UPLC-MS sample, which in general is rather less sensitive than GC-MS. It can of course not be excluded that the compound was destroyed during derivatization.

Since the hydrolysis experiment indicated acid labile compounds, enzymatic cleavage seemed a further possibility. For sulfatase treatment 400 μl of concentrated methanolic *N.annulata* extract were collected by UPLC UV-Vis fractionation in order to exclude any other components in the extract that might have an inhibiting effect. The solvent was evaporated and the extract taken up in 220 μl of deion-

ized water. As during the pre-experiments a control measurement was recorded by UPLC-MS. Then the protocol for enzymatic cleavage of model sulfated phenolic acids was applied (see section 2.2). After 1.5 hours no trace of a cleavage product with m/z 179 $[M-H]^-$ could be observed, but both metabolites with m/z 259 $[M-H]^-$ were still present. For the model substrates BS, mBS and 3,4CAS this was always a sufficient time for at least partial hydrolysis. A longer incubation time (4 hours) also did not change the result. Unfortunately, with the applied techniques and the limited material available no further insights could be gained that might lead to structure elucidation.

Although it can not be excluded that the two unknown compounds in *D. vermicularis* were simply not suitable substrates for the applied arylsulfatase protocol, the failure of both hydrolysis methods could also indicate that the loss of -80 found in *N. annulata* originates from the cleavage of a phosphate ester (" PO_3H ") instead of a sulfate ester. Additionally, a sulfonic acid moiety might be a further reason for the observed loss of m/z 80. The UV-Vis data obtained by Dr. Matthew Welling indicated an aromatic structure [56] and the QqQ-MS data during this study confirmed the presence of a carboxylic acid moiety connected to a CH_2 group. The loss of m/z 72 might additionally hint the presence of a further CH_2 group.

2.3.4 Summary of sulfated metabolites from *Dasycladus* spp.

In two members of the Dasycladaceae, *C. barbata* and *D. vermicularis*, hence unknown sulfated phenolic acids could be identified by UPLC-MS co-injection experiments. BS was found in addition to DHyCS in both algae, AS only in *D. vermicularis*. Despite the relationship of *D. vermicularis*, *C. barbata* and *N. annulata*, only the first two shared common metabolites, none of which were found in *N. annulata*. It is thus possible that the two unknown compounds in *N. annulata* are structurally not related to the identified ones. Further possibilities for structure elucidation would be the treatment with either a phosphatase or the use of alkalines to cleave a potential sulfonic acid. The use of special derivatization agents for these classes of compounds would also be worthwhile to test for further GC-MS measurements.

A question arising now was, if it is possible to assign a role of these secondary metabolites for *D. vermicularis* and *C. barbata*, since they were not found to be involved in their wound response, as was the other sulfated metabolite DHyCS.[56] Of additional interest was also the function of sulfatations and in what way the sulfate ester influences their biological activity.

The non-sulfated forms of both AS and especially BS, 4-hydroxyphenylacetic acid (A) and 4-hydroxybenzoic acid (B), are well known secondary plant metabolites. Both A and B were found in Greek aromatic plants, whose extracts showed antioxidant and antimicrobial activity.[140] Additionally, B was found in several mushroom species with antimicrobial activity [141] as well as in carrots (*Daucus carota*), where it seemed to play a role in plant defense [142] and in members of *Olea europaea*, where e.g. olives belong to [138]. Besides terrestrial plants, B was also identified in freshwater and marine algae [143] as well as in aqueous acidic extracts of various seagrasses, among them *Zostera marina* [144, 145]. Especially, the sodium salt of B showed antifouling activity against freshwater bacteria when dispersed in medium or included in silicone coatings.[146, 147] On the other hand, marine sulfate esters are not uncommon as metabolites and various properties were attributed to them. The structurally closely related ZS has been found to act as a strong antifoulant against freshwater and marine bacteria.[72, 74–76, 78, 79, 81] Aliphatic sulfate ester excreted by the water flea of the genus *Daphnia* caused the unicellular green alga *Scenedesmus subspicatus* to form colonies.[59] Sulfated polysaccharides found in species of the siphonous green algae *Codium* [60–64] have been reported to possess an immunostimulating effect [64] and exhibit strong antiviral activity in an early stage of virus binding, host cell penetration and viral reproduction[66–69]. Additionally, they showed strong anticoagulant activity, which increased with an increasing amount of sulfatation.[70, 71]

The following chapters are thus dedicated to unveil a possible function of the identified metabolites. Due to the close structural similarity to ZS, the impact of AS, BS and ZS and their non-sulfated forms on growth and biofilm formation of marine bacteria was investigated.

3 Filter disc assay

Filter disc assays are standard procedures for testing the impact of various compounds in different concentrations on bacterial growth. Small filter papers containing the test compounds are therefore placed on agar plates, where a bacterial pre-culture has been plated shortly before. The filter paper will release the substance into the surrounding agar and bacteria affected by it will not grow within a certain diameter surrounding the filter. By assuming similar diffusion coefficients of the compounds to be compared, the size of the inhibition zone (ZOI) reflects the bacterial response towards each treatment.

Compounds tested here were synthetic analogs of the two sulfated phenolic acids AS and BS, identified in members of the Dasycladaceae, as well as their non-sulfated forms A and B. The non-sulfated forms were found to possess among others, antimicrobial properties on a variety of organisms, as already discussed in section 2.3. During this assay their impact on growth of marine bacteria cultivated in our laboratory was investigated, namely *Pseudoalteromonas tetraodonis* (H11), *Pseudoalteromonas carrageenovora* (H92), *Cellulophaga lytica* (C.L.), *Dinoroseobacter shibae* (DINO), and three species isolated from *Ulva* spp. MS1, MS2 and MS3. This short experiment was supposed to provide first insights into how active the phenolic acids A and B are on these bacteria and in how far their activity is influenced by the sulfate ester present in AS and BS. Control plates with either no filters and some just treated with the solvent used to dissolve different treats were grown to ensure, that any observed effect is solely due to the treatment and not caused by a general condition of the culture or a toxicity of the solvents used. As a positive inhibition control different antibiotics, namely ampicillin, penicillin, streptomycin and an antibiotics mix of streptomycin, penicillin and neomycin (mix) were used to test the

hence unknown sensitivity of the applied bacteria towards these antibiotics. Final amounts of all compounds on the filters were 500 µg, 50 µg, 5 µg and 500 ng. After three days incubation at RT the zone of inhibition (ZOI) was estimated for each treatment.

All bacteria grew well under the conditions applied. After three days all plates with no filter papers or just those previously treated with different solvents (water, ethanol) showed a dense and homogeneous bacterial film.

3.1 Impact of AS, BS, A and B on bacterial growth

The sulfated phenolic acids AS and BS, as well as their non-sulfated forms A and B showed a small ZOI in all cultures ranging from 0.5 to 1 cm, but only when as much as 500 µg of each compound were applied on the filter (Figures 3.1 A-G). In each of the seven cultures the growth inhibiting effect of the non-sulfated forms seemed slightly higher (30 to 35 %) compared to the corresponding sulfate esters. The ostensible larger impact of the non-sulfated forms can presumably be ascribed to the fact that instead of equimolar, equal weights were used. Thus, samples containing the non-sulfated forms (A, B) contained about 35 % more substance on a molecular base than the sulfated ones. Although a growth inhibiting influence could be observed independent of the bacterial species tested, the concentration in which these additives became effective was rather high. Due to the differences concerning the molecular content of the sulfated and the non-sulfated forms, it seems reasonable to assume that the presence of the sulfate ester had no influence. Since the stability of the four additives AS, BS, A and B in presence of the tested marine bacteria was not monitored, it can not be distinguished if the substances simply only had a small impact on their growth, or if they were metabolized and detoxified.

In contrast to the universal impact of the sulfated phenolic acids and their non-sulfated forms was the efficiency of the tested antibiotics species dependent. None of the antibiotics used could inhibit growth of either test bacterium with an amount

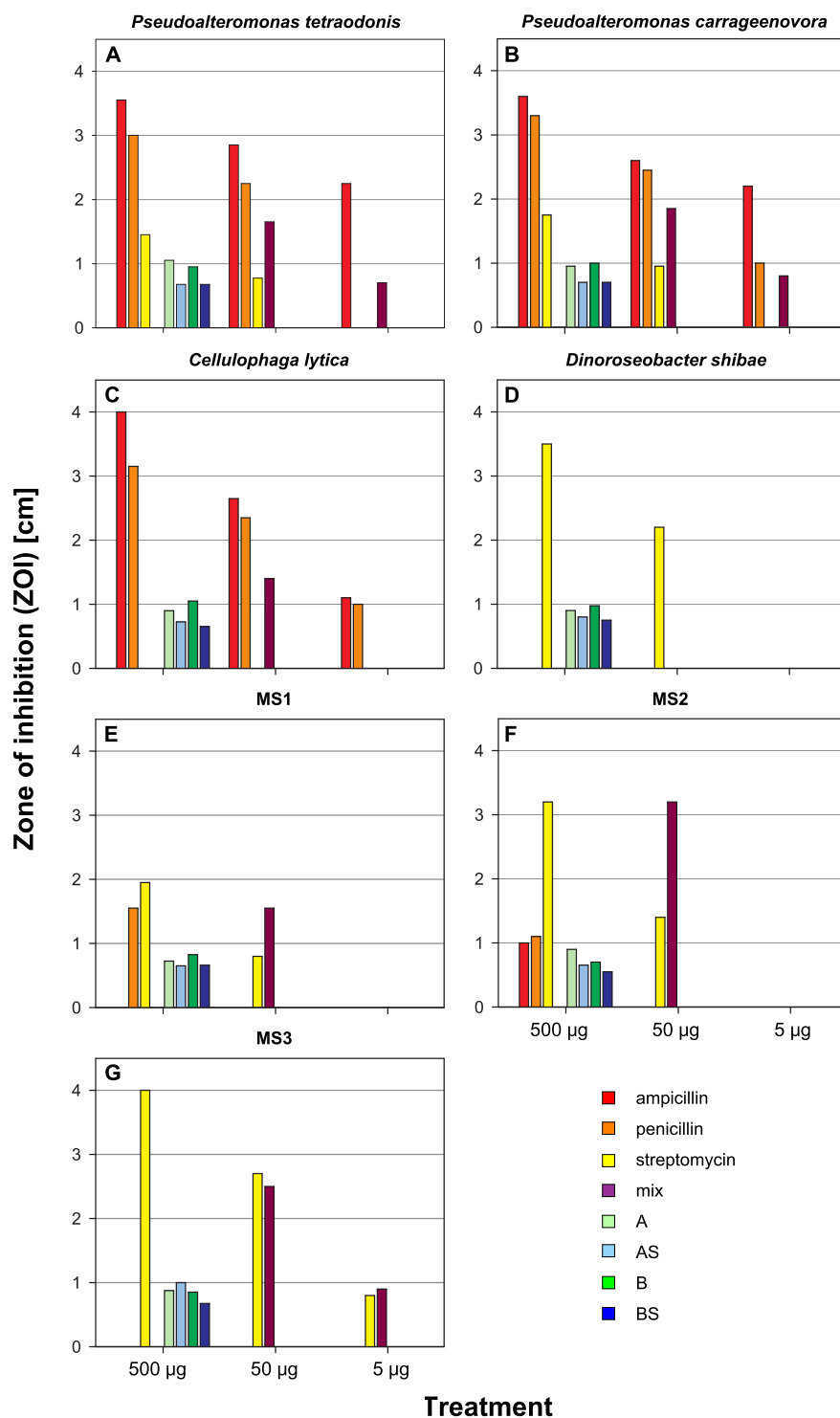


Figure 3.1: Filter disc assay with the phenolic acids A, B, and the sulfated phenolic acids AS, BS and the antibiotics ampicillin, penicillin, streptomycin and a mix (streptomycin, penicillin, neomycin). Zones of inhibition (ZOI) were estimated from 5, 50 and 500 ug of additive on the filter. (A) ZOI of additives on *P. tetraodonis*. (B) ZOI of additives on *P. carrageenovora*. (C) ZOI of additives on *C. lytica*. (D) ZOI of additives on *D. shibae*. (E) ZOI of additives on MS1. (F) ZOI of additives on MS2. (G) ZOI of additives on MS3.

as low as 500 ng. Growth of *P. tetraodonis* was inhibited by ampicillin and the mix applying only 5 µg on the filter. Penicillin and streptomycin could inhibit growth with 50 µg on the filter, but not below (Figure 3.1 A). *P. carrageenovora* was affected by ampicillin, penicillin and the mix with an amount as low as 5 µg, whereas streptomycin could only inhibit growth starting with 50 µg (Figure 3.1 B). *C. lytica* showed a resistance against streptomycin even at 500 µg on the filter. The mix was effective on this species starting from 50 µg, ampicillin and penicillin inhibited growth even at 5 µg on the filter (Figure 3.1 C). *D. shibae* showed a resistance against ampicillin, penicillin and the mix and was only inhibited by streptomycin at 50 µg and higher (Figure 3.1 D). The *Ulva* spp. isolate MS1 showed a resistance towards ampicillin, penicillin could only inhibit growth with the high amount of 500 µg, and streptomycin and the mix inhibited growth with 50 µg and higher (Figure 3.1 E). MS2 was inhibited by the mix and streptomycin applying 50 µg and higher, but by ampicillin and penicillin only with 500 µg on the filter (Figure 3.1 F). MS3 also was resistant against ampicillin and penicillin, but the mix and streptomycin could inhibit growth even at 5 µg on the filter (Figure 3.1 G).

Nevertheless, a direct, quantitative comparison of the effectiveness of the various antibiotics should be performed with care due to their different molar masses. The antibiotics neomycin and streptomycin have a much higher molecular weight (614.64 g mol⁻¹ and 581.57 g mol⁻¹) than ampicillin (349.41 g mol⁻¹) and penicillin (312.38 - 359.40 g mol⁻¹), thus, by using the same amount it has to be considered that antibiotics with a higher molecular weight might be more effective, since the actual amount of molecules present is lower.

3.2 Summary of the filter disc assay

This assay was a pre-experiment to provide first insights into the impact of the isolated substances AS and BS and their non-sulfated forms A and B on growth of marine bacteria. Antimicrobial effects of B have been discussed in the literature, although not with the species tested here.[138, 140, 141] It additionally provided

first insights, which bacterial species respond to a specific antibiotic treatment and what a reasonable concentration would be.

Since the phenolic acids, with and without sulfate ester, showed only a small impact on bacterial growth in high amounts, it can be assumed that the tested species are rather tolerant towards these compounds. Even at the highest amount applied (500 μg), ZOI was always smaller (0.5 - 1 cm) for AS, BS, A and B then for an effective antibiotic with the same amount applied (1 - 4 cm). Whereas the activity of the different antibiotics was highly species dependent, the small influence of the sulfated and non-sulfated phenolic acids seemed universal and no resistance towards these compounds could be observed. Thus, AS, BS, A and B seem reasonable candidates to be tested as low-toxic antifouling agents in the biofilm assays discussed in the following chapters, due to their structural similarity to the known antifoulant ZS.

4 Biofilm assay at the air-liquid-interface

This assay was initially performed to investigate, if the novel sulfated phenolic acids AS and BS, found in members of the Dasycladaceae, due to their structural similarity to zosteric acid (ZS) show a similar antifouling activity as the latter.[72, 74–76, 78, 79, 81] A fast method for investigating biofilm formation over time is the microtiter dish assay, where a biofilm is grown on walls of a multiwell plate.[148, 149] This method allows simultaneous monitoring of the impact of several additives on biofilm formation. Additionally, can bacterial growth be monitored by measuring the optical density (OD) directly within the plate until the start of biofilm formation. Biofilm formation, on the other hand, can only be evaluated indirectly by staining with a fluorophore or a dye that after subsequent dissolution can be quantified by absorption measurements.

During this assay two bacteria, on which a biofilm inhibiting effect of ZS has been shown in earlier studies were used. The biofilm of a non-pathogenic *Escherichia coli* (ATCC 25404) strain was found to be reduced by ZS in a microtiter dish assay by Villa *et. al* in 2010.[78] Another study which investigated biofilm formation on silicone coated glass plates could show that fouling of the marine bacterium *Vibrio natriegens* (ATCC 14048) was also reduced upon treatment with ZS.[81] ZS was hence assigned to be a positive biofilm inhibiting control, whose impact should act as an estimation of effectiveness for the two novel substances AS and BS. Additionally to the impact of these sulfated phenolic acids on biofilm formation, observations including a possible impact on cell growth, estimated by OD measurements, seemed also of vital importance in the context of current research on non-toxic antifouling

agents. Another crucial aspect, that has so far not been included in earlier studies on ZS, was the stability monitoring of the tested compounds in presence of bacteria by UPLC-MS. Pre-experiments already confirmed the long term stability of AS, BS and ZS in sterile medium and a general stability of sulfated phenolic acids against hydrolysis, as long as the pH value of the surrounding medium did not fall below 3. On the other hand, the sulfated phenolic acids BS and the dihydroxylated form of ZS, 3,4CAS, were readily hydrolyzed in the presence of an arylsulfatase (section 2.2). It was thus assumed that exhibited to sulfatase activity the non-sulfated form of each sulfated phenolic acid might be released into the medium. For *E. coli* sulfatase like enzymatic activity has once been described [150], but for *V. natriegens* none has been reported so far. Thus, a possible impact on biofilm formation of the non-sulfated forms of AS, BS and ZS, 4-hydroxybenzoic acid (B), 4-hydroxyphenylacetic acid (A) and *para*-coumaric acid (Z) was simultaneously investigated.

4.1 Experimental design

Purity of all synthesized (AS, BS, ZS) and commercially obtained (A, B, Z) additives was confirmed by NMR and UPLC-MS measurements (section 9). Each compound was used in a concentration of 2.05 mmol l^{-1} , which corresponds to 500 mg l^{-1} of ZS, an amount that has been shown effective concerning its antifouling activity in previous studies.[78, 81] Of each additive a sterile solution in medium suitable for each bacterial species was prepared. Additionally, a medium control sample without additives (M+) was prepared, to provide a condition, where in pre-experiments biofilm formation of both species has been observed. A further medium control was prepared without inoculation (M-) of bacteria as a reference during OD measurements and as a confirmation of initial medium sterility during preparation. After preparation of all treatments (AS, A, BS, B, ZS, Z, M+, M-), each solution except M- was inoculated with cells of a 24 hour pre-culture, resulting in a starting OD of 0.1. Then, several flat bottom 96 well plates were prepared as described in section 9. Each plate contained eight biological replicates of each treatment for

biofilm evaluation and three for UPLC-MS measurements to monitor the stability of the additives in presence of bacteria. All plates were incubated at 29°C without concussion, to prevent smearing of bacteria to the well wall, which might later be mistaken as biofilm. One plate was selected and specially marked. OD of this plate contents was measured immediately after inoculation and then hourly to obtain a growth curve of all treatments. OD values around 0.35 indicated the start of biofilm formation. However, a conventional bacterial growth curve with biofilm forming bacteria based on OD could not be obtained due to secretion of exopolymeric material also contributing to the OD. In such a case, OD simply increases constantly and the contribution of cells and exopolymeric material cannot be separated anymore. Thus, as soon as biofilm formation started, OD measurements were no longer taken into account. Despite this disadvantage, it is worthwhile to monitor OD, because information upon if any of the additives causes differences in lag- or exponential phase is still provided. Due to repeated movement during transportation, the plate for OD monitoring was not used for biofilm sampling.

When start of biofilm formation was indicated by an OD around 0.35, every hour one plate was removed from the incubator and sampled. First, OD was measured to observe if data corresponded to those of the plate used to compile the early growth curve. Then UPLC-MS samples (M+, ZS, Z, AS, A, BS, B) were transferred from the assigned wells into centrifugation tubes and the bacteria removed by centrifugation. The supernatant was pipetted into methanol containing *trans*-cinnamic acid as internal standard, leading to a sample dilution by a factor of ten. Methanol was used for UPLC-MS screening firstly to quench any remaining enzymatic activity and secondly to remove major parts of inorganic salts and peptides present in the medium.

Meanwhile for biofilm sampling immediately after removing the UPLC-MS samples, remaining well contents were rigorously shaken into a waste container and quickly dived into a bath of PBS buffer, to remove any unattached bacteria, e.g. in form of bacterial floc that, if sticking to the well wall, falsifies the biofilm result considerably. Plates were then additionally washed carefully in containers of deionized water. The

water was removed as far as possible by shaking the plate on paper towels. After air drying, the biofilm was stained for 15 minutes in a 0.1% crystal violet solution (CV).[148, 149] A previously empty column of 8 wells was additionally filled with CV solution, because CV also slightly stains the polystyrene of the well plates, and was used as a reference during absorption measurements to quantify the biofilm. After staining, CV was removed from the well with several subsequent washing steps in containers containing deionized water. Only when water remained colorless the washing was terminated. As an indirect estimation of the biofilm after drying, CV was dissolved from the biofilm by adding a mixture of ethanol:acetone (4:1) into each well. After 15 minutes the absorption of CV at 570 nm was measured, and referenced to the absorption of the first column, not containing biofilm.

4.2 Impact of AS, BS, ZS and their non-sulfated forms on biofilm formation of *Escherichia coli*

Biofilm formation of *E. coli* in well plates at 29 °C usually started around 7 to 8 hours after inoculation at the air-liquid-interface (Figure 4.1 A). Below that area, biofilm formation of this species was not observed. Already during the early stage of biofilm formation, 8 hours after inoculation, could be observed that the most noticeable inhibition was caused by Z, the non-sulfated form of ZS (Figure 4.1 A). After 11 and 13 hours, treatment Z inhibited biofilm still most effectively, recognizable easily by eye (Figure 4.1 A). Absorption measurements of CV dissolved from biofilms between 8 and 13 hours after inoculation confirmed this observation. These results clearly show that on all sampling points only Z could significantly reduce *E. coli* biofilm formation ($p < 0.001$), compared to the control (Figure 4.1 B). After 13 hours, when the experiment was terminated, biofilm coverage was still reduced by 30% compared to the control. The non-sulfated forms of the two sulfated phenolic acids found in members of the Dasycladaceae, A and B, also showed significantly inhibiting effects ($p < 0.001$), but only in the early stages and never reached a reduction as high as Z (Figure 4.1 B). The inhibiting effect decreased with time

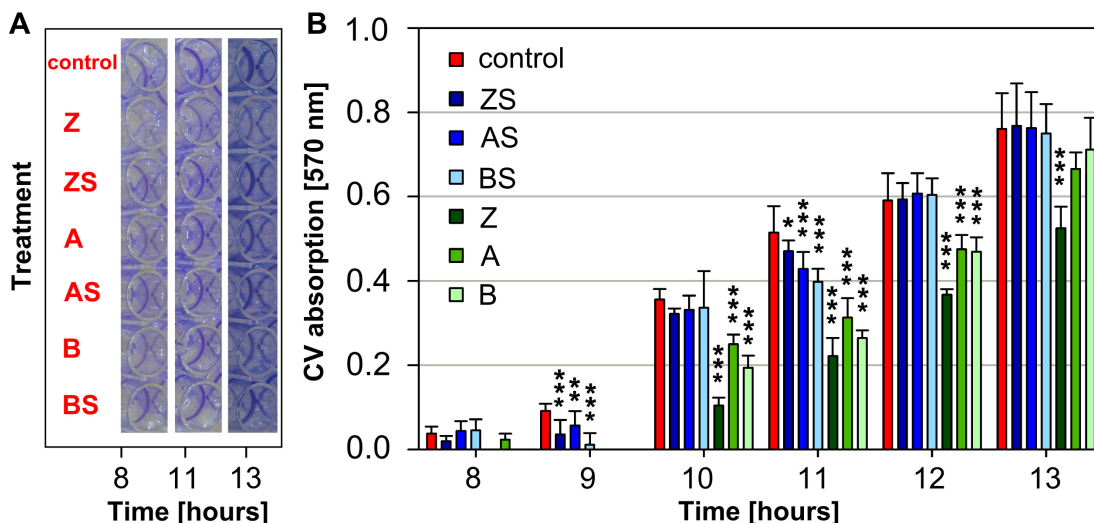


Figure 4.1: Formation of an *E. coli* biofilm during a period of 13 hours after inoculation. **A:** CV stained biofilm in polystyrene well plates at the air-liquid-interface of the control and the treatments Z, ZS, A, AS, B and BS after 8, 11 and 13 hours. During that time, the amount of biofilm increased for all treatments. After 8 hours biofilm development was much lower in treatment Z, and seemed reduced in treatments A and B. After 11 and 13 hours only in treatment Z was a distinct inhibition of biofilm formation recognizable by eye. None of the sulfated phenolic acids appeared to have had an impact on biofilm formation. **B:** Indirect estimation of biofilm by normalized CV absorption at 570 nm of dissolved CV from stained biofilms. Biofilm formation started 8 hours after inoculation. From hours 8 till 13 no long term difference between treatments ZS, AS and BS to the control was visible. Biofilm formation of treatments Z, A and B was delayed between hours 8 and 12, but only in Z biofilm formation remained significantly reduced after 13 hours. (mean \pm SD, n = 8. One way ANOVA (Holm-Šídák test): *** significantly different with $p < 0.001$, ** significantly different with $p < 0.01$, * significantly different with $p < 0.1$ to the control.)

and after 13 hours no significant difference between A, B and the control could be found anymore. Biofilm formation in presence of the sulfated phenolic acids AS, BS and ZS was inconstant until hour 11. After 9 hours a significant difference could be found for all three sulfated phenolic acids (ZS, BS: $p < 0.001$, AS: $p < 0.01$) compared to the control, which after 10 hours was not present anymore. After 11 hours a small reduction compared to the control could be found, but the reduction lay only around 8% for ZS, 15% for AS and 20% for BS. 12 and 13 hours after inoculation no difference between these three treatments and the control could be found. This strongly indicates, that the sulfated phenolic acids do not exhibit a long term inhibiting effect on *E. coli* biofilm formation.

Despite the varying responses of *E. coli* biofilms to the different treatments, bacterial growth in lag and exponential phase, during 0 and 8 hours after inoculation was

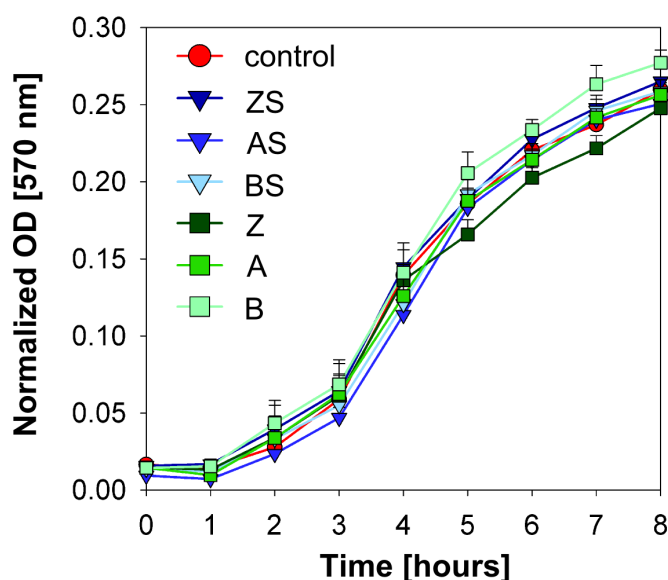


Figure 4.2: *E. coli* growth during lag and exponential phase until the start of biofilm formation after 8 hours. No remarkable differences in OD between treatments (ZS, Z, AS, A, BS, B) and the medium control are visible. Growth phases of all treatments exhibit a congruent course.

obviously not affected. Growth curves of all treatments show a congruent course and no significant differences in cell number could be found (Figure 4.2). The observed biofilm inhibiting effects of the non-sulfated forms A, B and Z seemed not to be caused by a corresponding reduction in cell number.

UPLC-MS screening of metabolites in medium shortly before the inoculation and 6, 11 and 15 hours after inoculation document that none of the additives was metabolized by this *E. coli* strain. Mean peak areas of the six additives ZS, Z, AS, A, BS and B, normalized by the peak area of the internal standard *trans*-cinnamic acid, remained constant over time (Figures 4.3 A-C). In none of the sulfated phenolic acid samples could the presence (Figures 4.3 B, C) or an increase in concentration (Figure 4.3 A) of the corresponding non-sulfated form be observed. Thus, this *E. coli* strain did not exhibit arylsulfatase activity, able to hydrolyze either of the three sulfated phenolic acids AS, BS and ZS, under the conditions applied here. The remarkable difference in peak areas between sulfated phenolic acids ZS, AS and BS and the non-sulfated forms Z, A and B are most likely caused by the strongly acidic proton of the sulfated phenolic acids. Ionizability (formation of the pseudo ion) in negative modus is presumably promoted, which is followed by an improved sensitivity of the MS system towards these substances. Peak areas of sulfated phenolic acid samples (AS, BS, ZS) were in general increased by factors between 3 and 6 compared to their

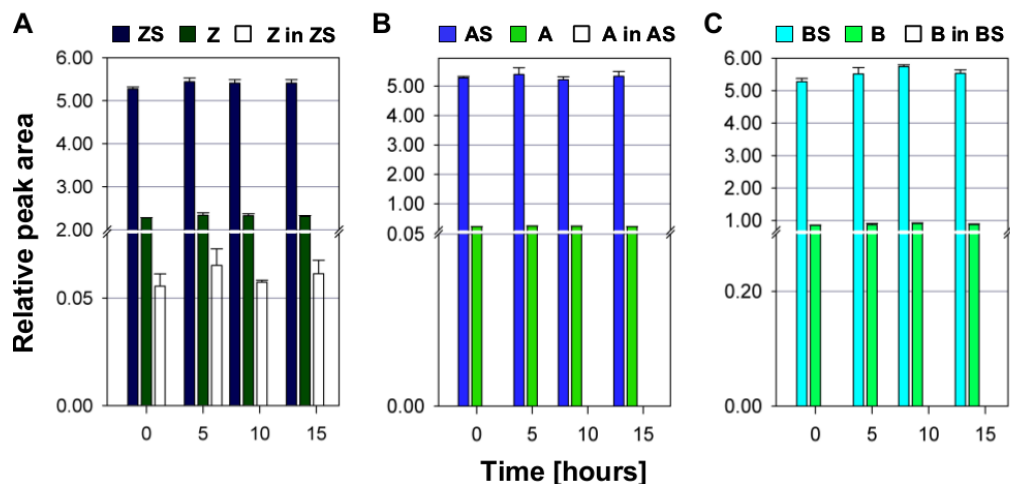


Figure 4.3: UPLC-MS screening of medium during biofilm formation of *E. coli* shortly before inoculation ($t = 0$) until 15 hours after. Figures **A** to **C** show relative peak areas of the additives Z, ZS, A, AS, B and BS, as well as a screening for the non-sulfated forms in samples of the sulfated phenolic acids "Z in ZS", "A in AS" and "B in BS". All peak areas were normalized to the internal standard *trans*-cinnamic acid. **A:** Concentrations of ZS and Z remained constant during 15 hours after inoculation. All samples of ZS show a constant minimal amount of Z (Z in ZS) before and after inoculation. **B:** Concentrations of AS and A remained constant during 15 hours after inoculation. No contamination of A in AS could be detected. **C:** Concentrations of BS and B remained constant during 15 hours after inoculation. No contamination of B in BS could be detected. (arithmetic mean \pm SD, $n = 3$)

non-sulfated forms of the same concentration. Merely in the ZS samples (Figure 4.3 A) could a minimal amount of non-sulfated educt (Z in ZS) be detected, whose concentration remained stable within the sampling period. The proportion was circa then 1% of the peak area of ZS.

The experiment was repeated twice with independent cultures and both times the same results could be obtained.

Combination of the microtiter dish assay with UPLC-MS screening, concerning the stability of the compounds, and cell growth monitoring provided a complete picture of the impact the applied compounds had on biofilm formation and growth of this specific *E. coli* strain. UPLC-MS measurements did not indicate sulfatase activity of this strain towards any of the three sulfated phenolic acids ZS, AS or BS during the length of the experiment. These measurements also showed that none of the six additives was metabolized, since their concentration remained constant on all sampling points. OD measurements confirmed that all samples started with a similar cell density and that bacterial growth was not remarkably influenced by any of the

additives during lag or exponential phase. During this study, only the non-sulfated form of ZS, *para*-coumaric acid (Z) proved to be a potent biofilm inhibitor of this *E. coli* strain. In accordance to that, neither of the other two sulfated phenolic acids identified in members of the Dasycladaceae AS and BS could inhibit biofilm formation. The non-sulfated forms of these metabolites, A and B, were found to slightly inhibit biofilm formation during the first 12 hours, but here no long term effect could be observed and the inhibition was less profound than that of Z.

With respect to the numerous studies published within the last years on antifouling effects assigned to ZS, including the specific tested strain in this study, these results were rather surprising. The first study concerning antifouling activity of ZS was performed by Todd *et al.* in 1993, who identified the structure of this compound isolated from *Zostera marina*. In addition to ZS, further structurally related phenolic acids (caffeic acid, ferulic acid) were sulfated and tested against fouling of marine bacteria of the *Acinetobacter* species isolated from *Zostera marina* leaves. Bacterial biofilm on glass slides was found to be inhibited by the sulfated phenolic acids but not by their non-sulfated forms.[72] This early study was performed during a time when tributyltin compounds (TBT) so far used as antifouling agents in paints for marine systems became criticized by several committees, due to its widespread toxicity and slow biodegradability. But only after the turn of the century the bans became more strict and a total ban was decided from January 1st in 2008 onwards, followed by an urgent search for non toxic, natural antifouling agents.[75] From 2005 onwards several studies headed by Cutright and Newby showed that ZS could successfully inhibit biofilm formation of marine and freshwater bacteria on silicone coated glass slides, regardless if the agent was dissolved in medium or incorporated into the silicone in concentrations ranging from 50 to 500 mg l⁻¹. [74–76] The same group also confirmed a low toxicity of ZS against tested bacteria and found that 50 % of the half maximal effective concentration (EC₅₀) per liter could already inhibit biofilm formation.[81] By treating fungi of the species *Candida albicans* with ZS during biofilm formation, cell adhesion on both hydrophobic and hydrophilic surfaces was reduced by at least 70 %. Interestingly, upon adding the sulfated methylester of ZS

no effect could be observed by Villa *et al.* in 2011.[79] A field assay by Boopalan *et al.* in 2011 showed antifouling (AF) activity of ZS loaded into zeolite particles, coupled to an epoxy coating. Stainless steel panels coated with ZS-loaded and ZS-free paint were immersed in sea water for 1 year. ZS loaded panels showed minor biofilm formation and no corrosion, whereas ZS free panels were exposed to corrosion and increased fouling.[77]

Additionally to these properties showed a study published by Stanley *et al.* in 2002 that ZS could inhibit adhesion of pathogenic fungal spores causing rice blast and bean anthracnose, both diseases leading to major crop loss.[73] ZS was also found to slightly inhibit *in vitro* early steps of virus-cell interactions of Dengue virus, although other, more complex compounds carrying amino groups were tested too and proved more effective.[80]

An experiment most closely related to this study was performed by Villa *et al.* in 2010 on the same *E. coli* strain as used by me and applying a similar experimental setup. Their study also detected a strong antifouling activity of ZS in concentrations of 500 mg l^{-1} and lower in contrast to results obtained during the present study. Villa *et al.* used different bacterial media both for culturing cells and during biofilm experiments, which were performed in mineral medium, a carbon source was not mentioned. It is known that nutrient deficiency can influence biofilm structure, amount and complexity. Several studies showed that less complex biofilm structures render the community to be more susceptible for antimicrobial agents.[151–153] Biofilm experiments presumably also started with a much higher cell number (10^6 cells/ml), also influencing biofilm formation. Quantification of biofilm was performed by staining attached bacteria with 4',6-diamidino-2-phenylindole (DAPI) and subsequent relation of cell number to fluorescence intensity. This study additionally revealed enhanced bacterial motility by 40% in presence of ZS, due to the additional synthesis of flagella. The increase in motility was suggested to be a reason for diminished biofilm formation.[78, 126] This assumption seems to contradict two other studies on biofilm formation of different *E. coli* strains by Pratt *et al.* in 1998 and Wood *et al.* in 2006 who demonstrated that additional to nutritional conditions,

motility itself is a crucial factor in biofilm formation and that strains deficient in motility and/or flagella synthesis produce only poor biofilms.[154, 155] The presence of flagella on the one hand was thought to be important for movement towards the surface and initial attachment, motility on the other hand for the overcome of surface repulsion, migration along the biofilm and thus biofilm spreading. The sensing of nutrition called chemotaxis on the other hand was found to be completely dispensable during biofilm formation.[154] It was hence assumed that once motility and flagella synthesis overcome a certain threshold, these initially inevitable factors for biofilm formation become adverse and result in diminished adhesion.[126]

Only one study performed by Geiger *et al.* in 2004 could not find a long term anti-fouling effect of ZS on activated sludge. Here, ZS was embedded in coatings of a biocompatible polyester (poly[3-hydroxyalkanoate-co-3-hydroxyalkenoate], PHAE). These coatings contained either dispersed ZS or ZS loaded microcapsules. In this study, ZS was only slightly active shortly after it was released.[156]

All these studies used various methods to unveil ZS activity and the variety of organisms tested lead to the assumption that ZS seems to be a potent, non-species dependent, non-toxic antifouling agent. The inactivity of the synthetic ZS used during this study in contrast to the potent antifouling performance of the non-sulfated form Z hence challenged these findings. UPLC-MS co-injection experiments with methanolic *Zostera marina* extract confirmed structural identity of synthetic and natural compounds (see section 9.4.4.1). Leaving experimental conditions aside, a general difference between the study performed here and all others just discussed can presumably be assigned to deviations in synthesis and purification strategies of ZS. As already discussed in chapter 2.1, many studies do not present comments on purity or analytics applied after synthesis of ZS.[74, 75, 77–80, 126, 156] Others mention that ZS samples still contained minimal amounts of educt Z [81], or noted the presence of Z/Z and Z/ZS anhydrides [73, 76], regardless of sulfatation agent and solvent used. Thus, it can be assumed that the occurrence of these side products is characteristic for the sulfatation process of phenolic acids. Except the early study from Todd *et al.* in 1993, who purified his synthesis product by HPLC, those

studies that mentioned purification [75, 77–79, 126] washed the raw product with an organic solvent and then precipitated salts from the aqueous phase by adding methanol. Due to the experiences during the present study, it seems possible that these products contained the anhydrides, which upon cleavage would release Z additionally to what might not have been sulfated. During this study no educt Z or any other side product could be detected by NMR, despite a rather high sample concentration during measurement (33.3 mg ml^{-1}) on a 400 MHz spectrometer, which should ensure a rather high sensitivity. Additionally, during the even more sensitive UPLC-MS measurements, no side products could be detected and the content of non-sulfated Z in the ZS sample was always around 1 %, as estimated by peak area comparison normalized to an internal standard. The purity of the sulfated phenolic acids AS, BS and ZS, as well as of their non-sulfated forms and the UPLC-MS monitoring of their stability in presence of bacteria ensured that any effect observed here could solely be attributed to each single compound. Despite the antifouling activity of Z demonstrated during this study, the assumption that likely contaminations of Z in ZS samples during other studies are responsible for the effect assigned to ZS can hardly be proven. Except during the study on antifouling activity of ZS from Todd *et al.* in 1993, who came to opposite results as already discussed, none of the other studies tested the non-sulfated form Z.

Despite the contradictory results obtained here in comparison to several others studies, the detected antifouling activity of A, B and especially Z appears not unreasonable when considering the various biological activities attributed to B and especially Z in the current literature. All three compounds are well known plant secondary metabolites. Z is found in plant cell walls [157–161], several mushroom species [141], fruits and vegetables [162, 163] as well as in freshwater and marine algae [143, 164]. As already mentioned, the sodium salt of B was discussed to be a potent antifouling agent against freshwater bacteria from Lake Erie.[147] A study by Tanveer *et al.* in 2012 demonstrated that Z, excreted by a weed associated with chickpea, could suppress germination of the latter and caused length reduction on shoots and roots.[160] Another allelochemical function of Z was revealed by a study from Seyedsayamdoost

et. al in 2011. The coccolithophore *Emiliana huxleyi* was found to release Z during senescence, upon which its associated bacteria *Phaeobacter gallaeciensis* produced algicides, which inhibited further algal growth.[164] Z has also been found to be a mild antioxidant [157, 162, 165, 166], in addition to antifungal [141, 167] and antibacterial activities [122, 168]. During a study by Li *et al.* Z could inhibit gene expression of a type III secretion system (T3SS) in *Dickeya dadanti*, a plant pathogen, belonging to the Enterobacteriaceae. T3SS is a protein secretion system capable of trans-locating virulence proteins directly into host cells.[122] Wells *et al.* in 2005 detected that viable cells of the *E. coli* strain O157:H7, common in cattle feces and pathogenic to humans, could be found in feces from cattle fed with corn silage. For cattle fed with brome grass, naturally containing Z, bacteria needed more than 120 days to recover in feces. Addition of Z to *E. coli* feces from corn silage fed cattle increased the bacterial death rate considerably, demonstrating an antibacterial activity of Z.[168]

Previous to the present assay, I tested the optimal conditions for biofilm formation of the used *E. coli* strain, including selection of medium, temperature and surface. Only when it was confirmed that the applied conditions promoted adhesion leading to an evaluable biofilm were the bacteria exposed to the different additives. A, AS, B, BS, Z and ZS were thus tested under favorable conditions for bacterial growth. It was accepted that under the conditions applied here, the highly pure ZS (and AS, BS) had no effect on biofilm formation of this strain in contrast to the non-sulfated forms and it seemed hence idle to further investigate possible reasons for the deviating results. Instead, the original aim to test which structural moieties of the sulfated phenolic acid ZS are responsible for the antifouling activity (sulfate ester, double bond, carboxyl group) and if structurally related compounds like AS and BS possess similar properties, was further pursued by repeating the established assay with another bacterium, whose biofilm formation has also been reported to be affected by ZS, namely *Vibrio natriegens*.[81]

4.3 Impact of AS, BS, ZS and their non-sulfated forms on biofilm formation of *Vibrio natriegens*

The marine biofilm forming bacterium *V. natriegens* was originally isolated from salt marshes and under optimal conditions can have a generation time of less than ten minutes and thus appeared a convenient model organism.[169] *V. natriegens* was found to form biofilms on stainless steel and thereby immensely increasing corrosion rates, causing substantial economical detriments for e.g. the shipping industries.[170] During a survey by Shieh *et. al* in 1989 several bacterial strains belonging to the *Vibrio* family were isolated from a *Zostera marina* bed.[171] As already discussed, this seagrass is the natural source of ZS. A biofilm inhibiting effect of ZS has been described for this strain by a study within the Ohio Sea Grant Project R/MB-002 and mentioned in a publication of Xu *et al.* in 2005.[81]

Unfortunately, the microtiter dish assay proved not applicable to this bacterium as it tends to form thick layers of bacterial floc when not moved during growth. Already after 5 to 6 hours a floc layer could be observed, covering the air-liquid-interface in each single well. A faint biofilm started to form after 12 hours (Figure 4.4). It was already noticeable that this faint layer is often partly overlain by strong patches of dense CV stained material, marked by a red arrow in Figure 4.4, that could not be removed by washing with PBS buffer. After 15 hours, several layers of stainable exopolymeric material could be observed, preventing any further distinction between floc sticking to the well wall and biofilm. Thus, with this assay, no predication about the impact of sulfated and non-sulfated phenolic acids on biofilm of *V. natriegens* could be made. Despite this drawback, interesting results could still be obtained by OD growth monitoring under the influence of the additives and UPLC-MS screening of the stability of the sulfated and non-sulfated phenolic acids in presence of bacteria, also included in the assay.

The impact of the six additives on *V. natriegens* cell growth, expressed by the OD before the start of biofilm formation provided a rather complex picture and indicated a remarkable influence of some substances on cell growth, presumably in

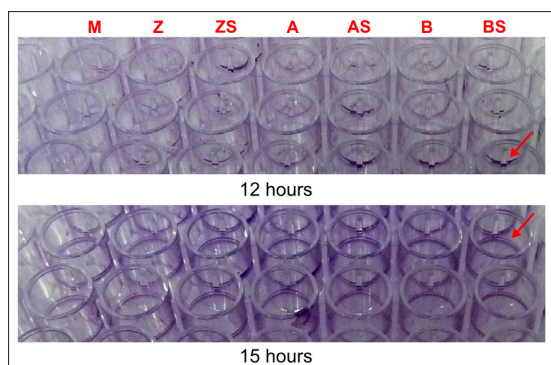


Figure 4.4: Biofilm of *V. natriegens* at the air-liquid-interface grown in medium with (Z, ZS, A, AS, B and BS) and without additives after 12 and 15 hours. Several layers of stained bacterial matter are visible, marked by red arrows. No distinction can be made between stained bacterial floc and biofilm.

lag and exponential phase. Due to slower growth compared to *E. coli*, OD was only measured every two hours. Statistical evaluation included all data points two hours after inoculation, all values are means originating from eight biological replicates. All treatments started with identical ODs (Figure 4.5 A and B). The control sample seemed to have an outlier around 8 hours where a sudden drop in OD could be observed, whereas all other six treatments showed a continuous increase of OD during the 12 hours of measurement. Figure 4.5 A shows an OD increase of the bacterial cultures exposed to the sulfated phenolic acids ZS, AS and BS and the medium control. OD values of treatments ZS and AS were significantly higher to the control on all data points taken into account ($p < 0.001$). The increase of the OD from two hours after inoculation onwards reaches values around 20% higher than control samples after 12 hours, indicating an increased cell number and thus a progression in growth. OD values of BS samples showed a congruent growth to the control, with the exception at eight hours after inoculation, where a significant difference between treatments BS and the control was found. This can presumably be attributed to the sudden drop of OD in the control sample. Treatments containing the non-sulfated phenolic acids Z, A and B appeared to either not or only slightly promote growth (Figure 4.5 B). Samples containing Z showed a more congruent course to the control until 8 hours after inoculation, but OD seemed to decrease after 10 ($p < 0.001$) and 12 ($p < 0.1$) hours, indicating a drop in cell growth. B seemed to promote growth on all sampling points taken into account ($p < 0.001$), but not as strong as ZS and AS. In samples B the increase lay only around 10% 12 hours after inoculation. Samples of treatments A seemed to slightly promote growth

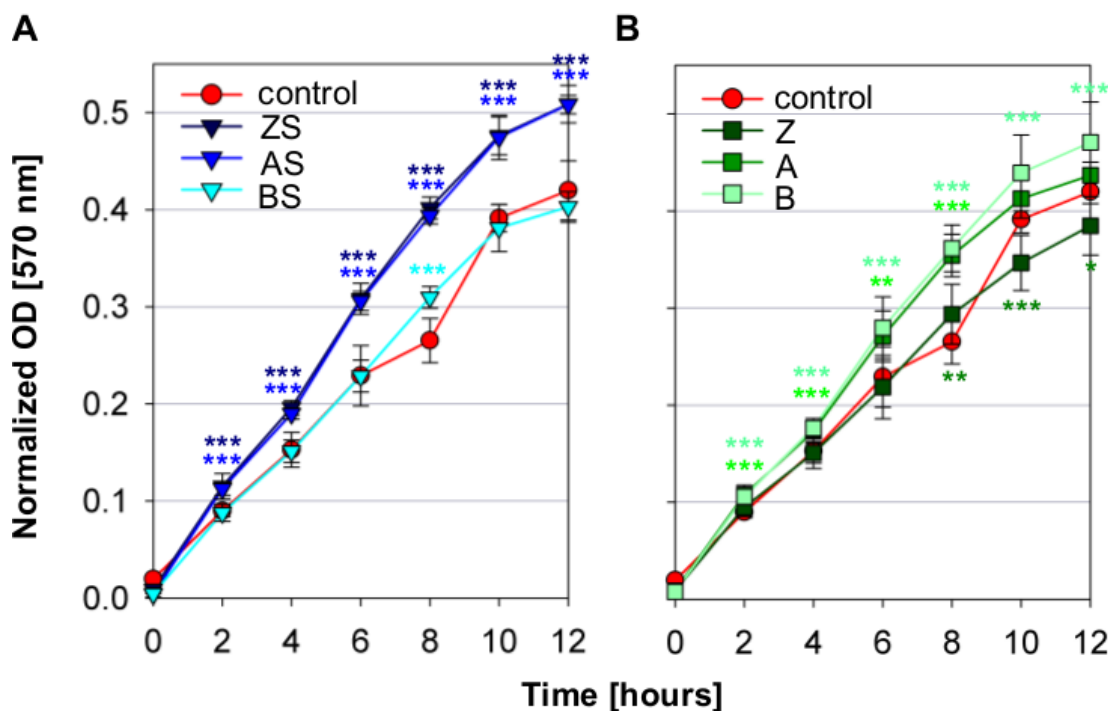


Figure 4.5: *V. natriegens* growth during lag and exponential phase until the start of biofilm formation 12 hours after inoculation. **A:** Growth of the control and in presence of the sulfated phenolic acids ZS, AS and BS. ZS and BS promoted growth during the first 12 hours. Samples BS were not significantly different, except 8 hours after inoculation, presumably due to the outlier in the control. **B:** Cell growth of the control and in the presence of phenolic acids Z, A and B. Treatment B promoted growth during the first 12 hours. A promoted growth until 10 hours after inoculation. Z samples were not significantly different until 10 hours after inoculation, when a slight decrease in OD was estimated compared to the control. The difference 8 hours after inoculation seems to be due to an outlier in the control. (mean \pm SD, n = 8. One way ANOVA (Holm-Šídák test): *** significantly different with $p < 0.001$, ** significantly different with $p < 0.01$, * significantly different with $p < 0.1$ to the control.)

until 10 hours after inoculation, similar to those containing B, ($p < 0.001$ 2, 4 and 8 hours, $p < 0.01$ 6 hours after inoculation), but afterwards seemed to be rather similar to the control.

UPLC-MS screening of the bacterial medium of *V. natriegens* during the length of the experiment containing the additives ZS, Z, AS, A, BS and B (Figures 4.6 A-C) also showed differences to the results obtained during the assay with *E. coli*. Peak areas of all samples are mean values from three biological replicates, normalized to the internal standard *trans*-cinnamic acid. All samples show a considerable difference in peak areas between sulfated phenolic acids and their non-sulfated forms, as already discussed in section 4.2.

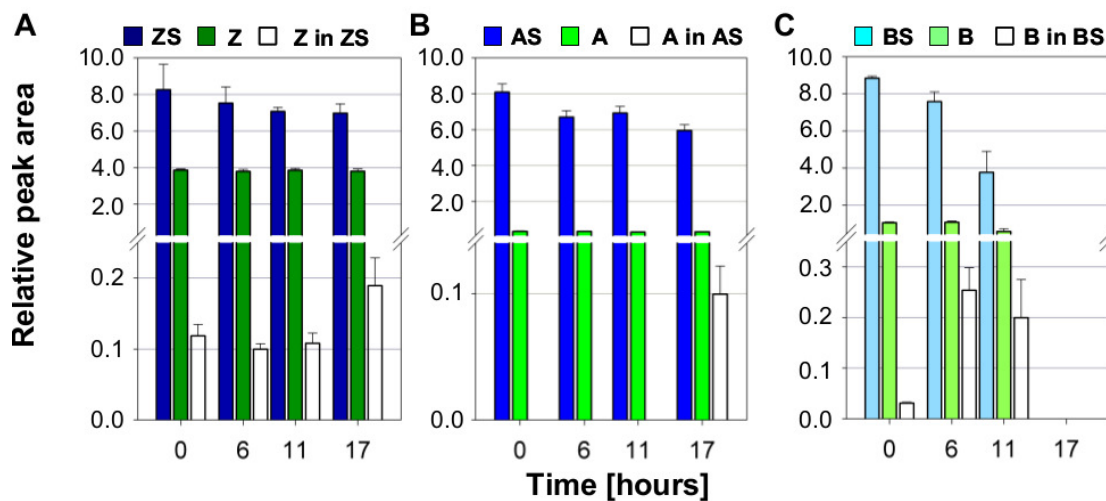


Figure 4.6: UPLC-MS screening of medium during biofilm formation of *V. natriegens* shortly after inoculation ($t = 0$) until 17 hours later. Figures **A** to **C** show relative peak areas of the additives Z, ZS, A, AS, B and BS, as well as a screening for non-sulfated forms in samples of the sulfated phenolic acids "Z in ZS", "A in AS" and "B in BS". All peak areas were normalized to the internal standard *trans*-cinnamic acid. **A:** Concentration of ZS decreased slightly, simultaneously Z in ZS increased after 17 hours. Concentration of Z remained constant. **B:** Concentration of AS decreased slightly, simultaneously A in AS suddenly appeared at 17 hours after. Concentration of A remained constant. **C:** Amount of BS decreased until it was not detectable anymore after 17 hours, simultaneously B in BS increased, but could not be detected after 17 hours as well. B also was not detectable after 17 hours.

Samples containing Z and A (Figures 4.6 A and B), showed no decrease in concentration of either substance on all sampling points, beginning shortly after inoculation (0) until 17 hours later, confirming that none of these substances was metabolized by *V. natriegens*. In contrast to Z and A, compound B was completely degraded by *V. natriegens* within 17 hours after inoculation. A decrease in concentration of B was noticeable 11 hours after inoculation. All samples containing the sulfated phenolic acids ZS, AS and BS showed a decrease in concentration over time in varying extents. In accordance to the decreasing concentration of the sulfated form, in all samples an increase in concentration of the corresponding non-sulfated form could be detected, indicating sulfatase activity of *V. natriegens*. Figure 4.6 A shows a slight decrease in concentration of ZS starting 6 hours after inoculation. After 17 hours an increase of "Z in ZS" could be observed. A similar process appeared in samples containing AS. Here the concentration of AS decreased slightly over 17 hours of inoculation, when "A in AS" could be detected for the first time. Presumable sulfatase activity could also be found in samples BS (Figure 4.6 C). Already

shortly after inoculation (point 0) a small amount of B in the BS sample could be detected, increasing until 6 hours after inoculation, congruent with a decrease of BS concentration. After 11 hours, "B in BS" started to decrease again and as in samples solely containing B none was detectable anymore after 17 hours, indicating that the sulfate ester of BS was cleaved by sulfatase activity, but additionally B and BS were completely metabolized by *V. natriegens*. Due to the different sensitivities of sulfated and non-sulfated phenolic acids during MS ionization, this allowed only a qualitative observation of a presumable sulfatase activity. No quantitative prediction can be made to verify, if the decrease in sulfated phenolic acids (ZS, AS, BS) corresponds to the amount of increase in the non-sulfated forms. As has been discussed in chapter 2.2 all substances remained stable at 30°C in sterile medium used for this species, thus, it can be assumed that the changes in concentration and the presence of the non-sulfated forms detected during this assay were due to bacterial activity. This is the first time that a sulfatase activity has been described for *V. natriegens*.

Although the microtiter dish assay with *V. natriegens* could not provide further insights regarding antifouling activity of the sulfated phenolic acids ZS, AS and BS and their non-sulfated forms, the combination of the biofilm experiment with cell growth monitoring and UPLC-MS screening provided important aspects for further assays. Bacterial growth seemed to be promoted by the sulfated compounds AS and ZS during the first twelve hours, in contrast to their non-sulfated forms. One possible assumption would be that the availability of additional sulfate due to cleavage of the sulfate ester was responsible for the growth promoting effect. UPLC-MS data on the other hand did not show an unambiguous decrease of the sulfated forms during the first twelve hours for samples AS and ZS. The presence of an additional sulfate salt contained in samples AS and ZS could be ruled out by elementary analysis of both synthetic standards. Interestingly, BS seemed not to promote growth during the first 12 hours, although sulfatase activity could already be detected 6 hours after inoculation by UPLC-MS measurements. Thus, the question why AS and ZS seemed to promote growth in lag and exponential phase remains unanswered. The

growth promoting effect of B on the other hand can presumably be assigned to the fact that this additive is completely metabolized and *V. natriegens* might have used it as an additional carbon source. Karegoudar *et al.* reviewed in 2000 that monohydroxybenzoic acids are degraded by many bacterial species.[172] Both the detected sulfatase activity of *V. natriegens* and its ability to metabolize 4-hydroxybenzoic acid, underline the importance to monitor the stability of additives during bioassays. Only then can be ensured to which compound any observed effect can be assigned to.

4.4 Summary of biofilm assays at the air-liquid-interface

The microtiter dish assay proved a fast method to test the impact of several treatments simultaneously, in combination with cell growth monitoring by OD measurements and stability screening of the additives by UPLC-MS. None of the pure synthetic analogous of ZS, originally isolated from *Zostera marina* [72], and the two novel sulfated metabolites AS and BS, identified in members of the Dasycladaceae influenced bacterial growth of *E. coli* in lag and exponential phase, whereas AS and ZS promoted growth during these phases in *V. natriegens*. UPLC-MS measurements revealed that in the presence of *E. coli* none of the additives was metabolized or hydrolyzed by sulfatase activity during 15 hours after inoculation. *V. natriegens* on the other hand showed sulfatase activity towards all three sulfated phenolic acids and additionally degraded BS and B completely within 17 hours post inoculation. Although *E. coli* growth was seemingly not affected by any of the six treatments, biofilm formation in samples containing Z was inhibited and in samples with A and B delayed. None of the sulfated phenolic acids ZS, AS and BS had an effect on *E. coli* biofilm formation at the air-liquid-interface. Due to excessive floc formation by *V. natriegens* during the microtiter-dish assay a result concerning the effect on biofilm formation of any of the six additives could not be obtained by this experiment. The question however arose, how the detected sulfatase activity and the subsequent

release of the non-sulfated form into the medium would affect biofilm formation. The contradictory results obtained during the assay performed with *E. coli* and the current literature as well as the inapplicability of the microtiter dish assay for *V. natriegens* were decisive reasons to repeat the approach with both strains by using a different experimental setup, which will be discussed in the following chapter.

5 Biofilm assay on PTFE plates

The microtiter dish assay discussed in chapter 4, allowing the investigation of biofilm formed at the air-liquid-interface, could not provide profound insights on the antifouling activity of the structurally related phenolic acids AS, BS (*Dasycladus* spp.), ZS (*Zostera marina*) and their non-sulfated forms against two biofilm forming strains of *E. coli* and *V. natriegens*. Thus, a change of the experimental setup seemed a reasonable strategy to bypass the drawbacks of the microtiter dish assay. The new assay should be applicable for both bacterial species allowing the comparison of a species dependent impact. The three aspects so far considered important, namely biofilm quantification, UPLC-MS stability screening of the additives and cell growth estimation should also still be included. Not only was this assay supposed to solve some of the contradictory results obtained by the microtiter dish assay, an insight on how far differing experimental conditions influence the impact of antifouling agents was also considered as an important additional information. Whereas during the microtiter dish assay a bacterial biofilm was formed at the air-liquid-interface requiring static conditions during growth, this assay should enable biofilm formation on surfaces beneath the air-liquid-interface allowing to bypass the interference of bacterial floc on biofilm determination.

5.1 Biofilm surface test for *E. coli* and *V. natriegens*

In preliminary experiments several surfaces were tested to conduct biofilm experiments within cultures of *E. coli* and *V. natriegens*. Surfaces included were microscopy cover glasses, white polytetrafluoroethylene (PTFE) plates and the silicon surface of a septum (Figure 5.1). As described in section 9.7.3 in detail, all plates

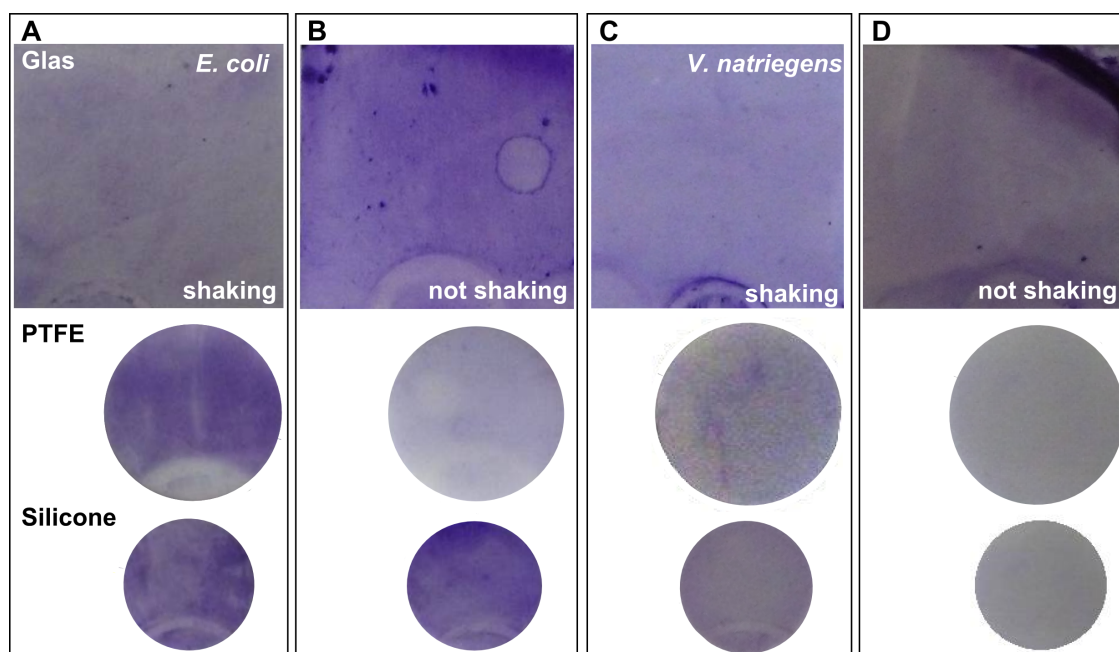


Figure 5.1: Biofilm formation of *E. coli* (A, B) and *V. natriegens* (C, D) on glass, PTFE plates and silicone covered septa. All samples were incubated at 30 °C either under shaking (A, C) or non-moving (B, D). Biofilms of different amounts could be observed on all samples after 3 days.

were tightened within a PTFE tube, such that each plate reached half into the tube. This setup allowed a homogeneous medium distribution, prevented scratching of plates against each other and ensured that bacterial coverage was not just due to an accumulation of settled bacteria (Figure 5.2). All samples were immersed in medium inoculated with pre-cultures of each bacterium. For each species three samples per material were placed on a shaker at 30 °C and three in a non-moving incubator also at 30 °C. After three days samples were removed from the medium, washed carefully and dyed with a 0.1 % crystal violet (CV) solution, to visualize the biofilm. On all surfaces growth of biofilm could be observed (Figure 5.1).

E. coli attached to all three surfaces but depending on the conditions during growth (shaking, not shaking) biofilm amount and homogeneity differed. On constantly moved samples, a dense biofilm grew on PTFE plates and silicone covered septa, whereas growth on glass was rather weak (Figure 5.1 A). Under non-shaking conditions biofilm formation on glass and silicone covered septa was dense but on PTFE plates it was rather weak (Figure 5.1 B). As during the microtiter dish assay, non-

shaking conditions proved not applicable for *V. natriegens*. After three days of incubation, the medium color of these samples changed from light brown to green and a 1 mm thick, dense carpet of floc covered the whole surface, which probably prevented oxygen transfer. Hence, biofilms on all surfaces were very weak (glass) or non-existent (PTFE, silicone), as is shown in Figure 5.1 D. Under shaking conditions, biofilm formation of *V. natriegens* could be observed on all surfaces, but the coverage was still weak. The experiment was repeated under shaking conditions for ten days, upon which a strong biofilm of this bacterium formed on all surfaces.

From all surfaces tested PTFE plates proved the most convenient. Biofilm coverage could be quantified under the microscope on both sides, increasing the amount of technical replicates. Quantitative evaluation of biofilm formation on the silicone covered septa was not possible by microscopy, due to its thickness. Glass slides allowed biofilm formation, but due to their fragility, this surface proved inconvenient too. On PTFE plates a homogeneous biofilm could be grown for both *E. coli* and *V. natriegens* under shaking. Additionally, PTFE material of tube and plates was autoclavable directly in the flasks used for bacterial cultivation.

5.2 Experimental design and image evaluation

If not noted otherwise, for all subsequent experiments two PTFE plates were equidistantly attached into a PTFE tube (Figure 5.2 A). Each plate provided two sides for biofilm formation, thus, leading to 4 sides per sample and a total of 12 samples for all three biological replicates. Per treatment and replicate 3 to 10 tubes were placed in a flask and completely covered with medium either without (control) or with additives (Z, ZS, A, AS, B, BS) in concentrations of 2.05 mmol l^{-1} . A UPLC-MS sample was taken shortly before inoculation. After inoculation all flasks were placed on a shaker either at room temperature or at 30°C and removed for sampling at designated time points, depending on the bacterium. At each sampling point $400 \mu\text{l}$ of each medium sample were removed for UPLC-MS screening and cell number estimation (see chapter 9.7.3), additionally to a tube containing PTFE plates for biofilm

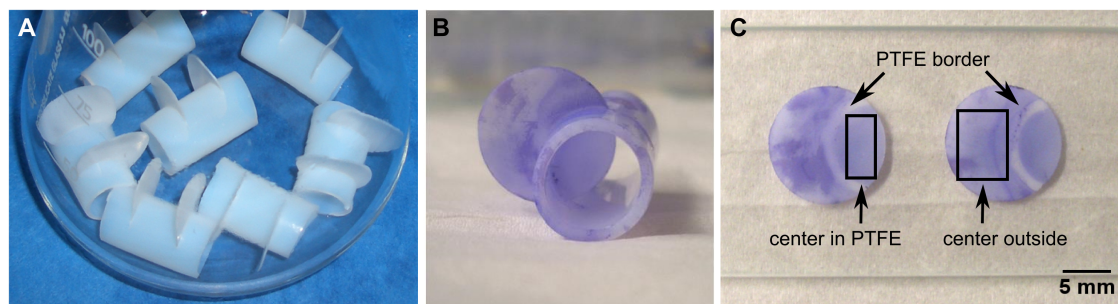


Figure 5.2: Experimental setup for biofilm development on PTFE tubes. **A:** PTFE tubes with PTFE plates firmly attached, before inoculation. **B:** PTFE tube and plate covered with *V. natriegens* biofilm after 9 days at 30 °C under shaking. **C:** The three different biofilm regions "PTFE border", "center in PTFE" and "center outside".

quantification. Tubes were washed carefully with PBS buffer and deionized water. After air drying, biofilm on plates was stained with a 0.1 % CV solution. The CV stained plates could be stored for a long time.

On the PTFE plates three different regions of biofilm growth could be distinguished for both bacteria. The earliest formation of biofilm could be observed at the "PTFE border", which was the region where the PTFE plates were attached to the PTFE tube (Figure 5.2 C). The second region where biofilm could be observed was the "center in PTFE", which is the area within the tube (Figure 5.2 C). A third region was defined as "center outside", which is the area of the plate outside the tube (Figure 5.2 C). Of all three regions, the "center in PTFE" proved to exhibit the most homogeneous biofilm coverage and since biofilm could grow protected within the tube, danger of scratching during shaking was eliminated. Thus, in all further experiments the biofilm was always evaluated in this region. Images of *V. natriegens* biofilms allowed a quantification by image processing, as described in the following paragraph. Images of *E. coli* biofilms were evaluated only qualitatively.

Quantitative evaluation of images was achieved by placing the PTFE plates tightly between two glass microscopy slides and fixing them with parafilm to create an even surface (Figure 5.2 C). Then an image from both sides of the "center in PTFE" region was taken using an inverted microscope, as is described in detail in section 9.1.6.

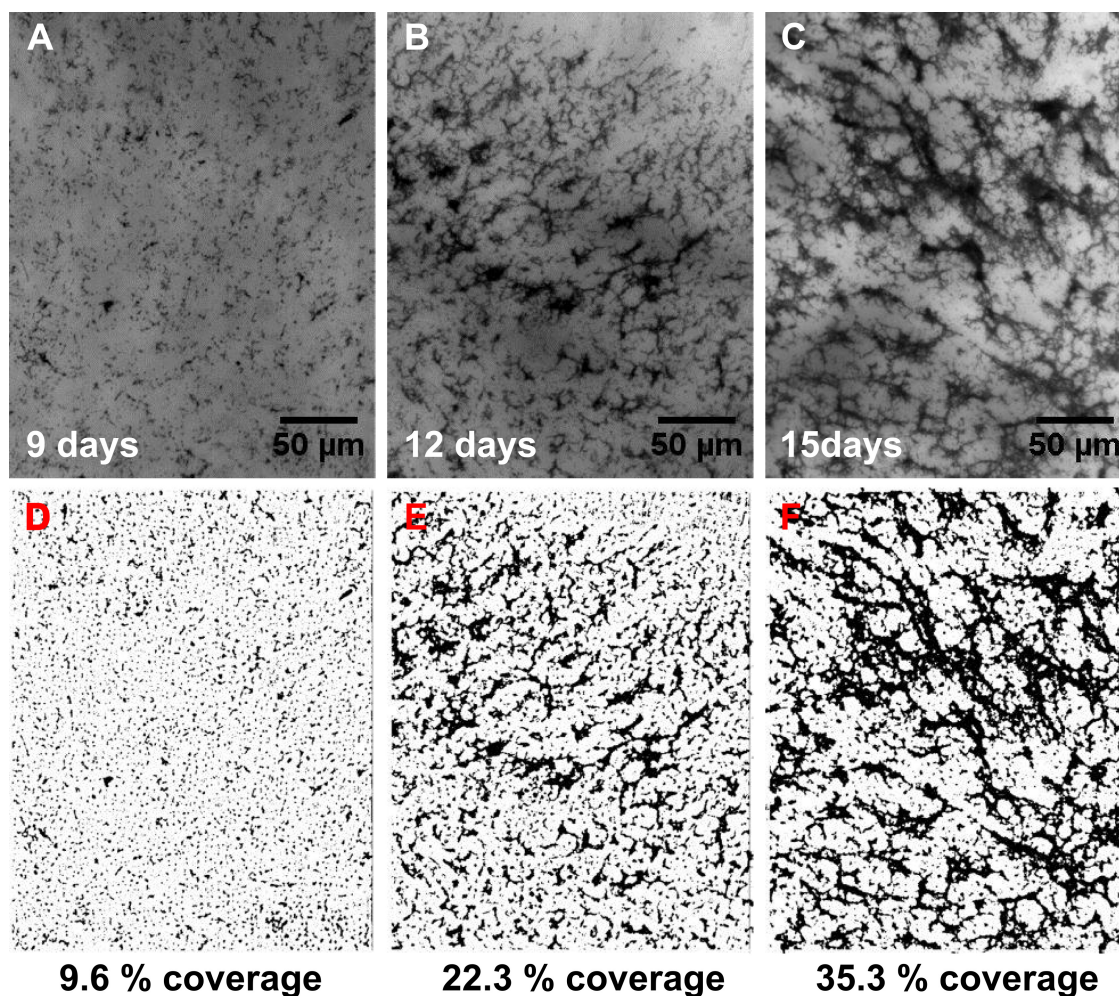


Figure 5.3: *V. natriegens* biofilm after 9 (A), 12 (B) and 15 (C) days. Image evaluation by analyzing black particles of binary images (D-F) resulted in 9.6% coverage after 9 (D), 22.3% coverage after 12 (E) and 35.3% coverage after 15 days (F).

Image processing for quantitative evaluation of biofilm coverage was performed by Image J. This program allowed transformation of the acquired RGB image (Figures 5.3 A-C) into a binary image, consisting only of black and white pixels, where the area of black pixels could be estimated, representing the biofilm coverage in percent (Figures 5.3 D-F). Therefore, the initial RGB picture was first converted to an 8 bit image and then processed by the dynamic thresholding tool to a binary image. Thresholding means to convert all pixels above a certain threshold to black and all remaining to white. Since microscopy images are rarely completely homogeneously illuminated, simply setting a threshold is often not possible due to large shadows originating from illumination gradients. In contrast, a dynamic threshold

divides a picture into small subareas, thereby intensity values of the local neighborhood of each pixel are statistically examined, thus, compensating illumination inhomogeneities.[173] To use this tool successfully, the area size of the neighborhood had to be large enough to cover sufficient foreground and background pixels. On the other hand a too large region had to be avoided, because this could violate the assumption of an approximately uniform illumination. The dynamic thresholding tool used with Image J provided different features how to evaluate the environment, and for the images obtained the "Max/Min image" was chosen as it most closely resembled the features of the original. The values for "Mask" (20-25) and "Constant" C (0-6) allowed the definition of the area size and varied depending on the amount of biofilm coverage. The main criterion for chosen values of each picture was the comparison of the obtained binary image with the original. By zooming into the picture, biofilm structure of original and binary image could be compared with regard to size, amount and form of pixels representing the biofilm. Figures 5.3 A-D show the procedure with different stages of a *V. natriegens* biofilm: small patches in early biofilm (A, D), medium coverage where patches are already connected (B, E) and dense biofilm with large patches (C, F). The algorithm proved to be applicable even on pictures containing biofilm structures largely differing in size, as can be observed on Figures 5.3 B and E.

5.3 Impact of AS, A, BS, B, ZS and Z on *E. coli* biofilm formation

Growth of *E. coli* biofilms at RT on PTFE plates beneath the medium surface was monitored after 12, 24, 48 and 72 hours. Biofilm formation after 12, 24 and 48 hours was rather inhomogeneous for all treatments and large variations could be observed even in samples of the same treatment (Figure 5.4). Early *E. coli* biofilms were characterized by small, branched stripes, sometimes including islands with homogeneous patches, independent of the treatment. Figure 5.4 shows six images

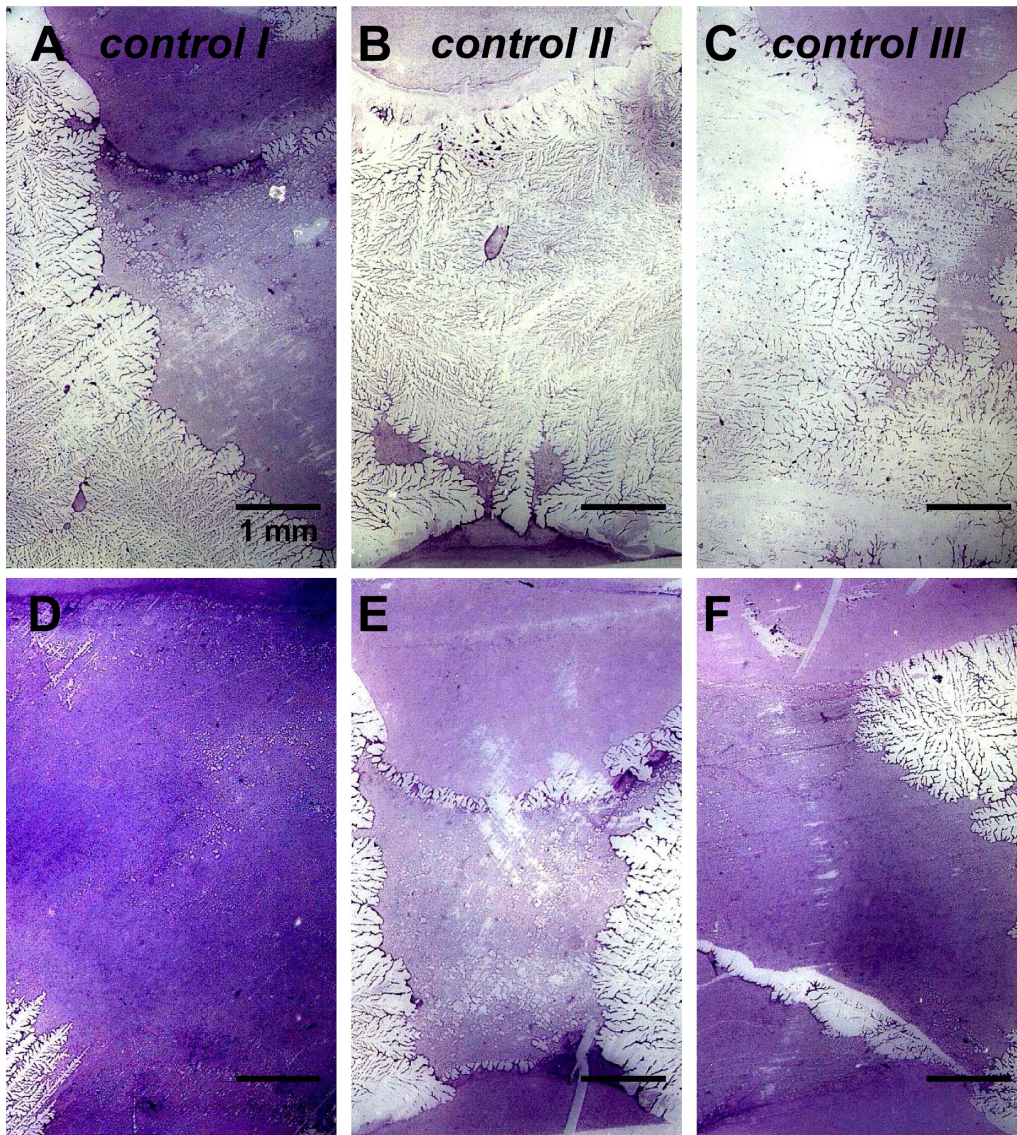


Figure 5.4: *E. coli* biofilm on PTFE plates after 12 hours without additives (control, replicates I (A, D), II (B, E), III (C, F)). The biofilm is characterized by large differences in coverage and shape. A, E show both branched and covered areas. B, C show mostly branched structures. D, F display large homogeneously covered areas.

of samples with no additives (control) after 12 hours, illustrating the inhomogeneity. Figures 5.4 D and F are characterized by dense and homogeneous biofilms, whereas images B and C are dominated by branched stripes and consequently much less coverage. Images A and E show both features. After 48 hours, biofilm features in all samples independent of the treatment changed to a more homogeneous coverage and after 72 hours all samples were covered with a dense, homogeneous biofilm (Fig-

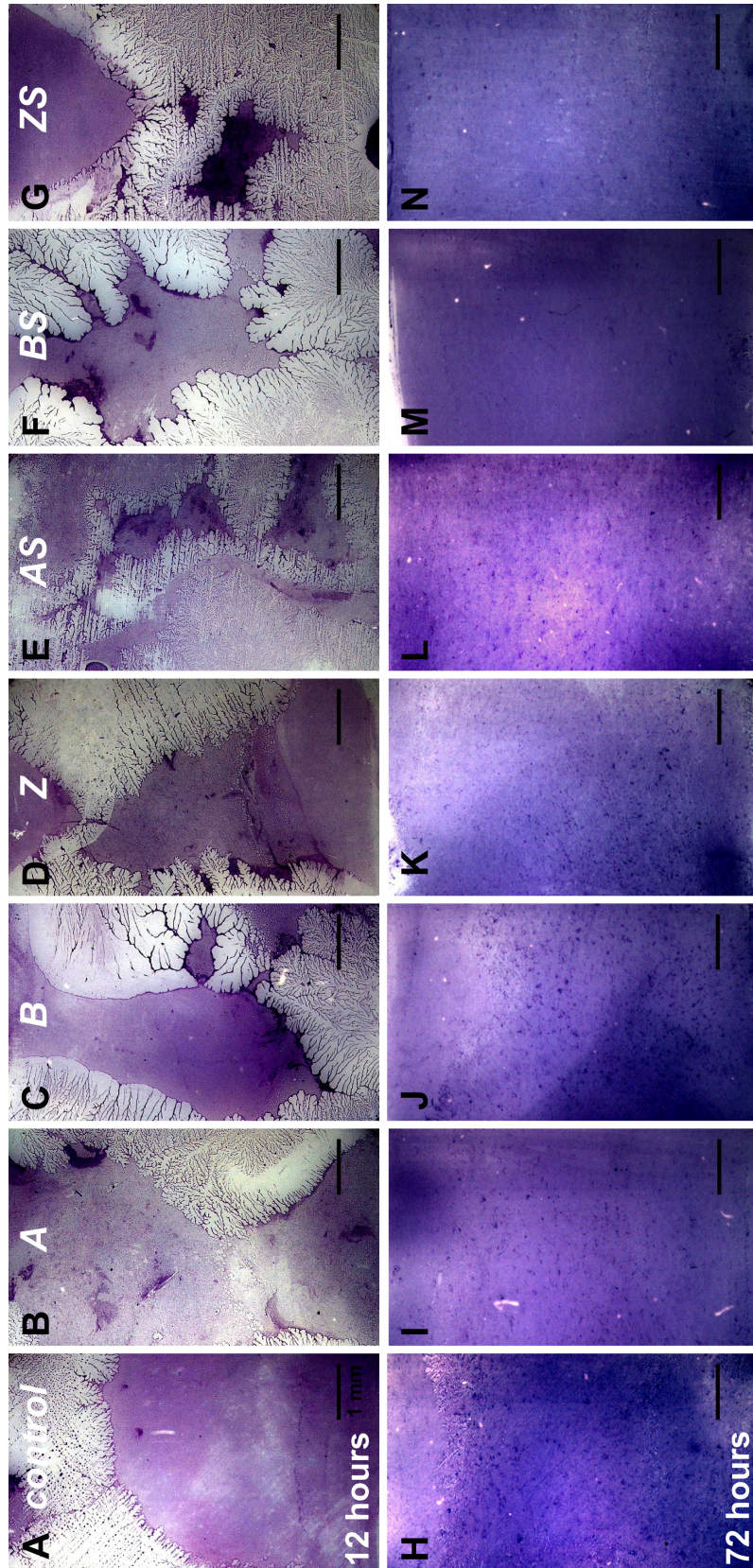


Figure 5.5: *E. coli* biofilm on PTFE plates growing in medium (control) without additives (A, H) and with A (B, I), B (C, J), Z (D, K), AS (E, L), BS (F, M) and ZS (G, N) in concentrations of 2.05 mmol l^{-1} . Slides A-G show biofilm formation after 12 hours, where a mixture of homogeneous patches and branched structures dominated. Slides H-N show biofilm formation after 72 hours and the inhomogeneous structures transformed into a homogeneous layer. No obvious differences between treatments neither after 12 nor after 72 hours could be observed. Scale bar = 1 mm

ures 5.5 H-N). Due to biofilm inhomogeneity, evaluation within the "center in PTFE" by the inverse microscope as described under section 5.2 would have lead to rather random results. Therefore, biofilm covered PTFE plates were magnified by a stereo microscope, each picture showing the complete "center in PTFE" region and not just a small fraction (image size 3.9×6.6 mm). Due to high light gradients during image capturing by the stereo microscope, the algorithm for quantitative evaluation with Image J as described in section 5.2 did not work for *E. coli*. Thus, images obtained by the stereo microscope were just evaluated qualitatively. Figure 5.5 shows a selection of *E. coli* biofilm development with treatments control, A, B, Z, AS, BS and ZS after 12 (A-G) and 72 hours (H-N). After 12 hours, from each treatment one picture was selected, representing a medium coverage, consisting of both branched and homogeneous island structures of biofilm. Biofilm coverage after 72 hours was homogeneous in all samples and treatments. In none of the six treatments an influence of any of the additives could be observed. Biofilm coverage was at any time comparable to that of the control sample with no additives (Figure 5.5).

Since no differences in biofilm formation could be observed for any of the treatments, estimation of cell growth was not performed during the assay.

UPLC-MS measurements confirmed a trend already observed in biofilm assays of this *E. coli* strain at the air-liquid-interface. None of the additives was metabolized even during a period of three days. Samples were taken right before and 24, 48 and 72 hours after inoculation. As internal standard for estimation of the relative peak area again *trans*-cinnamic acid was used. In none of the additives a decrease in concentration could be observed (Figure 5.6). Peak areas of the non-sulfated phenolic acids A, B and Z were rather constant with small standard deviations. Peak shapes of the non-sulfated forms and the internal standard were symmetric with the dilutions performed during sample preparation. In contrast, peak shapes of the sulfated phenolic acids in contrast showed tailing and fronting due to peak areas 4 to 10 times higher than those of the internal standard. This caused a rather large standard deviation of the relative peak area of the sulfated phenolic acids (Figure 5.6). None of the sulfated samples AS, BS and ZS contained traces of their non-sulfated

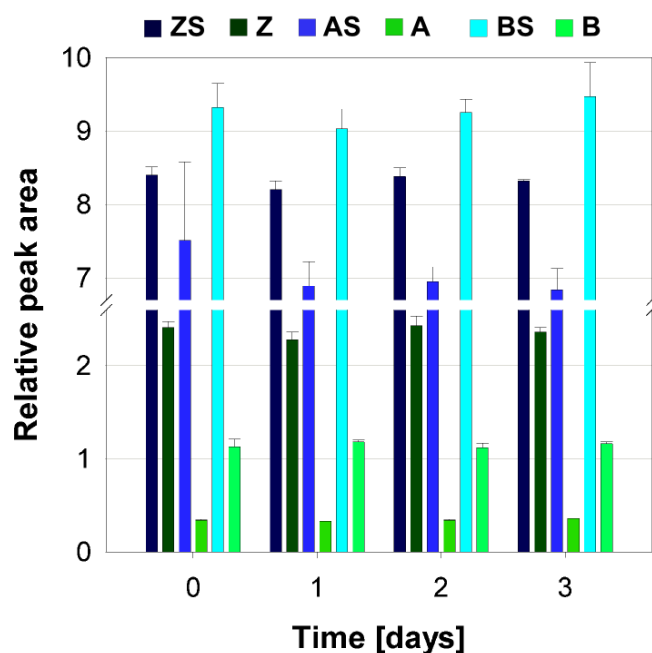


Figure 5.6: UPLC-MS measurements in *E. coli* biofilm assay on PTFE plates. Samples were taken before, and 1, 2 and 3 days after inoculation. Stability of all additives ZS, AS, BS, Z, A and B was monitored by using *trans*-cinnamic acid as internal standard. In none of the six samples could a decrease in concentration be observed, nor traces of non-sulfated forms be found in samples with sulfated additives. (arithmetic mean \pm SD, n=3)

forms, confirming long term stability of the sulfated phenolic acids in presence of this *E. coli* strain as already observed during the assay at the air-liquid-interface. Although a sulfatase like activity for a different *E. coli* strain has been reported once [150], under the conditions applied here, no indication of enzymatic hydrolysis could be detected.

UPLC-MS screening could not unveil differences concerning *E. coli* metabolic activity towards the six additives, both in this assay and the microtiter dish assay. Regarding biofilm formation, the differences in experimental conditions, such as surface, incubation time, shaking and temperature, however seem to have lead to rather distinct findings. *E. coli* biofilm formation at the air-liquid-interface was delayed by A and B and long term reduced by Z during 13 hours after inoculation. Biofilms grown on PTFE plates were not influenced by either one of the sulfated and non-sulfated phenolic acids (AS, BS, ZS, A, B, Z) after three days. All samples showed a dense and homogeneous biofilm. After 12 hours, where during the microtiter dish assay already a clear distinction between treatments could be made, biofilms on PTFE plates were rather inhomogeneous independent of the treatment. In none of the treatments a significant delay could be observed. Observation of biofilm coverage by light microscopy of course allowed no estimation of biofilm thickness. This how-

ever was considered as a negligible draw back, since it is widely agreed upon that a once developed biofilm often serves as a protection against antibacterial agents [82, 174] and additionally might provide a base for further colonization of micro- and macroorganisms, even of a different species [89]. Thus, within a homogeneous biofilm completely covering a surface, eventual differences in thickness seemed rather irrelevant. In this early stage of biofilm formation, it was expected that a reduction by 30 %, as could be observed during the microtiter dish assay with this strain by Z, would be clearly visible. Direct comparison of *E. coli* biofilm formation under two different experimental setups clearly demonstrates the strong dependence of the effectiveness of a treatment from the conditions applied. Both times bacteria were cultured in the same medium and additives were added in the same concentration, but the different conditions concerning surface, incubation temperature, shaking and incubation time were obviously sufficient to cause these deviating results. Thus, only *E. coli* biofilm formed at the air-liquid-interface was inhibited by Z under static conditions, whereas a biofilm formed below the medium surface was not affected by any of the additives. Again, no antifouling effect of ZS, as has been described in several studies (see section 4.2), could be found.

5.4 Impact of ZS and Z on biofilm formation of *V. natriegens*

Biofilm formation of *V. natriegens* at the air-liquid-interface was not evaluable (chapter 4.3), thus, the antifouling effect of the sulfated phenolic acids ZS (*Zostera marina*), AS and BS (Dasycladaceae) as well as their non-sulfated forms were tested with the biofilm assay on PTFE plates. Since results obtained for ZS and Z differed considerably from those obtained with metabolites identified in members of the Dasycladaceae, results for both groups will be discussed in separate sections. The effect of ZS and Z in concentrations of 2.05 mmol l^{-1} on biofilm formation of *V. natriegens* was tested on PTFE plates, with simultaneous monitoring of substance stability by UPLC-MS measurements and cell growth estimation in order to obtain

a complete overview of the influence of these substances on *V. natriegens*.

Pre-experiments with *V. natriegens* cultures showed higher growth rates and a consequently earlier start of biofilm formation at 30 °C compared to experiments performed at 23 °C (room temperature, RT). Thus, the impact of zosteric acid (ZS) and of the non-sulfated form *para*-coumaric acid (Z) was first investigated at 30 °C. Biofilm coverage in these treatments were compared to medium controls without additives. Treatments were performed in triplicates and sampling of each replicate provided 4 biofilm samples. For all treatments formation of biofilm at 30 °C started at day three. Afterwards, every second day a sample was taken until day 11 (Figure 5.7 B). Bacteria cultured in medium containing ZS exhibited no significant differences in biofilm coverage rates to bacteria in control samples. In both treatments a biofilm coverage of 25 to 35 % could be observed after 11 days (Figure 5.7 B). Only samples containing Z, the non-sulfated form of ZS showed a significant reduction in biofilm coverage compared to the control, starting at day 5. At all sampling points from day 3 onwards *p*-values of a one-way analysis of variance (ANOVA) lay below 0.001 when comparing samples containing Z to the control. Biofilm coverage in samples containing Z only reached maximum coverage rates of around 6 %, which was 4 to 5 times less than in control samples and treatments with ZS.

As during the *E. coli* experiments at the air-liquid-interface, only the non-sulfated form of ZS, Z, could effectively inhibit biofilm formation of *V. natriegens* at 30 °C. Since with the synthesis and work-up routine applied during this study, ZS showed no traces of educt Z in ¹H-NMR and only a fraction of around 1 % in UPLC-MS purity control, it was decided to test down to which concentration Z is able to inhibit biofilm formation. Due to the large amount of samples, for reasons of convenience, the experiment was repeated at RT, keeping in mind that temperature differences might influence the result. The experiment on PTFE plates was thus repeated at RT with ZS and Z in equal concentrations of 2.05 mmol l⁻¹ as before and additional samples containing Z in reduced amounts, of 50 (Z 50), 25 (Z 25), 10 (Z 10) and 5 % (Z 5) of the initial concentration. At RT (23 °C) biofilm formation started in all treatments at day 7, which was an expected delay compared to experiments per-

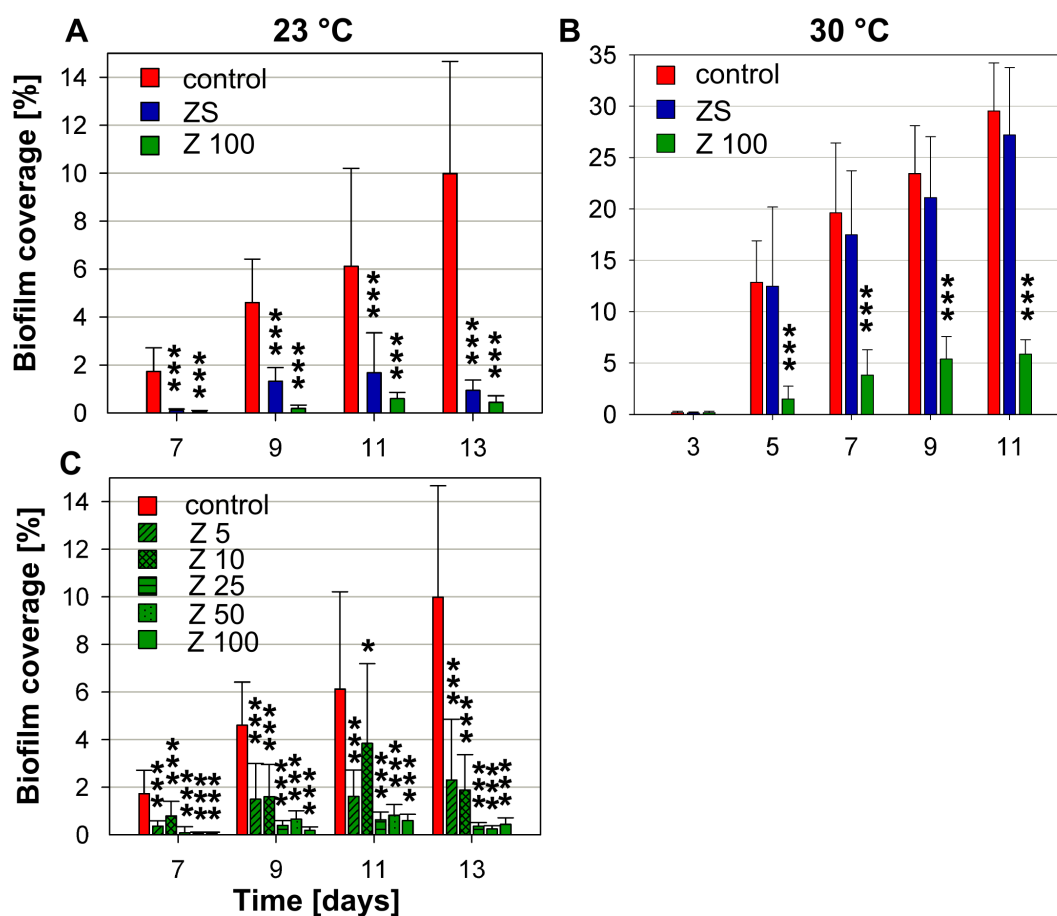


Figure 5.7: Biofilm coverage of *V. natriegens* with no additives (control) and in the presence of ZS and Z in concentrations of 2.05 mmol l^{-1} . **A:** Biofilm development during 13 days at RT (23°C). On all sampling days ZS and Z samples are significantly different from the control. **B:** Biofilm development during 11 days at 30°C . On all sampling days Z samples are significantly different from the control and treatment ZS. **C:** Biofilm development during 13 days at RT with Z in fractions of 2.05 mmol l^{-1} (Z100). 50% = Z 50, 25% = Z 25, 10% = Z 10, 5% = Z 5. On all sampling days Z 5, Z 25, Z 50 and Z 100 are significantly different from the control. Z 10 has an outlier on day 11. (mean \pm SD, $n = 3$. One way ANOVA (Holm-Šídák test): *** significantly different with $p < 0.001$, ** significantly different with $p < 0.01$, * significantly different with $p < 0.1$ to the control.)

formed at 30°C . From day 7 onwards biofilm samples were taken every second day until on day 13 the experiment was terminated (Figures 5.7 A, C). Also during this experiment samples for UPLC-MS measurements and cell growth estimation were taken, starting on day 0 and then every second day. The decrease in temperature to 23°C resulted in a remarkably reduced biofilm coverage after 13 days in the control samples (Figures 5.7 A and C). Whereas at 30°C a biofilm coverage around 30% could be observed, at this temperature only coverage rates around 10% could be

achieved, being two thirds less than at higher temperature. The inhibiting effect of Z could be confirmed at RT. For all sampling days starting at day 7 all different concentrations of Z, "Z 50", "Z 25", "Z 10" and "Z 5" showed a significant difference to the control with p -values below 0.001 (except treatment Z 10 at day 11 with $p < 0.1$ which nevertheless still was considered as significant). Even after 13 days Z samples in concentrations of 2.05 mmol l^{-1} showed an around 20 times reduced biofilm coverage compared to the control (Figure 5.7 A) and remarkably, even 5% ($125 \text{ } \mu\text{mol l}^{-1}$) of the original concentration (Figure 5.7 C) could still reduce biofilm formation by more than half compared to the control. This led to the conclusion that the non-sulfated form of ZS, *para*-coumaric acid (Z), is an effective biofilm inhibitor of *V. natriegens*, independent of the temperature. The inhibiting effect of Z seemed, however, more profound at RT, since its impact was stronger than at 30°C (Figure 5.7 A and B). Samples containing ZS in the experiment performed at RT however showed a surprising discrepancy to when the experiment was performed at 30°C . Suddenly a biofilm inhibiting effect of ZS could be observed too. On all sampling days (7, 9, 11 and 13) a significant difference ($p < 0.001$) between ZS samples and the control could be observed. Having proven now that Z is a very effective biofilm reducing agent also on *V. natriegens* independent of the temperature, the ostensible temperature dependent biofilm inhibiting effect of the sulfated form ZS seemed questionable.

UPLC-MS data for substance stability of experiments performed both at RT and at 30°C provided an explanation for these contradictory results. UPLC-MS data revealed, that in ZS samples at either RT or 30°C the concentration of ZS in the medium continuously decreased and simultaneously the amount of non-sulfated Z increased in medium originally just containing ZS. Figure 5.8 shows ion traces at RT of ZS (m/z 243.00 $[\text{M-H}]^-$), Z ("Z in ZS", m/z 163.05 $[\text{M-H}]^-$) and of the internal standard (IS) cinnamic acid (CA, m/z 147.05 $[\text{M-H}]^-$) in the negative mode within *V. natriegens* cultures containing ZS. The figure includes samples from five different time points. Sampling point 0 resembled the medium containing ZS shortly before inoculation. Here, only a minor trace of Z could be detected ($< 1\%$). Starting at

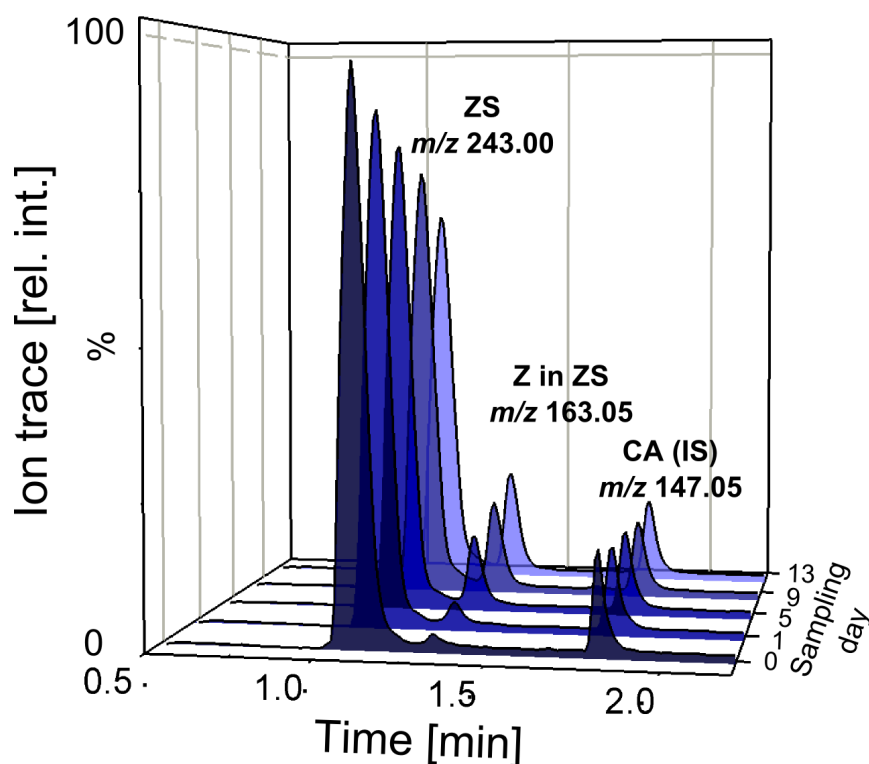


Figure 5.8: UPLC chromatograms of *V. natriegens* samples at RT containing ZS. The figure displays ion traces in the negative mode $[M-H]^-$ of ZS with m/z 243.00, the hydrolysis product of ZS, *para*-coumaric acid (Z in ZS), with m/z 163.05 and the internal standard (IS) cinnamic acid (CA) with m/z 147.05. During a 13 day period peak areas of ZS decreased, whereas simultaneously peak areas of Z in ZS within these samples increased, illustrating that the sulfate group of ZS is hydrolyzed by the bacteria and Z is released into the medium. Peak areas of the internal standard CA remained constant. (arithmetic mean \pm SD, $n=3$)

day 1 after the inoculation, the peak area of Z within the ZS samples ("Z in ZS") increased constantly during days 5, 9 and 13. Simultaneously, the peak area of ZS decreased from day 1 onwards until day 13. The peak area of the internal standard CA in the medium remained constant, showing no major instabilities of the UPLC-MS system during the measurements. When stability of the sulfated phenolic acids in sterile medium was tested over the same period of time under the same conditions (temperature, pH, movement), no such decomposition could be detected (chapter 2.2). Z was not metabolized during the experiment, neither at RT nor at 30 °C. The pH in medium containing bacteria and ZS at both temperatures also never dropped below 7 during the experiment and under these conditions sulfated phenolic acids

were not hydrolyzed (chapter 2.2). Thus, it seemed reasonable that sulfatase activity of *V. natriegens* was responsible for the release of Z into medium containing ZS as already observed in chapter 4.3. This led to the assumption that the biofilm inhibiting effect of ZS on *V. natriegens* at RT was just ostensible, and that the inhibiting substance was Z, released by sulfatase hydrolyzation of ZS. In order to proof this theory and directly compare if the decrease of ZS corresponded to the increase of Z and to what extent the sulfatase activity leading to the release of Z was temperature dependent, both ZS and Z in medium were quantified by UPLC-MS measurements. Therefore, an external calibration of Z and ZS was performed and the Z and ZS samples from both experiments measured again. For quantification of Z, cinnamic acid (CA) was used as internal standard as described before and an external calibration was performed ranging from 2.05×10^{-3} to 1.03×10^{-2} mmol l⁻¹ (see chapter 9.7.3.4). The solvent composition of the calibration standards corresponded to that of the UPLC-MS samples of the Z treatments. For quantification of ZS in *V. natriegens*, medium ZS samples were additionally diluted ten times with solvent A, due to the rather unsymmetrical peak shapes (compare chapter 4). Dilution of ZS samples with solvent A led to peaks with high peak symmetry, allowing the quantitative evaluation of peak areas. For quantification of ZS, another sulfated phenolic acid, BS, was used as internal standard, since its MS sensitivity was considered more similar to ZS than CA. External standards for ZS were prepared ranging from 5.13×10^{-3} to 2.56×10^{-2} mmol l⁻¹. External standards displayed the same solvent composition as the diluted ZS samples. All external standards were prepared in triplicates from stock solutions and measured once each. Calibration of Z and ZS was not aimed to estimate the absolute amount of ZS and Z in the bacterial medium, but rather to unveil, if the decrease of ZS corresponds to the increase of Z and if there is a temperature dependent difference in Z release from ZS samples. For reasons of better comprehensibility estimated molarities were expressed in % of the maximum concentration of ZS used in bacterial medium which was 2.05 mmol l⁻¹ (Figures 5.9 A, B). In *V. natriegens* samples grown at RT it could be seen that the concentration of ZS in the medium decreased from day 3 onwards to around 60%

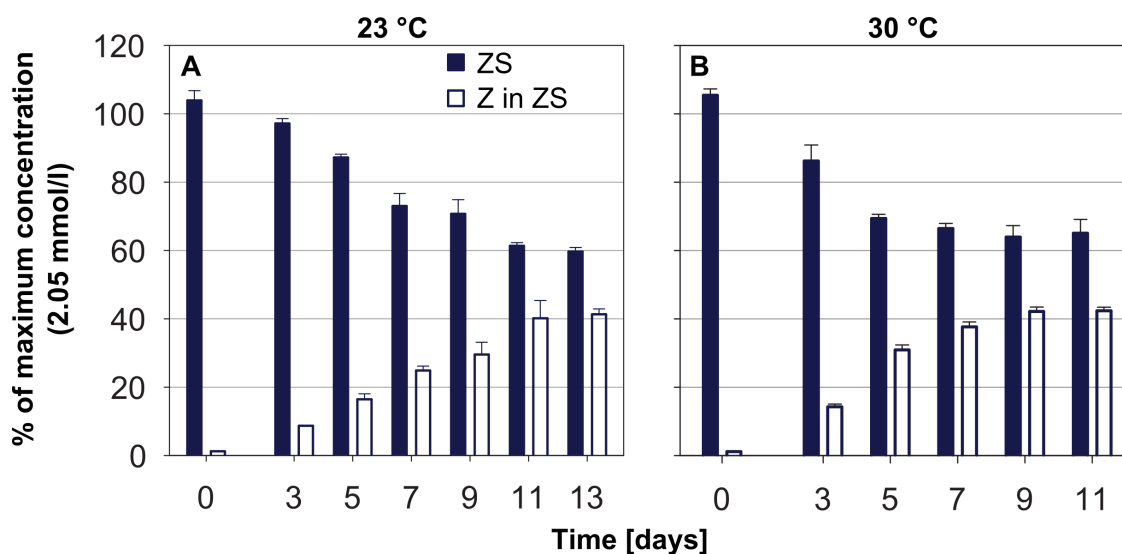


Figure 5.9: Quantification of ZS and "Z in ZS" at RT (23°C) (A) and at 30°C (B). Estimated amounts of each compound were expressed in % of the original concentration 2.05 mmol⁻¹. **A:** Starting from day three onwards, ZS content decreased till 60% of the original concentration at day 13, whereas "Z in ZS" increased by 40%. **B:** The same trend as at RT could be observed. The 60:40 % ratio of ZS and Z, however, is already reached 9 days after incubation. (arithmetic mean \pm SD, n=3)

of the original concentration on day 11 (Figure 5.9 A). In contrast, the concentration of Z in the ZS samples increased from day 3 onwards up to around 40% of the maximum concentration of 2.05 mmol⁻¹ (Figure 5.9 A). This measurement showed, that the concentration of ZS decreased by the exact amount that Z increased in the sample. The release of Z from ZS was temperature dependent such that an increase by 7°C, earlier led to a higher concentration of Z in the sample, reaching the ratio of 60% ZS to 40% Z already after 9 days (Figure 5.9 B). After 11 days this ratio did not seem to change anymore, independent of the culturing temperature. Although Z was released faster from ZS at 30°C than at RT, *V. natriegens* biofilm formation was not affected by Z originating from ZS hydrolyzation at the higher temperature. At RT biofilm formation started at day 7 (Figure 5.7 A), where according to the calibration Z was already present in ZS samples at least for 4 days and by then had reached a concentration of around 25% of 2.05 mmol⁻¹. In the concentration dependent impact experiment of pure Z, this amount of Z was already sufficient to significantly reduce biofilm formation (Figure 5.7 C). At 30°C biofilm formation started at day 3 (Figure 5.7 B) and here the concentration of Z in ZS was

only around 15%. Keeping in mind that the impact of Z on biofilm formation of *V. natriegens* was lower at higher temperatures, this might provide an explanation why at RT ZS has an ostensible effect that is due to Z released from ZS, whereas Z released from ZS at 30 °C does not affect biofilm formation. Obviously, Z could not disturb an already ongoing biofilm formation process, a phenomenon often observed upon the interaction of antibacterial agents and biofilms [82, 174].

A possible explanation why Z inhibited biofilm formation of *V. natriegens* might be provided by the estimation of cell growth during the experiment at RT. Cell numbers of the control were compared to that of samples containing ZS and Z each in concentrations of 2.05 mmol l⁻¹ (Figure 5.10 A), and "Z 25" and "Z 5" (Figure 5.10 B). Immediately after inoculation, cell numbers of all treatments were similar. All treatments (control, Z, ZS, "Z 5", "Z 25") entered the stationary phase after three days and started to decline after seven days. A one-way ANOVA (Holm-Šídák test) was performed on all samples from day 1 to 9, comparing control samples to the different treatments. Samples of *V. natriegens* containing Z as an additive with 2.05 mmol l⁻¹ are marked in dark green and were on all evaluated days significantly different to the control (with $p < 0.001$ on days 7 and 9, with $p < 0.01$ on days 1, 3 and 5). *V. natriegens* cell numbers of Z were reduced between 20 to 35% during days 1 to 7. Samples containing ZS in the same concentration as Z showed a more complicated picture during the evaluated time span. On day 1 could no statistically significant difference between samples containing ZS and the control be found, the mean cell number was slightly higher than in the control. This phenomenon had already been observed during OD measurements of *V. natriegens* cultures in the microtiter dish assay in the presence of this compound (section 4.3). But, as during that assay, a significant reduction of ZS concentration, hinting for a major release of sulfate into the medium that might be beneficial could also not be observed here by the UPLC-MS measurements. On day 3, however, a significant reduction in cell numbers of ZS treatments could be observed compared to the control (with $p < 0.1$). ZS samples showed cell numbers more similar to Z samples. A possible reason might be sought in the release of Z from ZS, that already took place at that time

(Figure 5.9 A). A similarity in cell numbers of ZS and Z samples could also be observed at day 7 and 9, which were both significantly different to the control ($p < 0.01$ on day 7 and $p < 0.001$ on day 9). Only day 5 seemed to display an exception, where no statistical significant difference between ZS and the control could be found. This can probably be attributed to the abnormally large standard deviation of ZS samples characterizing this day. Still, these data allowed the conclusion, that after day 3, when UPLC-MS measurements showed an continuous increase of Z in ZS samples, cell numbers of Z and ZS were similar and both were significantly reduced compared to control samples. A study by Xu *et al.* from 2005 found a more than 10 times higher toxicity of Z compared to ZS by using a standard Microtox[®] assay.[81] This assay uses bioluminescent bacteria and relates a reduction of bioluminescence to the toxicity of a compound.[175] Irrespective of the question, if the decreased cell numbers in *V. natriegens* samples containing Z were due to the toxicity of this compound or just due to a growth inhibiting effect, the significant reduction might be a contributing factor for reduced biofilm development. However, differences in cell numbers alone do not seem to be the sole reason for biofilm reductions, when growth curves of samples "Z 5" and "Z 25" were compared to control samples (Figure 5.10 B). The growth curve of "Z 25" had cell numbers 20 to 30 % lower than the control during the days 3 to 9 (Figure 5.10 B; days 3 and 7: $p < 0.001$; days 5 and 9: $p < 0.01$), similar to those of samples Z. Samples "Z 25" containing 25 % of the original 2.05 mmol l^{-1} (Z), also showed a similar reduction in biofilm formation as the Z samples at RT (Figure 5.7 C). Samples containing only 5 % of the original concentration of 2.05 mmol l^{-1} ("Z 5") had cell numbers never as low as samples Z and "Z 25". Cell number means of "Z 5" had rather large variations between the single sampling days, namely being significantly lower than control samples on days 3 and 7, but not significantly different on days 5 and 9. The overall progression of cell numbers in sample "Z 5" appeared to be more similar to the control. So assuming that in "Z 5" samples no overall reduction of cell number took place, this low concentration still was able to considerably reduce *V. natriegens* biofilm formation by more than half compared to the control (Figure 5.7 C). Thus, even if the

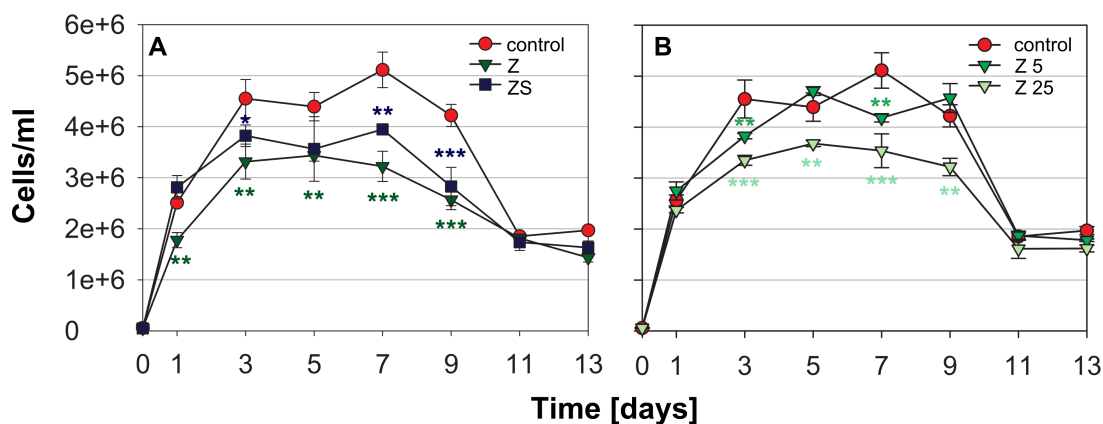


Figure 5.10: Cell number estimation during biofilm development of *V. natriegens* in presence of Z and ZS at RT (23 °C). **A:** Cell numbers of samples Z and ZS were significantly different from the control on all sampling days. **B:** Cell numbers of samples Z 25 were significantly different from the control on all sampling days, samples of Z 5 showed similar growth to the control, significant differences were not consequent (mean \pm SD, $n = 3$. One way ANOVA (Holm-Šidák test): *** significantly different with $p < 0.001$, ** significantly different with $p < 0.01$, * significantly different with $p < 0.1$ to the control.)

reduction in cell number constituted an additional factor for the decrease in biofilm formation of *V. natriegens* by Z, this compound was also found to be an effective biofilm inhibitor even in concentrations as low as $0.1025 \text{ mmol l}^{-1}$ (17 mg l^{-1}), an amount apparently not toxic or growth inhibiting to this strain.

Thus, as during the microtiter dish assay with *E. coli* no influence of ZS, which was often discussed as a potent antifouling agent during the recent years (chapter 4) on *V. natriegens*, could be found. The biofilm inhibiting effect of ZS at RT, also mentioned in a study by Xu *et al.* in 2005 [81], could be unambiguously proven by UPLC-MS screening to be ostensible. The presumably enzymatic hydrolysis of ZS by a sulfatase caused a release of Z into the medium. At RT, initial biofilm development was prolonged, starting at day 7, allowing a sufficient amount of Z to accumulate for biofilm inhibition. In contrast, a temperature increase by 7°C enhanced biofilm formation and seemed to moderate the antifouling effect of Z both when present from the beginning (sample Z) or released during the assay (sample ZS), obviously allowing *V. natriegens* biofilm formation to be less effected by this compound. At 30°C biofilm development started after 3 days and here the amount of Z released by sulfatase activity seemingly was not sufficient to interfere with an

already ongoing biofilm formation.

The concentration dependent biofilm assay with *V. natriegens* also unveiled that even minor contaminations ($0.1025 \text{ mmol l}^{-1}$) of educt Z in ZS samples initially present, e.g. from synthesis, can have a significant biofilm inhibiting effect. These results again underline the importance of initial substance purity as well as the monitoring of compound stability during a bioassay, ensuring the correct attribution of an observed impact.

Based on the data obtained during different biofilm assays with *E. coli* and *V. natriegens* a revised hypothesis concerning the antifouling activity of ZS can be derived. The sulfate ester ZS thus rather seems to display a storage form of the potent biofilm inhibiting agent *para*-coumaric acid Z. As already discussed in chapter 4.2 several allelochemical functions as well as antifungal and antibacterial activities have been attributed to this compound. Although Z seems a potent antifouling agent towards biofilm formation of *V. natriegens* on PTFE surfaces, the detrimental effect on cell growth in higher concentrations indicate that this compound is not non-toxic, as would be required for an environmental friendly agent.

5.5 Impact of AS, A, BS and B on biofilm formation of *V. natriegens*

The influence of the two synthetic sulfated phenolic acids AS and BS, identified in members of the Dasycladaceae and their non-sulfated forms was tested on biofilm formation of *V. natriegens* at 30°C under permanent agitation. All additives were used in concentrations of 2.05 mmol l^{-1} . Biofilm grown in medium without additives was used as a control. During the length of the experiment UPLC-MS samples were taken shortly before, and 1, 3, 5, 7 and 9 days after inoculation. Biofilm samples were taken after 3 days and then every second day until day 9. Biofilm formation started during day 3, where biofilm coverage ranged from 0 to 0.5% (Figure 5.11). A remarkable increase in biofilm formation could be observed from days 3 to 5 when bacterial coverage reached around 20% for control samples, AS, BS and

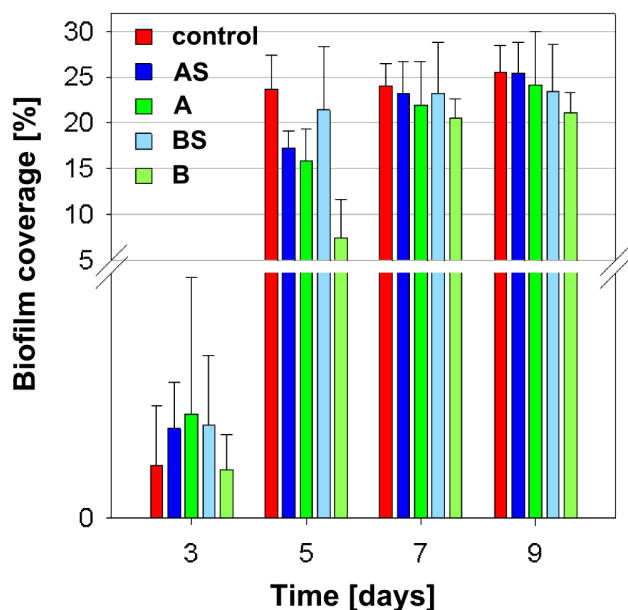


Figure 5.11: Biofilm development of *V. natriegens* on PTFE plates during 9 days at 30 °C in presence of AS, BS, A and B (2.05 mmol l^{-1}) and the control. Biofilm formation started 3 days after inoculation and reached levels between 20 and 25 % coverage from day 7 onwards for all treatments. Biofilm growth in sample B was delayed on day 5 compared to the other treatments. (arithmetic mean \pm SD, $n = 3$)

A. Biofilm formation in samples containing B was considerably lower, mean values only lay around 7 % coverage. From day seven onwards, the biofilm inhibiting effect of samples containing B seemed terminated, and in all samples PTFE surfaces were covered with a *V. natriegens* biofilm around 25 %. Thus, biofilm formation of *V. natriegens* was neither influenced by the two novel sulfated substances identified in members of the Dasycladaceae, nor by their non-sulfated forms A and B. Reduction of biofilm formation in sample B at day 5 rather seemed to have been a delay in biofilm development.

12 hours after inoculation all samples containing BS and B showed a remarkable color change within the bacterial medium ranging from light brown to deep purple that lasted for 12 hours. Afterwards, the medium color of these samples resembled that of the other treatments (A, AS) and the control. In UPLC-MS measurements of samples B and BS both additives could be detected in samples before inoculation ($t = 0$), but neither was detectable after sampling 24 hours later ($t = 1$) (Figure 5.13 B). This is in agreement with processes observed during the microtiter dish assay with *V. natriegens* (chapter 4.3). Here, both B and BS were completely degraded within 17 hours post inoculation. Previously also the non-sulfated form B could be found in BS samples (chapter 4.3), indicating sulfatase activity. Since during this

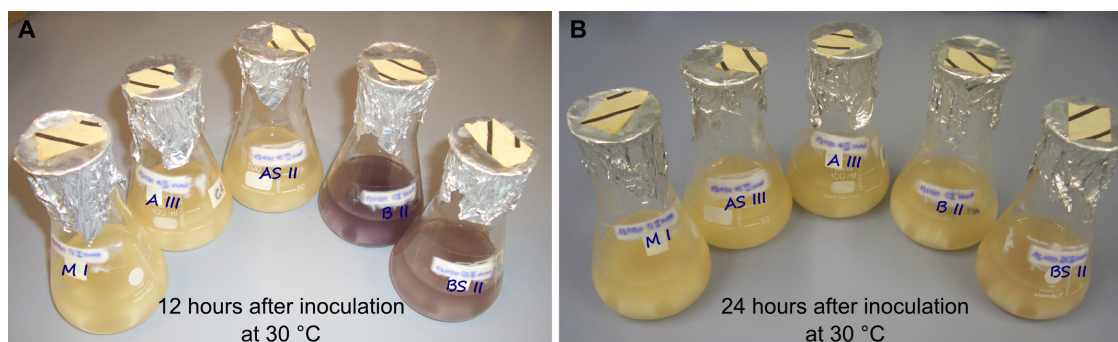


Figure 5.12: Color change in *V. natriegens* samples during exposure to B and BS (A) 12 hours after inoculation and complete discoloration after 24 hours (B) at 30 °C. During this time both B and BS were degraded completely.

assay samples were only taken 24 hours after inoculation, sulfatase activity can only be assumed based on the activity observed, when sampling points covered a closer time window in the experiment at the air-liquid-interface (chapter 4.3). The antibacterial and antifouling potential of B has already been discussed in chapter 4.3. The complete degradation of B by *V. natriegens* could thus be a detoxification strategy. In all sample replicates of AS sulfatase activity could be identified (Figure 5.13 A). A constant decrease of relative peak area of AS, accompanied by a gradual increase of the non-sulfated form A within the AS samples could be observed. In contrast to the hydroxybenzoic acids (BS, B), concentrations of 4-hydroxyphenylacetic acid A remained constant during the length of the experiment (Figure 5.13 A (green)). In contrast to B, A seems thus not to be metabolized. Since the presence of A on biofilm formation of *V. natriegens* was neither promoting nor inhibiting, the presence of A in the AS sample caused by sulfatase activity also played no role on biofilm formation. Since the sulfated metabolites found in members of the Dasycladaceae had no impact on biofilm formation, an estimation of cell numbers was not performed.

5.6 Summary of biofilm formation on PTFE plates

The biofilm assay using submerged PTFE plates allowed a quantitative evaluation of biofilm formation via image processing. Combination with UPLC-MS stability screening and cell number estimation provided profound insights on the impact of

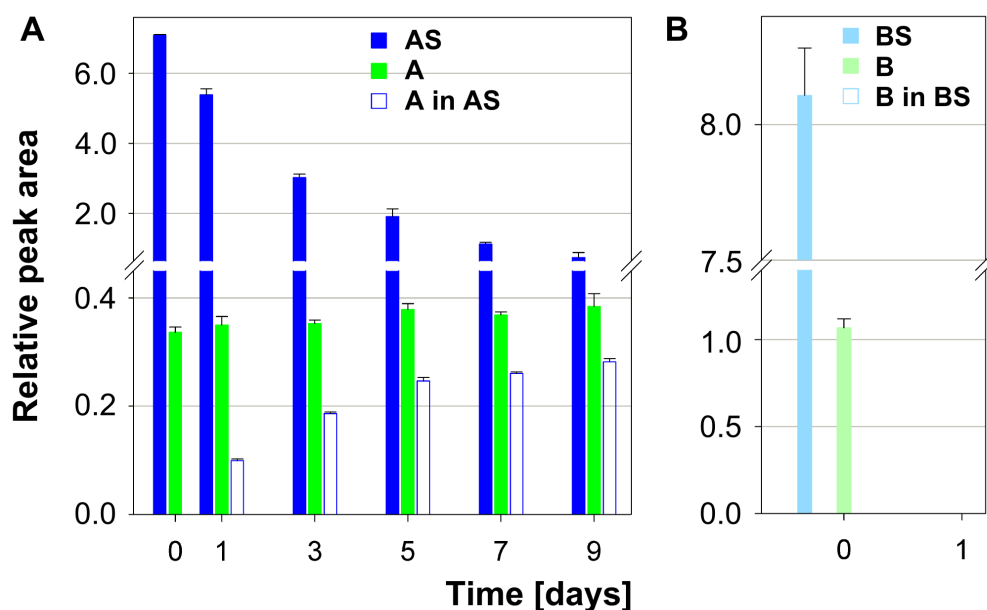


Figure 5.13: UPLC-MS screening of sulfatase activity in all samples and degradation of BS and B by *V. natriegens* at 30 °C. All peak areas were normalized to the internal standard *trans*-cinnamic acid. **A:** Concentration of AS decreased from day 1 onwards, simultaneously the amount of "A in AS" increased. Concentrations in samples just containing A remained constant. **B:** Neither B nor BS were detectable in medium containing *V. natriegens* cultures after 1 day. (arithmetic mean \pm SD, $n = 3$).

the sulfated phenolic acids AS, BS and ZS and their non-sulfated forms on biofilm and bacterial growth. *E. coli* biofilm formation on PTFE plates was not affected by any of the six additives, in contrast to the microtiter dish assay, where Z inhibited biofilm development at the air-liquid-interface. This indicates that potency of an antifouling agent can be dependent of the experimental conditions applied. *V. natriegens* biofilm formation on PTFE plates in contrast was effectively inhibited by Z, even in concentrations as low as $0.1025 \text{ mmol l}^{-1}$. Here, also the experimental factor temperature played an important role, in so far that the effect of Z was slightly attenuated at higher temperatures. The ostensible effect of ZS on *V. natriegens* biofilm formation at RT could be ascribed to Z, which was presumably released by sulfatase hydrolysis from ZS. Additionally it could be shown that Z in concentrations of $0.625 \text{ mmol l}^{-1}$ already reduced the cell number by 20 to 30 %, thus, showing growth inhibiting properties towards this species. Again also during this assay no antifouling activity of ZS could be detected.

6 Biofouling field assay with AS, BS and ZS at the coast of İzmir

Laboratory assays investigating the biofilm inhibiting potential of the sulfated phenolic acids ZS, AS and BS on single species cultures revealed that these rather display storage forms of the more potent non-sulfated ones. It could be shown that the active, non-sulfated form can be released into the medium by sulfatase activity. The field assay with a mixed marine community should hence provide first insights, if it is possible to utilize the sulfated phenolic acids as storage components in antifouling paints. A potentially slow release of the active compound due to metabolic activity of marine organisms might provide a long term antifouling effect.

6.1 Experimental design and evaluation

The antifouling field experiment was performed by Dr. Levent Cavas from the Dokuz Eylül University in İzmir, Turkey, during the main fouling season (June - August in 2013). The rosin based antifouling paints were prepared with synthesized AS, BS and ZS, provided from Jena. Antifouling effects of these compounds were compared with each other and to a control, only containing the paint components without additives. The rosin based antifouling paint contained Cu_2O , as an additional antifouling agent. Panels coated with either just the primer coating (preventing corrosion) and both primer coating and paint without additives were thus thought to function as positive controls. Paints including additives either contained AS, BS or ZS in weight ratios of 2, 4, 6 and 10%. With increasing amounts of additives, ratios of the pigment ZnO and binder were adapted accordingly (chapter 9.7.4). For each treatment a

steel panel was painted front and back. After drying, all panels were immersed into seawater at a depth of 50 cm by hanging them on a plastic line. The paints were tested for a period of 70 days from June 12 to August 8, 2013 at Levent Marina, İzmir, Turkey. Plates were removed every 10 to 14 days and a photograph of each sample was taken, before they were placed back into the seawater. Evaluation criteria for antifouling activity of test panels were adapted from Alyuruk *et al.* 2012, concerning abundance of settled micro- and macrofouling organisms.[176] Plates with no sign of a developing microfilm layer and consequently no fouling of higher organisms were described as level I. Level II was considered to exhibit a microfilm layer on the surface. Plates assigned level III showed macrofouling at its beginning state. When micro- and macrofouling organisms were readily present on the surface plates they were assigned level IV and, if macrofouling covered more than 50 % of the surface fouling was described as level V.

6.2 Impact of AS, BS and ZS on marine fouling

After 70 days immersed in seawater an unexpected conclusion could be drawn from the results obtained. Figure 9.7.4 G shows a primer coated plate, I a plate with biocide free paint and A, C and E plates of paint with the incorporated biocides AS, BS and ZS before immersion. After 70 days, as expected, the panels just treated with the primer coating were heavily fouled by macroorganisms, thus, assigned level V (Figure 9.7.4 H). The biocide free paint just containing 6 % CuO₂ in contrast exhibited no microslime layer, thus, was assigned the lowest fouling level I (Figure 9.7.4 J). Paint compositions with 2, 4 and 6 % of AS, BS and ZS incorporated showed either no biofilm (Figure 9.7.4 B 2 %, level I) or just a developing microslime layer (Figures 9.7.4 B (4, 6 %, level II), D (2 - 6 %, level II) and F (2 - 6 %), level II). On samples with 10 % ZS and BS macrofoulers already started to adhere, as marked by a red arrow in Figures 9.7.4 B and F (level III). Thus an increase in biocide content of either AS, BS and ZS seemingly promoted fouling compared to paint with a low amount or no additives.

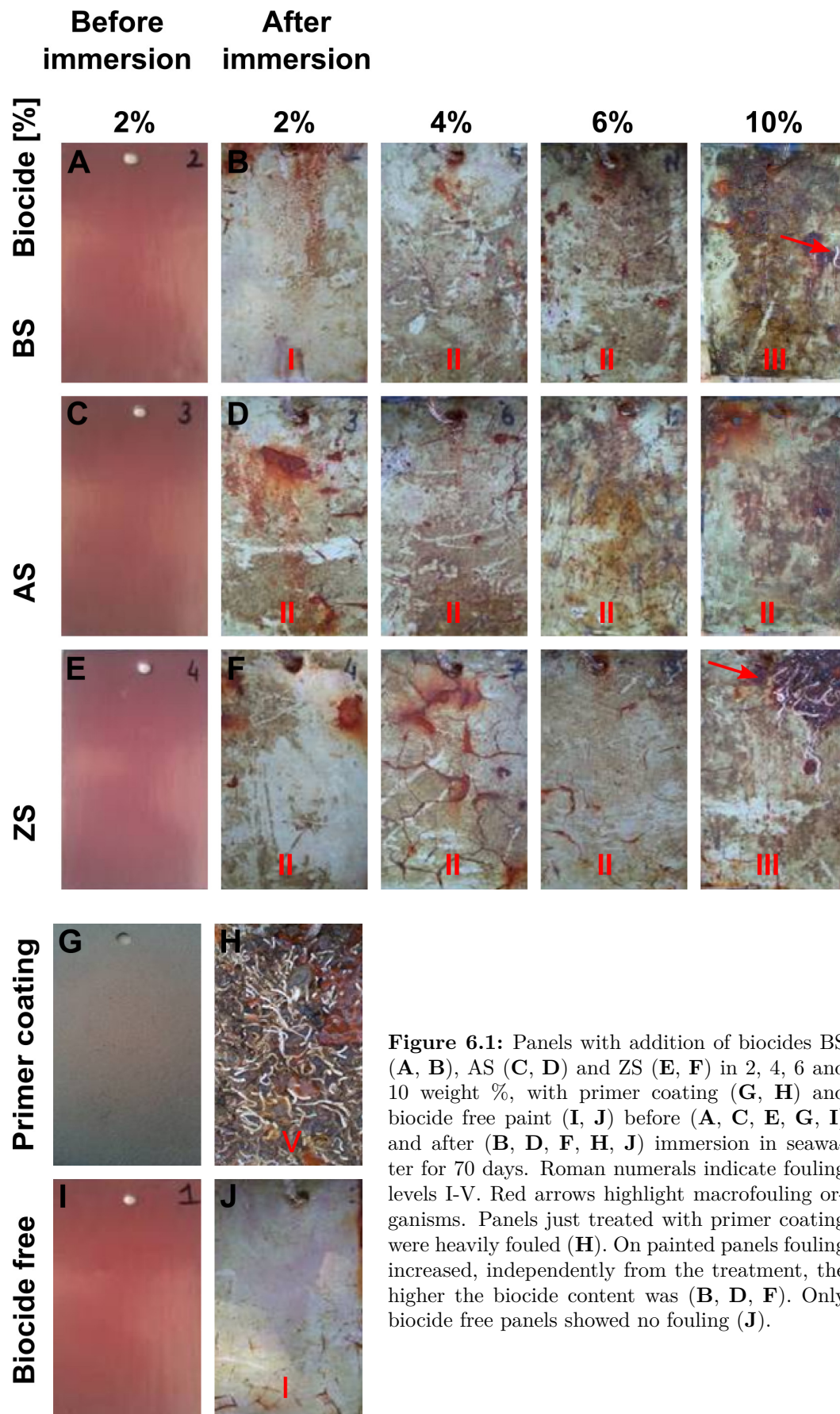


Figure 6.1: Panels with addition of biocides BS (A, B), AS (C, D) and ZS (E, F) in 2, 4, 6 and 10 weight %, with primer coating (G, H) and biocide free paint (I, J) before (A, C, E, G, I) and after (B, D, F, H, J) immersion in seawater for 70 days. Roman numerals indicate fouling levels I-V. Red arrows highlight macrofouling organisms. Panels just treated with primer coating were heavily fouled (H). On painted panels fouling increased, independently from the treatment, the higher the biocide content was (B, D, F). Only biocide free panels showed no fouling (J).

This assay was the first field test of the novel compounds AS and BS. According to Dr. Cavas, one problem during paint preparation was the non-solubility of the sulfated compounds in the solvent xylene, leading to increased aggregate formation. A more homogeneous distribution could be achieved by adding the anti-sagging agent Bentonite. A problem that still occasionally occurred with the applied paint composition was the emergence of cracks in the paint surface during immersion into seawater. Paint cracking was independent of the treatment and only occurred randomly, thus, any additional influences due to the cracks were supposed to be compensated by replicates.

The paint composition was based on the natural product rosin, isolated for example from pine trees, whose major components are derivatives of the diterpene abietic acid. Rosin based paints were originally classified as soluble antifouling paints. Meanwhile rosin is also included in self polishing paints.[177] These paints are a mixture of a polymer (Lutanol M40), a soluble binder (rosin) and usually copper based biocides.[95, 177] Copper ions are strong antimicrobial and antifungal agents, also active against many algae.[101, 178] Some algae (e.g. *Enteromorpha* spp., *Ectocarpus* spp., *Achnanthes* spp.), however, have a high tolerance towards this agent, thus, many paints contain an additional biocide, active against these species.[95, 101, 177] The biocides are slowly dissolved from the paint surface, leaving a porous structure. Since rosin is seawater soluble, this layer is also slowly dissolved, uncovering the next paint layer, with biocides and binder. Thus, a slow but continuous release of substances can be achieved.[95, 177]

Since this experiment was supposed to be a first test of the novel compounds BS and AS in comparison to the activity of ZS, nothing is known about the release rate of these compounds from the paint composition applied. Considering the high water solubility of the sulfated phenolic acids it seems reasonable, that a consequently high release rate from the paint might have led to a loss of antifouling activity. Still, if the sulfated phenolic acids were active a strong antifouling effect should have been observable in the beginning without a long term effect. But such a phenomenon could also not be detected. Already after the first sampling (9 days after immer-

sion) plates including sulfated phenolic acids were higher fouled, in a concentration dependent manner (see appendix 9.9). Assuming however, that the release rate of copper ions from the paint was constant for all treatments, the results obtained on the antifouling effects of AS, BS and ZS under natural conditions allows the conclusion that the presence of these sulfated compounds had compensated the antifouling effect of copper, thus, promoted fouling. Paints not containing AS, BS or ZS showed the lowest level of fouling, and the antifouling effect can presumably be attributed to the copper ions present. The higher the amounts of "biocides" (AS, BS and ZS) were, the less effective seemed the antifouling effect of the paint, although the proportion of copper remained constant in all treatments. On the other hand, it can of course not be excluded that a higher water soluble "biocide" content led to a much more porous paint structure due to leaching, also facilitating the release of copper ions and that the reduced antifouling performance was caused by such a mechanism. Only further experiments investigating simultaneously the concentration dependent leaching rate of the sulfated phenolic acids and copper ions from the paint would provide more profound insights to the underlying mechanisms. With the setup as applied for this assay could the sulfated phenolic acids not be utilized as a storage system for the more potent biofilm inhibitor, the non-sulfated form.

The antifouling activity of ZS has once been tested in the field by Boopalan *et al.* in 2011. Here, ZS was incorporated into zeolite particles, which were linked to an epoxy resin. The paint was applied on zinc phosphated mild steel panels and immersed in seawater for one year. Plates containing ZS loaded zeolite showed less fouling than those with unloaded particles. Based on the experiences on ZS synthesis and the activity of Z obtained during the present study, ZS preparation as described by the authors might still contain contaminations (chapter 2.1). Unfortunately, no further analytical data on the purity of ZS were provided.[77]

Considering the results obtained so far during this study, where not once biofilm inhibition by ZS, AS and BS was detected, it has to be investigated more detailed if it is possible to use these as storage forms for potent natural antifouling agents. The non sulfated form of ZS, Z, which showed rather convincing antifouling activ-

ity towards *E. coli* and the marine biofilm forming *V. natriegens* during laboratory assays (chapter 4, 5) was not included in the field assay. Due to the international co-operation and the limited time window for the field assay, its preparation started long before the experiments on the antifouling activity of the sulfated phenolic acids and their non sulfated forms in the laboratory. It might thus be worthwhile to test the direct antifouling activity of Z in the field as an alternative for the sulfated storage system. Despite the negative impact of Z on cell numbers of *V. natriegens* (chapter 5.4) and the toxicity as estimated by Xu *et al.* [81], might the application of Z as antifouling agent be justifiable, since it is a natural compound [141, 143, 157–164] which might be degraded and thus would not accumulate over the years, as TBT did [99].

7 UPLC-MS screening for secondary metabolites in *Codium fragile*

Analytical investigations by ultra-high-performance-liquid chromatography coupled to electro-spray-ionization mass spectrometry (UPLC-MS) concerning secondary metabolites of *Codium* spp. were motivated by the recent insights into the wound reactions of species belonging to the Caulerpaceae and Dasycladaceae (section 1.1). One reason for the invasive success of some *Codium* species might be sought in its high dispersal potential due to asexual proliferation by fragmentation. Although it has been known for a long time that *Codium* spp. can reproduce by fragmentation (section 1.1), the underlying chemical processes involved in wound sealing of this alga are still unknown. In wound responses of species belonging to the Caulerpaceae and Dasycladaceae a common feature was observed, despite that their species belong to different orders. In both cases an unreactive secondary metabolite is enzymatically transformed after wounding, releasing a highly reactive agent able to crosslink proteins and, thus, initiating the formation of a wound plug.[9, 10, 12, 30] The query if *Codium* species, which belong to the same class as the Caulerpaceae, exhibit a similar wound sealing mechanisms thus seemed reasonable. The high content of sulfated polysaccharides in many *Codium* spp. further encouraged to search for sulfated metabolites with a lower molecular weight, comparable to those detected in members of the Dasycladaceae (section 1.2).

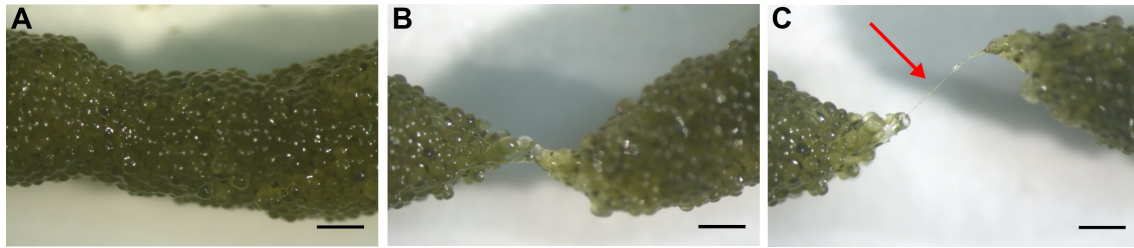


Figure 7.1: Microscopic images of the fragmentation of a *C. fragile* thallus by rupture. **A:** Untreated thallus. The surface is covered by utricles, medullary filaments can not be seen. **B:** Upon rupture thalli became peak shaped, while the surface is still covered by utricles. **C:** Shortly before complete separation thalli are still connected by one medullary filament. Further tearing will finally disrupt the filament leading to two fragments (scale bar = 0.5 mm).

7.1 Wound response of *Codium fragile*

First investigations of the wound response of *Codium* spp. were performed on *C. fragile*, originating from the west coast of Sweden.

Microscopic observations of the wound response in *C. fragile* already revealed significant differences to the wound reactions observed in members of the Dasycladaceae and Caulerpáceae (chapter 1.1). Figure 7.1 shows a *C. fragile* thallus fragmentation by rupture. The surface of the untreated thallus is completely covered by utricles (Figure 7.1 A). During rupture, the thalli of both sides become peak shaped, while the surface is still completely covered by utricles (Figure 7.1 B). Shortly before complete separation, fragments are still connected by one medullary filament (Figure 7.1 C), which upon further stretching will finally tear. Using a knife for fragmentation, a clear cut surface covered by utricles could be observed (data not shown). Neither cutting nor tearing revealed the internal structure as schematically shown in Figure ?? C.

Formation of a wound plug as observed after wounding of *D. vermicularis* and *C. prolifera* was thus for *C. fragile* not observed, indicating fundamental differences during the wound response. In both *C. prolifera* and *D. vermicularis* the developing wound plug could be observed under a microscope (Figure 1.2 A, C). By cutting thalli of *C. fragile* the cell structure of interwoven medullary filaments in the central part, connected to utricles constituting the external area could not be displayed. Here, every cut or rupture was still covered by utricles. Only by tearing a thallus

apart were single medullary filaments with diameters of around 0.05 mm shortly visible until final rupture. Under the magnification applied, a leaking of cell contents could not be observed from single torn filaments nor was the formation of a wound plug recognizable. If cell contents were only released from one single filament, the loss was presumably not as detrimental as during wounding of *C. prolifera* or *D. vermicularis*.

In order to detect a wound response on the molecular level by either GC- or LC-MS techniques two distinct sets of samples were prepared: an unwounded sample representing the non-stressed profile and samples which were first wounded and then extracted after defined time periods of 30 and 60 minutes. For extraction of either sample type, liquid nitrogen was used to stop enzymatic activity and to facilitate production of a fine powder. The fine algal powder was then extracted by several organic solvents covering different polarities, including methanol, ethylacetate, dichloromethane and hexane. Only in methanolic extracts of unwounded and wounded algae, measured by UPLC-MS, could a difference be detected, hence, this analytical method was applied for all further experiments. The established extraction procedure finally included the following steps: unwounded thalli were carefully dried by a paper towel, then frozen in liquid nitrogen and ground to a fine powder. Methanol was added, the sample unfrozen, vortexed, centrifuged and concentrated on a Chromabond[®] Easy SPE cartridge. For wounded samples, cells were crushed using a pistil and then left for 30 or 60 minutes. Afterwards, liquid nitrogen was added and the extraction procedure applied as described for unwounded samples. For each treatment three replicates were prepared. Additionally, the complete extraction procedure was repeated without algae to provide blank samples. Figure 7.2 A shows the UPLC-MS profile of an unwounded sample, recorded by electro-spray ionization (ESI) in the negative ionization modus. Peaks with ion traces present in all replicates were marked by a green star. In unwounded methanolic samples only very few polar substances were present (not marked), major metabolites appeared between 2 to 2.6 minutes, where the solvent composition rises from 66 to 77% acetonitrile, thus, representing rather non-polar components. 30 minutes post

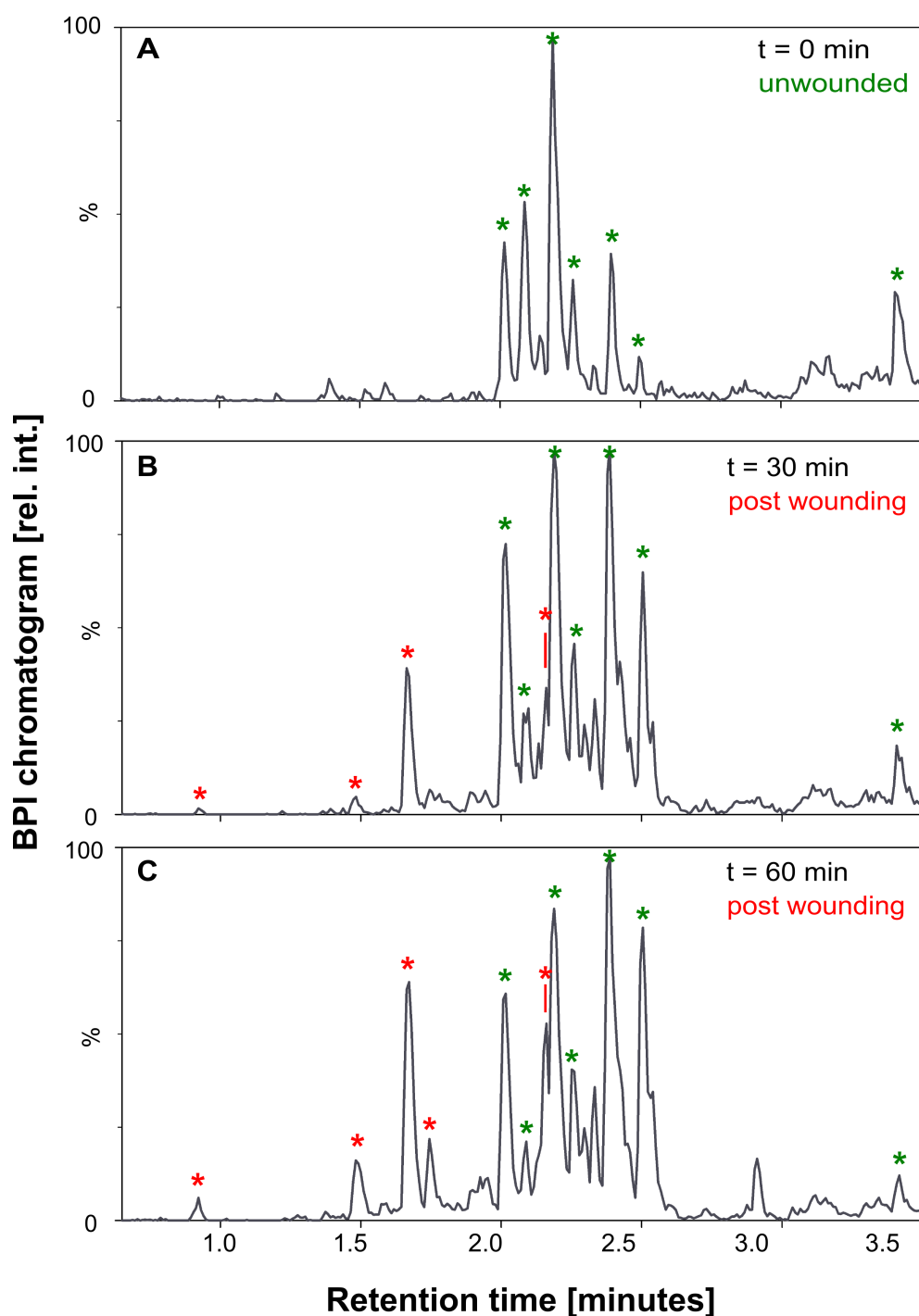


Figure 7.2: Base peak ion chromatogram (BPI) obtained by UPLC-MS screening in the negative modus of unwounded and wounded methanolic *C. fragile* extracts (method: standard). Compounds present in all replicates but not detectable in the blank are marked by green (unwounded) and red (wounded) stars. **A:** BPI chromatogram of an unwounded cell. Seven dominating compounds were found, marked by a green star. **B:** All seven compounds found in unwounded cells were still present in cells extracted 30 minutes post wounding, in addition to three more polar compounds and one compound with a similar polarity, marked by red stars. **C:** 60 minutes post wounding, one further polar compound at 1.75 minutes was found. All compounds detected 30 minutes post-wounding were still present. Results are representative for 3 experiments, including each 3 replicates.

wounding, the seven dominating compounds of unwounded cells were still present in addition to one novel compound with a similar polarity (R.T. 2.16 minutes) and three significantly more polar compounds (R.T. 0.92, 1.48, 1.66 minutes), marked by red stars (Figure 7.2 B). 60 minutes after wounding one further polar compound appeared after 1.75 minutes (Figure 7.2 C). For evaluation only those compounds present in all three replicates which additionally could not be detected in the blank sample were included (Figure 7.2, marked by stars). Ratios between single metabolites showed a rather high variation both in replicates of the same, and between different experiments.

In measurements of the same samples in the positive ionization modus, sensitivity towards most compounds seemed reduced, and no such clear differences between treatments were visible. Thus, compounds after wounding appeared rather ionizable by deprotonation with ESI-MS, presumably indicating the presence of acidic protons, as for example present in carboxylic acid moieties, phenols and alcohols. Mass spectra of the 5 compounds detected in the negative ionization modus 60 minutes after wounding show dominant ions ranging from m/z 241 to 329 $[M-H]^-$ (Figure 9.10 and 9.11 of the appendix). Due to the soft ionization technique used, these mass spectra reveal no obvious informations concerning the molecular structure. Merely the compound with m/z 329 $[M-H]^-$ (Figure 9.11) shows an isotopic pattern indicating the presence of several halogens as well as the clearly assignable sodium adduct $[M-2H+Na]^-$.

Compared to wound reactions of *Caulerpa* spp. and *Dasycladus* sp. described in chapter 1.1, fundamental differences could also be observed on a molecular level by UPLC-MS screening of methanolic extracts from *C. fragile*. Dominant compounds of unwounded algae from *Caulerpa* and *Dasycladus* spp. were not detectable even very shortly after wounding. They were enzymatically transformed into highly reactive intermediates, able to cross-link proteins, thus contributing to the formation of a wound plug. [10, 12] Thus, the morphological differences between species belonging to those and *C. fragile* are also reflected on a molecular level. Methanolic extracts of *C. fragile* contained common metabolites with identical ion traces and

retention times, in wounded and unwounded cells. Upon stress caused by wounding, polar compounds seemed to accumulate. *C. fragile* thus displays an interesting, so far unknown mechanism to cope with wounding and fragmentation. Further investigations of the specific role of the detected compounds in the wound response of this alga was not the focus of this thesis and remains to be investigated in detail.

7.2 UPLC-MS screening for sulfated metabolites

Dr. Matthew Welling detected several sulfated metabolites in some *Dasycladus* spp.. During this study, sulfate esters showed in the UPLC-MS negative ionization modus additionally to the molecular ion $[M-H]^-$ a characteristic, dominant fragment with a difference of -80. Mass ranges of these compounds were between m/z 200 and 300 $[M-H]^-$. [56]

In none of the metabolites with mass ranges from m/z 241-329 $[M-H]^-$ from extracts of either wounded or unwounded *C. fragile* cells could such a fragmentation pattern be observed by UPLC-MS measurements. Higher mass sulfated polysaccharides, identified in several *Codium* spp. were presumably not isolated by the extraction procedure applied. [60-64]

7.3 Summary

C. fragile displayed a very distinct wound reaction compared to algae belonging to *Caulerpa* and *Dasycladus* spp. Here, no transformation of present metabolites could be detected, but instead was the accumulation of new metabolites observed. *C. fragile* thus follows an interesting, so far unknown mechanism as a response to cell wounding and fragmentation. The identification of structure and specific function of the metabolites accumulating after wounding however was not the focus of this study and remains to be investigated. Sulfated secondary metabolites with a small molecular size as previously observed in some members of the Dasycladaceae (m/z 200-300 $[M-H]^-$) [56] could also not be detected.

8 Conclusions

Novel sulfated metabolites were previously detected by Dr. Matthew Welling in some members of the Dasycladaceae that were not involved in the alga's wound reaction. Based on data obtained by mass- and UV-Vis spectroscopy, these were assumed to be structurally related to the known antifouling agent zosteric acid (ZS).[56] Under the aspect of the recent quest for natural, environmentally friendly antifouling agents, the question arose if a similar biological activity could be assigned to these novel compounds, in case a structural relation should be confirmed.

By establishing a general synthesis and purification procedure applicable for creating sulfate esters of phenolic acids, coumarines and phenols, highly pure standards could be obtained. UPLC-MS co-injection experiments led to the identification of the sulfated metabolites 4-(sulfooxy)benzoic acid (BS) and 4-(sulfooxy)phenylacetic acid (AS) in *D. vermicularis* and BS in *C. barbata*. Some structural differences to the known antifoulant ZS are thus given. Investigations were initially focused both on the specific role the sulfate esters play during biofilm inhibition as well as in how far modifications of the aliphatic rests as present in AS, BS and ZS or the use of constitutional isomers would influence their biological effectivity.

Experiments preceding bioassays revealed that these phenolic acid sulfate esters were rather stable against chemical, but sensitive to enzymatic hydrolysis by sulfatases. Consequences drawn were first to establish a UPLC-MS stability screening method during bioassays and secondly, the inclusion of the non-sulfated forms (A, B, Z) to biofilm assays, in order to be able to distinguish how an eventual presence would affect biofilm inhibiting results. The final combination of different bioassays and bacterial species, UPLC-MS stability screening and bacterial growth monitoring provided a comprehensive overview of the various impacts AS, BS, ZS and their

non-sulfated forms had on biofilm development. All bioassays were performed in experimental conditions previously estimated to be favorable for biofilm formation. The initial aim to unveil the specific role of the phenolic acid sulfate ester in relation to further structural elements during biofilm inhibition led to a revision of the current consent of ZS activity. Although numerous suggested by various other studies, including both bacterial strains used (*E. coli*, *V. natriegens*), a biofilm inhibiting effect could neither be detected for ZS, nor for AS and BS by either of the three different assays performed at the air-liquid-interface, on PTFE plates submerged in medium and in the field. In contrast, especially the non-sulfated form of zosteric acid, Z, showed a strong biofilm inhibiting effect on both *E. coli* and *V. natriegens*, B could postpone biofilm development effectively, but had no long term influence. The impact of Z and B however, was dependent on the experimental setup applied. Thus was *E. coli* biofilm development at the air-liquid-interface delayed by B and reduced by Z until the end of the experiment, but none of the additives (AS, BS, ZS, A, B, Z) influenced biofilm formation on PTFE plates. Although Z inhibited biofilm at the air-liquid-interface, no impact on cell growth was detected. UPLC-MS measurements revealed no indications of sulfatase or other metabolic activity towards the sulfated and non-sulfated additives.

Different results were obtained for *V. natriegens*. Here, biofilm at the air-liquid-interface was not evaluable. UPLC-MS measurements however indicated pronounced sulfatase activity towards AS, BS and ZS as well as the complete metabolisation of BS and B. Growth monitoring by OD measurements revealed that sulfated phenolic acids possessed either no (BS) or a growth promoting (AS, ZS) effect before the start of biofilm formation of *V. natriegens*. Analytical monitoring during bioassays on PTFE plates confirmed the assumed sulfatase activity of *V. natriegens*. All three sulfated additives were partly hydrolysed and the non-sulfated form released into the medium. Additionally, B and BS were completely degraded.

Z proved a strong, temperature independent biofilm inhibitor for *V. natriegens*, even in a concentration as low as 0.10 mmol l^{-1} . B, as for *E. coli*, only postponed biofilm development, here presumably due to the rapid degradation of this additive. Os-

tensible inhibiting effects of ZS at room temperature (RT) could clearly be assigned to Z released by enzymatic hydrolyzation of ZS. In contrast to *E. coli* during the air-liquid-interface experiment, was *V. natriegens* cell number negatively affected by the presence of Z in high concentrations (0.51 to 2.05 mmol l⁻¹) during the PTFE plate assay. A concentration as low as 0.10 mmol l⁻¹ on the other hand did not affect growth of *V. natriegens*, but could significantly inhibit biofilm formation at RT. Thus, a reduction in cell number seems not to be the sole reason for reduced biofilm development.

During the biofouling field assay with a mixed community of microorganisms, again no biofilm inhibiting effect of AS, BS or ZS could be observed. Since coverage by fouling organisms rather increased with increasing concentration of sulfated additives, a settlement promoting effect can be assumed by these compounds.

The results obtained during the different biofilm assays leave room for the assumption that phenolic acid sulfate esters rather function as storage molecules for the potent, biofilm inhibiting non-sulfated forms, than being the active metabolites themselves. Divergent results to other studies including ZS can in case of *V. natriegens* clearly be assigned to the presence of sulfatase activity, releasing the highly active compound Z into the medium. For *E. coli* it can just be speculated that minor contaminations of educt and side products during synthesis might be more effective than ZS, or that different experimental conditions influenced its impact.

This study emphasizes the importance to use compounds with high purity during bioassays and to monitor the stability of additives in presence of metabolically active organisms, to ensure that any observed effect will be assigned to the correct compound. Results also highlighted how dependent a compounds impact can be on experimental conditions.

A second project of this thesis was concerned with UPLC-MS screenings of *C. fragile*, a siphonous green alga as members of the Dasycladaceae and Caulerpaceae. Of special interest was thus, if *C. fragile* follows a similar reaction to wounding as was previously unveiled for these [9, 10, 12, 30] and if sulfated metabolites are present as in members of the Dasycladaceae [56].

Sulfated metabolites similar to AS, BS and ZS could in *C. fragile* not be detected by UPLC-MS measurements. These measurements also revealed, that *C. fragile* reacts with a fundamentally different process to cell wounding than some members of the Dasycladaceae and Caulerpaceae, where the rapid transformation of secondary metabolites enables biopolymerisation reactions leading to a visible wound plug. In contrast to that were in *C. fragile* all metabolites present in unwounded cell extracts still detected in wounded cells. But upon wounding additional compounds accumulated, predominately with a higher polarity than those present already before wounding. Formation of a wound plug was also not observable by microscopy. A possible cause for the different response in *C. fragile* might be sought in its more complex thallus morphology. *C. fragile* thalli are composed of many thin and interwoven medullary filaments, whereas species belonging to the Caulerpaceae and Dasycladaceae consist of only one siphon. Upon wounding of *C. fragile* by rupture, very few of the many filaments were actually torn. Morphology thus seems to constitute a first step in minimizing the detrimental effects caused by wounding for this specific siphonous green algae. A further investigation of *C. fragile*'s interesting wound response and the metabolites involved was, however, not in the focus of this thesis.

To conclude, with insights gained during this study a new hypothesis can be derived. The sulfatation of potent biofilm inhibiting phenolic acids (Z, B) thus might constitute a measure of detoxification and thus enables intracellular storage. This phenomenon has already been observed for two sulfated metabolites of marine origin [12, 57] and seems also to be valid for the sulfated metabolites ZS (*Zostera marina*), AS and BS (some Dasycladaceae). In how far especially Z would be applicable as a non-toxic antifouling agent remains to be evaluated. A further interesting aspect for future studies would be a closer investigation of the role ZS plays for *Zostera marina* were it originally was isolated from. Valuable insights might be provided by a screening for sulfatase activity and if an intra- or extracellular increase of ZS or Z would be detectable during fouling pressure on *Z. marina*.

9 Materials and Methods

9.1 Instruments and materials

9.1.1 NMR

NMR spectra were recorded on a 400 MHz Bruker Avance spectrometer. Chemical shifts are listed in δ , relative to TMS. Coupling constants J are given in Hertz (Hz).

9.1.2 UPLC-ESI-MS (UPLC-MS)

Ultra-High-Performance-Liquid-Chromatography (UPLC) was performed on a Acquity[®] Ultra-Performance LC system (Waters, Milford, MA, USA), coupled to a quadrupole time-of-flight (QToF) MicroMass spectrometer (Waters Micromass, Manchester, England). Separation was performed on a UPLC[®] C18-BEH column (2.1 mm \times 50 mm, particle size 1.7 μ m) from Waters and later on a Kinetex C18 column (2.1 mm \times 50 mm, particle size 1.7 μ m) from Phenomenex. All samples were eluted using a gradient solvent composition. Solvent A was composed of 98 % water and 2 % acetonitrile plus 0.1 % formic acid, solvent B solely contained acetonitrile plus 0.1 % formic acid. Only UPLC grade solvents from Fisher Scientific (United Kingdom) were used. Tables 9.1 to 9.5 show the applied UPLC methods.

Electro-spray-ionization (ESI) mass spectra (MS) were recorded with a micro-channel detector (MCP) detector voltage of 2300 V, a cone gas flow of 10 l h⁻¹ and a desolvation gas flow of 700 l h⁻¹. The desolvation temperature was set to 300 °C, the source temperature to 120 °C. For all experiments a collision energy of 10 eV was applied. The capillary voltage was set to 2700 V in negative and 3000 V in positive ionization modus. Additionally a photo diode array (PDA) detector was connected

time [minutes]	A [%]	B [%]
0.0	100	0
0.2	100	0
3.0	0	100
4.0	0	100
4.5	100	0
5.0	100	0

Table 9.1: Method **standard**

time [minutes]	A [%]	B [%]
0.0	100	0
0.2	100	0
1.8	82	18
4.5	0	100
5.5	0	100
6.0	100	0
6.5	100	0

Table 9.3: Method **sulfmet**

time [minutes]	A [%]	B [%]
0.0	100	0
0.2	100	0
2.5	91	9
5.0	0	100
6.0	0	100
6.5	100	0
7.0	100	0

Table 9.5: Method **co-injection 2**

time [minutes]	A [%]	B [%]
0.0	100	0
0.2	100	0
4.0	0	100
4.5	0	100
5.5	100	0
6.5	100	0

Table 9.2: Method **biofilm**

time [minutes]	A [%]	B [%]
0.0	100	0
0.5	100	0
1.0	99	1
4.0	98.8	1.2
5.0	0	100
6.5	100	0
7.5	100	0

Table 9.4: Method **co-injection**

time [minutes]	A [%]	B [%]
0.0	100	0
1.0	100	0
8.0	85	15
11.0	0	100
16.0	0	100
18.5	100	0
20.0	100	0

Table 9.6: Method **sulfmetTQ**

between the UPLC and the MS systems, allowing to record wavelengths from 190 to 500 nm.

9.1.3 HPLC-ESI-Triple-Quad-MS

High-Performance-Liquid-Chromatography (HPLC) was performed with an Agilent Series 1100 LC system, coupled to a triple-quadrupole mass spectrometer of the PE Sciex API 3000 series. Solvents A and B were prepared as described for UPLC-ESI-MS measurements, except that HPLC grade solvents were used (VWR, Germany). For chromatographic separation, a 150 mm Zorbax C18 column from Agilent was used. The LC method for detection of sulfated metabolites is

described in table 9.6. Mass spectra were recorded in negative ionization modus and product ions were detected (PI MS2) with a collision energy of 30 eV.

9.1.4 GC-MS

Gaschromatography-mass spectrometry (GC-MS) measurements were performed on an ISQ Trace GC Ultra[®] from Thermo Scientific. The GC program started at 60 °C for 1 minute and the temperature was then increased by 15 °C min⁻¹ to 310 °C, which was held for ten minutes. Injector temperature was set to 300 °C and split flow to 10 ml min⁻¹ at a split ratio of 10. Electron ionization (EI) recorded masses ranged from 50 to 800 amu. For chromatographic separation an Agilent Dura Guard DB-5ms (length 30 m, pre-column 10 m, diameter 0.25 mm, filmthickness 0.25 µm) column was installed.

9.1.5 Mithras plate reader

Optical density (OD) measurements of bacterial cultures and absorption of crystal violett (CV) in solution were measured on a Mithras LB940 (Berthold Technologies, Germany) plate reader. OD and CV absorption were measured at 570 nm, the lamp energy was set to 11 000 V with a scan time of 0.1 s. Before CV absorption measurements plates were shaken for 10 s. Each measurement was performed in triplicates.

9.1.6 Microscopes

Pictures for counting bacterial cells were recorded on a Leica DM 2000 microscope, equipped with a HI Plan 40×0.65 objective (Leica). CV stained biofilms on PTFE plates were evaluated with the inverted Leica DMIL LED, equipped with a Leica C Plan 10×0.22 objective. Biofilms of *E. coli* were investigated with a Leica MZ6 stereo microscope. All three microscopes could be connected to a Leica DFC280 camera system.

9.1.7 Solvents and chemicals

Solvents for synthesis were either obtained from Sigma Aldrich (Germany) or VWR (Germany). For Liquid Chromatography and algae extraction only UPLC grade solvents from Fisher Scientific (United Kingdom) were used. Ultra pure water was generated by a MicroPure system from TKA, Germany (conductivity $0.055 \mu\text{S cm}^{-1}$). Origin of chemicals is noted for each substance in the corresponding section.

9.1.8 Buffer solutions

9.1.8.1 Phosphate buffered saline

For a phosphate buffered saline (PBS) solution 0.8 g of NaCl (Sigma Aldrich, Germany), 1.78 g $\text{Na}_2\text{HPO}_4 \cdot 2\text{H}_2\text{O}$ (Sigma Aldrich, Germany), 0.2 g KCl (Sigma Aldrich, Germany) and 0.27 g KH_2PO_4 (Sigma Aldrich, Germany) were dissolved in 1 l ultra pure water and the pH adjusted to 7.4 with HCl. The buffer was stored at room temperature (RT) and used for three weeks.

9.1.8.2 TRIS-HCl buffer

For a 0.25 M Tris HCl solution 30.29 g of Tris (tris(hydroxymethyl)aminomethane), (Carl Roth, Germany), were dissolved in 200 ml of ultra pure water and the pH at RT adjusted with diluted HCl to 7.2. Then the solution was filled up to a volume of 1 l and stored at 4°C in the dark. Since the pH of Tris HCl buffer is temperature dependent, a small fraction was always taken from the stock and the pH newly adjusted just before an experiment to achieve the right pH at the temperature the experiment was performed.

9.2 Synthesis of sulfated phenolic acids

9.2.1 General method

The following section describes a general routine for the synthesis of several sulfated phenolics, in mg to g scales. Several publications describe syntheses using a variety of solvents and sulfatation reactants, but none of these provided a product of either the required amount or purity for this study. [72, 74, 78, 79, 126] Important designations concerning amounts of reactants and solvents used are described in the specified sections. If defined amounts of solvents during workup are not given, their volume did not influence the outcome. For reactants with one sulfatation site, equimolar amounts of the sulfatation reagent sulfur trioxide pyridine complex (Pyr*SO₃) and the reactant were used. For phenolic acids with two possible reaction sites the amount of Pyr*SO₃ was doubled. Approximately 100 ml per 50 mmol of reactant of water free pyridine were added as solvent and the reaction mixture was stirred in a round neck flask at RT for 48 hours. The initial suspension was usually dissolved within 4-7 hours. Pyridine was removed by rotor evaporation to yield a yellow to brown oil. The oil was dissolved in as little water as possible and the pH (~3-4) adjusted to ~6-7 with a 25 % potassium hydroxide (KOH) solution. The aqueous solution was then washed three times with the same volume of ethyl acetate. During the first two washing steps a precipitate formed, not containing product, which was filtered off after phase separation. The ethyl acetate phase was colored orange to brown at first, whereas the aqueous phase became lighter. During the third washing step, no coloring of the ethyl acetate phase and no further precipitation occurred. The ethyl acetate phase was discarded, the aqueous phase concentrated by rotor evaporation to yield a brown to yellow, slightly damp raw product (Figure 2.2 F). This raw product occasionally contained educt and two major side products, detectable by UPLC-MS measurements, presumably sulfated (X/XS) and non-sulfated (X/X) anhydrides. The presence of these side products could be minimized by using Pyr*SO₃ only in stoichiometric amounts. The raw product could be purified by two different routines.

9.2.1.1 Purification - analytical scale

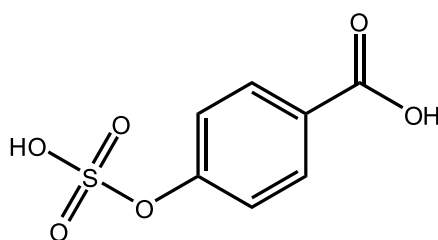
For analytical amounts (mg), as needed for co-injection experiments, hydrophilic-interaction-chromatography (ZIC[®]-HILIC, from SeQuant[®]) solid phase extraction cartridges (SPE) proved most efficient. Therefore, 200 mg of raw product were dissolved in 2 to 4 ml of ultra pure water and the seven fold amount of acetonitrile was added, so that no precipitation occurred. A 500 mg ZIC[®]-HILIC SPE cartridge was washed first with 4 ml water, by applying slight pressure with a syringe equipped with a small tube fitting tightly inside the cartridge. Then the cartridge was conditioned with 4 ml of a 9 to 1 (v:v) acetonitrile/water mixture. The sample in the acetonitrile/water mixture was then loaded onto the cartridge by pushing the solvent slowly through the material (approximately 2 drops per s). The absorption material was then washed with 4 ml of acetonitrile and the sample eluted with ultra pure water containing 0.1 % of formic acid. The water was removed to yield a white powder. UPLC-MS measurements showed no side products. Although the purity of the compounds obtained by the ZIC[®]-HILIC method as estimated by UPLC-MS measurements was high, the yield was poor and the effort high and not transferable for purifying larger amounts. This procedure was applicable to *p*-, *m*-, *o*-BS and AS. From the raw product could 5 to 20 weight percent pure compound be obtained.

9.2.1.2 Purification - large scale

The raw product was dissolved in as little water as possible and the pH 7 solution adjusted to pH 10 with a 25 % KOH solution. The solution was then stirred for 1 hour in a 60 °C water bath to cleave the anhydride side product, providing sulfated product and educt. With diluted H₂SO₄ the pH was adjusted back to pH 6 - 7. Water was removed by rotary evaporation. The yellowish powder was dissolved again in as little water as possible, by slightly warming the solution in a 40 °C water bath if necessary. This procedure was essential for the following salt precipitating step. Too much water reduced the efficiency of the salt precipitation, whereas falling under the solubility of the sulfated product, parts might be lost during the precipitation. To this aqueous solution twice the amount of methanol was added to precipitate

salts. The precipitate was filtered off and washed with a further single amount of methanol. The solution was then left standing at RT over night without stirring. A crystallization, presumably of K_2SO_4 , took place. The precipitate was filtered off and the solution evaporated to dryness. The yellowish, damp powder was then taken up in 1/10 the amount of methanol used to precipitate salts and placed into an ultrasonic bath until a fine suspension of a white powder and yellowish solution was achieved. The solution was filtered off, evaporated again and the suspension step repeated with half the amount of methanol. More than 2 repetitions did not lead to an increase in yield. If the obtained powder was still yellowish, the ultrasonic bath step was repeated once. After removal of methanol through a funnel filter, vacuum was turned off and the powder was suspended in acetone to dissolve remaining educt, present from the cleavage of the anhydride. Acetone was removed by vacuum, and the washing step repeated two more times, until in UPLC-MS measurements no educt could be detected. The product was dried at 70 °C, until the weight did not change anymore. Yields lay usually around 60 % to 80 %. For the rare cases this routine was not applicable an alternative synthesis is described in detail.

9.2.2 4-(Sulfoxy)benzoic acid (BS)



15 g 4-hydroxybenzoic acid (**B**, $M=138.12 \text{ g mol}^{-1}$, 108 mmol, Sigma Aldrich, Germany) and 17.2 g Pyr^*SO_3 ($M=159.16 \text{ g mol}^{-1}$, 108 mmol, Alfa Aesar, Germany), were dissolved in 200 ml water free pyridine (Sigma Aldrich, Germany). The procedure followed the workup as described in the general method section.

Analytical scale

With this approach 13.4 mg of a white powder (6.7 weight % of raw product loaded on the HILIC cartridge) could be obtained. UPLC-MS measurements showed only product.

Large scale

The batch described above yielded 13.5 g of a fine white powder (57%).

Product BS:

¹H NMR (400 MHz, DMSO [D6] + 0.8 % formic acid):

δ (ppm): 7.22 (d, 2H); 7.84 (d, 2H)

¹³C NMR (400 MHz, DMSO [D6] + 0.8 % formic acid):

δ (ppm): 119.33, 126.59, 130.45, 156.93, 164.64

(Figure 9.2 of the appendix)

Elementary analysis of BS:

Found: C 38.44 %, H 1.62 %, S 14.32 %

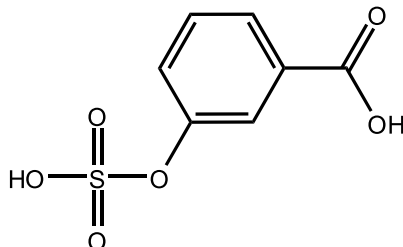
Theoretical: C 38.50 %, H 2.70 %, S 14.70 %

UPLC-MS:

m/z [M-H]⁻: 216.99

R.T. [minutes]: 0.89 (method: **standard**, C18 BEH column, Waters) or 1.33 (method: **co-injection**, C18 BEH column, Waters) or 0.89 (method: **biofilm**, C18 column, Phenomenex).

9.2.3 3-(Sulfooxy)benzoic acid (mBS)



1.5 g 3-hydroxybenzoic acid (**mB**, $M=138.12 \text{ g mol}^{-1}$, 10.9 mmol, Sigma Aldrich, Germany) and 1.7 g Pyr*SO₃ ($M=159.16 \text{ g mol}^{-1}$, 10.9 mmol, Alfa Aesar, Germany), were dissolved in 20 ml water free pyridine (Sigma Aldrich, Germany). The procedure followed the workup as described in the general method section.

Analytical scale

With this approach 22.3 mg of a white powder (11.2 weight % of raw product loaded on the HILIC cartridge) could be obtained. UPLC-MS measurements showed only product.

Large scale

Half of the raw product from the batch described above yielded 0.59 g of a fine white powder (49.5 %).

Product mBS:

¹H NMR (400 MHz, DMSO [D6] + 0.8 % formic acid):

δ (ppm): 7.34 (m, 1H), 7.37 (m, 1H), 7.63 (m, 1H), 7.77 (m, 1H)

¹³C NMR (400 MHz, DMSO [D6] + 0.8 % formic acid):

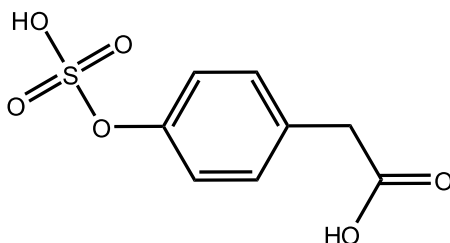
δ (ppm): 121.24, 124.05, 124.82, 128.95, 132.22, 153.55, 167.33

UPLC-MS:

m/z [M-H]⁻: 216.99

R.T. [minutes]: 2.12 (method: **co-injection**, C18 BEH column, Waters) or 0.92 (method: **biofilm**, C18 column, Phenomenex).

9.2.4 4-(Sulfooxy)phenylacetic acid (AS)



7.5 g of 4-hydroxyphenylacetic acid (**A**, $M=152.15 \text{ g mol}^{-1}$, 52 mmol, Sigma Aldrich, Germany) and 8.3 g Pyr^*SO_3 ($M=159.16 \text{ g mol}^{-1}$, 52 mmol, Alfa Aesar, Germany) were dissolved in 100 ml dry pyridine (Sigma Aldrich, Germany). The procedure followed the workup as described in the general method section.

Analytical scale

With this approach 38 mg of a white powder (19 weight % of raw product loaded on the HILIC cartridge) could be obtained.

Large scale

The batch described above yielded 9.2 g of a fine white powder (76 %).

Product AS:

$^1\text{H NMR}$ (400 MHz, DMSO [D6] + 0.8% formic acid):

δ (ppm): 3.11 (s, 2H), 6.98 (d, 2H), 7.08 (d, 2H)

$^{13}\text{C NMR}$ (400 MHz, DMSO [D6] + 0.8% formic acid):

δ (ppm): 45.93, 119.89, 129.30, 135.26, 150.82, 174.06

(Figure 9.1 of the appendix)

Elementary analysis of AS potassium salt:

Found: C 32.24 %, H 1.87 %, S 10.83 %

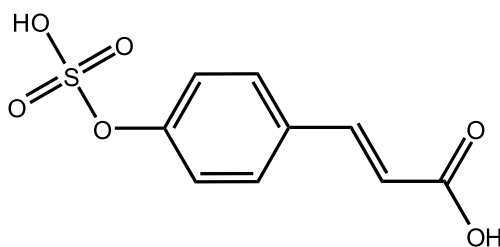
Theoretical: C 35.55 %, H 2.61 %, S 11.86 %

UPLC-MS:

m/z [M-H]⁻: 231.00

R.T. [minutes]: 1.07 (method: **standard**, C18 BEH column, Waters) or 2.25 (method: **co-injection**, C18 BEH column, Waters) or 0.95 (method: **biofilm**, C18 column, Phenomenex)

9.2.5 Zosteric acid (ZS)



13.05 g of *para*-coumaric acid (**Z**, M=164.16 g mol⁻¹, 79.5 mmol, Alfa Aesar, Germany) and 12.60 g Pyr*SO₃ (M=159.16 g mol⁻¹, 79.5 mmol, Alfa Aesar, Germany) were dissolved in 160 ml water free pyridine (Sigma Aldrich, Germany). The procedure followed the workup as described in the general method section.

Large scale

The batch described above yielded 11.2 g of a fine white powder (58 %).

Product ZS:

¹H NMR (400 MHz, DMSO [D6] + 0.8 % formic acid):

δ (ppm): 6.40 (d, 1H, J = 15.7 Hz), 7.19 (d, 2H), 7.48 (d, 1H, J = 15.7 Hz), 7.57 (d, 2H)

¹³C NMR (400 MHz, DMSO [D6] + 0.8 % formic acid):

δ (ppm): 118.73, 120.36, 128.95, 129.19, 142.73, 155.12, 168.13

Signals correspond to [72] (Figure 9.3 of the appendix).

Elementary analysis of ZS potassium salt:

Found: C 33.86 %, H 1.81 %, S 6.35 %

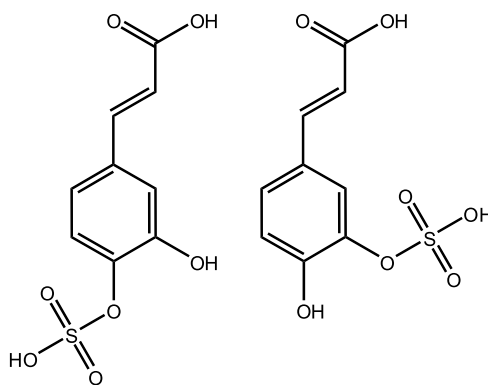
Theoretical: C 38.84 %, H 1.09 %, S 11.52 %

UPLC-MS:

m/z [M-H]⁻: 243.00

R.T. [minutes]: 0.96 (method: **standard**, C18 column, Phenomenex) or 1.10 (method: **biofilm**, C18 column, Phenomenex).

9.2.6 3-(Sulfoxy)-4-hydroxycinnamic acid, 4-(sulfoxy)-3-hydroxycinnamic acid (3,4CAS)



3.2 g of caffeic acid (**CA**, $M=180.16 \text{ g mol}^{-1}$, 17.8 mmol, Simga Aldrich Germany) and 6 g Pyr^*SO_3 ($M=159.16 \text{ g mol}^{-1}$, 37.8 mmol, Alfa Aesar, Germany) were dissolved in 40 ml water free pyridine (Sigma Aldrich, Germany). The procedure followed the workup as described in the general method section, with 1.2 g of raw product.

Large scale

The work up of 1.2 g raw product yielded 0.6 g of a light brown powder.

Product isomeric mixture of 3,4CAS:

$^1\text{H NMR}$ (400 MHz, DMSO [D6] + 0.8% formic acid):

δ (ppm): 6.22 (B) and 6.24 (A) (d, 1H, $J = 15.7$ Hz), 7.27 (dd, 1H), 7.45 (B) and 7.46 (A) (d, 1H, $J = 15.7$ Hz), 7.55 (d, H), 7.73 (d, 1H)

The $^1\text{H NMR}$ showed five strong signals of one isomer (A), slightly shifted downfield compared to the educt and some smaller signals from the other isomer (B) where only two could be assigned to the double bond due to their 3J coupling. The others are partly overlaid by the signals from the isomer A (Figure 9.4 of the appendix).

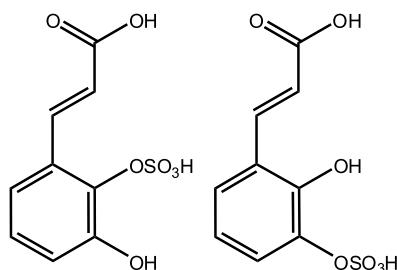
UPLC-MS:

m/z [M-H] $^-$: 258.99

R.T. [minutes]: 1.70 and 1.80 (method: **sulfmet**, C18 column, Phenomenex).

UPLC-MS measurements showed two peaks with the same m/z value, indicating the presence of two constitutional isomers. The first eluting peak showed a slightly larger peak area (Figure 9.7 A).

9.2.7 2-(Sulfoxy)-3-hydroxycinnamic acid, 3-(sulfoxy)-2-hydroxycinnamic acid (2,3CAS)



In the first step 2,3-hydroxycinnamic acid (2,3CA) was synthesized according to a slightly modified synthesis route from [130]. Briefly, 3.8 g (carbethoxymethylene)-

triphenylphosphorane ($M = 348.37 \text{ g mol}^{-1}$, 10.9 mmol, Sigma Aldrich, Germany) and 1.5 g 2,3-dihydroxybenzaldehyde ($M = 138.12 \text{ g mol}^{-1}$, 10.9 mmol, Sigma Aldrich, Germany) were dissolved in 12.5 ml methanol. This solution was slowly dropped into a solution of 2.2 g K_2CO_3 in 19 ml methanol. After the solutions were combined, the mixture was placed into a boiling water bath and heated for 3 hours. UPLC-MS screening proved the presence of an intermediate product, the ethylester of the dihydroxycinnamic acid with a m/z $[\text{M-H}]^-$ of 207. The solvent was removed from the reaction product and the oily product was dissolved in 23 ml water. To this solution 10 ml of a 50% NaOH solution were added dropwise and then heated to boil for 30 s. Immediately after, the mixture was placed in an ice bath and 4 ml of a 37% HCl solution were added, after which little precipitate formed. The final product was extracted from the aqueous phase with three times 50 ml ethylacetate and diethylether, the organic phases were combined and dried over Na_2SO_4 to yield a yellow oily product of approximately 20 mg. In UPLC-MS measurements product with the m/z $[\text{M-H}]^-$ of 179 could be found as the major component. This raw product was immediately transformed to the mixture of sulfate esters (2,3CAS) without further purification.

Therefore 20 mg of raw product ($M = 180.16 \text{ g mol}^{-1}$, 0.1 mmol) and 46.9 mg Pyr^*SO_3 ($M = 159.16 \text{ g mol}^{-1}$, 0.3 mmol, Alfa Aesar, Germany) were dissolved in 3 ml of water free pyridine (Sigma Aldrich, Germany). The further procedure followed the general method for formation of phenolic sulfate esters including the ethylacetate washing step. This yellow raw product showed two peaks in UPLC-MS measurements with a m/z $[\text{M-H}]^-$ of 258.99.

UPLC-MS:

2,3 CA:

m/z $[\text{M-H}]^-$: 179.03

R.T. [minutes]: 1.40 (method: **standard**, C18 column, Phenomenex).

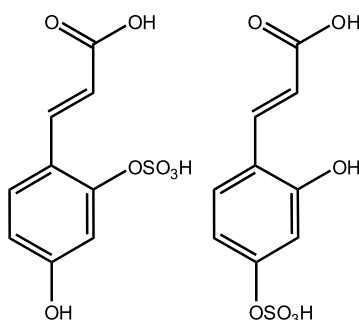
2,3 CAS:

m/z $[M-H]^-$: 258.99

R.T. [minutes]: 2.59 and 2.84 (method: **co-injection 2**, C18 column, Phenomenex).

UPLC-MS measurements showed two peaks with the same m/z value, indicating the presence of two constitutional isomers.

9.2.8 2-(Sulfooxy)-4-hydroxycinnamic acid, 4-(sulfooxy)-2-hydroxycinnamic acid (2,4CAS)



9.2.8.1 Sulfatation with Pyr^*SO_3

0.5 g of 2,4-dihydroxycinnamic acid (2,4CA, $M = 180.16 \text{ g mol}^{-1}$, 2.8 mmol, Sigma Aldrich, Germany) and 1.2 g Pyr^*SO_3 ($M = 159.16 \text{ g mol}^{-1}$, 7.5 mmol, Alfa Aesar, Germany) were dissolved in 7 ml of water free pyridine (Sigma Aldrich, Germany). The further procedure followed the general method for formation of phenolic sulfate esters including the ethylacetate washing step, yielding 1.4 g of a moist yellow brown powder. UPLC-MS measurements revealed two products.

UPLC-MS:

2,4CAS (Pyr^*SO_3):

m/z $[M-H]^-$ 259.57: Isomer A: 215.46 (100 %)/259.50 (80 %)/241.50 (10 %) and isomer B: 259.57 (100 %)/241.45 (45 %)/215.50 (10 %)

R.T. [minutes]: 2.24 (A) and 2.44 (B) (method: **co-injection 2**, C18 column, Phenomenex).

9.2.8.2 Sulfatation with chlorosulfonic acid

0.3 g of 2,4-dihydroxycinnamic acid (2,4CA, $M = 180.16 \text{ g mol}^{-1}$, 1.2 mmol, Sigma Aldrich, Germany) were dissolved under argon in 12 ml of water free pyridine (Sigma Aldrich, Germany) in an ice bath. 200 μl of chlorosulfonic acid ($M = 116.53 \text{ g mol}^{-1}$, 3 mmol, Alfa Aesar, Germany) were added dropwise under stirring. After 30 minutes the ice bath was removed and the reaction mixture stirred for one more hour at RT. Pyridine was removed, the raw product taken up in 10 ml water and brought to pH 7 with a 25 % KOH solution, which was then washed three times with 20 ml of ethylacetate to yield a few mg of a light yellow powder.

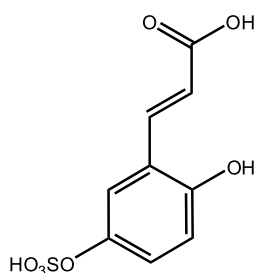
UPLC-MS:

2,4CAS (chlorosulfonic acid):

m/z $[M-H]^-$: 1. 259.45 (100 %)/215.37 (40 %)/179.23 ((10 %) and 2. 241.40 (100 %)/161.28 (10 %)

R.T. [minutes]: 1.92 and 2.27 (method: **co-injection 2**, C18 column, Phenomenex).

9.2.9 5-(Sulfoxy)-2-hydroxycinnamic acid (2,5CAS)



5-(sulfoxy)cinnamic acid was generated in a two step synthesis from sulfatation of 6-hydroxycoumarine and subsequent hydrolysis of the 6-(sulfoxy)coumarine adapted from [131] with minor modifications. For sulfatation, 100 mg of 6-hydroxycoumarine ($M = 162.14 \text{ g mol}^{-1}$, 0.62 mmol, Sigma Aldrich, Germany) and 300 mg of Pyr^*SO_3 ($M = 159.16 \text{ g mol}^{-1}$; 1.8 mmol, Alfa Aesar, Germany) were dissolved in 6 ml water free pyridine (Sigma Aldrich, Germany). The synthesis followed the general method

including the desalting step with methanol, to yield 140 mg of raw product.

UPLC-MS:

6-sulfooxycoumarine:

m/z [M-H]⁻: 240.96 with a fragment of 161.02

R.T. [minutes]: 2.34 (method: **co-injection 2**, C18 column, Phenomenex).

For generation of 5-(sulfooxy)cinnamic acid 83 mg of 6-(sulfooxy)coumarine (M = 242.14 g mol⁻¹, 0.34 mmol, raw product) were dissolved in 520 µl of a 25 % Na₂SO₃ solution. The solution was heated to boil under stirring, then the stirrer was turned off and the solution left to cool to RT. After 1.5 hours 220 µl of a 50 % KOH solution were added dropwise and heated to boil for a few minutes under stirring. Then the mixture was placed in an ice bath and 1 ml methanol containing 10 % formic acid were added, the precipitate was filtered off, the solvents removed and the beige product taken up in methanol again. This raw product showed two sulfated compounds in UPLC-MS measurements, educt and presumably the hydrolysis product 5-(sulfooxy)cinnamic acid. The hydrolysis product 2,5CAS was assumed to be the *trans* isomer, based on publications of Adams *et al.* in 1948 and López-Castillo *et al.* in 2013. [131, 179]

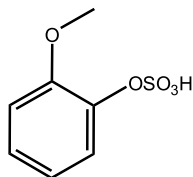
UPLC-MS:

cleavage product:

m/z [M-H]⁻: fragments of 215.02 (100 %) and 259.01 (30 %)

R.T. [minutes]: 2.0 (method: **co-injection 2**, C18 column, Phenomenex).

9.2.10 1-(Sulfooxy)-2-methoxybenzene (2MOPS)



1 g of 2-methoxyphenol ($M = 124.14 \text{ g mol}^{-1}$, 8 mmol, Alfa Aesar, Germany) and 3.8 g of Pyr^*SO_3 ($M=159.16 \text{ g mol}^{-1}$, 24 mmol, Sigma Aldrich, Germany) were dissolved in 18 ml of water free pyridine (Sigma Aldrich, Germany). The synthesis route followed the general method including the desalting step with methanol and ultrasonic bath treatments yielding 2.26 g of a beige solid.

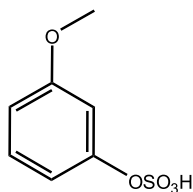
UPLC-MS:

2-MOPS:

m/z $[\text{M-H}]^-$: 202.97

R.T. [minutes]: 0.91 (method: **standard**, C18 column, Phenomenex).

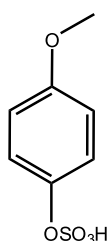
9.2.11 1-(Sulfooxy)-3-methoxybenzene (3MOPS)



884 μl of 3-methoxyphenol ($M = 124.14 \text{ g mol}^{-1}$, 8 mmol, Alfa Aesar, Germany) and 3.8 g of Pyr^*SO_3 ($M=159.16 \text{ g mol}^{-1}$, 24 mmol, Sigma Aldrich, Germany) were dissolved in 16 ml of water free pyridine (Sigma Aldrich, Germany). The synthesis route followed the general method including the desalting step with methanol and ultrasonic bath treatments, yielding 1.13 g of a beige powder.

UPLC-MS:

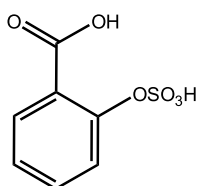
3-MOPS:

 m/z [M-H]⁻: 203.00R.T. [minutes]: 1.05 (method: **standard**, C18 column, Phenomenex).**9.2.12 1-(Sulfoxy)-4-methoxybenzene (4MOPS)**

1 g of 4-methoxyphenol ($M = 124.14 \text{ g mol}^{-1}$, 8 mmol, Alfa Aesar, Germany) and 3.8 g of Pyr*SO₃ ($M=159.16 \text{ g mol}^{-1}$, 24 mmol, Sigma Aldrich, Germany) were dissolved in 16 ml of water free pyridine (Sigma Aldrich, Germany). The synthesis route followed the general method including the desalting step with methanol and ultrasonic bath treatments, yielding 3.19 g of a beige powder.

UPLC-MS:

4-MOPS:

 m/z [M-H]⁻: 202.97R.T. [minutes]: 0.95 (method: **standard**, C18 column, Phenomenex).**9.2.13 2-(Sulfoxy)benzoic acid (oBS)**

The sulfatation of 2-hydroxybenzoic acid was adapted from a method by Todd *et al.* 1993 [72]. 3 g of 2-hydroxybenzoic acid ($M = 180.16 \text{ g mol}^{-1}$, 21 mmol, Sigma Aldrich, Germany) were dissolved under argon in 40 ml water free pyridine (Sigma Aldrich, Germany) in an ice bath. 1.4 ml of chlorosulfonic acid ($M = 116.53 \text{ g mol}^{-1}$, 21 mmol, Alfa Aesar, Germany) were added drop wise under stirring. After 30 minutes the ice bath was removed and the reaction mixture stirred for one more hour at RT. Pyridine was removed and the raw product taken up in 20 ml ultra pure water and brought to pH 7 with a 25 % KOH solution, which was then washed three times with 40 ml of ethylacetate to yield 2.5 g of a beige powder.

Analytical scale

With this approach 27.6 mg of a white powder (13,8 weight % of raw product loaded on the HILIC cartridge) could be obtained. UPLC-MS measurements showed no side products.

UPLC-MS:

oBS:

m/z $[M-H]^-$: 216,95 (100 %)/ 137,01 (27 %)

R.T. [minutes]: 1.55 (method: **co-injection**, C18-BEH column, Waters).

9.3 Stability of sulfated phenolic acids

9.3.1 pH dependent stability of 3,4CAS

Chemical stability of the sulfated phenolic acids in aqueous solution was tested in the presence of formic acid, HCl, H_2SO_4 (pH 1, 3 and 5) and KOH (pH 7, 9, 11 and 13). 3,4CAS was herein used as a model substance. For each test approximately 60 mg were dissolved in 1 to 2 ml of ultra pure water. Adding different amounts of formic acid, HCl and H_2SO_4 pH values of 1, 3 and 5 were adjusted. The ultra pure water showed a pH of 6, and was adjusted to pH 7 with 1 M KOH. Three more

samples were prepared with a 1 M KOH solution to pH 9, 11 and 13. All samples were adjusted to a final volume of 4 ml. One part was incubated in a water bath at 80 °C, the other was left at RT, both under shaking. After 30, 60, 270 minutes and 24 hours 1 ml was taken from each formic acid or KOH sample and neutralized either with KOH or formic acid to pH 7. Samples containing HCl or H₂SO₄ were left for 30 minutes, 1, 2 and 4 hours before sampling and neutralizing. Then 100 µl of each sample were pipetted into 900 µl of methanol, vortexed and centrifuged at 13.000 rpm for 15 minutes. The supernatant was transferred into glass vials and screened by UPLC-MS for the non-sulfated hydrolysis product (method: **co-injection 2**).

9.3.2 HCl hydrolysis of sulfated metabolites in *N. annulata*

Solvent was evaporated in a N₂ stream from 2 ml of methanolic *N. annulata* extract (see section 9.4.3) leading to approximately 1 mg dried extract. This was dissolved in 100 µl ultra pure water under vortexing. 10 µl were removed and pipetted into 100 µl solvent A (9.1.2), centrifuged (13.000 rpm, 15 minutes) and transferred to a glass vial for the UPLC-MS measurement "before". The remaining 90 µl were adjusted with diluted HCl to a pH of 1 and filled up to a volume of 1 ml with ultra pure water. The sample was then placed in an 80 °C water bath under stirring for 3 hours, after which a slight turbidity could be noticed. The solution was cooled to RT neutralized with KOH to pH 6-7. Then the solution was reduced to approximately 500 µl under an N₂ stream. 100 µl of this solution were diluted with solvent A (sample 2), another 100 µl were added to 100 µl methanol and centrifuged (13.000 rpm, 15 minutes) (sample 1). The remaining 300 µl were extracted three times with 1 ml methyl-tert-butylether (MTBE), which proved a suitable extraction solvent for phenolic acids from aqueous solution. MTBE was evaporated under an N₂ stream and taken up in 150 µl of methanol (sample 3). Samples 1-3 were screened by UPLC-MS (methods **sulfmet**, **biofilm**) for molecules with m/z [M-H-80]⁻ 179, which would indicate the loss of "SO₃".

After complete solvent evaporation, sample 3 was derivatized for GC-MS measurements according to a protocol from Vidoudez [139]. Briefly, 50 µl of a methoxyamine

solution in pyridine (20 mg ml^{-1}), were added to the dried sample, vortexed and then incubated for 1 hour at 60°C and further 9 hours at RT. Then $50 \mu\text{l}$ of N-methyl-N-tri-methylsilyltrifluoroacetamid (MSTFA) solution, containing a retention time index mixture of different alkanes, were added and the solution was incubated for 1 hour at 40°C . The sample was transferred to a glass vial and measured by GC-MS, as described in section 9.1.4.

9.3.3 Enzymatic hydrolysis by an arylsulfatase

Enzymatic hydrolysis experiments of the synthetic phenolic acid sulfate esters 3,4CAS, *m*-, *o*- and *p*-BS and of the fractionated, presumably sulfated metabolites from *N. annulata* were performed with a sulfatase type VI from *Aerobacter aerogenes* (Sigma Aldrich, S1629) according to a published protocol.[137] Briefly, stock solutions in deionized water (4 mg/ml) of the synthetic analogs were prepared and diluted ten times. Methanolic *N. annulata* extract was fractionated by UPLC (PDA detection). Thus, fractions from 20 runs with $20 \mu\text{l}$ injection volume containing the two isomers were collected. The solvent was evaporated and the remainings dissolved in $220 \mu\text{l}$ deionized water. Off all samples a UPLC-MS measurement was performed with the method **biofilm** (table 9.2) before sulfatase addition, to screen for the absence of the non-sulfated forms. Then, $200 \mu\text{l}$ of each sample were mixed with $250 \mu\text{l}$ of 0.25 M Tris-HCl buffer at pH 7.2 (section 9.1.8.2) and incubated for 30 minutes at 37°C . Finally, $50 \mu\text{l}$ of sulfatase were added, carefully mixed and incubated for further 1.5 hours at 37°C . Solvents were then evaporated and the samples dissolved in $200 \mu\text{L}$ of methanol, vortexed, centrifuged and immediately measured with UPLC-MS (**biofilm**, table 9.2). Chromatograms were then screened for the presence of non-sulfated forms, recognizable by the loss of m/z -80 (" SO_3 ").

9.3.4 Stability of sulfated phenolic acids in sterile medium

Solutions of A, B, Z, AS, BS and ZS in Marine Broth (Carl Roth) in concentrations of 2.05 mmol l^{-1} were sterile filtered ($0.2 \mu\text{m}$) into autoclaved 4 ml glass vials, each

in triplicates. A sample was taken immediately afterwards and after leaving the samples for 11 days on a shaker (150 rpm, 30 °C). For UPLC-MS measurements 100 µl of solution were added to 900 µl methanol containing 6.75 mmol l⁻¹ *trans*-cinnamic acid as internal standard (IS). Samples were vortexed, centrifuged (15 minutes, 13,000 rpm), transferred to glass vials and stored at -26 °C until measured with the method **biofilm** (table 9.2).

9.4 Cultivation and extraction of algae

9.4.1 *Codium fragile*

C. fragile was collected at the west coast of Sweden, north of Göteborg, end of October 2009 and shipped on ice to Jena. The algae were kept in a medium prepared from Instant Ocean nitrate free artificial sea salt (Aquarium Systems, France), without further nutrients at 6 °C and a light/dark cycle of 14/10. Constant air flow was ensured by an air pump.

For algae extraction, tools were prepared as follows: mortar and pistil were cleaned with sand and deionized water, then thoroughly rinsed with ultra pure H₂O, acetone and finally methanol. Glass ware and spatulas were thoroughly rinsed with methanol.

For wounding experiments three replicates per sample were prepared, on time points I (0 minutes), II (30 minutes) and III (60 minutes) post wounding. For each replicate 6 to 8 g of wet algal material were used. For unwounded control samples, the alga was immediately placed into liquid nitrogen, ground to a fine powder and then 4 ml of methanol were added. For wounded samples II and III, algae were wounded with the pistil, left for the designated time, then liquid nitrogen and methanol was added. The samples in methanol were thawed, transferred to glass vials with solvent resistant lids, vortexed and then centrifuged for 14 minutes at 20 °C at 6.000 rpm. For removal of remaining salts Chromabond® Easy SPE cartridges (Macherey-Nagel) were used. These were rinsed two times with 4 ml H₂O (UPLC grade, Fisher Scientific, United Kingdom) by using a syringe with a small piece of Teflon® tube attached

to push the solvent through the cartridge. The extract supernatant was transferred onto the cartridge and pushed through with the syringe setup by approximately 2 drops/s. The cartridge was then washed two times with 4 ml ultra pure water and finally the metabolites eluted with 6 ml of methanol and collected in a glass tube. The volume was reduced under a N₂ stream to approximately 500 to 800 µl. For blank measurements the complete procedure was repeated just with methanol. All extracts were transferred into glass vials and stored at −26 °C.

9.4.1.1 UPLC-MS measurements of *Codium* sp. extracts

Extracts of wounding experiments were measured on a C18-Waters column with the method **standard**.

9.4.2 *Dasycladus vermicularis*

D. vermicularis was collected by Dr. Matthew Welling in the Florida Keys in 2009, still attached to a stone and brought to Jena. The alga was kept in a medium prepared from Instant Ocean nitrate free artificial sea salt (Aquarium Systems, France), without further nutrients at RT and no air flow. Instant Ocean was exchanged monthly. Extraction was performed as described in section 9.4.1, except that no solid phase extraction was applied. Therefore, 4 ml of methanol per 1 g of wet algae material were used. Samples were stored at −26 °C.

9.4.2.1 UPLC-MS measurements of *D. vermicularis* extracts

Extracts were measured on a C18 column from Waters with the methods **sulfmet** and **co-injection**. Best peak shapes were obtained by removal of methanol in a N₂ stream and subsequent uptake of the sample in 4 times the original volume of solvent A. The solution was vortexed, centrifuged and immediately measured.

9.4.3 *Neomeris annulata* and *Cymopolia barbata*

Extracts of *N. annulata* were prepared in Florida (USA) by Dr. Matthew Welling (2009) and Prof. Georg Pohnert (2011) in cold methanol with freshly harvested algal material. Extracts of *C. barbata* were made by Dr. Jennifer Sneed (2012, Florida, USA) and Stefanie Wolfram (2013, Georgia, USA) with algae ordered from www.live-plants.com. Both times *C. barbata* arrived not cooled and rather stressed, recognizable by the yellowish/brown coloring of the water and the fishy smell. Extractions were performed in cold methanol (Florida) or with liquid nitrogen and methanol (Georgia), and shipped as evaporated extracts, which were then taken up again in methanol in Jena.

9.4.3.1 UPLC-MS measurements of *N. annulata* and *C. barbata* extracts

Extracts were measured on a C18 column from Phenomenex with the methods **sulfmet** and **co-injection**. Best peak shapes were obtained by preparing the samples in solvent A as described in section 9.4.2.1.

9.4.4 Extraction of zosteric acid from *Zostera marina*

2.5 g of freshly harvested *Zostera marina* (Helgoland, Germany, 2012) were carefully dried with a tissue, then extracted with 5 ml of methanol as described in section 9.4.1, except for the solid phase purification step. The extracts were stored in glass vials at -26°C .

9.4.4.1 UPLC-MS measurements of *Z. marina* extracts

Extracts were measured on a C18 column (Phenomenex) with the method **sulfmet**. Best peak shapes were obtained by measuring the samples tenfold diluted in solvent A (9.1.2). To confirm structural identity, UPLC-MS co-injection experiments of synthetic and natural zosteric acid were performed as described under section 9.5.

9.5 Identification of sulfated metabolites by UPLC-MS

For identification of the unknown sulfated metabolites in *D. vermicularis*, *C. barbata* and *N. annulata* UPLC retention times and MS spectra of the extracts and of the potential synthetic standards were compared using samples in methanol. Then co-injection experiments were performed to confirm the identity. Therefore, the concentrations of metabolites in the algal samples were roughly estimated by an external calibration with the synthetic standards. For BS calibration standards ranging from 10 to 80 $\mu\text{g ml}^{-1}$ in steps of 10 and for AS standards from 50 to 400 μg in steps of 50 were prepared in triplicates. Then, equal amounts of algal extract and the synthetic sample with most similar concentrations were mixed, namely 20 $\mu\text{g l}^{-1}$ for BS and 150 $\mu\text{g l}^{-1}$ for AS. The solvent was removed and the sample taken up in half the amount of solvent A. After centrifugation (15 minutes, 13,000 rpm), samples were immediately measured by UPLC-MS with the methods **co-injection** for *D. vermicularis* and **co-injection 2** for *C. barbata* and *N. annulata*. If peak areas were doubled without major changes in peak symmetry, peaks were considered as co-eluting, confirming the identity of the tested metabolites.

9.6 Cultivation and storage of bacteria

For biofilm assays two different biofilm forming bacteria were used: a non-pathogenic strain *Escherichia coli* (ATCC 25404, DSM 5698) belonging to the enterobacteria family and a strain of the marine bacterium *Vibrio natriegens* (ATCC 14048, DSM 759). Both strains were obtained from DSMZ (Deutsche Sammlung von Mikroorganismen und Zellkulturen GmbH) as freeze-dried pellets and were revived as recommended by DSMZ. For culturing of *E. coli*, medium recommended by DSMZ for this strain was prepared. Therefore, 10 g of peptone (Carl Roth), 5 g yeast extract (Fluka), 10 g sodium chloride (Carl Roth) and 1 g of D+ Glucose (Sigma Aldrich) were dissolved in 990 ml of Millipore Water (0.055 μS) and the pH adjusted to 7.4

with 10 M NaOH. The medium was autoclaved for 15 minutes at 121 °C. Before use, 5 ml of a 1 M CaCl₂×2H₂O and 5 ml of a 1 M MgSO₄×7H₂O were added through a sterile filter (0.2 µm). *V. natriegens* was grown in Marine Broth (Carl Roth) containing 1.94 % of NaCl, as recommended by DSMZ.

For longtime storage of both bacterial strains glycerol stocks were prepared. Therefore, freeze-dried pellets were revived according to DSMZ and grown for 48 hours at RT on a shaker. From this culture an overnight culture was prepared by adding 200 µl of the pre-culture into 20 ml of the respective medium. This culture was grown for 24 hours at RT during shaking. For preparation of the glycerol stocks 600 µl of sterile bacterial medium were thoroughly mixed with 600 µl autoclaved glycerol. To this 600 µl of the 24 hour culture were added and carefully mixed. Vials were put into a Mr. Frosty™ Freezing Container (Nalgene via VWR) with isopropanol (cooling rate approximately -1 °C min^{-1}) and kept for 24 hours at -80 °C . After that time, samples could be stored at -80 °C . For each experiment a new glycerol stock was used. Therefore, the stock was thawed at 37 °C for 15 minutes, then medium was inoculated with 2 % v/v of the stock. This pre-culture was grown for 24 hours at the desired temperature under shaking. From this culture fresh medium was inoculated with 1 % v/v and grown for 24 hours. This pre-culture was then used for inoculating cultures for the biofilm experiments.

For filter disc assays marine bacteria were provided by Dr. Carsten Paul und Jan Grüneberg. Experiments were performed with one week old cultures grown at RT under shaking (100 rpm/min). Media used for the different bacterial species are listed in table 9.7.

9.7 Bioassays

9.7.1 Filter disc assay

A filter disc assay was used to test a growth inhibiting impact of the two from *D. vermicularis* isolated sulfated metabolites AS and BS and their non-sulfated forms A and B on different marine bacteria. Various antibiotics (ampicillin, peni-

strain	short	medium	origin
<i>Pseudoalteromonas tetraodonis</i>	H11	Difco TM Marine Broth 2216	Wichels 2004 [180]
<i>Pseudoalteromonas carrageenovora</i>	H92	Difco TM Marine Broth 2216	Wichels 2004 [180]
<i>Cellulophaga lytica</i>	C.L.	DSMZ Medium 172	DSM 2039
<i>Dinoroseobacter shibae</i>	DINO	Difco TM Marine Broth 2216	DSM 16493
?	MS1	Difco TM Marine Broth 2216	<i>Ulva sp.</i> isolate
?	MS2	Difco TM Marine Broth 2216	<i>Ulva sp.</i> isolate
?	MS3	Difco TM Marine Broth 2216	<i>Ulva sp.</i> isolate

Table 9.7: Bacteria and culture media used for filter disc assay.

substance	origin	solvent
B	Sigma Aldrich	ethanol
A	Sigma Aldrich	ethanol
BS	synthesized	water
AS	synthesized	water
ampicillin	Sigma Aldrich	ethanol
penicillin	Sigma Aldrich	water
streptomycin	Sigma Aldrich	water
streptomycin penicillin neomycin	Sigma Aldrich	water

Table 9.8: Additives and solvents used in filter disc assay.

cillin, streptomycin, and a mix of streptomycin, penicillin and neomycin) were used as references. Agar plates were prepared from a solution of 1000 ml ultra pure water, 40.1 g Marine Broth (Carl Roth) and 15 g agar which was brought to boil while stirring. After complete dissolution, the agar was autoclaved and immediately afterwards 20 ml of agar were pipetted to polystyrene petri dishes (diameter 9 cm). The plates were left to cool under the sterile bench, then tightly sealed and stored at 4°C until used.

Stock solutions of all additives in concentrations of 100 mg ml⁻¹ were sterile filtered and then diluted with sterile deionized water to concentrations of 10, 1 and 0.1 mg ml⁻¹. The antibiotics mix was only available in a stock solution of 1 mg l⁻¹. As release material of the additives, paper filters (VWR, Art. No. 516-0801) were punched into circular plates with a diameter of 5 mm, which were then autoclaved

for 15 minutes at 121 °C. Each substance was tested in 4 different dilutions and 1 solvent blank on each of the seven bacteria. Therefore, 5 µl of a dilution or solvent were pipetted to a filter plate, leaned against the petri dish lid and left a few minutes for solvent evaporation. In the meantime, 100 µl of the undiluted, dense bacterial culture were distributed on the agar plate. The dried filter papers of an additive in different concentrations were then placed on the designated positions on the agar plate. Each bacterium was additionally distributed without filters on an agar plate as a growth control. The plates were sealed and left at RT until a dense bacterial film was grown. After three days, zones of inhibition were measured. The diameter of each inhibition zone was measured two times and the mean value taken.

9.7.2 Biofilm formation at the air-liquid-interface

For testing the impact of sulfated phenolics and their non-sulfated forms on growth and biofilm formation of *E. coli* and *V. natriegens* at the air-liquid-interface sterile 96 well plates (Cellstar, F-bottom, polystyrole) were used. This assay simultaneously allowed to investigate the stability of the additives in presence of bacteria by UPLC-MS screening.

Substances tested were BS (m= 17.9 mg), AS (m= 19.02 mg), ZS (m= 20.0 mg) and the non-sulfated educts B (m= 11.3 mg, Sigma Aldrich, Germany), A (m= 12.5 mg, Alfa Aesar, Germany) and Z (m= 13.4 mg, Alfa Aesar, Germany).

Sample preparation

In 8 sterile Falcon tubes (Sarstedt) 40 ml of appropriate bacterial medium was provided (see section 9.6). The six substances (Z, ZS, A, AS, B, BS) were each dissolved in the tube, leading to a final concentration of 2.05 mmol l⁻¹. Two tubes with medium remained as blanks. From all of the 8 solutions 30 ml were filtered through 0.2 µm sterile filters into new, sterile Falcon tubes. Into 6 solutions containing additives and one medium blank 300 µl of a 24 hour preculture (see section 9.6) were pipetted, leading to the following solutions: M- (medium containing neither bacteria nor additives), M+ (medium containing bacteria but no additives), Z, ZS,

	1	2	3	4	5	6	7	8	9	10	11	12
A		M+	Z	ZS	A	AS	B	BS	M-	M+	M+	M+
B		M+	Z	ZS	A	AS	B	BS	M-	Z	Z	Z
C		M+	Z	ZS	A	AS	B	BS	M-	ZS	ZS	ZS
D		M+	Z	ZS	A	AS	B	BS	M-	A	A	A
E		M+	Z	ZS	A	AS	B	BS	M-	AS	AS	AS
F		M+	Z	ZS	A	AS	B	BS	M-	B	B	B
G		M+	Z	ZS	A	AS	B	BS	M-	BS	BS	BS
H		M+	Z	ZS	A	AS	B	BS	M-			

Table 9.9: Filling scheme of a 96-well plate for biofilm formation in presence of additives (A, AS, B, BS, Z and ZS) at the air-liquid-interface.

A, AS, B, BS. With these solutions 12 96-well plates were filled according to the scheme in table 9.9. In each well 200 μ l of a solution were pipetted; care was taken to not touch the well with the pipette tip and to avoid air bubbles by pipetting very slowly. Both measures were necessary to avoid that bacterial material dried at the well inner well wall, which might later be mistakenly be understood as biofilm. Row 1 (A-H) was always left empty, rows 2 (A-H) - 8 (A-H) contained 8 biological replicates for biofilm formation, rows 9A - 12G contained three replicates of each sample for UPLC-MS screening of metabolites in presence of bacteria. All plates were then carefully transported to an incubator at 29 °C and not moved anymore before evaluation, to avoid swapping of bacterial medium within the well, which might later be misinterpreted as biofilm.

Monitoring of bacterial growth via optical density

One plate was labeled specially and used to monitor the optical density (OD) hourly to observe bacterial growth in the presence of the additives until the start of production of exo-polymeric material leading to biofilm formation. Measurements also served as a rough estimation, when biofilm formation would start. The biofilms of this plate were not evaluated, due to repeated movement. OD was measured on a Mithras plate reader (section 9.1.5). M- was used as a reference during OD measurements, and values for medium containing bacteria were normalized to these values. M- had an OD fluctuating around 0.15 ± 0.02 . After the start of biofilm formation OD measurements might not only represent bacterial cells, but also exo-polymeric

material which additionally contributed to the signal. Thus, these OD measurements do not lead to a complete growth curve, but only show bacterial growth in lag and exponential phase.

UPLC-MS screening of additives

When it was assumed that biofilm formation would start, a plate was removed from the incubator and first samples for UPLC-MS measurements were taken. Therefore, 190 μl were transferred from each well into Eppendorf Tubes[®] and centrifuged at 5.000 rpm for 15 minutes. During that time a stable bacterial pellet formed. 100 μl of the supernatant were pipetted into 900 μl of methanol containing 0.1 mg ml^{-1} cinnamic acid as internal standard (IS). Methanol was used for two reasons: namely to quench eventually remaining enzyme activity and to precipitate the majority of salts from the UPLC-MS sample. Samples were centrifuged for 15 minutes at 13.000 rpm, the supernatant transferred to glass vials and stored at $-26\text{ }^{\circ}\text{C}$ until measurement with the method **biofilm** (see table 9.2). This method allowed separation of all three sulfated as well as the three non-sulfated substances and the internal standard, with an acceptable peak shape of the sulfated metabolites.

Peak areas were evaluated by hand using the MassLynx software (Waters), because the integrated automatic tool QuanLynx always required corrections for the sulfated samples. From peak areas of the replicates mean values and standard deviations were calculated using Microsoft Excel (2007) and graphs were created with Sigma Plot (11.0, Systat Software GmbH).

Biofilm evaluation via crystal violet absorption

Immediately after taking UPLC-MS samples, the plate was prepared for biofilm evaluation according to [148, 149]. Plates were turned up side down and the medium contents poured into a waste container, then immediately dipped into a container containing PBS buffer (section 9.1.8.1) and thoroughly washed, to remove bacterial floc (formed at the medium surface, due to the static conditions during growth), which can seriously falsify the biofilm evaluation when sticking to the well border. The plates were then washed in two further containers with deionized water and air

dried for 15 minutes. After drying, 200 µl of a 0.1 % crystal violet solution (CV, Sigma Aldrich, Germany) were added to each well, including wells 1 A-H as a CV reference (CV also slightly stains polystyrene) and also in rows 8 (A-H) as a negative biofilm control (M-). The biofilm was incubated for 15 minutes, then CV solution was removed and the plates washed in several containers with deionized water until no coloring of water was observed. The plates were shaken vigorously to remove most of the remaining water and dried by air. When all plates were dried, 200 µl of a 80:20 (v:v) mixture of ethanol:acetone were pipetted in each stained well, and left for 15 minutes until CV was completely dissolved. Afterwards, plates were measured on a Mithras plate reader under shaking (10s) as described in section 9.1.5. The mean value of the CV blank in rows 1A-H was used for normalization.

Statistical analysis

Statistical analysis for the bioassays described in section 9.7.2 and 9.7.3 were performed using Sigma Plot 11.0 (Systat Software GmbH). For comparison of two mean values a t-test was used. For comparison of several mean values to a control, one way ANOVA with the therein included Holm-Šidák test was used. Samples with $p < 0.001$ to the control were assigned ***, those with $p < 0.1$ ** and those with $p < 0.1$ *.

9.7.3 Biofilm formation below the air-liquid-interface

9.7.3.1 Surface test for biofilms of *E. coli* and *V. natriegens*

For biofilm assays below the air-liquid-interface the following surfaces were tested for *E. coli* and *V. natriegens*: glass microscopy coverglasses (VWR, 22 mm × 22 mm), PTFE plates (VWR, diameter 12 mm, white) and Silicone septa (Thermo Fisher, Red PTFE/White Silicone, diameter 8 mm). For each material two plates were fixed equidistantly in a PTFE tube (VWR, PTFE, white, translucent, diameter 1 cm, inside 8 mm) sliced in one third, so that the plate stuck half into the tube, allowing sufficient flow through of medium. All materials were rinsed with ethanol and only touched with gloves. The tubes with the plates were put into a glass beaker, sealed

with aluminum foil and autoclaved for 15 minutes at 121 °C. Two tubes containing glass slides were each put into 12 sterile 250 ml Erlenmeyer flasks, for tubes containing silicone or PTFE plates also 2 were put into 12 sterile 100 ml Erlenmeyer flasks. 250 ml flasks were filled with 150 ml of the respective medium and inoculated with 1.5 ml of a bacterial pre-culture. 100 ml flasks were filled with 50 ml of medium and inoculated with 500 µl pre-culture (section 9.6). Thus, six biological replicates of each material and bacteria were prepared. Three replicates of each material and bacteria were placed on a shaker (30 °C, 100 rpm), the remaining samples were kept in an incubator without shaking (30 °C). After three days tubes were removed, washed with deionized water and dried. The tubes were stained with a 0.1 % CV solution for 15 minutes and afterwards carefully washed until no coloration of water was observed. After drying, the plates were carefully removed by cutting the tube and observed under the microscope (section 9.1.6). The silicone surface was the only one not evaluable under the microscope due to its thickness.

9.7.3.2 Biofilm growth test of *V. natriegens* on PTFE plates

The experiment as described under section 9.7.3.1 was repeated with *V. natriegens* growing on PTFE plates over a period of 15 days. This time, for each condition (on shaker, not shaking, both 30 °C) three replicates with 4 tubes containing two plates were prepared in 100 ml flasks. Samples were taken under the sterile bench after 5, 9, 12 and 15 days. Thereby, a tube was removed from each replicate per sampling day, followed by image evaluation to quantify biofilm coverage according to section 9.7.3.3.

9.7.3.3 Biofilm formation of *E.coli* and *V. natriegens* on PTFE plates with additives

Sample preparation

Additives tested were BS (m= 76.1 mg), AS (m= 80.62 mg), ZS (m= 85.12 mg) and the non-sulfated educts B (m= 48.2 mg, Sigma Aldrich, Germany), A (m= 53.3 mg, Alfa Aesar, Germany) and Z (m= 57.4 mg, Alfa Aesar, Germany). In sterile glass

containers 170 ml of appropriate medium (section 9.6) were provided. The additives were each dissolved in medium, leading to a final concentration of 2.05 mmol l^{-1} . One medium sample remained without additives as a control. 100 ml Erlenmeyer flasks were equipped with 5 - 10 PTFE tubes containing each two PTFE plates. From all the different solutions 3 times 50 ml were sterile filtered ($0.2 \mu\text{m}$) into the flasks, leading to three biological replicates per sample. Then, each flask was inoculated with 500 μl bacterial pre-culture (section 9.6). After inoculation, flasks were placed on a shaker (150 rpm) either at RT ($\sim 23^\circ\text{C}$) or at 30°C (see below). Samples were taken at designated time points for the estimation of biofilm coverage (1), cell number (2) and for UPLC-MS screening (3) to test the stability of the metabolites in presence of bacteria. The following experiments were performed according to this scheme:

I. *E. coli*: in presence of Z, ZS, A, AS, B, BS and the control M at RT (23°C) on a shaker (150 rpm). The experiment was performed once. Biofilm samples were taken at 12, 24, 48 and 72 hours after inoculation, UPLC-MS samples additionally before inoculation.

II. *V. natriegens*: with Z, ZS, A, AS, B, BS and M at 30°C on a shaker (150 rpm). The experiment was performed twice with Z, ZS, A, AS and M, once additionally with B and BS. Samples (biofilm, UPLC-MS, cell number) were taken every second day, starting from day 1 until day 11 and additionally was a cell number sample taken right after inoculation and a UPLC-MS sample right before inoculation.

III. *V. natriegens*: with ZS (2.05 mmol l^{-1}), "Z 100" (2.05 mmol l^{-1}), "Z 50" ($1.025 \text{ mmol l}^{-1}$), "Z 25" ($0.512 \text{ mmol l}^{-1}$), "Z 10" ($0.205 \text{ mmol l}^{-1}$), "Z 5" ($0.1025 \text{ mmol l}^{-1}$) and M at 23°C . Samples (biofilm, UPLC-MS, cell number) were taken every second day, starting from day 1 until day 13, and additionally was a cell number sample taken right after inoculation and a UPLC-MS sample right before inoculation.

Biofilm sampling

For biofilm sampling (1) one tube was removed from each flask (see section 9.7.3.3)

and washed in three glass containers with water, to remove bacteria not attached to the surface of a plate. The tube with the plates was air dried and dyed in a 0.1 % CV solution for 15 minutes. The CV solution was carefully washed from the tubes and the tubes air dried. After drying, tubes were cut so that the PTFE plates could easily be removed without scratching the biofilm. The two plates of each sample/replicate were then tightly clipped between two glass microscope slides (VWR, Germany) and fixed with parafilm. Then, a picture of the biofilm in the "center at PTFE" (section 5.2) region was taken of both plates on both sides, with the camera-microscope as described in section 9.1.6. Thus, for each single biological replicate consisting of two plates 4 biofilm images were taken. With three biological replicates this provided a mean value of 12 images for each sample and time point. Images for *V. natriegens* were evaluated as described under 9.7.3.3, for *E. coli* evaluation was performed only qualitatively.

UPLC-MS screening of additives

For UPLC-MS screening (3) 400 µl of each sample solution were transferred to an Eppendorf tube and centrifuged for 15 minutes at 5.000 rpm. Then 100 µl of the supernatant were pipetted into 900 µl methanol containing cinnamic acid (0.1 mg/l) as an internal standard and further treated and measured as described in section 9.7.2.

Monitoring bacterial growth via cell counting

For cell number estimation, 290 µl of the remaining 300 µl medium covering the bacterial pellet (see paragraph "UPLC-MS screening of additives", section 9.7.3.3) were removed, thereby care was taken not to touch the bacterial pellet. 290 µl of PBS buffer were added and the sample vortexed rigorously until the bacterial pellet was completely dissolved. Then the sample was centrifuged again at 5.000 rpm for 15 minutes. 290 µl of the supernatant were removed and replaced with 390 µl of fresh PBS buffer. The sample was vortexed again until complete solution of the bacterial pellet. The washing step with PBS was necessary due to the exopolymeric material produced by the bacteria, which caused them to clump together in the medium.

This led to an inhomogeneous distribution under the microscope, making counting cells impossible. Two times washing in buffer solved that problem. Finally, 8 μl of a 25 % glutaraldehyde solution (0.5 %, Sigma Aldrich, Germany) were added and the sample shortly vortexed. These samples were stored in the dark at 4 °C.[181]

For cell counting, samples were vortexed and diluted with PBS buffer such that approximately 250 - 400 cells were in one square with an area of 0.04 mm² of a Neubauer improved counting chamber. For loading cells, 15 μl of a diluted sample were carefully pipetted into on the counting chamber. The bacteria were then left to settle for 25 minutes. This time was necessary for settlement, but should not be elongated much, because then solvent evaporation leads to an interfering concentration change of cells. For counting cells, a picture was taken with the camera-microscope setup described in section 9.1.6. The camera, however, could not show the whole area of one of the 25 central squares with 0.04 mm². Thus, in ImageJ a new square was adjusted containing cells within the inner lines of the three allowing volume adjustment (0.1861 mm \times 0.1884 mm \times 0.1000 mm). Three pictures were taken of the 25 central squares, one in the center and two at opposite sides at the border. Each sample was loaded on both sides of the chamber, leading in total to six pictures to count per sample. Cells were counted with the ImageJ cell counter tool (version 1.47v). Cell numbers of the six pictures were added together and with these the cell number per sample estimated. Then mean values and standard deviations of the cell numbers of the three replicates were calculated.

Biofilm evaluation via quantitative image evaluation

Observation of the CV stained biofilm coverage was most evenly in the "center at PTFE" region (section 5.2) and this area was quantitatively analyzed by ImageJ (version 1.47v) based on dynamic thresholding as described by [182] and references therein. Therefore, the image was first converted to an 8 bit image and then transformed into a binary image by using the dynamic threshold 1d tool (Mask= 20, C= 0-6, display Max/Min Image). Biofilm was shown in black pixels and the thus thresholded image was compared to the original, if particle size and form fitted. The

binary image was then analyzed with the particle analyzer tool. The estimated coverage by black particles in % was then used to calculate the mean biofilm coverage.

Statistical analysis

Statistical evaluation of this assay was performed as described under 9.7.2.

9.7.3.4 Calibration of ZS and Z in ZS samples after presence of *V. natriegens* by UPLC-MS

To calibrate the amount of Z released during the degradation of ZS by *V. natriegens* via UPLC-MS, external standards of ZS and Z were prepared as well as a dilution of the ZS samples. For each standard, three replicates were prepared, which were measured once (as for the samples from the experiment). For calibration of Z, a stock solution of Z was prepared in the concentration of 2.05 mmol l^{-1} ("Z 100") in Marine Broth (MB, Carl Roth, Germany). Of this solution samples containing 50 ("Z 50"), 35 ("Z 35"), 30 ("Z 30"), 25 ("Z 25"), 20 ("Z 20"), 15 ("Z 15"), 10 ("Z 10"), 5 ("Z 5") and 1 ("Z 1") % of the original concentration were prepared as listed in table 9.10. For Z calibration, cinnamic acid was used as internal standard (IS) from a stock solution of 0.1 mg/ml dissolved in methanol. Sample preparation followed the routine described in section 9.7.2.

To monitor the degradation of ZS to Z over time by *V. natriegens*, the original samples containing ZS (2.05 mmol l^{-1}) were diluted by a factor of 10 with solvent A (section 9.1.2) to obtain a better peak shape. As internal standard for the calibration of ZS, BS was used. Therefore, a stock solution of BS in solvent A was prepared with a concentration of $1.025 \text{ mmol l}^{-1}$. For sample dilution, 890 μl A were pipetted into an Eppendorf tube and 10 μl BS stock were added, then 100 μl from the ZS sample (section 9.7.2) were added. The diluted sample was then centrifuged at 13.000 rpm for 15 minutes and 950 μl transferred into a glass vial and stored for a short time at $-26 \text{ }^\circ\text{C}$.

The calibration standards for ZS were then prepared in two subsequent steps so that they matched the solvent composition of the diluted sample. First stock solutions of

sample	methanol + IS [μl]	stock Z [μl]	MB [μl]
Z 100	900	100	0
Z 50	900	50	50
Z 35	900	35	65
Z 30	900	30	70
Z 25	900	25	75
Z 20	900	20	80
Z 15	900	15	85
Z 10	900	10	90
Z 5	900	5	95
Z 1	900	1	99

Table 9.10: External calibration standards for Z. MB: Marine Broth, IS: Internal standard.

sample	methanol + IS [μl]	stock ZS [μl]	MB [μl]
ZS 125	900	100 I	0
ZS 100	900	100 II	0
ZS 75	900	75 II	25
ZS 50	900	50 II	50
ZS 25	900	25 II	75
ZS 10	900	10 II	90
ZS 5	900	5 II	95

Table 9.11: External calibration standards for ZS. I: Stock solutions from stock I. II: Stock solutions from stock II. MB: Marine Broth, IS: Internal standard.

ZS in Marine Broth (MB) were prepared in concentrations of 2.56 mmol l^{-1} (stock I) and 2.05 mmol l^{-1} (stock II) and then mixed with methanol containing the internal standard as listed in table 9.11. Stock solutions contained 125 ("ZS 125"), 100 ("ZS 100"), 75 ("ZS 75"), 50 ("ZS 50"), 25 ("ZS 25"), 10 ("ZS 10") and 5 ("ZS 5") % of the concentration originally contained in the ZS sample.

These samples were centrifuged for 15 minutes at 13.000 rpm and 100 μl from the supernatant were pipetted into 890 μl solvent A and 10 μl BS solution ($1.025 \text{ mmol l}^{-1}$) were added. These samples were vortexed, centrifuged, transferred into glass vials and stored for a short time at -26°C until measurement. Diluted ZS samples and undiluted Z samples of one experiment as well as ZS and Z calibration standards were measured pooled, with no interruption of the UPLC-MS system (method **biofilm**).

9.7.4 Biofouling field assay at the coast of İzmir, Turkey

The biofouling field assay was performed by Dr. Levent Cavas, from the Dokuz Eylül University, İzmir-Turkey. The substances tested (AS, BS, ZS) were synthesized in Jena and sent to Turkey, shortly before the experiment started. The rosin based antifouling paints [183] were prepared with synthesized analogous of AS and BS (found in Dasycladaceae) and ZS (found in *Zostera marina*). The antifouling effects of these compounds were compared with each other and to a control panel, only containing the paint composition without additives. The commercial primer coating and commercial rosin based antifouling paint containing very small amounts of Cu_2O (also an antifoulant), were thought to function as positive controls (heavy fouling). First, rosin was dissolved in xylene, then sunflower oil, Lutanol M40, ZnO , Cu_2O , CaCO_3 , additives and Bentonite (anti-sagging) were incorporated at weight ratios as given in table 9.12.

Steel panels were treated with sandpaper and primer coating was applied in order to prevent corrosion. Then, the antifouling paints were applied by a brush on two sides of the steels. Painted steels were allowed to dry for one week at RT. The painted steel panels were immersed into seawater at a depth of 50 cm by hanging on a plastic apparatus. The paints were tested for a period of 70 days from June 12 to August 8, 2013 at Levent Marina, İzmir, Turkey. Fouling criteria, concerning abundance of settled micro- and macro-fouling organisms, for evaluation of the surfaces of the antifouling test panels were adapted from [176]. The fouling criteria used in this study constitute five fouling levels:

Level 1. No fouling organisms on the surface.

Level 2. Microfilm layer formation is present on the surface.

Level 3. Microfilm layer is present and macrofouling is at the beginning state.

Level 4. Micro- and macrofouling organisms are present on the surface.

Level 5. The surface is heavily fouled (>50%) by micro- and macrofouling organisms.

Paint	Binder		Plasti- cizer	Pigment		Sol- vent	Stabi- lizer	Additive			Anti- sagging
	Rosin	Oil		ZnO	Cu ₂ O			Xylene	CaCO ₃	AS	
1	24%	6%	6%	12%	6%	38%	5%	-	-	-	3%
2	24%	6%	6%	12%	6%	38%	3%	2%	-	-	3%
3	24%	6%	6%	12%	6%	38%	3%	-	2%	-	3%
4	24%	6%	6%	12%	6%	38%	3%	-	-	2%	3%
5	24%	6%	6%	10%	6%	38%	3%	4%	-	-	3%
6	24%	6%	6%	10%	6%	38%	3%	-	4%	-	3%
7	24%	6%	6%	10%	6%	38%	3%	-	-	4%	3%
8	21%	6%	6%	8%	6%	37%	3%	10%	-	-	3%
9	21%	6%	6%	8%	6%	37%	3%	-	10%	-	3%
10	21%	6%	6%	8%	6%	37%	3%	-	-	10%	3%
11	23%	6%	6%	10%	6%	37%	3%	6%	-	-	3%
12	23%	6%	6%	10%	6%	37%	3%	-	6%	-	3%
13	23%	6%	6%	10%	6%	37%	3%	-	-	6%	3%

Table 9.12: Paint compositions for the biofouling field assay in İzmir, Turkey.

Bibliography

- [1] D. Menzel. How do giant plant-cells cope with injury - the wound response in siphonous green algae. *Protoplasma*, 144(2-3):73–91, 1988.
- [2] <http://www.britannica.com>. 30.06.2014.
- [3] D. Menzel. Plug formation and peroxidase accumulation in two orders of siphonous green algae (*Caulerpales* and *Dasycladales*) in relation to fertilization and injury. *Phycologia*, 19(1):37–48, 1980.
- [4] L. Tornbom and L. Oliveira. Wound-healing in *Vaucheria longicaulis* Hop-paugh var. *Macounii* Blum. 1. Cytomorphological study of the wound response. *New Phytologist*, 124(1):121–133, 1993.
- [5] J. W. La Claire II. Cytomorphological aspects of wound-healing in selected Siphonocladales (Chlorophyceae). *Journal of Phycology*, 18(3):379–384, 1982.
- [6] M. Welling, G. Pohnert, F. C. Küpper, and C. Ross. Rapid biopolymerisation during wound plug formation in green algae. *Journal of Adhesion*, 85(11):825–838, 2009.
- [7] T. W. Dreher, B. R. Grant, and R. Wetherbee. Wound response in siphonous alga *Caulerpa simpliciuscula* C. Ag.: Fine-structure and cytology. *Protoplasma*, 96(1-2):189–203, 1978.
- [8] T. W. Dreher, D. B. Hawthorne, and B. R. Grant. The wound response of the siphonous green algal genus *Caulerpa*. 3. Composition and origin of the wound plugs. *Protoplasma*, 110(2):129–137, 1982.
- [9] V. Jung and G. Pohnert. Rapid wound-activated transformation of the green algal defensive metabolite caulerpenyne. *Tetrahedron*, 57(33):7169–7172, 2001.
- [10] V. Jung, T. Thibaut, A. Meinesz, and G. Pohnert. Comparison of the wound-activated transformation of caulerpenyne by invasive and noninvasive *Caulerpa* species of the Mediterranean. *Journal of Chemical Ecology*, 28(10):2091–2105, 2002.

-
- [11] S. Adolph, V. Jung, J. Rattke, and G. Pohnert. Wound closure in the invasive green alga *Caulerpa taxifolia* by enzymatic activation of a protein cross-linker. *Angewandte Chemie-International Edition*, 44(18):2806–2808, 2005.
- [12] M. Welling, C. Ross, and G. Pohnert. A desulfatation-oxidation cascade activates coumarin based cross-linkers in the wound reaction of the giant unicellular alga *Dasycladus vermicularis*. *Angewandte Chemie-International Edition*, 50(33):7691–7694, 2011.
- [13] D. Santini-Bellan, P. M. Arnaud, G. Bellan, and M. Verlaque. The influence of the introduced tropical alga *Caulerpa taxifolia*, on the biodiversity of the Mediterranean marine biota. *Journal of the Marine Biological Association of the United Kingdom*, 76(1):235–237, 1996.
- [14] P. Bartoli and C. F. Boudouresque. Transmission failure of parasites (Digenea) in sites colonized by the recently introduced invasive alga *Caulerpa taxifolia*. *Marine Ecology-Progress Series*, 154:253–260, 1997.
- [15] R. Raniello, E. Mollo, M. Lorenti, M. Gavagnin, and M. C. Buia. Phytotoxic activity of caulerpenyne from the Mediterranean invasive variety of *Caulerpa racemosa*: a potential allelochemical. *Biological Invasions*, 9(4):361–368, 2007.
- [16] G. Pergent, Ch.-F. Boudouresque, O. Dumay, Ch. Pergent-Martini, and S. Wyllie-Echeverria. Competition between the invasive macrophyte *Caulerpa taxifolia* and the seagrass *Posidonia oceanica*: contrasting strategies. *BMC Ecology*, 8(20), 2008.
- [17] V. Amico, G. Oriente, M. Piattelli, C. Tringali, E. Fattorusso, S. Magno, and L. Mayol. Caulerpenyne, an unusual sesquiterpenoid from green alga *Caulerpa prolifera*. *Tetrahedron Letters*, (38):3593–3596, 1978.
- [18] R. Lemée, D. Pesando, M. Durand-Clément, A. Dubreuil, A. Meinesz, A. Guerriero, and F. Pietra. Preliminary survey of toxicity of the green alga *Caulerpa*

- taxifolia* introduced into the Mediterranean. *Journal of Applied Phycology*, 5 (5):485–493, 1993.
- [19] J. P. Girard, C. Graillet, D. Pesando, and P. Payan. Calcium homeostasis and early embryotoxicity in marine invertebrates. *Comparative Biochemistry and Physiology C-Pharmacology Toxicology and Endocrinology*, 113(2):169–175, 1996.
- [20] C. F. Boudouresque, R. Lemée, X. Mari, and A. Meinesz. The invasive alga *Caulerpa taxifolia* is not a suitable diet for the sea urchin *Paracentrotus lividus*. *Aquatic Botany*, 53(3-4):245–250, 1996.
- [21] I. Galgani, D. Pesando, J. Porthe-Nibelle, B. Fossat, and J. P. Girard. Effect of caulerpenyne, a toxin extracted from *Caulerpa taxifolia* on mechanisms regulating intracellular pH in sea urchin eggs and sea bream hepatocytes. *Journal of Biochemical Toxicology*, 11(5):243–50, 1996.
- [22] D. Pesando, R. Lemée, C. Ferrua, P. Amade, and J.-P. Girard. Effects of caulerpenyne, the major toxin from *Caulerpa taxifolia* on mechanisms related to sea urchin egg cleavage. *Aquatic Toxicology*, 35(3-4):139–155, 1996.
- [23] M. L. Pedrotti, B. Marchi, and R. Lemée. Effects of *Caulerpa taxifolia* secondary metabolites on the embryogenesis, larval development and metamorphosis of the sea urchin *Paracentrotus lividus*. *Oceanologica Acta*, 19(3-4): 255–262, 1996.
- [24] R. Lemée, D. Pesando, C. Issanchou, and P. Amade. Microalgae: A model to investigate the ecotoxicity of the green alga *Caulerpa taxifolia* from the Mediterranean sea. *Marine Environmental Research*, 44(1):13–25, 1997.
- [25] D. Pesando, P. Huitorel, V. Dolcini, P. Amade, and J. P. Girard. Caulerpenyne interferes with microtubule-dependent events during the first mitotic cycle of sea urchin eggs. *European Journal of Cell Biology*, 77(1):19–26, 1998.

- [26] D. Pesando, C. Pesci-Bardon, P. Huitorel, and J. P. Girard. Caulerpenyne blocks MBP kinase activation controlling mitosis in sea urchin eggs. *European Journal of Cell Biology*, 78(12):903–910, 1999.
- [27] A. A. Erickson, V. J. Paul, K. L. Van Alstyne, and L. M. Kwiatkowski. Palatability of macroalgae that use different types of chemical defenses. *Journal of Chemical Ecology*, 32(9):1883–1895, 2006.
- [28] V. J. Paul and W. Fenical. Chemical defense in tropical green algae, order caulerpales. *Marine Ecology - Progress Series*, 34:157–169, 1986.
- [29] V.J. Paul and K.L. Van Alstyne. Activation of chemical defenses in the tropical green algae *Halimeda* spp. *Journal of Experimental Marine Biology and Ecology*, 160:191–203, 1992.
- [30] G. Cimino, A. Crispino, V. Di Marzo, M. Gavagnin, and J. D. Ros. Oxytoxins, bioactive molecules produced by the marine opisthobranch mollusk *Oxynoe olivacea* from a diet-derived precursor. *Experientia*, 46(7):767–770, 1990.
- [31] C. Ross, F. C. Küpper, V. Vreeland, H. Waite, and R. S. Jacobs. The wound repair mechanism in the giant unicellular chlorophyte *Dasycladus vermicularis* is a two-stage process. *Phycologia*, 44(4):140, 2005.
- [32] D. Menzel, R. Kazlauskas, and J. Reichelt. Coumarins in the siphonalean green algal family Dasycladaceae Kutzing (Chlorophyceae). *Botanica Marina*, 26(1):23–29, 1983.
- [33] F. Sollai, P. Zucca, E. Sanjust, D. Steri, and A. Rescigno. Umbelliferone and esculetin: Inhibitors or substrates for polyphenol oxidases? *Biological and Pharmaceutical Bulletin*, 31(12):2187–2193, 2008.
- [34] C. Ross, F. C. Küpper, V. Vreeland, J. H. Waite, and R. S. Jacobs. Evidence of a latent oxidative burst in relation to wound repair in the giant unicellular Chlorophyte *Dasycladus vermicularis*. *Journal of Phycology*, 41(3):531–541, 2005.

-
- [35] P. C. Silva. The dichotomous species of *Codium* in Britain. *Journal of the Marine Biological Association of the United Kingdom*, 34(3):565–577, 1955.
- [36] P. C. Silva and H. B. S. Womersley. The genus *Codium* (Chlorophyta) in southern Australia. *Australian Journal of Botany*, 4(3):261–289, 1956.
- [37] F. I. Dromgoole. Occurrence of *Codium fragile* ssp. *tomentosoides* in New Zealand waters. *New Zealand Journal of Marine and Freshwater Research*, 9(3), 1975.
- [38] E. Y. Dawson and M. S. Foster. Seashore plants of California. *Quarterly Review of Biology*, 58(4):584–585, 1982.
- [39] J. T. Carlton and J. A. Scanlon. Progression and dispersal of an introduced alga - *Codium fragile* ssp. *tomentosoides* (Chlorophyta) on the atlantic coast of North America. *Botanica Marina*, 28(4):155–165, 1985.
- [40] S. J. Campbell. Occurrence of *Codium fragile* ssp. *tomentosoides* (Chlorophyta: Bryopsidales) in marine embayments of southeastern Australia. *Journal of Phycology*, 35(5):938–940, 1999.
- [41] A. C. Mathieson, C. J. Dawes, L. G. Harris, and E. J. Hehre. Expansion of the asiatic green alga *Codium fragile* ssp. *tomentosoides* in the Gulf of Maine. *Rhodora*, 105(921):1–53, 2003.
- [42] A. González and B. Santelices. A dichotomous species of *Codium* (Bryopsidales, Chlorophyta) is colonizing northern Chile. *Revista Chilena de Historia Natural*, 77(2):293–304, 2004.
- [43] J. Provan, S. Murphy, and C. A. Maggs. Tracking the invasive history of the green alga *Codium fragile* ssp. *tomentosoides*. *Molecular Ecology*, 14(1):189–194, 2005.
- [44] C. D. Nyberg and I. Wallentinus. Can species traits be used to predict marine macroalgal introductions? *Biological Invasions*, 7(2):265–279, 2005.

- [45] P. E. Neill, O. Alcalde, S. Faugeron, S. A. Navarrete, and J. A. Correa. Invasion of *Codium fragile* ssp. *tomentosoides* in northern Chile: A new threat for *Gracilaria* farming. *Aquaculture*, 259(1-4):202–210, 2006.
- [46] F. Goecke, V. Hernández, M. Bittner, M. González, J. Becerra, and M. Silva. Fatty acid composition of three species of *Codium* (Bryopsidales, Chlorophyta) in Chile. *Revista de Biología Marina y Oceanografía*, 45(2):325–330, 2010.
- [47] R. Hoffman, E. Shemesh, M. Ramot, Z. Dubinsky, Y. Pinchasov-Grinblat, and D. Iluz. First record of the Indo-Pacific seaweed *Codium arabicum* Kutz. (Bryopsidales, Chlorophyta) in the Mediterranean sea. *Botanica Marina*, 54(5):487–495, 2011.
- [48] A. V. González, M. E. Chacana, and P. C. Silva. *Codium bernabei* sp. nov. (Bryopsidales, Chlorophyta), a coalescing green seaweed from the coast of Chile. *Phycologia*, 51(6):666–671, 2012.
- [49] J. Ramus. Differentiation of green alga *Codium fragile*. *American Journal of Botany*, 59(5):478–482, 1972.
- [50] M. H. Yang, G. Blunden, F. L. Huang, and R. L. Fletcher. Growth of a dissociated, filamentous stage of *Codium* species in laboratory culture. *Journal of Applied Phycology*, 9(1):1–3, 1997.
- [51] E. Hwang, J. Baek, and C. Park. Cultivation of the green alga, *Codium fragile* (Suringar) Hariot, by artificial seed production in Korea. *Journal of Applied Phycology*, 20(5):469–475, 2008.
- [52] N. Nanba, R. Kado, H. Ogawa, and Y. Komuro. Formation and growth of filamentous thalli from isolated utricles with medullary filaments of *Codium fragile* spongy thalli. *Aquatic Botany*, 73(3):255–264, 2002.
- [53] N. Nanba, R. Kado, H. Ogawa, T. Nakagawa, and Y. Sugiura. Effects of irradiance and water flow on formation and growth of spongy and filamentous thalli of *Codium fragile*. *Aquatic Botany*, 81(4):315–325, 2005.

- [54] R. L. Fletcher, G. Blunden, B. E. Smith, D. J. Rogers, and B. C. Fish. Occurrence of a fouling, juvenile, stage of *Codium fragile* ssp. *tomentosoides* (Goor) Silva (Chlorophyceae, Codiales). *Journal of Applied Phycology*, 1(3):227–237, 1989.
- [55] D. M. Li, F. Lu, G. C. Wang, and B. C. Zhou. Assembly of the protoplasm of *Codium fragile* (Bryopsidales, Chlorophyta) into new protoplasts. *Journal of Integrative Plant Biology*, 50(6):752–760, 2008.
- [56] M. A. Welling. The role of sulfated metabolites in the wound response of siphonous green algae. *PhD Thesis*, 2010. École Polytechnique Fédérale de Lausanne.
- [57] C. Thoms and P. J. Schupp. Activated chemical defense in marine sponges—a case study on *Aplysinella rhax*. *Journal of Chemical Ecology*, 34(9):1242–1252, 2008.
- [58] V. Gewin. Functional genomics thickens the biological plot. *PLOS Biology*, 3(6):949–953, 2005.
- [59] K. Yasumoto, A. Nishigami, F. Kasai, T. Kusumi, and T. Ooi. Isolation and absolute configuration determination of aliphatic sulfates as the *Daphnia* kairomones inducing morphological defense of a phytoplankton. *Chemical and Pharmaceutical Bulletin*, 54(2):271–274, 2006.
- [60] A. K. Siddhanta and M. Shanmugam. Metabolites of tropical marine algae of the family Codiaceae (Chlorophyta): chemistry and bioactivity. *Journal of the Indian Chemical Society*, 76(7):323–334, 1999.
- [61] M. I. Bilan, E. V. Vinogradova, A. S. Shashkov, and A. I. Usouy. Structure of a highly pyruvylated galactan sulfate from the Pacific green alga *Codium yezoense* (Bryopsidales, Chlorophyta). *Carbohydrate Research*, 342(3-4):586–596, 2007.

- [62] J. M. Estevez, P. V. Fernández, L. Kasulin, P. Dupree, and M. Ciancia. Chemical and *in situ* characterization of macromolecular components of the cell walls from the green seaweed *Codium fragile*. *Glycobiology*, 19(3):212–228, 2009.
- [63] P. V. Fernández, M. Ciancia, A. B. Miravalles, and J. M. Estevez. Cell-wall polymer mapping in the coenocytic macroalga *Codium vermilara* (Bryopsidales, Chlorophyta). *Journal of Phycology*, 46(3):456–465, 2010.
- [64] M. Tabarsa, S. Karnjanapratum, M. Cho, J. K. Kim, and S. You. Molecular characteristics and biological activities of anionic macromolecules from *Codium fragile*. *International Journal of Biological Macromolecules*, 59:1–12, 2013.
- [65] G. Jiao, G. Yu, J. Zhang, and H.S. Ewart. Chemical structures and bioactivities of sulfated polysaccharides from marine algae. *Marine Drugs*, 9(2):196–223, 2011.
- [66] J. B. Lee, K. Hayashi, M. Maeda, and T. Hayashi. Antiherpetic activities of sulfated polysaccharides from green algae. *Planta Medica*, 70(9):813–817, 2004.
- [67] Y. Ohta, J. B. Lee, K. Hayashi, and T. Hayashi. Isolation of sulfated galactan from *Codium fragile* and its antiviral effect. *Biological and Pharmaceutical Bulletin*, 32(5):892–898, 2009.
- [68] J. B. Lee, Y. Ohta, K. Hayashi, and T. Hayashi. Immunostimulating effects of a sulfated galactan from *Codium fragile*. *Carbohydrate Research*, 345(10):1452–1454, 2010.
- [69] A. R. Soares, M. C. S. Robaina, G. S. Mendes, T. S. L. Silva, L. M. S. Gestinari, O. S. Pamplona, Y. Yoneshigue-Valentin, C. R. Kaiser, and M. T. V. Romanos. Antiviral activity of extracts from Brazilian seaweeds against herpes simplex virus. *Revista Brasileira de Farmacognosia-Brazilian Journal of Pharmacognosy*, 22(4):714–723, 2012.

- [70] A. K. Siddhanta, M. Shanmugam, K. H. Mody, A. M. Goswami, and B. K. Ramavat. Sulphated polysaccharides of *Codium dwarkense* Boergs. from the west coast of India: chemical composition and blood anticoagulant activity. *International Journal of Biological Macromolecules*, 26(2-3):151–154, 1999.
- [71] P. V. Fernández, I. Quintana, A. S. Cerezo, J. J. Caramelo, L. Pol-Fachin, H. Verli, J. M. Estevez, and M. Ciancia. Anticoagulant activity of a unique sulfated pyranosic (1 → 3)-beta-l-arabinan through direct interaction with thrombin. *Journal of Biological Chemistry*, 288(1):223–233, 2013.
- [72] J. S. Todd, R. C. Zimmerman, P. Crews, and R. S. Alberte. The antifouling activity of natural and synthetic phenolic acid sulfate esters. *Phytochemistry*, 34(2):401–404, 1993.
- [73] M. S. Stanley, M. E. Callow, R. Perry, R. S. Alberte, R. Smith, and J. A. Callow. Inhibition of fungal spore adhesion by zosteric acid as the basis for a novel, nontoxic crop protection technology. *Phytopathology*, 92(4):378–383, 2002.
- [74] C. A. Barrios, Q. W. Xu, T. Cutright, and B. M. Z. Newby. Incorporating zosteric acid into silicone coatings to achieve its slow release while reducing fresh water bacterial attachment. *Colloids and Surfaces B-Biointerfaces*, 41(2-3):83–93, 2005.
- [75] Q. W. Xu, C. A. Barrios, T. Cutright, and B. M. Z. Newby. Assessment of antifouling effectiveness of two natural product antifoulants by attachment study with freshwater bacteria. *Environmental Science and Pollution Research*, 12(5):278–284, 2005.
- [76] B. M. Z. Newby, T. Cutright, C. A. Barrios, and Q. W. Xu. Zosteric acid - an effective antifoulant for reducing fresh water bacterial attachment on coatings. *JCT Research*, 3(1):69–76, 2006.

- [77] M. Boopalan and A. Sasikumar. Studies on biocide free and biocide loaded zeolite hybrid polymer coatings on zinc phosphated mild steel for the protection of ships hulls from biofouling and corrosion. *Silicon*, 3(4):207–214, 2011.
- [78] F. Villa, D. Albanese, B. Giussani, P. S. Stewart, D. Daffonchio, and F. Cappitelli. Hindering biofilm formation with zoosteric acid. *Biofouling*, 26(6):739–752, 2010.
- [79] F. Villa, B. Pitts, P. S. Stewart, B. Giussani, S. Roncoroni, D. Albanese, C. Giordano, M. Tunesi, and F. Cappitelli. Efficacy of zoosteric acid sodium salt on the yeast biofilm model *Candida albicans*. *Microbial Ecology*, 62(3):584–598, 2011.
- [80] C. R. Rees, J. M. Costin, R. C. Fink, M. McMichael, K. A. Fontaine, S. Isern, and S. F. Michael. *In vitro* inhibition of Dengue virus entry by p-sulfoxy-cinnamic acid and structurally related combinatorial chemistries. *Antiviral Research*, 80(2):135–142, 2008.
- [81] Q. W. Xu, C. A. Barrios, T. Cutright, and B. M. Z. Newby. Evaluation of toxicity of capsaicin and zoosteric acid and their potential application as antifoulants. *Environmental Toxicology*, 20(5):467–474, 2005.
- [82] J. W. Costerton, Z. Lewandowski, D. E. Caldwell, D. R. Korber, and H. M. Lappin-Scott. Microbial biofilms. *Annual Review of Microbiology*, 49:711–745, 1995.
- [83] D. Lindsay and A. von Holy. Bacterial biofilms within the clinical setting: what healthcare professionals should know. *Journal of Hospital Infection*, 64(4):313–325, 2006.
- [84] P. Stoodley, K. Sauer, D. G. Davies, and J. W. Costerton. Biofilms as complex differentiated communities. *Annual Review of Microbiology*, 56:187–209, 2002.
- [85] G. O’Toole, H. B. Kaplan, and R. Kolter. Biofilm formation as microbial development. *Annual Review of Microbiology*, 54:49–79, 2000.

-
- [86] K. P. Lemon, A. M. Earl, H. C. Vlamakis, C. Aguilar, and R. Kolter. Biofilm development with an emphasis on *Bacillus subtilis*. *Bacterial Biofilms*, 322: 1–16, 2008.
- [87] C. M. Waters and B. L. Bassler. *Quorum sensing: Cell-to-cell communication in bacteria*, volume 21, pages 319–346. 2005.
- [88] T. K. Gallaher, S. H. Wu, P. Webster, and R. Aguilera. Identification of biofilm proteins in non-typeable *Haemophilus influenzae*. *BMC Microbiology*, 6, 2006.
- [89] P. Y. Qian, S. C. K. Lau, H. U. Dahms, S. Dobretsov, and T. Harder. Marine biofilms as mediators of colonization by marine macroorganisms: Implications for antifouling and aquaculture. *Marine Biotechnology*, 9(4):399–410, 2007.
- [90] D. M. Yebra, S. Kiil, and K. Dam-Johansen. Antifouling technology - past, present and future steps towards efficient and environmentally friendly antifouling coatings. *Progress in Organic Coatings*, 50(2):75–104, 2004.
- [91] H. C. Flemming. Biofouling in water systems - cases, causes and countermeasures. *Applied Microbiology and Biotechnology*, 59(6):629–640, 2002.
- [92] M. E. Callow and J. E. Callow. Marine biofouling: a sticky problem. *Biologist*, 49(1):10–4, 2002.
- [93] A. Rosenhahn, S. Schilp, H. J. Kreuzer, and M. Grunze. The role of "inert" surface chemistry in marine biofouling prevention. *Physical Chemistry Chemical Physics*, 12(17):4275–4286, 2010.
- [94] E. Almeida, T. C. Diamantino, and O. de Sousa. Marine paints: The particular case of antifouling paints. *Progress in Organic Coatings*, 59(1):2–20, 2007.
- [95] I. Banerjee, R. C. Pangule, and R. S. Kane. Antifouling coatings: Recent developments in the design of surfaces that prevent fouling by proteins, bacteria, and marine organisms. *Advanced Materials*, 23(6):690–718, 2011.

-
- [96] J. P. Marechal and C. Hellio. Challenges for the development of new non-toxic antifouling solutions. *International Journal of Molecular Sciences*, 10(11):4623–4637, 2009.
- [97] F. A. Guardiola, A. Cuesta, J. Meseguer, and M. A. Esteban. Risks of using antifouling biocides in aquaculture. *International Journal of Molecular Sciences*, 13(2):1541–1560, 2012.
- [98] K. A. Dafforn, J. A. Lewis, and E. L. Johnston. Antifouling strategies: History and regulation, ecological impacts and mitigation. *Marine Pollution Bulletin*, 62(3):453–465, 2011.
- [99] C. Alzieu. Impact of tributyltin on marine invertebrates. *Ecotoxicology*, 9(1-2):71–76, 2000.
- [100] IMO-MEPC 38. Terms of reference for a corresponding group on the reduction of harmful effects of the use of antifouling paints for ships. *IMO-MEPC Paper MEPC 38/WP*, 6, 1996.
- [101] I. Omae. General aspects of tin-free antifouling paints. *Chemical Reviews*, 103(9):3431–3448, 2003.
- [102] C. M. Grozea and G. C. Walker. Approaches in designing non-toxic polymer surfaces to deter marine biofouling. *Soft Matter*, 5(21):4088–4100, 2009.
- [103] C. M. Magin, S. P. Cooper, and A. B. Brennan. Non-toxic antifouling strategies. *Materials Today*, 13(4):36–44, 2010.
- [104] S. Cao, J. D. Wang, H. S. Chen, and D. R. Chen. Progress of marine biofouling and antifouling technologies. *Chinese Science Bulletin*, 56(7):598–612, 2011.
- [105] T. Murosaki, N. Ahmed, and J. P. Gong. Antifouling properties of hydrogels. *Science and Technology of Advanced Materials*, 12(6), 2011.

-
- [106] M. De Kwaadsteniet, M. Botes, and T. E. Cloete. Application of nanotechnology in antimicrobial coatings in the water industry. *Nano*, 6(5):395–407, 2011.
- [107] N. Fusetani. Biofouling and antifouling. *Natural Product Reports*, 21(1):94–104, 2004.
- [108] E. Ralston and G. Swain. Bioinspiration - the solution for biofouling control? *Bioinspiration and Biomimetics*, 4(1):015007, 2009.
- [109] M. Salta, J. A. Wharton, P. Stoodley, S. P. Dennington, L. R. Goodes, S. Werwinski, U. Mart, R. J. K. Wood, and K. R. Stokes. Designing biomimetic antifouling surfaces. *Philosophical Transactions of the Royal Society A-Mathematical Physical and Engineering Sciences*, 368(1929):4729–4754, 2010.
- [110] P.-Y. Qian, Y. Xu, and N. Fusetani. Natural products as antifouling compounds: recent progress and future perspectives. *Biofouling*, 26(2):223–234, 2010.
- [111] A. J. Scardino and R. de Nys. Mini review: Biomimetic models and bioinspired surfaces for fouling control. *Biofouling*, 27(1):73–86, 2011.
- [112] R. J. Cremllyn. *Chlorosulfonic acid: A versatile reagent*. The Royal Society of Chemistry, Cambridge, 1 edition, 2002.
- [113] G. N. Burkhardt and A. Lapworth. XCV. Arylsulphuric acids. *Journal of the Chemical Society*, 129:684–690, 1926.
- [114] J. Feigenbaum and C. A. Neuberg. Simplified method for the preparation of aromatic sulfuric acid esters. *Journal of the American Chemical Society*, 63(12):3529–3530, 1941.
- [115] A. Richter and D. Klemm. Regioselective sulfation of trimethylsilyl cellulose using different SO₃-complexes. *Cellulose*, 10(2):133–138, 2003.

- [116] D. Kusch. Sulphur trioxide-pyridine complex: A versatile organic reagent. *Speciality Chemicals Magazine*, 26(10):40–41, 2006.
- [117] Y. Liu, I. F. F. Lien, S. Ruttgaizer, P. Dove, and S. D. Taylor. Synthesis and protection of aryl sulfates using the 2,2,2-trichloroethyl moiety. *Organic Letters*, 6(2):209–212, 2004.
- [118] G. T. Gunnarsson, M. Riaz, J. Adams, and U. R. Desai. Synthesis of per-sulfated flavonoids using 2,2,2-trichloro ethyl protecting group and their factor Xa inhibition potential. *Bioorganic and Medicinal Chemistry*, 13(5):1783–1789, 2005.
- [119] L. S. Simpson and T. S. Widlanski. A comprehensive approach to the synthesis of sulfate esters. *Journal of the American Chemical Society*, 128(5):1605–1610, 2006.
- [120] A. Bunschoten, J. A. W. Kruijtzter, J. H. Ippel, C. J. C. de Haas, J. A. G. van Strijp, J. Kemmink, and R. M. J. Liskamp. A general sequence independent solid phase method for the site specific synthesis of multiple sulfated-tyrosine containing peptides. *Chemical Communications*, (21):2999–3001, 2009.
- [121] L. J. Ingram, A. Desoky, A. M. Ali, and S. D. Taylor. O- and N-sulfations of carbohydrates using sulfuryl imidazolium salts. *Journal of Organic Chemistry*, 74(17):6479–6485, 2009.
- [122] Y. Li, Q. Peng, D. Selimi, Q. Wang, A. O. Charkowski, X. Chen, and C.-H. Yang. The plant phenolic compound p-coumaric acid represses gene expression in the *Dickeya dadantii* type III secretion system. *Applied and Environmental Microbiology*, 75(5):1223–1228, 2009.
- [123] S. C. Miller. Profiling sulfonate ester stability: Identification of complementary protecting groups for sulfonates. *Journal of Organic Chemistry*, 75(13):4632–4635, 2010.

- [124] Q. Zhang, K. S. Raheem, N. P. Botting, A. M. Z. Slawin, C. D. Kay, and D. O'Hagan. Flavonoid metabolism: the synthesis of phenolic glucuronides and sulfates as candidate metabolites for bioactivity studies of dietary flavonoids. *Tetrahedron*, 68(22):4194–4201, 2012.
- [125] R.C. Zimmerman, R.S. Alberte, J.S. Todd, and P. Crews. Phenolic acid sulfate esters for prevention of marine biofouling. *US Patent 5607741*, 1997.
- [126] F. Villa, W. Remelli, F. Forlani, A. Vitali, and F. Cappitelli. Altered expression level of *Escherichia coli* proteins in response to treatment with the antifouling agent zosteric acid sodium salt. *Environmental Microbiology*, 14(7):1753–1761, 2012.
- [127] D. R. Edwards, D. C. Lohman, and R. Wolfenden. Catalytic proficiency: The extreme case of S-O cleaving sulfatases. *Journal of the American Chemical Society*, 134(1):525–531, 2012.
- [128] S. J. Benkovic. Studies on sulfate esters. 2. carboxyl group catalysis in hydrolysis of salicyl sulfate. *Journal of the American Chemical Society*, 88(23):5511–5515, 1966.
- [129] A. F. Hollemann and N. Wiberg. *Lehrbuch der Anorganischen Chemie*. W. de Gruyter, Berlin - New York, 101 edition, 1995.
- [130] J. F. E. Dupin and J. Chenault. Phase-transfer catalyzed Wittig-Horner synthesis preparation of hydroxycinnamic esters from *ortho*-hydroxy aromatic-aldehydes obtention of hydroxycinnamic acids. *Synthetic Communications*, 15(7):581–586, 1985.
- [131] R. Adams and J. Mathieu. A new synthesis of atranol (2,6-dihydroxy-4-methylbenzaldehyde) and the corresponding cinnamic acid. *Journal of the American Chemical Society*, 70(6):2120–2122, 1948.
- [132] M. Miyazaki and J. Fishman. Acid catalyzed hydrolysis of estrogen aryl sulfates. Effects of hydroxyl substitution. *Steroids*, 12(4):465–474, 1968.

- [133] E. J. Fendler and J. H. Fendler. Hydrolysis of nitrophenyl and dinitrophenyl sulfate esters. *Journal of Organic Chemistry*, 33(10):3852–3859, 1968.
- [134] G. N. Burkhardt, W. G. K. Ford, and E. Singleton. 4. The hydrolysis of arylsulphuric acids. part I. *Journal of the Chemical Society*, pages 17–25, 1936.
- [135] K. S. Dodgson, B. Spencer, and K. Williams. Studies on sulphatases: 13. Hydrolysis of substituted phenyl sulphates by the arylsulphatase of *Alcaligenes metalcaligenes*. *Biochemical Journal*, 64(2):216–221, 1956.
- [136] S. R. Hanson, M. D. Best, and C. H. Wong. Sulfatases: Structure, mechanism, biological activity, inhibition, and synthetic utility. *Angewandte Chemie-International Edition*, 43(43):5736–5763, 2004.
- [137] H. Freiser and Q. Jiang. Optimization of the enzymatic hydrolysis and analysis of plasma conjugated gamma-CEHC and sulfated long-chain carboxychromanols, metabolites of vitamin E. *Analytical Biochemistry*, 388(2):260–265, 2009.
- [138] D. Ryan, M. Antolovich, P. Prenzler, K. Robards, and S. Lavee. Biotransformations of phenolic compounds in *Olea europaea* L. *Scientia Horticulturae*, 92(2):147–176, 2002.
- [139] Ch. Vidoudez. Diatom metabolomics. *PhD Thesis*, 2010. Friedrich-Schiller-Universität Jena, Germany.
- [140] C. Proestos, I. S. Boziaris, G. J. E. Nychas, and M. Komaitis. Analysis of flavonoids and phenolic acids in greek aromatic plants: Investigation of their antioxidant capacity and antimicrobial activity. *Food Chemistry*, 95(4):664–671, 2006.
- [141] M. J. Alves, I. C. Ferreira, H. J. Froufe, R. M. Abreu, A. Martins, and M. Pintado. Antimicrobial activity of phenolic compounds identified in wild mush-

- rooms, SAR analysis and docking studies. *Journal of Applied Microbiology*, 115(2):346–357, 2013.
- [142] D. Sircar, C. Mukherjee, T. Beuerle, L. Beerhues, and A. Mitra. Characterization of p-hydroxybenzaldehyde dehydrogenase, the final enzyme of p-hydroxybenzoic acid biosynthesis in hairy roots of *Daucus carota*. *Acta Physiologiae Plantarum*, 33(5):2019–2024, 2011.
- [143] L. Onofrejeva, J. Vasickova, B. Klejdus, P. Stratil, L. Misurcova, S. Kracmar, J. Kopecky, and J. Vacek. Bioactive phenols in algae: The application of pressurized-liquid and solid-phase extraction techniques. *Journal of Pharmaceutical and Biomedical Analysis*, 51(2):464–470, 2010.
- [144] O. Zapata and C. McMillan. Phenolic-acids in seagrasses. *Aquatic Botany*, 7(4):307–317, 1979.
- [145] R. C. Quackenbush, D. Bunn, and W. Lingren. HPLC determination of phenolic-acids in the water-soluble extract of *Zostera marina* L. (eelgrass). *Aquatic Botany*, 24(1):83–89, 1986.
- [146] H. Haque, T. J. Cutright, and B. M. Z. Newby. Effectiveness of sodium benzoate as a freshwater low toxicity antifoulant when dispersed in solution and entrapped in silicone coatings. *Biofouling*, 21(2):109–119, 2005.
- [147] A. A. Al-Juhni and B. Zh. Newby. Incorporation of benzoic acid and sodium benzoate into silicone coatings and subsequent leaching of the compound from the incorporated coatings. *Progress in Organic Coatings*, 56(2-3):135–145, 2006.
- [148] J. H. Merritt, D. E. Kadouri, and G. A. O’Toole. Growing and analyzing static biofilms. *Current protocols in microbiology*, Chapter 1:Unit 1B.1, 2005.
- [149] G. A. O’Toole, L. A. Pratt, P. I. Watnick, D. K. Newman, V. B. Weaver, and R. Kolter. Genetic approaches to study of biofilms. *Biofilms*, 310:91–109, 1999.

-
- [150] P. J. O'Brien and D. Herschlag. Sulfatase activity of *E. coli* alkaline phosphatase demonstrates a functional link to arylsulfatases, an evolutionarily related enzyme family. *Journal of the American Chemical Society*, 120(47):12369–12370, 1998.
- [151] R. Kolter, D. A. Siegele, and A. Tormo. The stationary phase of the bacterial life cycle. *Annual Review of Microbiology*, 47:855–874, 1993.
- [152] H. M. Dalton, A. E. Goodman, and K. C. Marshall. Diversity in surface colonization behavior in marine bacteria. *Journal of Industrial Microbiology*, 17(3-4):228–234, 1996.
- [153] P. I. Watnick, C. M. Lauriano, K. E. Klose, L. Croal, and R. Kolter. The absence of a flagellum leads to altered colony morphology, biofilm development and virulence in *Vibrio cholerae* O139. *Molecular Microbiology*, 39(2):223–235, 2001.
- [154] L. A. Pratt and R. Kolter. Genetic analysis of *Escherichia coli* biofilm formation: roles of flagella, motility, chemotaxis and type I pili. *Molecular Microbiology*, 30(2):285–293, 1998.
- [155] T. K. Wood, A. F. G. Barrios, M. Herzberg, and J. Lee. Motility influences biofilm architecture in *Escherichia coli*. *Applied Microbiology and Biotechnology*, 72(2):361–367, 2006.
- [156] T. Geiger, P. Delavy, R. Hany, J. Schleuniger, and M. Zinn. Encapsulated Zosteric acid embedded in poly 3-hydroxyalkanoate coatings - protection against biofouling. *Polymer Bulletin*, 52(1):65–72, 2004.
- [157] Y. Xing and P. J. White. Identification and function of antioxidants from oat groats and hulls. *Journal of the American Oil Chemists' Society*, 74(3):303–307, 1997.
- [158] L. E. Bartley, M. L. Peck, S.-R. Kim, B. Ebert, Ch. Manisseri, D. M. Chiniquy, R. Sykes, L. Gao, C. Rautengarten, M. E. Vega-Sánchez, P. I. Benke, P. E.

- Canlas, P. Cao, S. Brewer, F. Lin, Wh. L. Smith, X. Zhang, J. D. Keasling, R. E. Jentoff, S. B. Foster, J. Zhou, A. Ziebell, G. An, H. V. Scheller, and P. C. Ronald. Overexpression of a BAHD acyltransferase, OsAt10, alters rice cell wall hydroxycinnamic acid content and saccharification. *Plant Physiology*, 161(4):1615–1633, 2013.
- [159] G. X. Pan, J. L. Bolton, and G. J. Leary. Determination of ferulic and p-coumaric acids in wheat straw and the amounts released by mild acid and alkaline peroxide treatment. *Journal of Agricultural and Food Chemistry*, 46(12):5283–5288, 1998.
- [160] A. Tanveer, M. K. Jabbar, A. Kahliq, A. Matloob, R. N. Abbas, and M. M. Javaid. Allelopathic effects of aqueous and organic fractions of *Euphorbia dracunculoides* Lam. On germination and seedling growth of chickpea and wheat. *Chilean Journal of Agricultural Research*, 72(4):495–501, 2012.
- [161] Kh. Latreche and F. Rahmania. High extracellular accumulation of p-hydroxybenzoic acid, p-hydroxycinnamic acid and p-hydroxybenzaldehyde in leaves of *Phoenix dactylifera* L. affected by the brittle leaf disease. *Physiological and Molecular Plant Pathology*, 76(2):144–151, 2011.
- [162] G. W. Plumb, S. J. Chambers, N. Lambert, B. Bartolomé, R. K. Heaney, S. U. Wanigatunga, O. I. Aruoma, B. Halliwell, and G. Williamson. Antioxidant actions of fruit, herb and spice extracts. *Journal of Food Lipids*, 3(3):171–188, 1996.
- [163] M. N. Clifford. Chlorogenic acids and other cinnamates – nature, occurrence and dietary burden. *Journal of the Science of Food and Agriculture*, 79(3):362–372, 1999.
- [164] M. R. Seyedsayamdost, R. J. Case, R. Kolter, and J. Clardy. The Jekyll-and-Hyde chemistry of *Phaeobacter gallaeciensis*. *Nature Chemistry*, 3(4):331–335, 2011.

- [165] J. L. Torres y Torres and J. P. N. Rosazza. Reactions of p-coumaric acid with nitrite: Product isolation and mechanism studies. *Journal of Agricultural and Food Chemistry*, 49(3):1486–1492, 2001.
- [166] K. Aaby, E. Hvattum, and G. Skrede. Analysis of flavonoids and other phenolic compounds using high-performance liquid chromatography with coulometric array detection: Relationship to antioxidant activity. *Journal of Agricultural and Food Chemistry*, 52(15):4595–4603, 2004.
- [167] A. Lanoue, V. Burlat, G. J. Henkes, I. Koch, U. Schurr, and U. S. R. Röse. *De novo* biosynthesis of defense root exudates in response to *Fusarium* attack in barley. *New Phytologist*, 185(2):577–588, 2010.
- [168] J. E. Wells, E. D. Berry, and V. H. Varel. Effects of common forage phenolic acids on *Escherichia coli* O157:H7 viability in bovine feces. *Applied and Environmental Microbiology*, 71(12):7974–7979, 2005.
- [169] R. G. Eagon. *Pseudomonas natriegens*, a marine bacterium with a generation time of less than 10 minutes. *Journal of Bacteriology*, 83(4):736–737, 1962.
- [170] S. Cheng, K.-T. Lau, S. Chen, X. Chang, T. Liu, and Y. Yin. Microscopical observation of the marine bacterium *Vibrio natriegens* growth on metallic corrosion. *Materials and Manufacturing Processes*, 25(5):293–297, 2010.
- [171] W. Y. Shieh, U. Simidu, and Y. Maruyama. Enumeration and characterization of nitrogen-fixing bacteria in an eelgrass (*Zostera marina*) bed. *Microbial Ecology*, 18(3):249–259, 1989.
- [172] T. B. Karegoudar and C. K. Kim. Microbial degradation of monohydroxybenzoic acids. *Journal of Microbiology*, 38(2):53–61, 2000.
- [173] J. Hagmar, C. Brackmann, T. Gustavsson, and A. Enejder. Image analysis in nonlinear microscopy. *Journal of the Optical Society of America A-Optics Image Science and Vision*, 25(9):2195–2206, 2008. ISSN 9.

- [174] T. F. C. Mah and G. A. O'Toole. Mechanisms of biofilm resistance to antimicrobial agents. *Trends in Microbiology*, 9(1):34–39, 2001.
- [175] J. M. Ribo and K. L. E. Kaiser. Photobacterium phosphoreum toxicity bioassay. I. test procedures and applications. *Toxicity Assessment*, 2(3):305–323, 1987.
- [176] E. C. Kandemir, H. Alyuruk, and L. Cavas. Fouling organisms on the rebars and protection by antifouling paint. *Anti-Corrosion Methods and Materials*, 59(5):215–219, 2012.
- [177] D. M. Yebra, S. Kiil, K. Dam-Johansen, and C. Weinell. Reaction rate estimation of controlled-release antifouling paint binders: Rosin-based systems. *Progress in Organic Coatings*, 53(4):256–275, 2005.
- [178] J. S. Chapman. Biocide resistance mechanisms. *International Biodeterioration and Biodegradation*, 51(2):133–138, 2003.
- [179] N. N. López-Castillo, A. D. Rojas-Rodríguez, B. M. Porta, and M. J. Cruz-Gómez. Process for the obtention of coumaric acid from coumarin: Analysis of the reaction conditions. *Advances in Chemical Engineering and Science*, 3(3), 2013.
- [180] A. Wichels, C. Hummert, M. Elbrächter, B. Luckas, C. Schutt, and G. Gerdt. Bacterial diversity in toxic *Alexandrium tamarense* blooms off the Orkney Isles and the Firth of Forth. *Helgoland Marine Research*, 58(2):93–103, 2004.
- [181] Y. Q. Chao and T. Zhang. Optimization of fixation methods for observation of bacterial cell morphology and surface ultrastructures by atomic force microscopy. *Applied Microbiology and Biotechnology*, 92(2):381–392, 2011.
- [182] <http://homepages.inf.ed.ac.uk/rbf/HIPR2/adpthrsh.htm>, 06.05.2014.
- [183] N. Mert, G. Topcam, and L. Cavas. RP-HPLC optimization of econeal by using artificial neural networks and its antifouling performance on the Turkish coastline. *Progress in Organic Coatings*, 77(3):627–635, 2014.

Appendix

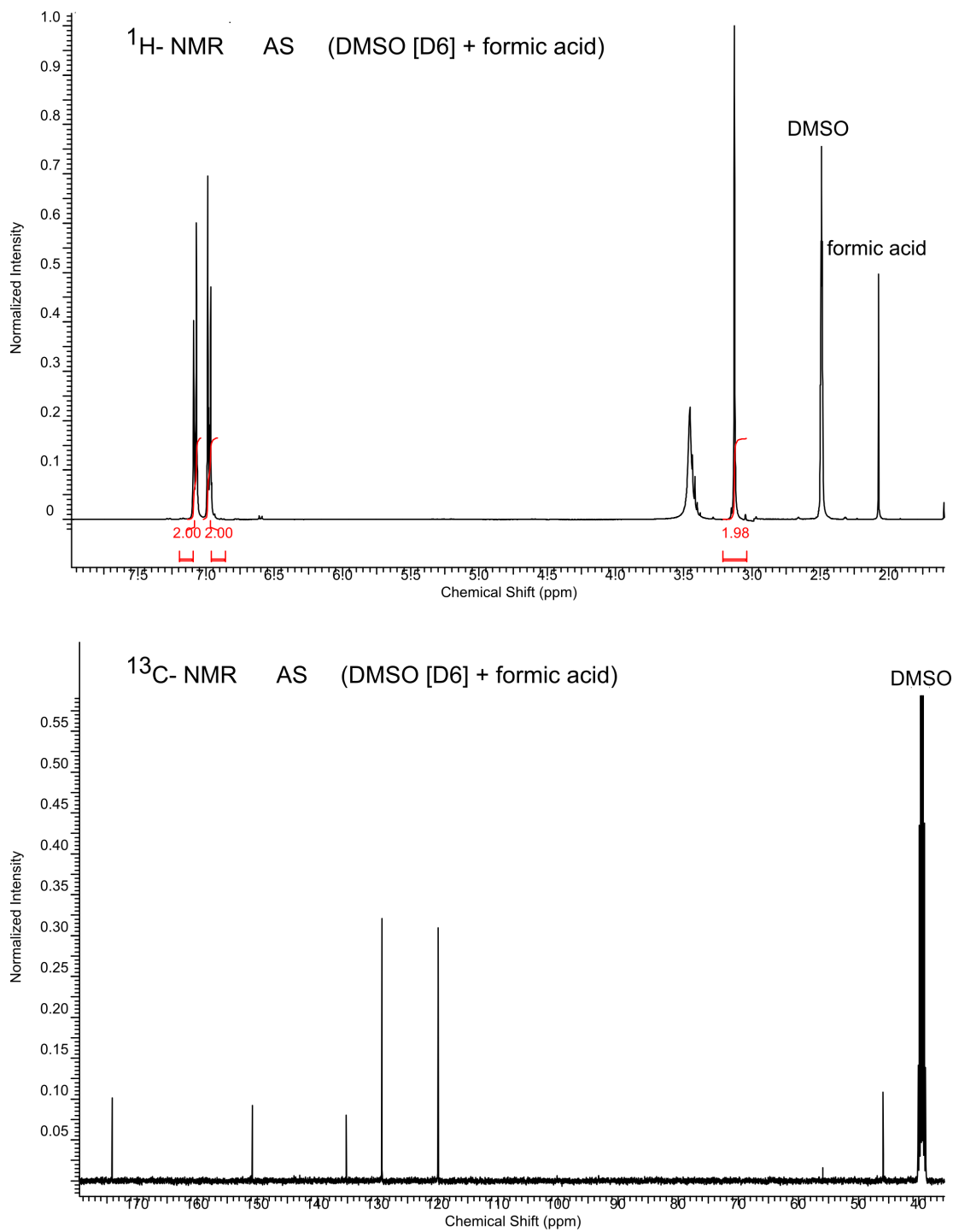


Figure 9.1: ^1H and ^{13}C NMR of synthetic AS.

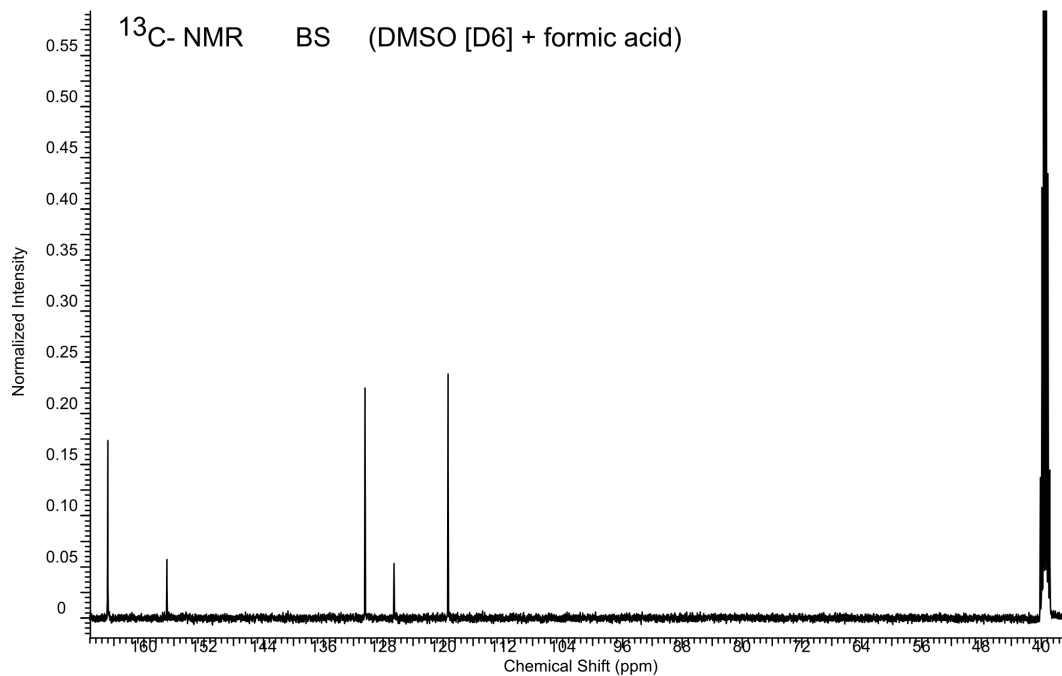
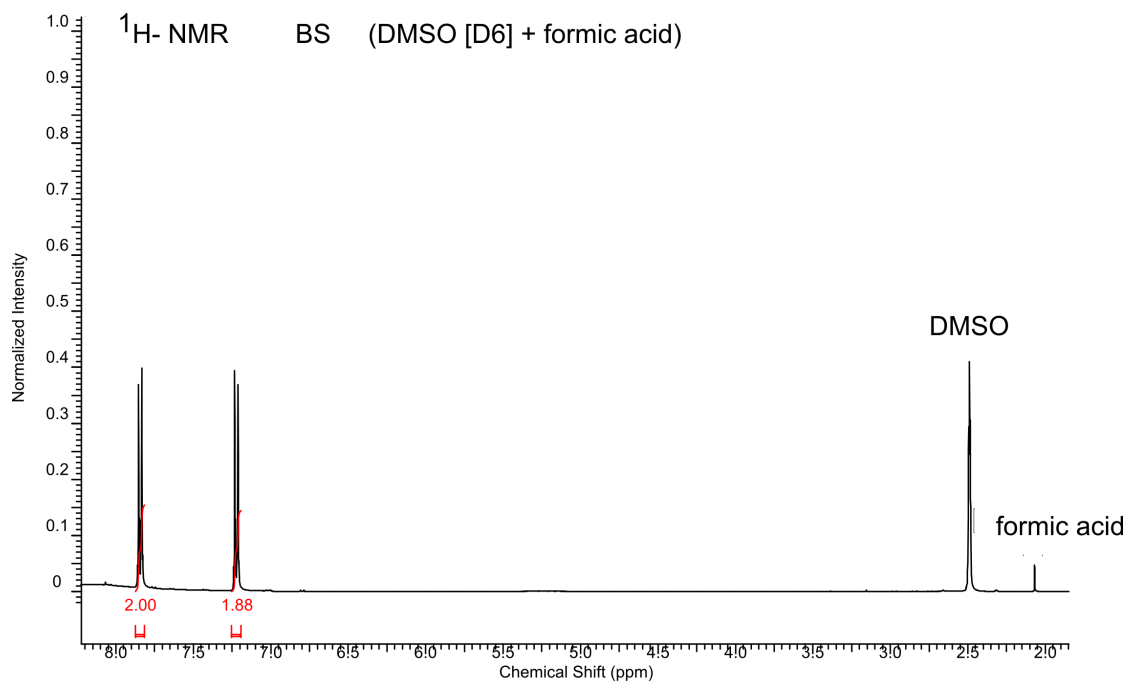


Figure 9.2: ^1H and ^{13}C NMR of synthetic BS.

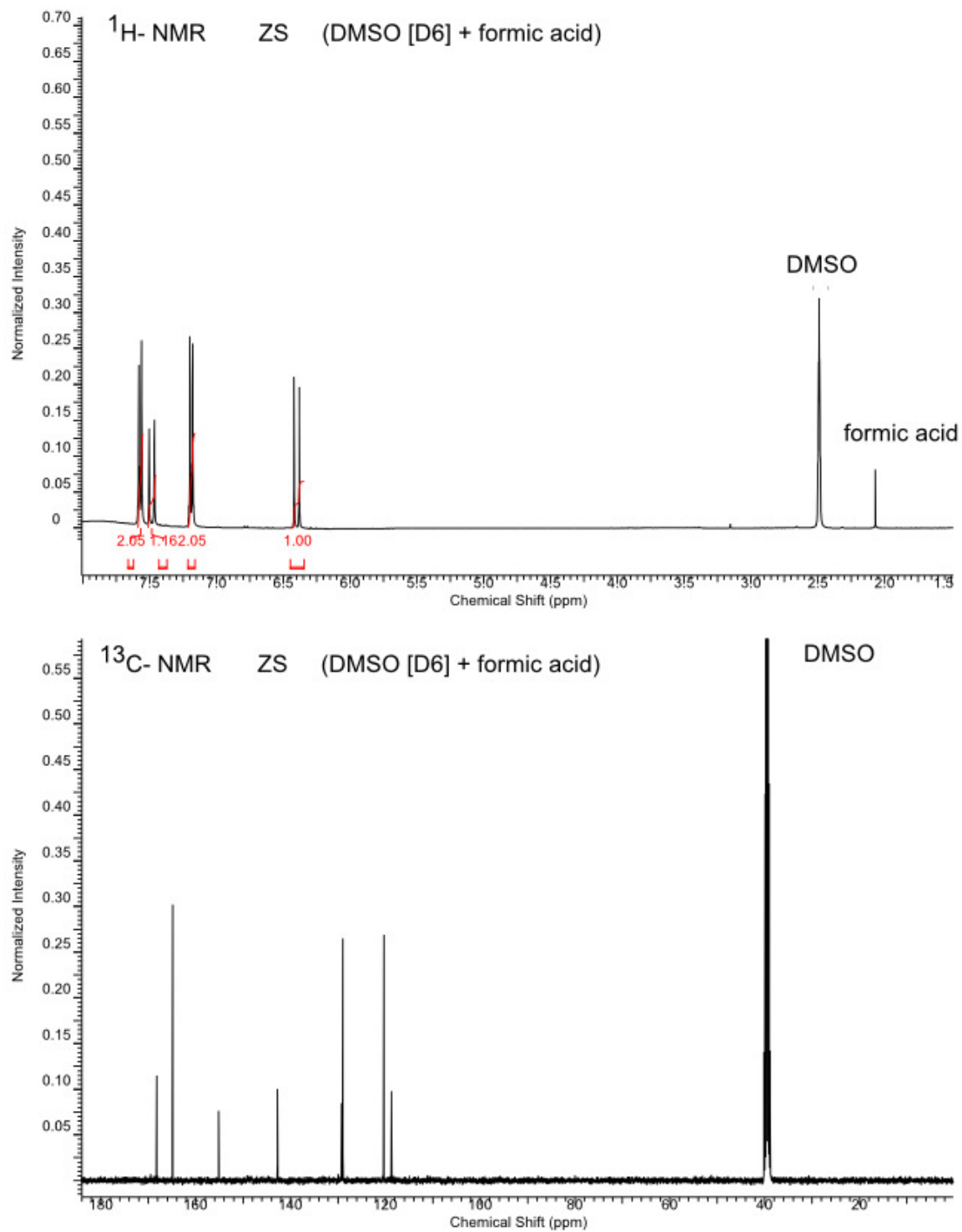


Figure 9.3: ^1H and ^{13}C NMR of synthetic ZS.

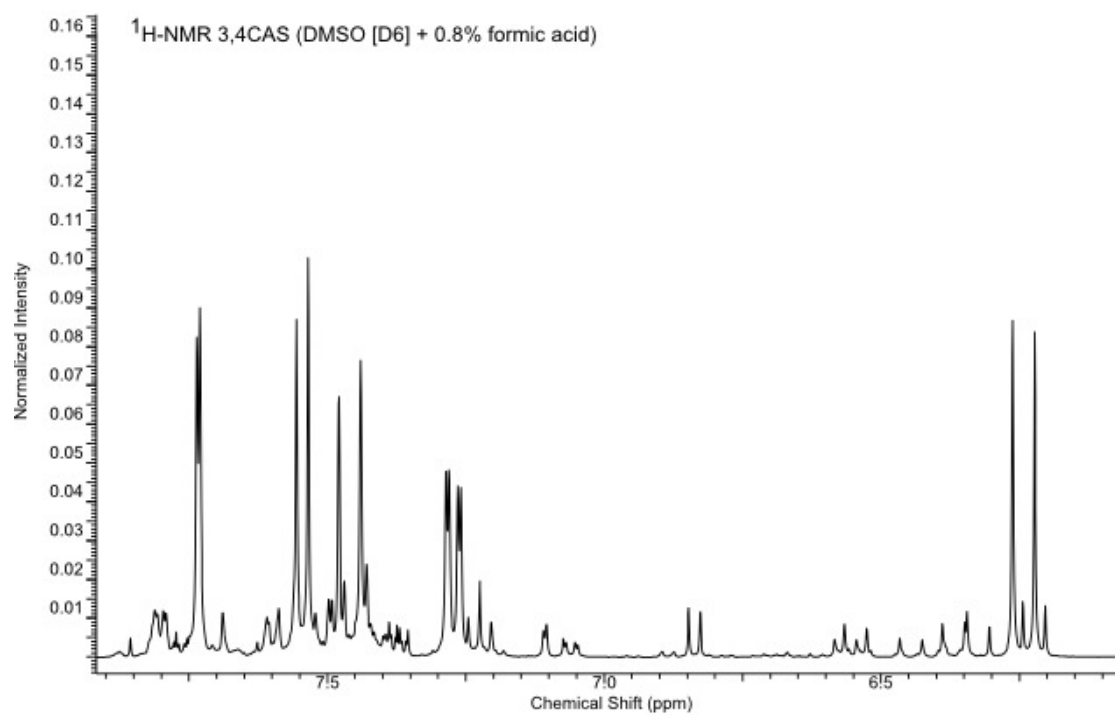


Figure 9.4: ¹H of the isomeric mixture 3,4CAS.

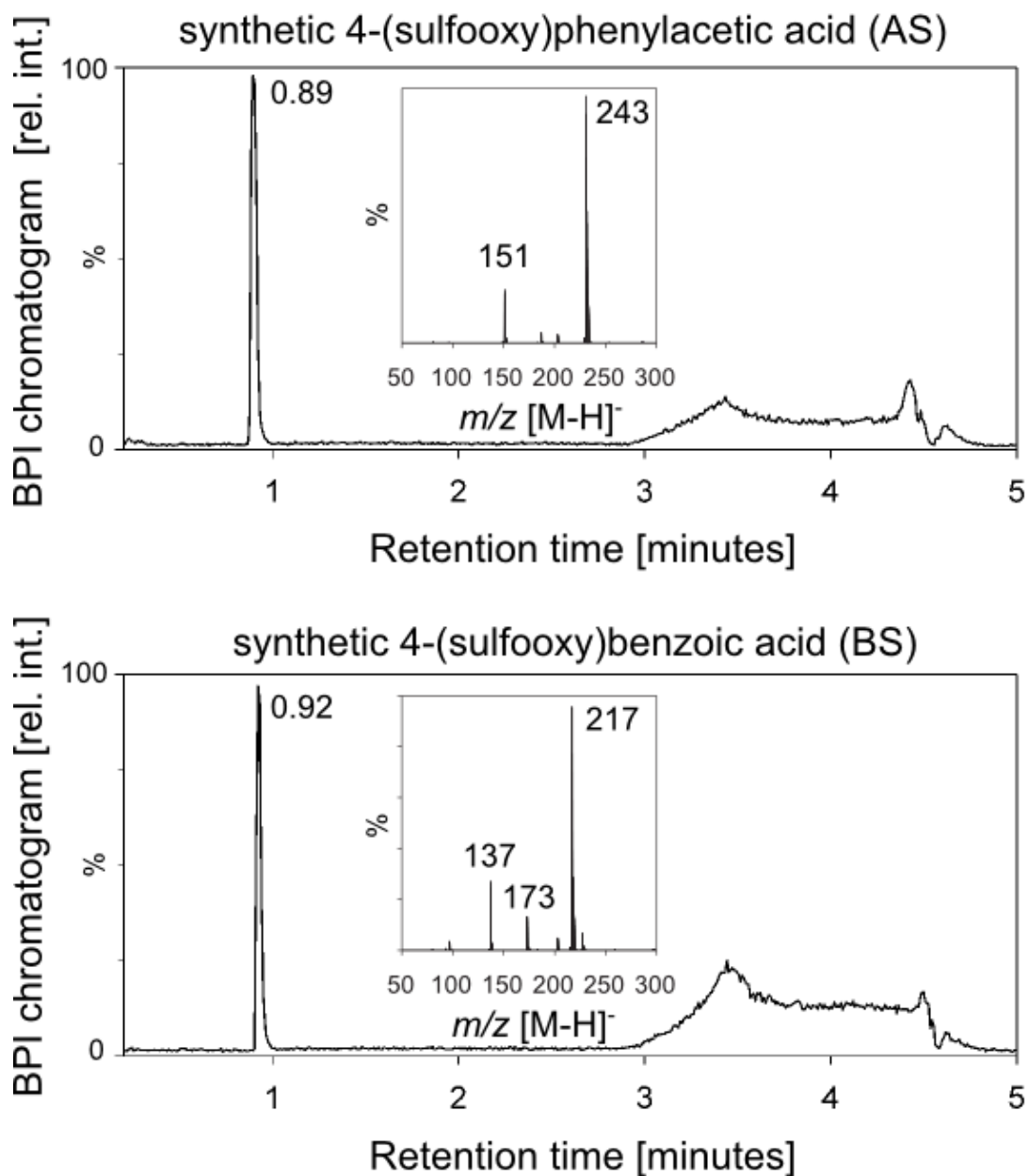


Figure 9.5: UPLC chromatograms and MS spectra of synthetic AS and BS.

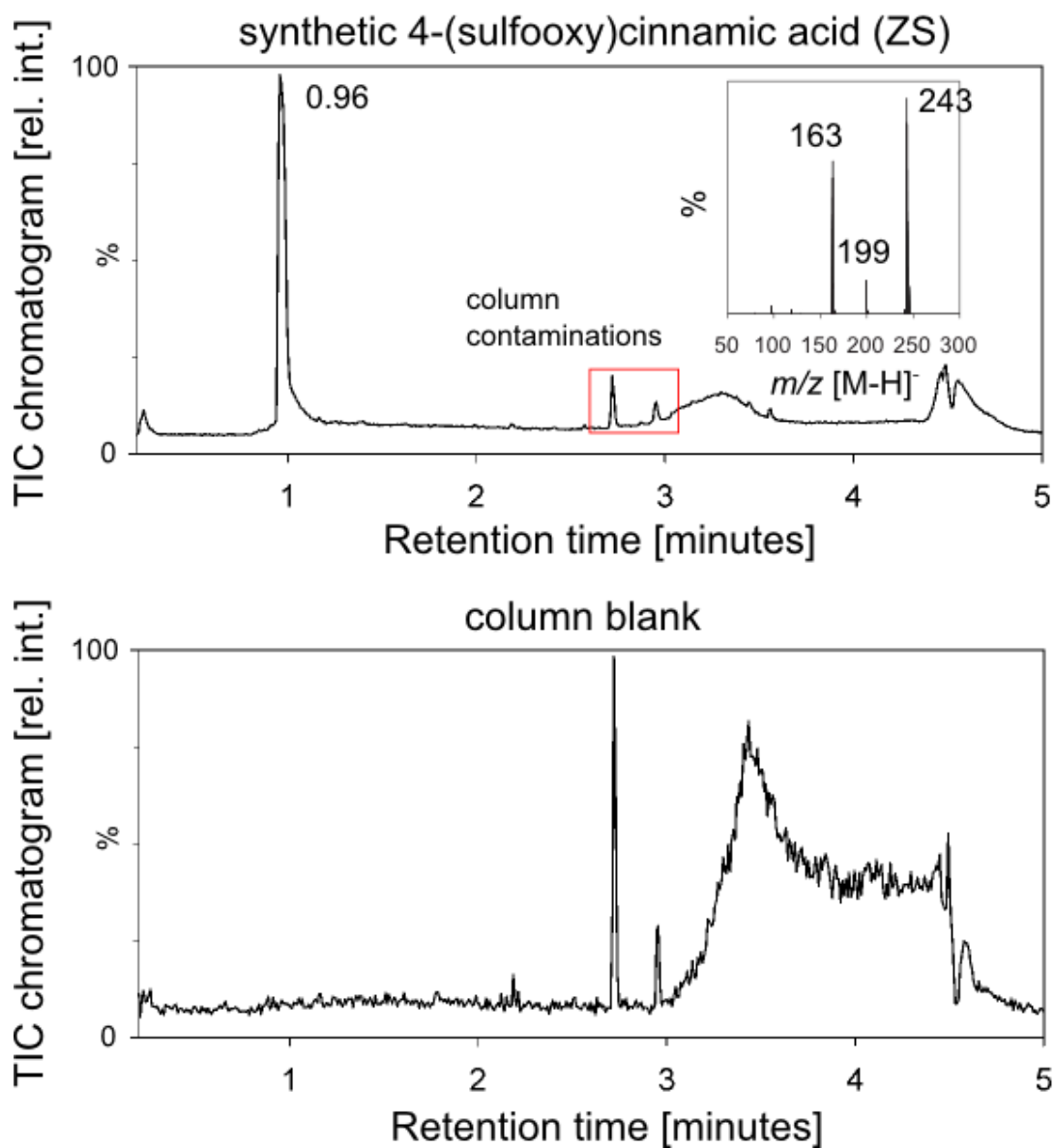


Figure 9.6: UPLC chromatogram and MS spectrum of synthetic ZS.

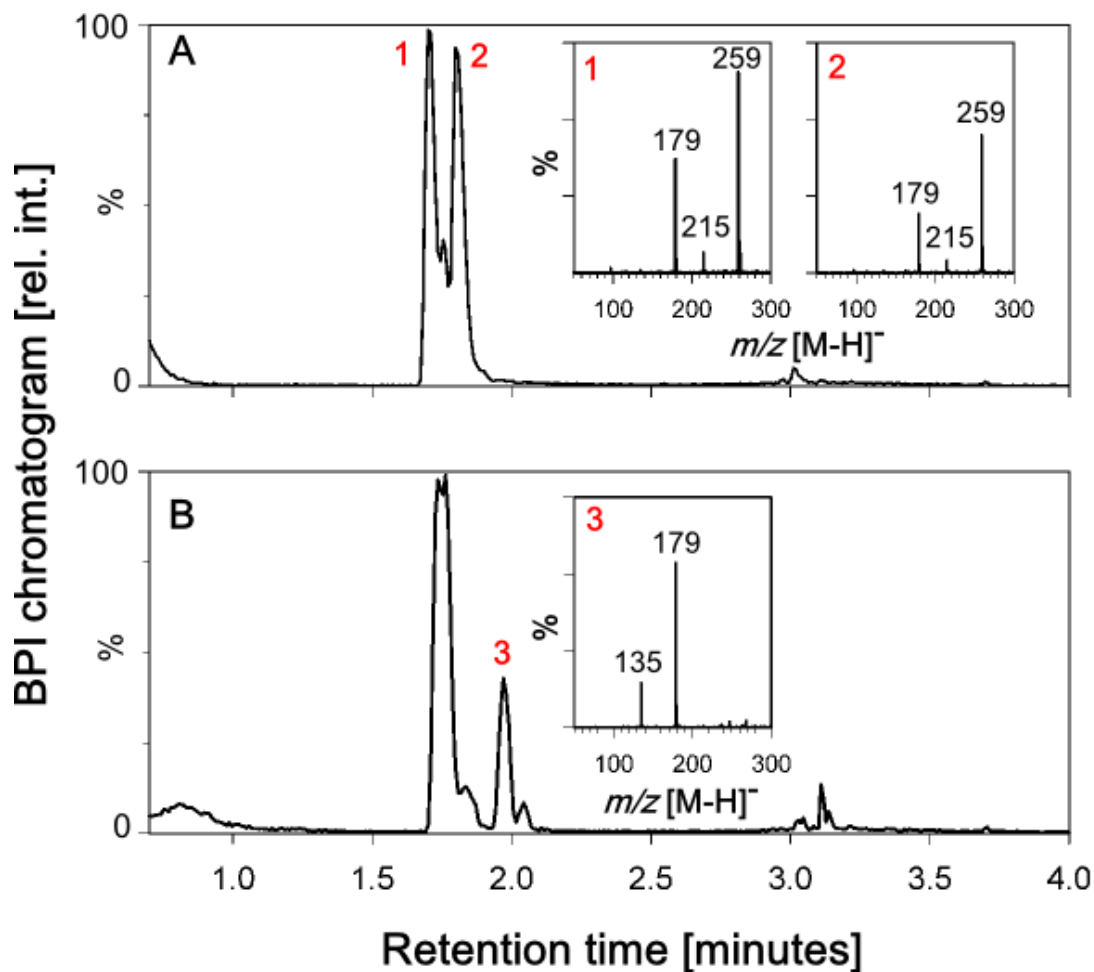


Figure 9.7: UPLC-MS monitoring of the enzymatic cleavage of 3,4CAS by an arylsulfatase. **A:** BPI chromatogram showing the two isomers of pure 3,4CAS at 1.70 (1) and 1.80 (2) minutes and the corresponding mass spectra before sulfatase treatment. **B:** BPI chromatogram showing the two isomers of pure 3,4CAS at 1.70 (1) and 1.80 (2) minutes, and its cleavage product 3,4CA at 1.97 minutes with the corresponding mass spectrum, after sulfatase treatment.

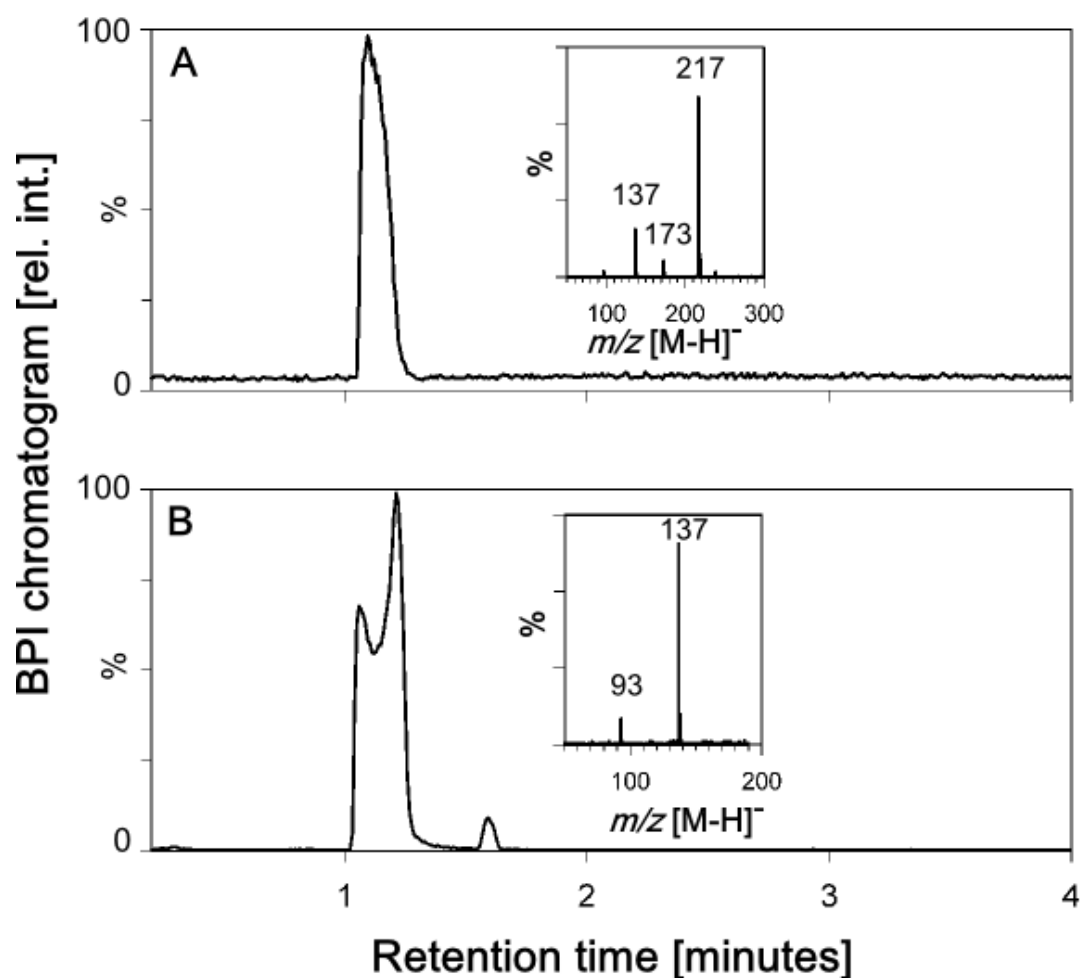


Figure 9.8: UPLC-MS monitoring of the enzymatic cleavage of BS by an arylsulfatase. **A:** BPI chromatogram showing pure BS at 1.10 minutes and the corresponding mass spectrum before sulfatase treatment. **B:** BPI chromatogram showing pure BS at 1.10 minutes, and its cleavage product B at 1.58 minutes with the corresponding mass spectrum, after sulfatase treatment. The unsymmetrical peak shape of BS results from a sample overload in order to be able to detect the low amount of B.

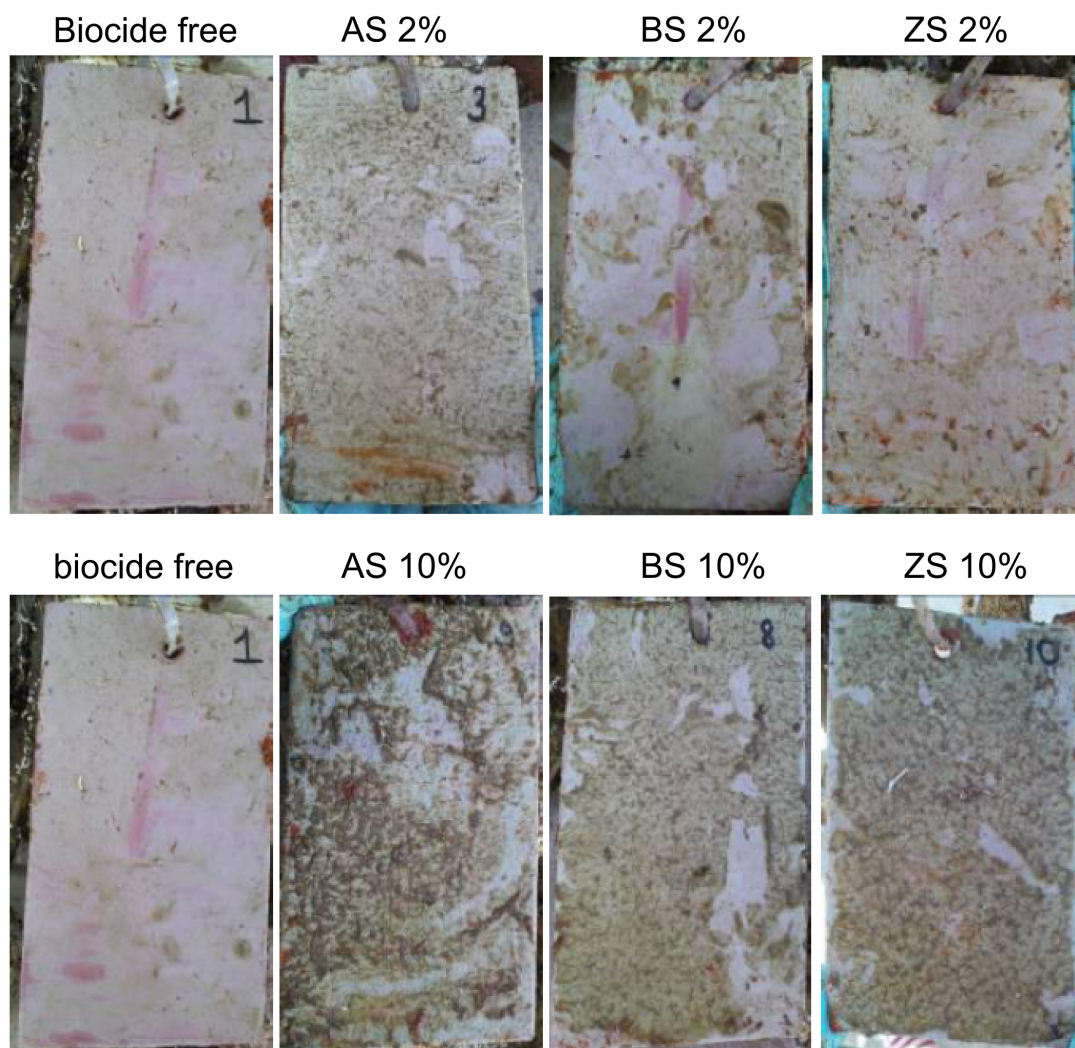


Figure 9.9: Field assay plates after two weeks with 2 and 10% biocide.

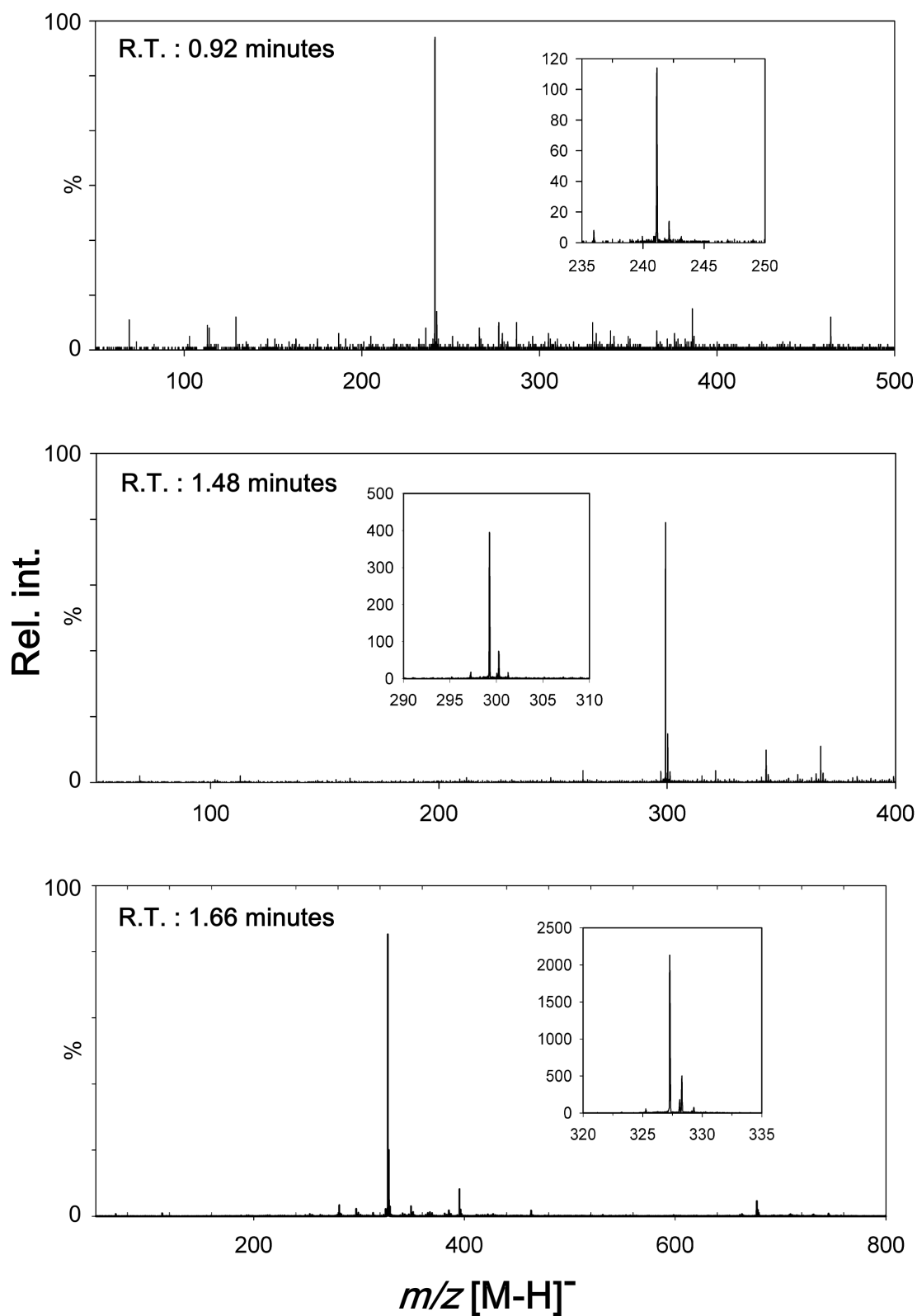


Figure 9.10: Mass spectra of methanolic *Codium fragile* extracts 60 minutes after wounding. Spectra originate from peaks marked by red stars in the chromatogram of Figure 7.2 C.

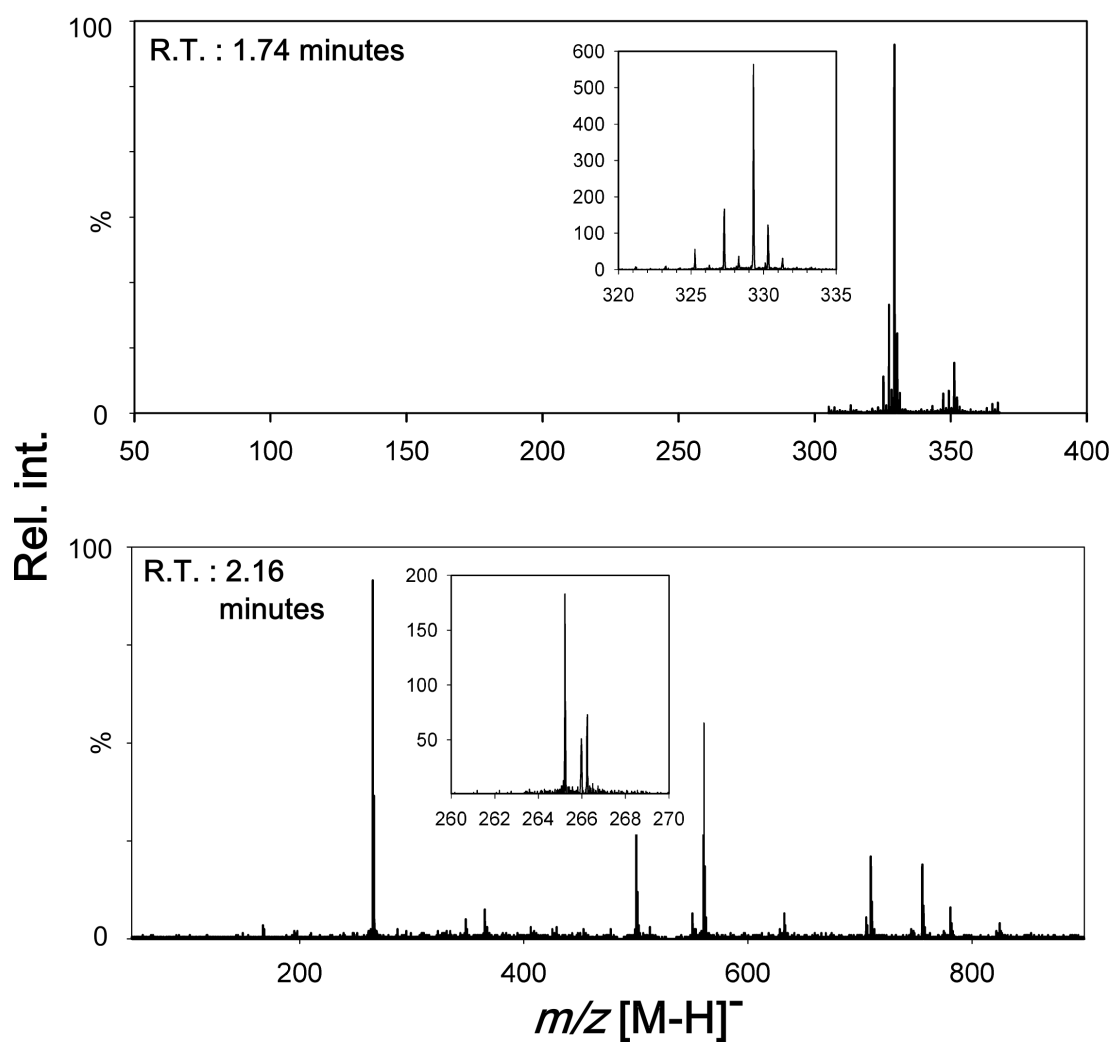


Figure 9.11: Mass spectra of methanolic *Codium fragile* extracts 60 minutes after wounding. Spectra originate from peaks marked by red stars in the chromatogram of Figure 7.2 C.

Selbständigkeitserklärung

Ich erkläre, dass ich die vorliegende Arbeit selbstständig und unter Verwendung der angegebenen Hilfsmittel, persönlichen Mitteilungen und Quellen angefertigt habe.

Jena,

Caroline Kurth